THE MINOR PLANET BULLETIN

BULLETIN OF THE MINOR PLANETS SECTION OF THE ASSOCIATION OF LUNAR AND PLANETARY OBSERVERS

VOLUME 52, NUMBER 4, A.D. 2025 OCTOBER-DECEMBER 279.

LIGHTCURVES AND ROTATION PERIODS OF NEAR-EARTH ASTEROIDS (137170) 1999 HF1 AND 2025 GB

Heiko Duin
Bredenkamp Observatory (L65)
Am Bredenkamp 6, 28203 Bremen, GERMANY
heiko.duin@web.de

(Received: 2025 May 7)

Photometric observations of two near-Earth asteroids were conducted to determine their synodic rotation periods. It was found for (137170) 1999 HF1 that P = 2.3193 ± 0.0003 h with A = 0.150 ± 0.03 mag and for 2025 GB that P = 0.172 ± 0.0003 h with A = 1.04 ± 0.08 mag.

Photometric observations of the two near-Earth asteroids (137170) 1999 HF1 and 2025 GB were carried out at the Bredenkamp Observatory (L65) in April and May 2025 using a 0.23-m Schmidt-Cassegrain telescope mounted on an EQ6-Pro mount and a monochrome ZWO ASI533MM Pro CMOS camera operated at a chip temperature of -10°C. The observations were made with a clear filter and with the telescope operating with a focal reducer at f/6.3. Exposure times were 30 s for (137170) 1999 HF1 and 3.4 s for 2025 GB, which had a high sky motion of around 140 arcsec/minute. The planning of observations had been done with *NeoPlanner* (Haeusler, 2025), image acquisition software was *NINA* (Berg, 2025).

All images were calibrated with dark and flat frames and were software-binned 3×3 resulting in an image scale of 1.50 arcsec/pix. Data reduction and period analysis were performed with *Tycho Tracker Pro v12* (Parrott, 2025). In both cases, the asteroid and five comparison stars were measured for differential photometry. The comparison stars were selected from the ATLAS catalogue (Tonry et al., 2018) using V magnitudes with color indices in the range of 0.5 < B-V < 0.95 covering the typical color range of asteroids. Some observations with inference from nearby stars have been discarded. Data were light-time corrected and phase-angle corrections were made by applying a H-G model. Data points have been binned in sets of 2 to reduce the number of data points on the lightcurve and to make it easier to read.

(137170) 1999 HF1 is a binary Aten-type near-Earth asteroid (Pravec et al., 2006) discovered by LONEOS on 1999 04/20 (ESA NEOCC, 2025). Pravec et al. (2006) report an orbital period of 14.03 h confirmed by Marchis et al. (2012) who measured an orbital period of 14.04 h. The observations presented here show no obvious signs of the satellite in the data (even though the data in the second half of the short period seems to be a little more scattered between single runs than in the first half). The reason for that may lie in the fact that the observation runs were just about 3 h and less having not enough coverage of the 14.02 h period. The Asteroid Light Curve Database (LCDB) (Warner et al., 2009) contains several previous-reported rotation periods for the main body. The summary table for this asteroid shows a rotation period of 2.3192 h with amplitudes ranging from 0.12 mag to 0.26 mag. The measured synodic period of 2.3193 (±0.0007) h with an amplitude of 0.172 mag is in very good agreement with the data reported from the LCDB. All observations were carried out on five nights in 2025 between 04/12 and 05/05.

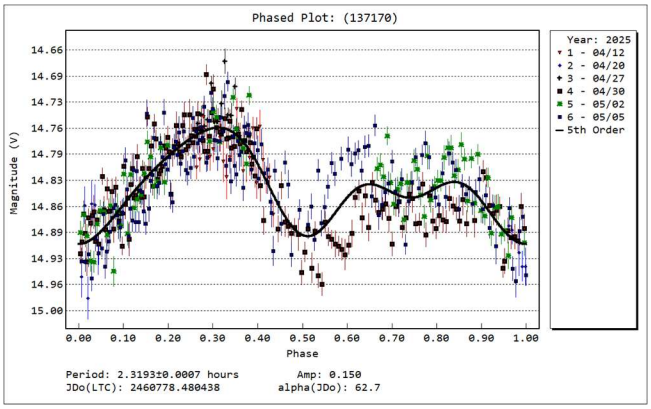

Number	Name	yyyy mm/dd	Phase	L_{PAB}	B_{PAB}	Period(h)	P.E.	Amp	A.E.	Grp
137170	1999 HF1	2025 04/12-05/05	57.8,62.7	201	49	2.319	0.0007	0.15	0.03	NEA
	2025 GB	2025 04/02	32.7,35.1	190	17	0.172	0.0001	1.04	0.08	NEA

Table I. Observing circumstances and results. The phase angle is given for the first and last date. If preceded by an asterisk, the phase angle reached an extrema during the period. L_{PAB} and B_{PAB} are the approximate phase angle bisector longitude/latitude at mid-date range (see Harris et al., 1984). Grp is the asteroid family/group (Warner et al., 2009).

2025 GB is an Apollo-type near-Earth asteroid which was discovered on 2025 04/01 by ATLAS-HKO, Haleakala (ESA NEOCC, 2025). With an absolute magnitude of H=24.5 mag it is expected to have a size of 30-70 meters (ESA NEOCC, 2025). Due to its high apparent speed nine fields were necessary for observations resulting in nine sets of measurements with a time difference of 10 m between these sets. Preliminary results of analyses of the synodic rotation period have been reported on the Minor Planet Mailing List (MPML, 2025) independently by P.-J. Dekelver, D. Bamberger, P. Birtwhistle and C. Gerhard with values ranging from 0.1718 to 0.1729 h (10.31 to 10.38 m). The measured synodic period of 0.1720 h (10.32 m) is in good agreement with these results.

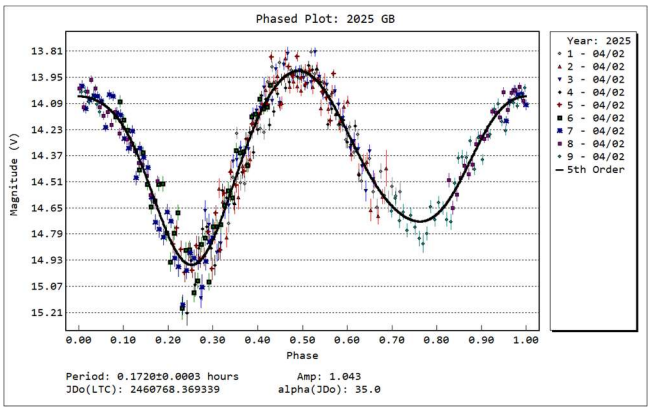

Acknowledgements

Acknowledgements go to Bernhard Haeusler for providing *NeoPlanner*, to Stefan Berg for providing *NINA*, and to Daniel Parrot for providing *Tycho Tracker Pro*.

References

Berg, S. (2025). "Nightime Imaging 'N' Astronomy (NINA)." *https://nighttime-imaging.eu/*

ESA NEOCC (2025). Search for Asteroids. *https://neo.ssa.esa.int/search-for-asteroids*

Haeusler, B. (2025). "NEO Planner." *https://www.k87dettelbachvineyardobservatory.bayern/NeoPlanner.htm*

Harris, A.W.; Young, J.W.; Scaltriti, F.; Zappala, V. (1984). "Lightcurves and phase relations of the asteroids 82 Alkmene and 444 Gyptis." *Icarus* **57**, 251-258.

Marchis, F.; Enriquez, J.E.; Emery, J.P.; Mueller, M.; Baek, M.; Pollock, J.; Assafin, M.; Vieira Martins, R.; Berthier, J.; Vachier, F. and 6 coauthors. (2012). "Multiple asteroid systems: Dimensions and thermal properties from Spitzer Space Telescope and ground-based observations." *Icarus* **221**, 1130-1161.

MPML (2025). "Rotation Period of NEO 2025 GB." *https://groups.io/g/mpml/topic/112264575#msg40509*

Parrot, D. (2025). Tycho software. *https://www.tycho-tracker.com*

Pravec, P.; Scheirich, P.; Kusnirák, P.; Sarounová, L.; Mottola, S.; Hahn, G.; Brown, P.; Esquerdo, G.; Kaiser, N.; Krzeminski, Z. and 47 coauthors (2006). "Photometric survey of binary near-Earth asteroids." *Icarus* **181**, 63-93.

Tonry, J.L.; Denneau, L.; Flewelling, H.; Heinze, A.N.; Onken, C.A.; Smartt, S.J.; Stalder, B.; Weiland, H.J.; Wolf, C. (2018). "The ATLAS All-Sky Stellar Reference Catalog." *Astrophys. J.* **867**, A105.

Warner, B.D.; Harris, A.W.; Pravec, P. (2009). "The Asteroid Lightcurve Database." *Icarus* **202**, 134-146. 2023 October Release #2. *https://minplanobs.org/mpinfo/ph*

LIGHTCURVE ANALYSIS OF NEO 2025 EF4

Peter Birtwhistle
Great Shefford Observatory
Phlox Cottage, Wantage Road
Great Shefford, Berkshire, RG17 7DA
UNITED KINGDOM
peter@birtwhistle.org.uk

Grant Privett
LPMR Observatory (Y82)
Broad Chalke, UK

Wayne Hawley
Old Orchard Observatory (Z09)
Fiddington, UK

Jean-François Gout
Tree Gate Farm Observatory (W05)
Starkville, USA

Mohammad Shawkat Odeh
Al-Khatim Observatory (M44)
Abu Dhabi, UAE

Alexander R. Pratt
Almalex Observatory (Z92)
Leeds, UK

(Received: 2025 May 11)

The analysis of photometric observations of the NEO 2025 EF4 obtained by a collaboration of six observers in three countries during March 2025 indicates that Apollo 2025 EF4 has tumbling rotation with a dominant synodic period of 0.26049 ± 0.00001 h, amplitude 0.55 ± 0.15 mag and a secondary period of 0.23552 ± 0.00002 h, amplitude 0.29 ± 0.15 mag.

Following an alert on a forum of the British Astronomical Association's Asteroid and Remote Planets (ARPS) section, six observers from three countries mobilized to observe the newly discovered Apollo 2025 EF4 (*H = 24.6, D ~36 m, albedo pV = 0.2 assumed*) as it passed Earth at 1.2 Lunar Distances (459,000 km) on 2025 Mar 15.41 UTC (Kechin et al., 2025). Observations were obtained over a period of 32.6 h, spanning either side of the close approach. Apparent magnitude ranged between +13 and +14 throughout, with the apparent speed reaching 145 arcsec/min in the hours following perigee. Photometry was measured by the individual observers, using *Astrometrica* (Raab, 2025), *Tycho* (Parrott, 2025), *Tangra* (Pavlov, 2022) and bespoke Python routines utilising Astropy, Numpy & Scipy libraries. Photometry reference data was obtained from the Gaia DR2, DR3 and ATLAS (Tonry et al., 2018) star catalogues, further details including a summary of the equipment used are listed in Table III. Birtwhistle used a total of 5138 photometric measurements from 85 sessions for the lightcurve analysis using *MPO Canopus* (Warner, 2023) which incorporates the Fourier algorithm developed by Harris (Harris et al., 1989). Adjustments to the zero-points of the individual sessions were made to minimise the RMS of the overall fit to accommodate the differences in equipment, star catalogues and mag bands selected by the observers. 2025 EF4 reached opposition 2 hours after close approach and the photometric measurements span phase angles from 53.7° at the start of the observing period, reducing to 44.7° near opposition, before increasing again to 54.7° by the last session.

The linearly scaled period spectrum plot from a 4th order analysis indicates the best-fit solution is at ~0.26 h. A series of increasingly inferior solutions at multiples of that period imply the best-fit period has a significant contribution from the first harmonic, likely to lead to a monomodal lightcurve. Also apparent is another series of weaker RMS minima at multiples of ~0.24 h suggesting that non-principal axis rotation (NPAR) or tumbling is present.

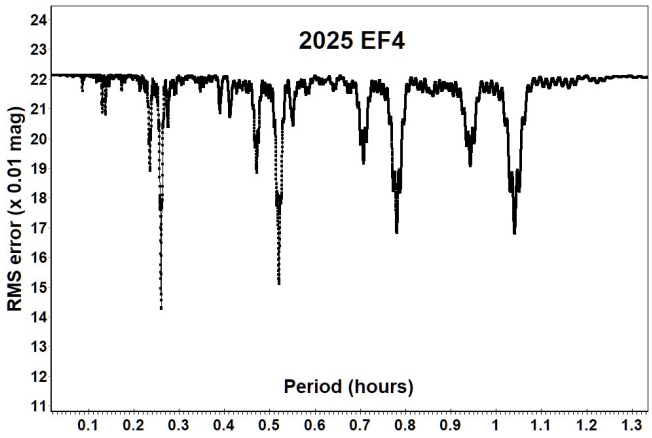

The *MPO Canopus* Dual Period Search function was used to search for NPAR solutions for rotation and precession and the resulting best-fit lightcurves are given, labelled P1 and P2, where:

P1 = 0.26049 ± 0.00001 h (~15.6 min), amplitude 0.55 ± 0.15
P2 = 0.23552 ± 0.00002 h (~14.1 min), amplitude 0.29 ± 0.15

A weaker solution, consisting of the same dominant P1 period but with a secondary period P3 of 0.1373 h (~8.2 min) was also located, but it is noted that the frequency of the P3 period is just a linear combination of the frequencies of P1 and P2, where:

3/P1 – 1/P2 = 1/P3.

Although this analysis is not able to determine which of the two periods are due to rotation and which to precession, it is expected that 2025 EF4 may be rated on the Principal Axis Rotation (PAR) scale defined in Pravec et al. (2005) as PAR = -3 where *NPA rotation is reliably detected with the two periods resolved. An ambiguity of the periods solution may be tolerated provided the resulting spectrum of frequencies with significant signal is the same for the different solutions*. (Petr Pravec, personal communication).

The NPAR solution indicates the full amplitude of the tumbling rotation was 0.84 mag.

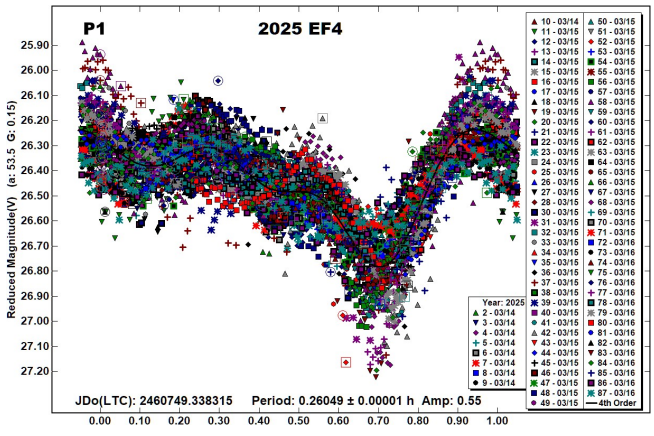

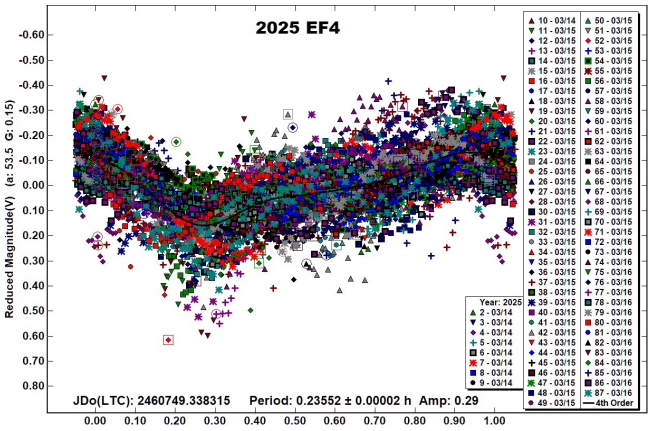

No previously reported results for 2025 EF4 have been found in the Asteroid Lightcurve Database (Warner et al., 2009), from searches via the Astrophysics Data System (ADS, 2025) or from wider searches apart from Diepvens (2025), where two raw (unphased) lightcurve plots are given. These were obtained with a 0.20-m f/9 refractor + CCD from Olmen observatory (MPC Code C23), with 2.6 h of coverage being acquired starting on 2025 Mar 15.89 UTC and a further 0.6 h starting on 2025 Mar 16.92 UTC. The earlier plot completely overlaps and closely matches a raw plot of the photometry measurements in this paper for the same time range.

Number	Name	Integration times	Max intg/Pd	Min a/b	Pts	Flds
	2025 EF4	0.3-8.0	0.009[1]	1.3*	5138	85

Table I. Ancillary information, listing the integration times used (seconds), the fraction of the period represented by the longest integration time (Pravec et al., 2000), the calculated minimum elongation of the asteroid (Zappala et al., 1990), the number of data points used in the analysis and the number of times the telescopes were repositioned to different fields. Note: * = Value uncertain, based on phase angle > 40°, 1 = Calculated using the shorter of the NPAR periods.

Acknowledgements

The authors express their great appreciation for the help Dr. Petr Pravec, Astronomical Institute, Czech Republic gave reviewing a draft of the NPAR analysis of 2025 EF4. This work has made use of data from the European Space Agency (ESA) mission Gaia (*https://www.cosmos.esa.int/gaia*), processed by the Gaia Data Processing and Analysis Consortium (DPAC, *https://www.cosmos.esa.int/web/gaia/dpac/consortium)*. Funding for the DPAC has been provided by national institutions, in particular the institutions participating in the Gaia Multilateral Agreement.

References

ADS (2025). Astrophysics Data System. *https://ui.adsabs.harvard.edu/*

Diepvens, A. (2025). 2025 EF4 Lightcurve. *https://www.astronomie.be/alfons.diepvens/cometimages/NEO/lightcurve/2025-EF4.html*

Harris, A.W.; Young, J.W.; Scaltriti, F.; Zappala, V. (1984). "Lightcurves and phase relations of the asteroids 82 Alkmene and 444 Gyptis." *Icarus* **57**, 251-258.

Harris, A.W.; Young, J.W.; Bowell, E.; Martin, L.J.; Millis, R.L.; Poutanen, M.; Scaltriti, F.; Zappala, V.; Schober, H.J.; Debehogne, H.; Zeigler, K. (1989). "Photoelectric Observations of Asteroids 3, 24, 60, 261, and 863." *Icarus* **77**, 171-186.

JPL (2025). Small-Body Database Lookup. *https://ssd.jpl.nasa.gov/tools/sbdb_lookup.html*

Kechin, Y.; Lipunov, V.; Gorbovskoy, E.; Buckley, D.; Balanutsa, P.; Panchenko, I.; Zhirkov, K.; Kuznetsov, A.; Gress, O.; Antipov, G.; Tiurina, N.; Gout, J.-F.; Sankovich, A. (2025) "2025 EF4." MPEC 2025-E163. *https://minorplanetcenter.net/mpec/K25/K25EG3.html*

Parrott, D. (2025). Tycho Software. *https://www.tycho-tracker.com*

Pavlov, H. (2022). Tangra software. *http://www.hristopavlov.net/Tangra/Tangra.html*

Pravec, P.; Hergenrother, C.; Whiteley, R.; Sarounova, L.; Kusnirak, P.; Wolf, M. (2000). "Fast Rotating Asteroids 1999 TY2, 1999 SF10, and 1998 WB2." *Icarus* **147**, 477-486.

Pravec, P.; Harris, A.W.; Scheirich, P.; Kušnirák, P.; Šarounová, L.; Hergenrother, C.W.; Mottola, S.; Hicks, M.D.; Masi, G.; Krugly, Yu.N.; Shevchenko, V.G.; Nolan, M.C.; Howell, E.S.; Kaasalainen, M.; Galád, A. and 5 colleagues. (2005). "Tumbling Asteroids." *Icarus* **173**, 108-131.

Raab, H. (2025). Astrometrica software, version 4.15.0.460. *http://www.astrometrica.at/*

Tonry, J.L.; Denneau, L.; Flewelling, H.; Heinze, A.N.; Onken, C.A.; Smartt, S.J.; Stalder, B.; Weiland, H.J.; Wolf, C. (2018). "The ATLAS All-Sky Stellar Reference Catalog." *Astrophys. J.* **867**, A105.

Warner, B.D.; Harris, A.W.; Pravec, P. (2009). "The Asteroid Lightcurve Database." *Icarus* **202**, 134-146. Updated 2023 Oct. *https://www.minorplanet.info/php/lcdb.php*

Number	Name	yyyy mm/dd	Phase	L_{PAB}	B_{PAB}	Period(h)	P.E.	Amp	A.E	PAR	H
	2025 EF4	2025 03/14-03/16	*53.7,54.7	158	9	0.26049	0.00001	0.55	0.15	-3	24.6
						0.23552	0.00002	0.29	0.15		

Table II. Observing circumstances and results. The phase angle is given for the first and last date. If preceded by an asterisk, the phase angle reached an extrema during the period. L_{PAB} and B_{PAB} are the approximate phase angle bisector longitude/latitude at mid-date range (see Harris et al., 1984). Amplitude error (A.E.) is calculated as √2 × (lightcurve RMS residual). PAR is the expected Principal Axis Rotation quality detection code (Pravec et al., 2005) and H is the absolute magnitude at 1 au from Sun and Earth taken from the Small-Body Database Lookup (JPL, 2025).

Warner, B.D. (2023). MPO Software, Canopus version 10.8.6.20. Bdw Publishing, Colorado Springs, CO. *https://minplanobs.org/BdwPub/*

Zappala, V.; Cellini, A.; Barucci, A.M.; Fulchignoni, M.; Lupishko, D.E. (1990). "An analysis of the amplitude-phase relationship among asteroids." *Astron. Astrophys*. **231**, 548-560.

Observer, Observatory (MPC code)	Telescope	Detector	Filter / mag band	Star Catalogue	Photometry software	Obs. span 2025 March UTC	Sessions / Points
Birtwhistle, Great Shefford Observatory (J95)	0.41-m f/6.3 SCT	CCD	None / G	Gaia DR3	Astrometrica	14.86-16.05	52 / 3324
Privett, LPMR Observatory, Broad Chalke, UK (Y82)	0.3-m f/4 Newtonian	CCD	None / G	Gaia DR3	(Python)	15.82 - 15.93	6 / 941
Hawley, Old Orchard Observatory, Fiddington, UK (Z09)	0.35-m f/6.7 SCT	CCD	SDSS r' / SR	ATLAS	Tycho	15.80 - 15.84	11 / 341
Gout, Tree Gate Farm Observatory, Starkville, USA (W05)	0.28-m f/1.9 SCT	CMOS	None / V	ATLAS	Tycho	16.12 - 16.19	6 / 319
Odeh, Al-Khatim Observatory, Abu Dhabi, UAE (M44)	0.36-m f/7.7 SCT	CMOS	None / SR	ATLAS	Tycho	15.68 - 15.70	8 / 198
Pratt, Almalex Observatory, Leeds, UK (Z92)	0.28-m f/4 SCT	CMOS	None / V	Gaia DR3	Tangra	14.85 - 15.91	2 / 15

Table III. Equipment list.

761 BRENDELIA: A NEWLY IDENTIFIED BINARY ASTEROID FROM PRO-AM COLLABORATION

Milagros Colazo
Astronomical Observatory Institute, Faculty of Physics
Adam Mickiewicz University, ul. Słoneczna 36, 60-286 Poznań
POLAND
Grupo de Observadores de Rotaciones de Asteroides (GORA)
ARGENTINA
https://aoacm.com.ar/gora/index.php
milirita.colazovinovo@gmail.com

Carlos Colazo
Observatorio Astronómico El Gato Gris (MPC I19)
Tanti, Córdoba, ARGENTINA

Víctor Amelotti
Observatorio Astronómico Naos (GORA NAO)
Alta Gracia, Córdoba, ARGENTINA|
Observatorio Astronómico Naos 2 (GORA NA2)
Alta Gracia, Córdoba, ARGENTINA

Raúl Melia
Observatorio de Raúl Melia Carlos Paz (GORA RMC)
Carlos Paz, Córdoba, ARGENTINA

Néstor Suárez
Observatorio Antares (MPC X39)
Pilar, Buenos Aires, ARGENTINA

Francisco Santos
Observatorio Astronómico Giordano Bruno (MPC G05)
Piconcillo, Córdoba, ESPAÑA

Bruno Monteleone
OsservatorioAstronomico “La Macchina del Tempo” (MPC M24)
Ardore Marina, Reggio Calabria, ITALIA

Giuseppe Ciancia
CapoSudObservatory (GORA CS1)
Palizzi Marina, Reggio Calabria, ITALIA

Aldo Wilberger
Observatorio Los Cabezones (MPC X12)
Santa Rosa. La Pampa, ARGENTINA

Mario Morales
Observatorio de Sencelles (MPC K14)
Sencelles, Mallorca, Islas Baleares, ESPAÑA

Marcos Anzola
Observatorio Astronómico Vuelta por el Universo (GORA OMA)
Córdoba, Córdoba, ARGENTINA

Ariel Stechina
Observatorio de Ariel Stechina 1 (GORA OAS)
Reconquista, Santa Fe, ARGENTINA

Damián Scotta
Observatorio de Damián Scotta 1 (GORA ODS)
San Carlos Centro, Santa Fe, ARGENTINA

Alberto García
Observatorio Río Cofio (MPC Z03)
Robledo de Chavela, Madrid, ESPAÑA

Emilio Primucci
Observatorio Pueyrredón (MPC X38)
Pilar, Buenos Aires, ARGENTINA

(Received: 2025 May 28)

Photometric observations taken by GORA observatories during 2024 July 24 - August 5 revealed that minor planet 761 Brendelia is a binary system with an orbital period of 57.079 ± 0.016 h. Mutual eclipse/occultation events that are 0.6-0.8-magnitude deep suggest that both components are of similar sizes. This configuration also suggests that the pair has reached tidal coupling, which would explain why their rotation periods are both 58 hours. Eclipses are occurring every 29 hours. We applied relative photometry assigning V magnitudes to the calibration stars. The image acquisition was performed without filters and with exposure times of a few minutes. All images used were corrected using dark frames and, in some cases, bias and flat-field corrections were also used. Photometry measurements were performed using *FotoDif* software and for the analysis, we employed *Períodos* software (Mazzone, 2012).

761 Brendelia is a main-belt asteroid discovered in 1913 by F. Kaiser. Classified as a SC-type asteroid according to the Tholen taxonomy, it is a member of the Koronis family (Nesvorny et al., 2015). The diameter is 20.763 km. The reported rotational period for this asteroid is 57.96 h (Durech et al., 2018).

Between 2024 July 24 and October 20, we recorded ten significant brightness drops (0.6- to 0.8-magnitude deep) in the asteroid’s lightcurve that cannot be explained by its rotational modulation alone (Fig. 1). The first two events were detected serendipitously. After observing the second brightness dip, we hypothesized that these were mutual eclipses caused by the alignment of two components of a previously undetected binary system.

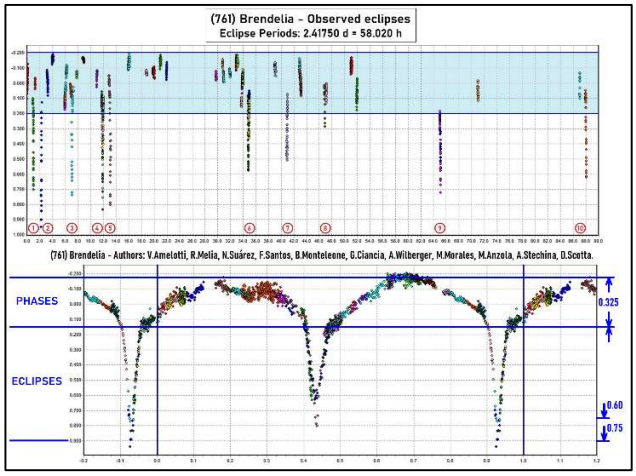

Fig. 1: Observed eclipses of (761) Brendelia.

Our analysis indicates that 761 Brendelia is likely a binary asteroid system. The components appear to orbit their common center of mass with a period of approximately 58 hours, producing mutual eclipses approximately every 29 hours. During the observation window, the Sun was aligned with the orbital plane of the system, enabling the detection of these eclipses; this was an unexpected outcome since our initial objective was simply to determine the rotational period and lightcurve (Table I).

Eclipse period: 2.41750 d = 58.020 h			
Eclipse N°	**Date**	**UT**	**Phase:**
1	25/7/2024	02:19	0.424
2	26/7/2024	07:19	0.924
3	31/7/2024	03:22	0.924
4	4/8/2024	23:24	0.924
5	6/8/2024	04:25	0.424
6	27/8/2024	22:35	0.424
7	2/9/2024	23:38	0.924
8	9/9/2024	00:41	0.424
9	27/9/2024	03:50	0.924
10	20/10/2024	03:02	0.424

Table I: Observed eclipses of (761) Brendelia.

This geometric alignment, apparently never recorded before, provided the unique conditions necessary to reveal the binary nature of 761 Brendelia. GORA happened to be observing the asteroid at precisely the right time. With this evidence, we submitted two reports to the Central Bureau for Astronomical Telegrams (CBAT) of the International Astronomical Union (IAU) in early August, requesting the issuance of an electronic telegram officially crediting GORA with the discovery. *IAU Electronic Telegram No. 5435* was subsequently published on 2024 August 21.

One of the immediate questions that arose was whether or not the eclipses might have been missed in previous observations. Assuming that the observed brightness dips were caused by mutual shadow projection — i.e., eclipses — between the two components of the system as illuminated by the Sun, we set out to estimate past "eclipse seasons" (Table II) based on GORA's observations and the known orbital parameters of 761 Brendelia.

(761) Brendelia - ECLIPSING BINARY ECLIPSE SEASONS IN THE PAST				
Orbital period		**4,843827343 years**	**Date**	**Elong.**
Half of the		**2,421913671 years**		
orbital period		**884,6039685 days**		
Time 2° eclipse GORA		**2460517,80763 GJD**	**26/7/2024**	**176,6**
-1	Ephemerides -1	2459633,20366 GJD	22/2/2022	**148,7**
-2	Ephemerides -2	2458748,59969 GJD	22/9/2019	**109,8**
-3	Ephemerides -3	2457863,99572 GJD	20/4/2017	82,8
-4	Ephemerides -4	2456979,39176 GJD	17/11/2014	**56,4**
-5	Ephemerides -5	2456094,78779 GJD	16/6/2012	**35,6**
-6	Ephemerides -6	2455210,18382 GJD	13/1/2010	**11,7**
-7	Ephemerides -7	2454325,57985 GJD	13/8/2007	**5,8**
-8	Ephemerides -8	2453440,97588 GJD	11/3/2005	**31,0**
-9	Ephemerides -9	2452556,37191 GJD	8/10/2002	**48,1**
-10	Ephemerides -10	2451671,76795 GJD	7/5/2000	76,0

Table II: Estimate past "eclipse seasons."

We took as a reference the date of minimum brightness observed during the second eclipse among the ten recorded by GORA between 2024 July and October. The parameters used for the calculation were:

- Orbital period: 4.8438273428 d
- Date of the second observed eclipse: JD 2460517.80763 (2024 July 26, 07:19 UT)

Since two opportunities for eclipses occur per orbital period, we subtracted half the orbital period successively from the reference date to project previous eclipse events. We also assumed that each "eclipse season" spans approximately six months, or twice the duration over which we observed eclipses during 2024.

However, we did not know the exact duration of each eclipse season, since the inclination of the mutual orbit relative to the heliocentric orbit is unknown. If the inclination were $i = 0°$, eclipses would be continuous; if $i = 90°$, eclipse seasons would be very brief. Similarly, the maximum and minimum distances between the two components are not precisely known; only rough estimates exist. Based on our observations, which span over 88 days, it is evident that the inclination $i << 90°$ and/or the mutual distance $d << 93$ km. These conditions would favor the extension of eclipse seasons (Fig. 2).

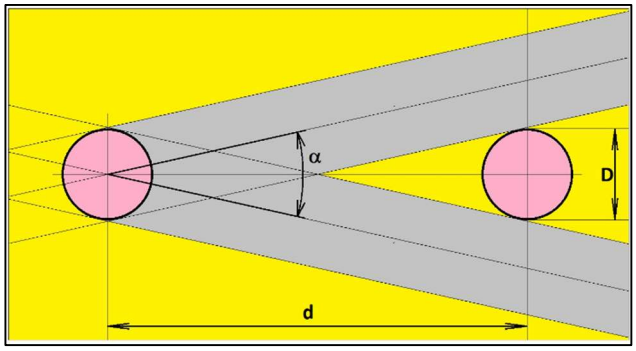

Fig. 2: Eclipse seasons assuming i = 90°.

Eclipse seasons = α*P/360°; Tg (α/2) = D/d; (assuming $i = 90°$)

with: Eclipse seasons > 88 days;
$P = 1769$ days;
$D \approx 14.7$ km;
$a \approx 72$ km.

this gives $\alpha > 17.9°$ and $d < 93$ km (with conditions for short eclipse seasons).

We also examined the solar elongation of Brendelia during those periods, an important observational factor:

- When elongation is near 180° (opposition), the asteroid is observable throughout much of the night, being closest to Earth and at peak brightness.
- When elongation is near 0° (conjunction), the asteroid is unobservable at night, farthest from Earth, and at minimum brightness.

We then compared the epochs of all published observations of 761 Brendelia with the eclipse seasons we calculated. We computed ten such seasons retroactively, the asteroid having been observed seven times since the start of this century.

From this comparison, we find that all seven published lightcurve phase diagrams were constructed using data obtained outside the predicted eclipse seasons (Table III). This may explain why the binary nature of 761 Brendelia was not detected in previous studies prior to the GORA observations.

Ephemerides (Ref: 2° eclipse GORA)		Observations in the past		
Date	Elongation	From	To	Authors
26/7/2024	176,6	23/7/2024	19/10/2024	M. Colazo et al.
22/2/2022	148,7	No observational data		
22/9/2019	109,8	No observational data		
20/4/2017	82,8	No observational data		
17/11/2014	56,4	10/3/2013	21/4/2013	Stefphen M. Slivan et al.
16/6/2012	35,6	No observational data		
13/1/2010	11,7	20/5/2009	17/6/2009	Stefphen M. Slivan et al.
13/8/2007	5,8	2/3/2008	14/3/2008	Stefphen M. Slivan et al.
		9/12/2006	10/2/2007	Stefphen M. Slivan et al.
11/3/2005	31,0	6/9/2005	7/10/2005	Stefphen M. Slivan et al.
8/10/2002	48,1	21/2/2003	20/5/2003	Stefphen M. Slivan et al.
7/5/2000	76,0	No observational data		

Table III: Observations made in the past.

Another question that arose following the discovery was whether or not eclipses will be observable again in the future (Table IV).

(761) Brendelia - ECLIPSING BINARY ECLIPSE SEASONS IN THE FUTURE				
Orbital period		4,843827343 years	Date	Elong.
Half of the orbital period		2,421913671 years 884,6039685 days		
Time 2° eclipse GORA		2460517,80763 GJD	26/7/2024	176,6
1	Ephemerides 1	2461402,41160 GJD	27/12/2026	128,7
2	Ephemerides 2	2462287,01557 GJD	30/5/2029	99,0
3	Ephemerides 3	2463171,61954 GJD	1/11/2031	68,7
4	Ephemerides 4	2464056,22350 GJD	3/4/2034	49,2
5	Ephemerides 5	2464940,82747 GJD	4/9/2036	23,0
6	Ephemerides 6	2465825,43144 GJD	5/2/2039	6,1
7	Ephemerides 7	2466710,03541 GJD	9/7/2041	18,5
8	Ephemerides 8	2467594,63938 GJD	11/12/2043	36,8
9	Ephemerides 9	2468479,24335 GJD	13/5/2046	62,0
10	Ephemerides 10	2469363,84731 GJD	14/10/2048	85,2

Table IV: Estimate in the future “eclipse seasons.”

We again used as a reference the date of minimum brightness observed during the second eclipse among the ten recorded by GORA between 2024 July and October. This time, we successively added half of the orbital period to that reference date and calculated ten eclipse seasons projected into the future.

In addition to the current favorable season for eclipse observations, we will have another opportunity to observe such events toward the end of 2026. In mid-2029, another potential eclipse season is predicted; however, detection may be more difficult due to the system's quadrature position relative to the Sun, which reduces observational windows and visibility. To encounter similarly optimal conditions for observing eclipses again, we will likely need to wait until the second half of the current century.

Based on the observational evidence and lightcurve analysis, several working hypotheses have been proposed to explain the physical and dynamical characteristics of the 761 Brendelia binary system.

Size of the Components: Based on the depth of the brightness drops observed in two consecutive events (eclipse and occultation), we infer that both components have similar dimensions. This symmetry supports the classification of the system as a binary asteroid, rather than a primary asteroid with a smaller satellite.

Synchronization of Rotation and Revolution. Our proposed model envisions the system as composed of two rugby ball-shaped ellipsoids, co-orbiting in a tidally locked configuration. That is, both bodies have achieved tidal synchronization, meaning that their rotation period equals their orbital period, or approximately 58 hours. This would account for the presence of two minima and two maxima in the published lightcurves, consistent with the classical bimodal shape model expected for a single elongated ellipsoidal body.

Phase Diagram. If both components are ellipsoidal, it is plausible that their alignment with Earth occurs when their major axes are pointed toward the observer, coinciding with the minima in the phase diagram. Conversely, the maxima occur when we observe the long sides of both ellipsoids from the side.

Orbital Size and System Resolution. We estimate the duration of each eclipse to be approximately 3 hours. If both components have similar diameters (D), their orbits should also be comparable in size. During an eclipse, each body would traverse an arc approximately equal to its own diameter.

According to physicist Robert Johnston, the equivalent diameter of each component is about 14.7 km. Based on GORA’s observations, Johnston estimates the semi-major axis of each orbit to be 72 km.

The maximum separation between the two components would slightly exceed 200 km. From Earth, this corresponds to an angular separation of approximately 0.14 arcseconds — below the resolving power of most conventional telescopes. This explains why the system cannot be visually resolved using standard observational equipment.

Finally, we present the results from two key diagrams. Fig. 3, which includes eclipses, allowed us to determine the periodicity of these events. Meanwhile, Fig. 4, without eclipses, provided the data needed to identify the rotation periods of both components. Together, these findings confirm the binary nature of 761 Brendelia and underscore the importance of continued Pro-Am collaboration in advancing asteroid research.

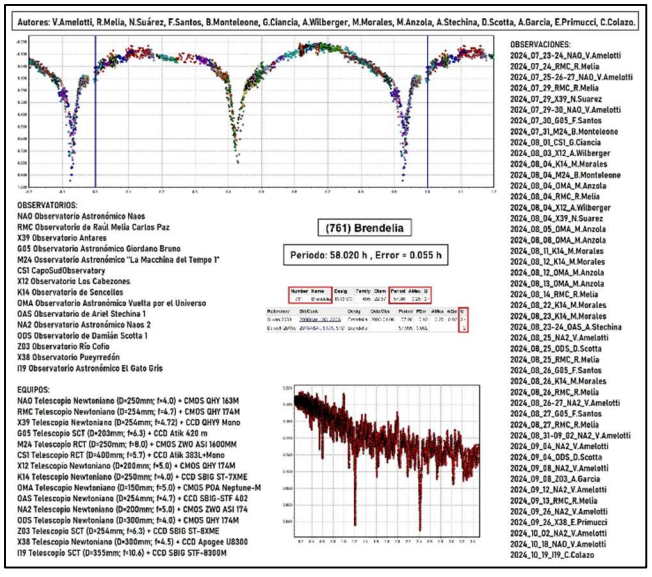

Fig. 3: Observations made with eclipses.

Number	Name	yy/ mm/dd- yy/ mm/dd	Phase	L_{PAB}	B_{PAB}	Period(h)	P.E.	Amp	A.E.	Grp
761	Brendelia	24/07/27-24/10/20	*04.3,21.4	311	-2	57.98	0.06	0.28	0.03	KOR

Table 5. Observing circumstances and results. The phase angle is given for the first and last date. If preceded by an asterisk, the phase angle reached an extremum during the period. L_{PAB} and B_{PAB} are the approximate phase angle bisector longitude/latitude at mid-date range (see Harris et al., 1984). Grp is the asteroid family/group (Warner et al., 2009). KOR: 158 Koronis.

Observatory	Telescope	Camera
G05 Obs.Astr.Giordano Bruno	SCT (D=203mm; f=6.3)	CCD Atik 420 m
I19 Obs.Astr.El Gato Gris	SCT (D=355mm; f=10.6)	CCD SBIG STF-8300M
K14 Obs.Astr.de Sencelles	Newtonian (D=250mm; f=4.0)	CCD SBIG ST-7XME
M24 Oss.Astr.La Macchina del Tempo	RCT (D250mm; f=8.0)	CMOS ZWO ASI 1600MM
X12 Obs.Astr.Los Cabezones	Newtonian (D=200mm; f=5.0)	CMOS QHY 174M
X38 Observatorio Pueyrredón	Newtonian (D=300mm; f=4.5)	CCD Apogee U8300
X39 Obs.Astr.Antares	Newtonian (D=250mm; f=4.72)	CCD QHY9 Mono
Z03 Obs.Astr.Río Cofio	SCT (D=254mm; f=6.3)	CCD SBIG ST-8XME
CS1 CapoSudObservatory	RCT (D=400mm; f=5.7)	CCD Atik 383L+Mono
NAO Obs.Astr.Naos	Newtonian (D=250mm; f=4.0)	CMOS QHY 163M
NA2 Obs.Astr.Naos 2	Newtonian (D=200mm; f=5.0)	CMOS ZWO ASI 174
OAS Obs.Astr.de Ariel Stechina 1	Newtonian (D=254mm; f=4.7)	CCD SBIG STF-402
ODS Obs.Astr.de Damián Scotta 1	Newtonian (D=300mm; f=4.0)	CMOS QHY 174M
OMA Obs.Astr.Vuelta por el Universo	Newtonian (D=150mm; f=5.0)	CMOS POA Neptune-M
RMC Obs.Astr.de Raúl Melia Carlos Paz	Newtonian (D=254mm; f=4.7)	CMOS QHY 174M

Table 6. List of observatories and equipment.

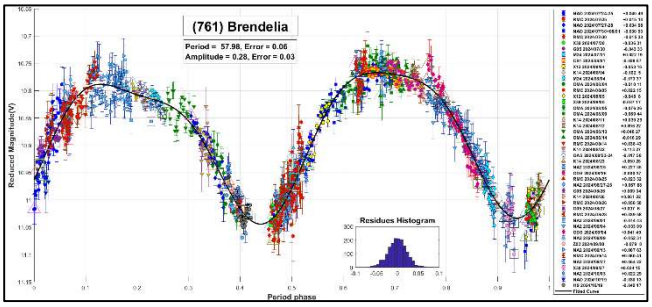

Figure 4: Phase diagram without eclipses.

Acknowledgements

We want to thank Julio Castellano for his *FotoDif* program that we used for preliminary analyses, Fernando Mazzone for his *Períodos* program, which was used in final analyses, and Matías Martini for his *CalculadorMDE v0.2* that was used for generating ephemerides used in the planning stage of the observations. This research made use of the Small Bodies Data Ferret supported by the NASA Planetary System (*https://sbnapps.psi.edu/ferret/*). This research made use of data and/or services provided by the International Astronomical Union's Minor Planet Center.

References

Durech, J.; Hanus, J.; Ali-Lagoa, V. (2018). "Asteroid models reconstructed from the Lowell Photometric Database and WISE data." *Astron. Astrophys*. **617**, A57.

Harris, A.W.; Young, J.W.; Scaltriti, F.; Zappala, V. (1984). "Lightcurves and phase relations of the asteroids 82 Alkmene and 444 Gyptis." *Icarus* **57**, 251-258.

Mazzone, F.D. (2012). Períodos sotware, version 1.0. *http://www.astrosurf.com/salvador/Programas.html*

Nesvorny, D.; Broz, M.; Carruba, V. (2015). "Identification and Dynamical Properties of Asteroid Families." In *Asteroids IV* (P. Michel, F. DeMeo, W.F. Bottke, R. Binzel, Eds.). Univ. of Arizona Press, Tucson, also available on astro-ph.

Warner, B.D.; Harris, A.W.; Pravec, P. (2009). "The Asteroid Lightcurve Database." *Icarus* **202**, 134-146. *https://minplanobs.org/mpinfo/ph*

TWO NEW LIGHTCURVES FOR 1209 PUMMA AND ITS OBLIQUITY AND LIGHTCURVE AMPLITUDE

W. Romanishin
1933 Whispering Pines Cir., Norman, OK 73072
wromanishin@ou.edu

(Received: 2025 May 28)

1209 Pumma is an asteroid showing relatively sharp V-shaped dips in its lightcurve. Two new lightcurves are presented that should aid future shape modelling.

1209 Pumma has an orbital period of 5.643 y, a semimajor axis of 3.170 AU, an eccentricity of 0.127, and an orbital inclination of 6°.9. The October 2023 version of the asteroid lightcurve database of Warner et al. (2009) lists Pumma as a member of the Hygiea family. However, Mothé-Diniz et al. (2001) suggest it is an interloper, based on spectroscopic evidence. Only a single lightcurve is found in the lightcurve database for this object. This lightcurve was obtained in 2012 by Casulli and Roy (2013) and has a high-quality rating (Q=3).

As part of a program to reobserve asteroids which show sharp narrow minima in their lightcurves, the author obtained two new lightcurves of Pumma. Photometry on three nights in April 2023 was obtained using the 0.43-m telescope at the Heavens Mirror Observatory in Chile (IAU code X02). Two-minute exposures through a Red filter were obtained spanning 19.8 hours in total, resulting in 478 usable images. Another lightcurve was obtained over four nights in July 2024 using the 0.5-m T72 iTelescope at Deep Sky Chile (IAU code X07). Over a total span of 14.8 hours, 371 two minute exposures were made through a luminance filter. Observations of standard stars in the Landolt system (Clem and Landolt, 2013) provided excellent transformations between the luminance and Red filters and the standard R system.

The lightcurves below present absolute R mags, H(R), derived assuming G=0.15 (Bowell et al., 1989). The points were fit with a smooth spline curve. The standard deviation scatter around the fit is 0.018 mag for the 2023 points and 0.011 mag for the 2024 lightcurve. Note that the absolute mag of the maxima of the 2023 and 2024 lightcurves agree very well.

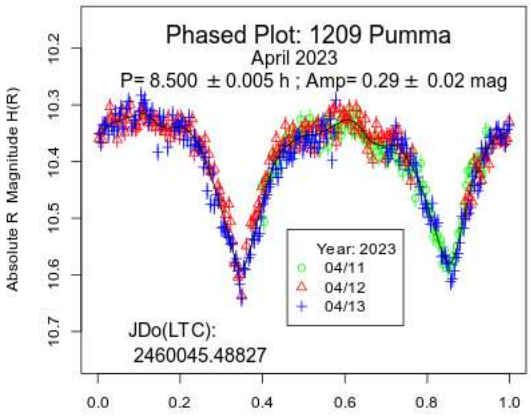

Fig. 1. Phased absolute magnitude plot from April 2023. The median observed R mag was around 14.7.

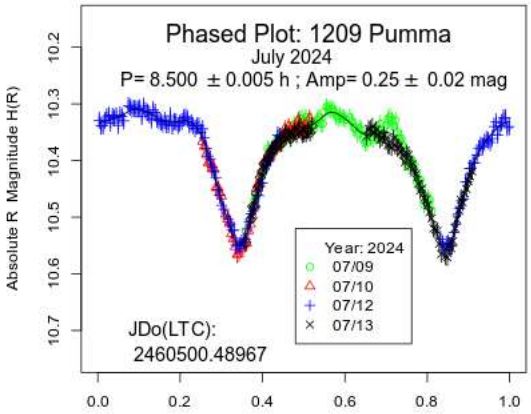

Fig. 2. Lightcurve from July 2024. The median observed R mag was around 14.1.

Casulli and Roy (2013) report a period of 8.5001 h. For the 2024 data reported here, a period was found by phasing with a range of periods and finding the minimum standard deviation around the smooth spline fit. A period of 8.500 h was derived, matching the Casulli and Roy (2013) period.

The three available lightcurves have similar amplitudes: 0.28 mag in 2012, 0.29 mag in 2023 and 0.25 mag in 2024. The 2023 lightcurve was obtained when Pumma was close to 2 revolutions around the Sun from its position when the 2012 lightcurve was measured. The angle between the 2012 and 2023 orbital positions as seen from the Sun is about 17°. The 2024 lightcurve was obtained when the object was close to 90° from the midpoint of the 2012 and 2023 orbital positions. The fact that the amplitudes of the three lightcurves are similar suggests that the rotational axis obliquity is roughly perpendicular to the orbital plane of Pumma and that the true amplitude is near 0.29 mag. However, as the 2012 and 2023 orbital positions are close together, we basically have only two independent positions with measured amplitude, so additional measurements are needed to nail down the true lightcurve amplitude and obliquity.

The October of 2025 opposition will find Pumma at an orbital position almost 180° from the midpoint of the 2012 and 2023 orbital positions. The opposition in December 2026 will occur when Pumma will be close to 180° from the midpoint between the 2012+2023 and 2024 orbital positions. Thus, measurement of the amplitude in December 2026 should allow a much-improved measurement of the actual lightcurve amplitude and orbital obliquity and might provide enough data for shape modelling.

Acknowledgements

This research has made use of data and/or services provided by the Jet Propulsion Laboratory HORIZONS system and the Minor Planet Center of the International Astronomical Union.

References

Bowell, E.; Hapke, B.; Domingue, D.; Lumme, K.; Peltoniemi, J.; Harris, A.W. (1989). "Application of Photometric Models to Asteroids." In: Binzel, R.P.; Gehrels, T.; Matthews, M.S. (Eds.), Asteroids II. Univ of Arizona Press, pp. 524-556, Tucson.

Number	Name	yyyy mm/dd	Phase	L_{PAB}	B_{PAB}	Period(h)	P.E.	Amp	A.E.	Grp
1209	Pumma	2023 04/11-04/13	5.0-5.6	191	8	8.500	0.005	0.29	0.02	MB-O
1209	Pumma	2024 07/09-07/13	2.9-1.7	293	-3	8.500	0.005	0.25	0.02	MB-O

Table I. Observing circumstances and results. The phase angle is given for the first and last date. If preceded by an asterisk, the phase angle reached an extrema during the period. L_{PAB} and B_{PAB} are the approximate phase angle bisector longitude/latitude at mid-date range (see Harris et al., 1984). Grp is the asteroid family/group (Warner et al., 2009).

Casulli, S.; Roy, R. (2013). "Curves of rotation of asteroids and comets, CdR, CdL." *http://obswww.unige.ch/~behrend/r001209a.png*

Clem, J.L.; Landolt, A.U. (2013). "Faint UBVR Standard Star Fields." *Astronomical Journal,* **146**, 88.

Harris, A.W.; Young, J.W.; Scaltriti, F.; Zappala, V. (1984). "Lightcurves and Phase Relations of the Asteroids 82 Alkmene and 444 Gyptis." *Icarus* **57**, 251-258.

Mothé-Diniz, T.; Di Martino, M.; Bendjoya, P.; Doressoundiram, A.; Migliorini, F. (2001). "Rotationally Resolved Spectra of 10 Hygiea and a Spectroscopic Study of the Hygiea Family." *Icarus* **152**, 117-126.

Warner, B.D.; Harris, A.W.; Pravec, P. (2009). "The Asteroid Lightcurve Database." *Icarus* **202**, 134-146. Updated 2023 Oct. *http://www.minorplanet.info/lightcurvedatabase.html*

LIGHTCURVE ANALYSIS FOR (36197) 1999 TZ91

Gonzalo Fornas (J57)
Asociación Valenciana de Astronomía
(Centro Astronómico Alto Turia)
C/ Profesor Blanco 16. 46014 Valencia, SPAIN
gon@iicv.es

Frederick Pilcher
Organ Mesa Observatory (G50)
4438 Organ Mesa Loop
Las Cruces NM 88011 USA

(Received: 2025 June 22)

Photometric observations are reported for (36197) 1999 TZ91. We derived the rotational synodic period of 12.23275 ± 0.0004 h and amplitude 0.8 mag.

We report on the photometric analysis for the main-belt asteroid (36197) 1999 TZ1 by observatory codes G50 and J57. Due to the period being very close to 12 hours, we collaborated between the two observatories located in the USA and Spain to obtain the complete lightcurve of this previously unstudied asteroid. The data were obtained during April and May of 2025. We present graphic results of the data analysis, with the plot phased to a given period.

Observatory	Telescope	CCD
C.A.A.T. J57	17" DK	QHY- 600
Organ Mesa. G50	14" SCT	SBIG STL 1001E

Table I. List of instruments used for the observations.

Images were measured using *MPO Canopus* (Bdw. Publishing) with a differential photometry technique. The comparison stars were restricted to near solar-color to minimize color dependencies, especially at larger air masses. The lightcurves show the synodic rotation period. The amplitude (peak-to-peak) that is shown is that for the Fourier model curve and not necessarily the true amplitude.

(36197) 1999 TZ91. This middle main-belt asteroid of the Chioris family was discovered on 1999 Oct 2 at Socorro by LINEAR. We made observations on 2025 April 9 to May 17. From our data we derive a synodic rotation period of 12.23275 ± 0.0004 h and an amplitude of 0.8 mag. There are no previous results for this asteroid.

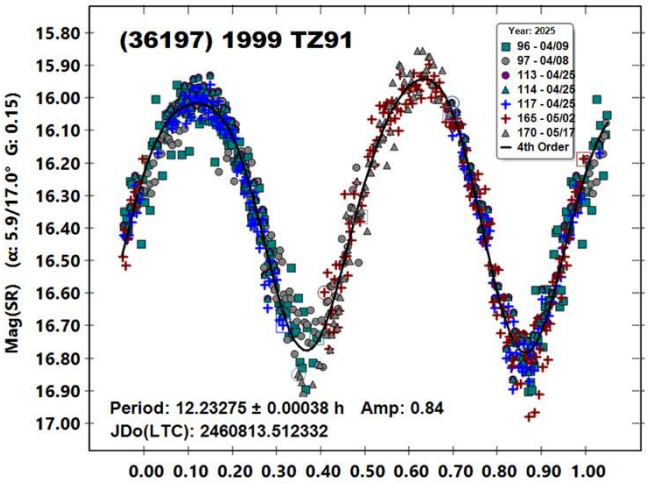

References

Harris, A.W.; Young, J.W.; Scaltriti, F.; Zappala, V. (1984). "Lightcurves and phase relations of the asteroids 82 Alkmene and 444 Gyptis." *Icarus* **57**, 251-258.

Warner, B.D.; Harris, A.W.; Pravec, P. (2009). "The Asteroid Lightcurve Database." *Icarus* **202**, 134-146. Updated 2016 Sep. *http://www.minorplanet.info/lightcurvedatabase.html*

Number	Name	mm/dd	Phase	L_{PAB}	B_{PAB}	Period(h)	P.E.	Amp	A.E.	Grp
36197	1999 TZ9	2025/4/9 - 5/17	5.9,16.7	205.2	7.6	12.23275	0.0004	.84	0.05	MB-M

Table I. Observing circumstances and results. The phase angle values are for the first and last date. L_{PAB} and B_{PAB} are the approximate phase angle bisector longitude and latitude at mid-date range (see Harris et al., 1984). Grp is the asteroid family/group (Warner et al., 2009). MB-I/O: Main-belt inner/outer; NEA: Near Earth Asteroid; MC: Mars-Crosser.

LIGHTCURVES OF ASTEROID (1363) HERBERTA IN 2023 AND 2024

Abigail G. Ramsey, Francis P. Wilkin, Eduardo Castro,
Glauk Hizmo, Dimitrios-Vasileios Zora
Union College
Department of Physics and Astronomy
807 Union St.
Schenectady, NY 12308
wilkinf@union.edu

(Received: 2025 June 16)

We present a composite lightcurve for Koronis family asteroid (1363) Herberta in 2024 based on six nights, and a lightcurve from a single night in 2023. The amplitude was 0.16 ± 0.04 mag in 2024 and 0.14 ± 0.02 mag in 2023. Our derived period of 3.0166 ± 0.0003 h is consistent with previous results.

To increase the completeness of rotational studies of Koronis family objects (Slivan et al., 2003; Slivan et al., 2023), we have revisited (1363) Herberta. This object is one of the largest members lacking a pole solution (Slivan, 2025). Previously reported synodic periods for Herberta are 3.015 ± 0.005 h (Black et al., 2016) and 3.016 ± 0.002 h (Wilkin et al., 2022).

Observations were planned using *Koronisfamily.com* (Slivan, 2003). In 2023, images were obtained at CHI-1 on April 24. In 2024, images were obtained over five nights at the Union College Observatory and one night on T72. Further information on the telescopes, cameras, and filters used is given in Table I. Observation dates are specified within the legends of the lightcurve figures. The exposure times were 240 s for CHI-1 and UCO, and 180 s for T72.

The images were processed for bias, dark, and flat field corrections, and photometry was performed using *AstroImageJ* (Collins et al., 2017). Ephemerides obtained from the JPL Horizons web app (JPL, 2025) were used to correct for light travel time.

The magnitude values for individual nights in 2024 were shifted to match the brightnesses of the corresponding local extrema because different comparison stars were used. The period was adjusted to obtain a self-consistent composite. We obtained a period of 3.0166 ± 0.0003 h for 2024 and 3.0 ± 0.2 h for 2023. Both values agree with our previously derived period, as well as other reported periods. The amplitudes in 2024 and 2023 were 0.16 ± 0.04 mag and 0.14 ± 0.02 mag, respectively.

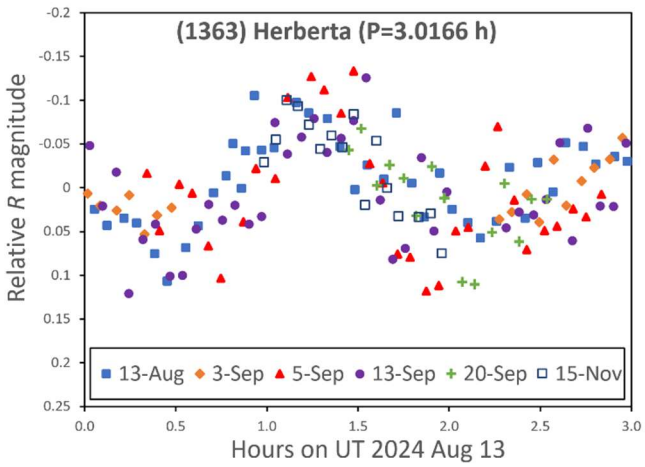

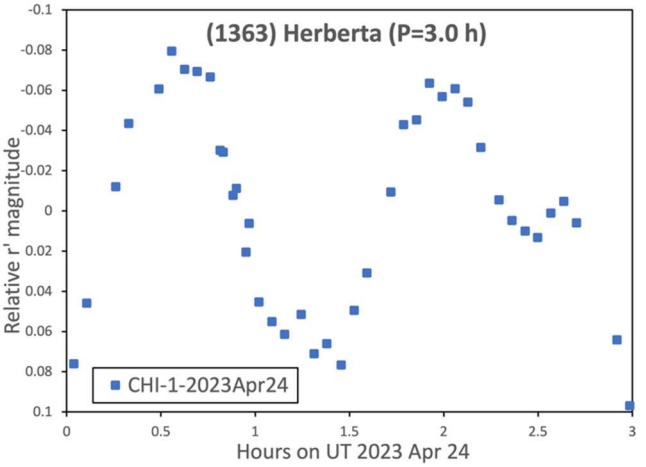

Acknowledgments

Observations at CHI-1 were funded by the Union College Faculty Research Fund. We are grateful to Dr. S.Slivan for suggestions that improved the manuscript.

References

Black, S.; Linville, D.; Michalik, D.; Wolf, M.; Ditteon, R. (2016). "Lightcurve Analysis of Asteroids Observed at the Oakley Southern Sky Observatory: 2015 December - 2016 April." *Minor Planet Bull.* **43**, 287-289.

Name	Site	Telescope	Camera	Array	Filter	FOV (′)	Scale (″/pix)
UCO	Schenectady, NY	0.50-m f/8.1	SBIG STXL-11002	2004×1336×9μm	*R*	30×20	0.93
T72	Rio Hurtado, Chile	0.51-m CDK f/6.8	FLI-ML16200	4500×3600×6μm	*R*	26.9×21.5	0.36
CHI-1	Rio Hurtado, Chile	0.61-m RC f/6.8	QHY 600M Pro	9576×6382×3.8μm	*r′*	31×20.7	0.39

Table I. Telescopes and Cameras. CDK=Corrected Dall Kirkham.

Number	Name	yyyy mm/dd	Phase	L_{PAB}	B_{PAB}	Period(h)	P.E.	Amp	A.E.
1363	Herberta	2024 08/13-11/15	*7.6,20.8	339	1	3.0166	0.0003	0.16	0.04
1363	Herberta	2023 04/24	8.4	234	0	3.0	0.2	0.14	0.02

Table II. Observing circumstances and results. The phase angle is given for the first and last dates. If preceded by an asterisk, the phase angle reached an extremum during the period. L_{PAB} and B_{PAB} are the approximate phase angle bisector longitude/latitude at mid-date range.

Collins, K.A.; Kielkopf, J.F.; Stassun, K.G.; Hessman, F.V. (2017). "AstroImageJ: Image Processing and Photometric Extraction for Ultra-precise Astronomical Light Curves." *Astron. J.* **153**, 77-89.

JPL (2025). Horizons System. *https://ssd.jpl.nasa.gov/horizons/app.html#/*

Slivan, S.M. (2003). "A Web-based tool to calculate observability of Koronis program asteroids." *Minor Planet Bull*. **30**, 71-72.

Slivan, S.M.; Binzel, R.P.; Crespo de Silva, L.D.; Kaasalainen, M.; Lyndaker, M.M.; Krčo, M. (2003). "Spin vectors in the Koronis family: Comprehensive results from two independent analyses of 213 rotation lightcurves." *Icarus* **162**, 285-307.

Slivan, S.M. (2025). *Personal communication*.

Slivan, S.M.; Hosek Jr., M.; Kurzner, M.; Sokol, A.; Maynard, S.; Payne, A.V.; Radford, A.; Springmann, A.; Binzel, R.P.; Wilkin, F.P.; Mailhot, E.A.; Midkiff, A.H.; Russell, A.; Stephens, R.D.; Gardiner, V.; Reichart, D.E.; Haislip, J.; La Cluyze, A.; Behrend, R.; Roy, R. (2023). "Spin vectors in the Koronis family: IV. Completing the sample of its largest members after 35 years of study." *Icarus* **394**, A115397.

Wilkin, F.P.; Bromberg, J.; AlMassri, Z.; Beauchaine, L.; Nguyen, M. (2022). "Lightcurve for Koronis Family Member (1363) Herberta." *Minor Planet Bull*. **49**, 253.

PHOTOMETRIC OBSERVATIONS OF ASTEROID 3760 POUTANEN

Alessandro Marchini, Riccardo Papini, Fabio Salvaggio
Astronomical Observatory, University of Siena (K54)
Via Roma 56, 53100 - Siena, ITALY
marchini@unisi.it

(Received: 2025 July 15)

Photometric observations of the inner main-belt asteroid 3760 Poutanen were conducted to verify its synodic rotation period. We found and confirmed: P = 2.956 ± 0.001 h with A = 0.18 ± 0.03 mag.

CCD photometric observations of the inner main-belt asteroid 3760 Poutanen were carried out in April-May 2025 at the Astronomical Observatory of the University of Siena (K54) to verify its synodic rotation period, determined by the same authors in 2017 (Salvaggio et al., 2017). We used a 0.30-m *f*/5.6 Maksutov-Cassegrain telescope, SBIG STL-6303E NABG CCD camera; the pixel scale was 2.30 arcsec when binned at 2×2 pixels. We used a Clear filter and 300 seconds of exposure time.

Data processing and analysis were done with *MPO Canopus* (Warner, 2018). All images were calibrated with dark and flat-field frames and the instrumental magnitudes converted to R magnitudes using solar-colored field stars from a version of the CMC-15 catalogue distributed with *MPO Canopus*. Table I shows the observing circumstances and results.

3760 Poutanen (1984 AQ) was discovered by E. Bowell at Anderson Mesa on 1984 January 8 and named in honor of Markku Poutanen, a Finnish astronomer active in the observation of asteroid lightcurves. It is an inner main-belt asteroid with a semi-major axis of 2.532 AU, eccentricity 0.184, inclination 10.493°, and an orbital period of 4.03 years. Its absolute magnitude is H = 12.59 (JPL, 2025).

Observations were conducted over three nights and collected 180 data points. The period analysis confirms a rotational period of P = 2.956 ± 0.001 h with an amplitude A = 0.18 ± 0.03 mag, in perfect agreement with that published by the same authors in 2017 and with the results published in LCDB in subsequent years (Benishek, 2018, 2021, 2022; Ďurech et al., 2020; Pál et al., 2020; Franco et al., 2021).

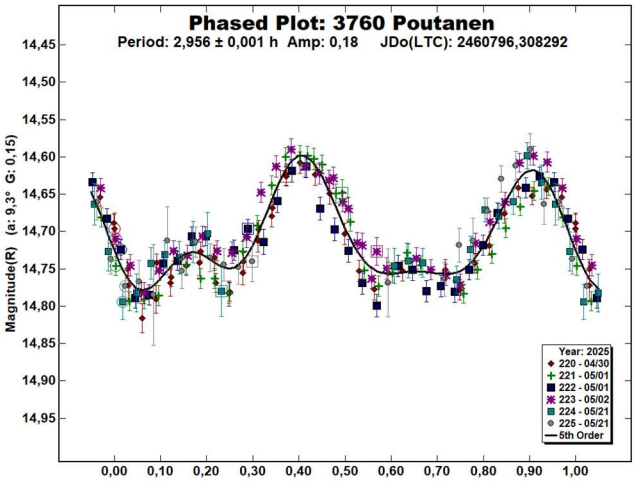

Number	Name	2025/mm/dd	Phase	L_{PAB}	B_{PAB}	Period(h)	P.E.	Amp	A.E.	Grp
3760	Poutanen	04/30-05/21	9.3,14.6	219	14	2.956	0.001	0.18	0.03	MB-I

Table I. Observing circumstances and results. The phase angle is given for the first and last date. If preceded by an asterisk, the phase angle reached an extremum during the period. LPAB and BPAB are the approximate phase angle bisector longitude/latitude at mid-date range (see Harris et al., 1984). Grp is the asteroid family/group (Warner et al., 2009).

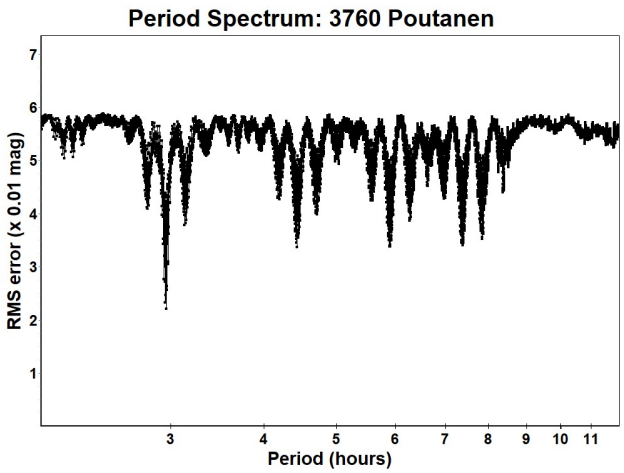

References

Benishek, V. (2018). "Lightcurve and Rotation Period Determinations for 29 Asteroids." *Minor Planet Bull.* **45**, 82-91.

Benishek, V. (2021). "Lightcurve and Rotation Period Determinations for 25 Asteroids." *Minor Planet Bull.* **48**, 280-285.

Benishek, V. (2022). "CCD Photometry of 29 Asteroids at Sopot Astronomical Observatory: 2020 July-2021 September." *Minor Planet Bull.* **49**, 38-44.

Ďurech, J.; Tonry, J.; Erasmus, N.; Denneau, L.; Heinze, A.N.; Flewelling, H.; Vančo, R. (2020). "Asteroid models reconstructed from ATLAS photometry." *A&A* **643**, A59.

Franco, L.; Marchini, A.; Iozzi, M.; Scarfi, G.; Montigiani, N.; Mannucci, M.; Aceti, P.; Banfi, M.; Mortari, F.; Galli, G.; Bacci, P.; Maestripieri, M.; Valvasori, A.; Guido, E. (2021). "Collaborative Asteroid Photometry from UAI: 2021 April-June." *Minor Planet Bull.* **48**, 372-374.

Harris, A.W.; Young, J.W.; Scaltriti, F.; Zappala, V. (1984). "Lightcurves and phase relations of the asteroids 82 Alkmene and 444 Gyptis." *Icarus* **57**, 251-258.

JPL (2025). Small Body Database Search Engine. *https://ssd.jpl.nasa.gov*

Pál, A.; Szakáts, R.; Kiss, C.; Bódi, A.; Bognár, Z.; Kalup, C.; Kiss, L.L.; Marton, G.; Molnár, L.; Plachy, E.; Sárneczky, K.; Szabó, G.M.; Szabó, R. (2020). "Solar System Objects Observed with TESS - First Data Release: Bright Main-belt and Trojan Asteroids from the Southern Survey." *ApJS* **247**, 26.

Salvaggio, F.; Marchini, A.; Papini, R. (2017). "Rotation Period Determination for 3760 Poutanen and 14309 Defoy." *Minor Planet Bull.* **44**, 354-355.

Warner, B.D.; Harris, A.W.; Pravec, P. (2009). "The Asteroid Lightcurve Database." *Icarus* **202**, 134-146. Updated 2023 Oct. 1. *https://minplanobs.org/mpinfo/php/lcdb.php*

Warner, B.D. (2018). MPO Software, MPO Canopus v10.7.7.0. Bdw Publishing. *http://bdwpublishing.com/*

LIGHTCURVE AND ROTATION PERIOD OF MAIN-BELT ASTEROID 3961 ARTHURCOX

Melissa N. Hayes-Gehrke, Carter Delavan-Hoover,
Chase Johnston, Pranav Krishnamurthy, Cyrille Longkeng,
Emily McNeal, Salem Mengistu, James Mooney,
Aleko Samblanet, Trevor Scholz, Kaleb Ward,
Hannah White, Grace Whitken
University of Maryland
Astronomy Department
1113 PSC bldg 415
College Park, MD 20742 USA
mhayesge@umd.edu

(Received: 2025 June 3)

Five nights of observations of 3961 Arthurcox between 2025 March 30 and April 23 were combined to create a phased lightcurve. After analysis of observation data with *MPO Canopus*, the rotation period was determined to be 57.01 ± 0.25 h.

Images of 3961 Arthurcox were collected using a 0.50-m f/6.8 reflector equipped with an FLI-PL6303E CCD camera. Images were collected on 2025 March 30, April 3, April 5, April 21, and April 23 using the *iTelescope* software (iTelescope, 2025) to control the image sequences with a luminance filter and exposure time of five minutes. *MPO Canopus* version 12 (Warner, 2024) was used along with the ATLAS Star Catalog (Tonry, et al., 2018) for photometry and analysis. Each image was inspected using *DS9* to ensure it was fit for photometry (SAOImage DS9, 2025). A preliminary lightcurve was generated in *MPO Canopus* using Fourier analysis.

3961 Arthurcox is a main-belt asteroid discovered on 1962 July 31 by the Goethe Link Observatory at Brooklyn, with a semi-major axis of 2.621 AU and an eccentricity of 0.154 (JPL, 2025). According to the Asteroid Lightcurve Database (LCDB; Warner, et al., 2009), 3961 Arthurcox was most recently determined to have a magnitude of H = 12.3 ± 0.1, and an albedo of A = 0.20 ± 0.03.

A third-order Fourier lightcurve was generated in *MPO Canopus* to fit a P = 57.01 ± 0.25 h with an amplitude of A = 0.57 ± 0.22 mag for a light-time corrected zero-point of JD = 2460769.2 for the starting date of the phased lightcurve. This fit results in an RMS value of 60.5 mmag. A search of the LCDB did not yield any prior rotation period determinations for the asteroid 3961 Arthurcox. The period spectrum of 3961 Arthurcox confirms that the asteroid has a long rotation period, but also shows that the period of 57.01 h is not largely preferable to similar periods. More observations of 3961 Arthurcox would help determine a more accurate period.

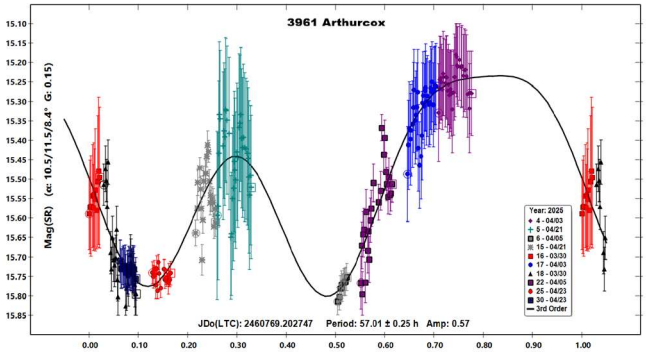

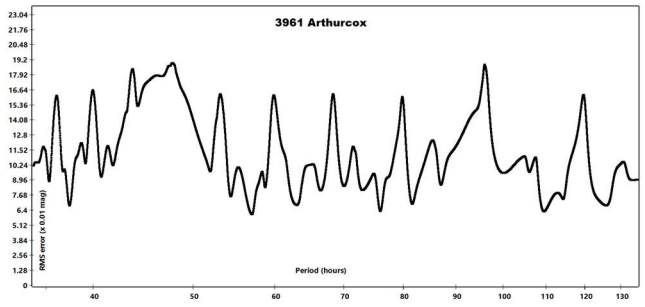

References

Harris, A.W.; Young, J.W.; Scaltriti, F.; Zappala, V. (1984). "Lightcurves and phase relations of asteroids 82 Alkmene and 444 Gyptis." *Icarus* **57**, 251-258.

iTelescope (2025). Leaders in internet astronomy since 2006. (n.d.). iTelescope. *https://www.itelescope.net*

JPL (2025). Small-Body Database Browser - JPL Solar System Dynamics website. *http://ssd.jpl.nasa.gov/sbdb.cgi*

SAOImage DS9 (2025). Chandra X-ray Science Center (CXC). *https://sites.google.com/cfa.harvard.edu/saoimageds9*

Tonry, J.L; Denneau, L.; Flewelling, H.; Heinze, A.N.; Onken, C.A.; Smartt, S.J.; Stalder, B.; Weiland, H.J.; Wolf, C. (2018). "The ATLAS All-sky Stellar Reference Catalog." *The Astrophysical Journal* **867**, 105-121.

Warner, B.D.; Harris, A.W.; Pravec, P. (2009). "The Asteroid Lightcurve Database." *Icarus* **202**, 134-146. Updated 2016 Sep. *http://www.minorplanet.info/lightcurvedatabase.html*

Warner, B.D. (2024). *MPO Canopus* version 12. Bdw Publishing. *http://www.bdwpublishing.com/*

Number	Name	yyyy mm/dd	Phase	L_{PAB}	B_{PAB}	Period(h)	P.E.	Amp	A.E.	Grp
3961	Arthurcox	2025 03/30-04/23	*11.5, 8.4	209.1	-15.9	57.01	0.25	0.57	0.22	MB

Table I. Observing circumstances and results. The phase angle is given for the first and last date. If preceded by an asterisk, the phase angle reached an extrema during the period. L_{PAB} and B_{PAB} are the approximate phase angle bisector longitude/latitude at mid-date range (see Harris et al., 1984). Grp is the asteroid family/group (Warner et al., 2009).

ROTATION PERIOD DETERMINATION FOR 3048 GUANGZHOU

Massimiliano Mannucci, Nico Montigiani
Associazione Astrofili Fiorentini
Osservatorio Astronomico Margherita Hack (A57)
Florence, ITALY
info@astrofilifiorentini.it

(Received: 2025 June 15)

CCD photometric observations of the main-belt asteroid 3048 Guangzhou were obtained over three nights from January to March 2025. Analysis of the lightcurve using *MPO Canopus* revealed a synodic rotation period of 3.81040 ± 0.00004 hours with a peak-to-peak amplitude of 0.18 magnitudes. The result is in perfect agreement with previous determinations.

3048 Guangzhou was discovered on 8 October 1964 by astronomers at the Purple Mountain Observatory near Nanjing, China, under its provisional designation 1964 TH1. It was later named after the city of Guangzhou, the capital of Guangdong province. It is a main-belt asteroid with a semi-major axis of 2.39772 AU, eccentricity e = 0.1473, inclination i = 1.939°, and an orbital period of 3.7128 years. Its absolute magnitude is H = 13.26 (JPL, 2025; MPC, 2025).

To refine its rotational characteristics a photometric campaign was conducted during the first three months of 2025 to confirm its rotation period and contribute updated lightcurve data to the scientific community. Observations were conducted from January 3rd to March 4th, 2025, at the Osservatorio Astronomico Margherita Hack (MPC code A57) using a Celestron C14 Schmidt-Cassegrain telescope equipped with an SBIG ST10-XME CCD camera and an R-band photometric filter. Standard calibration procedures were followed, including dark subtraction and flat-field correction, using the software *Astroart 6* (Warner, 2006). Differential photometry and period analysis were performed using *MPO Canopus* software (Warner, 2021).

A composite lightcurve was produced from the combined data of three nights for a total amount of 240 data points. The analysis yielded a well-defined synodic rotation period of 3.81040 ± 0.00004 hours, with a lightcurve amplitude of 0.18 ± 0.01 magnitudes. The phased lightcurve is shown in Figure 1.

This result is in excellent agreement with the period reported by Benishek (2021), based on observations from the Sopot Astronomical Observatory, as well as with the values listed in the Lightcurve Database (LCDB; Warner et al., 2009).

Acknowledgements

The authors thank the MPC and the Lightcurve Database (LCDB) team for providing access to orbital and photometric data. *MPO Canopus* was used for the photometric analysis.

References

Benishek, V. (2021). "Photometry of 12 Asteroids from Sopot Astronomical Observatory: 2020 October-December." *Minor Planet Bulletin* **48(2)**, 117-119.

Harris, A.W.; Young, J.W.; Scaltriti, F.; Zappala, V. (1984). "Lightcurves and phase relations of the asteroids 82 Alkmene and 444 Gyptis." *Icarus* **57**, 251-258.

JPL (2025). Small-Body Database Browser. *http://ssd.jpl.nasa.gov/sbdb.cgi#top*

MPC (2025). MPC Database. *https://minorplanetcenter.net/db_search/*

Warner, B.D. (2006). A Practical Guide to Lightcurve Photomretry and Analysis (2nd edition). Springer, New York.

Warner, B.D.; Harris, A.W.; Pravec, P. (2009). "The Asteroid Lightcurve Database." *Icarus* **202**, 134-146. *https://www.minorplanet.info/php/lcdb.php*

Warner, B.D. (2021). MPO Software, MPO Canopus v10.8.5.0. Bdw Publishing. *http://minorplanetobserver.com*

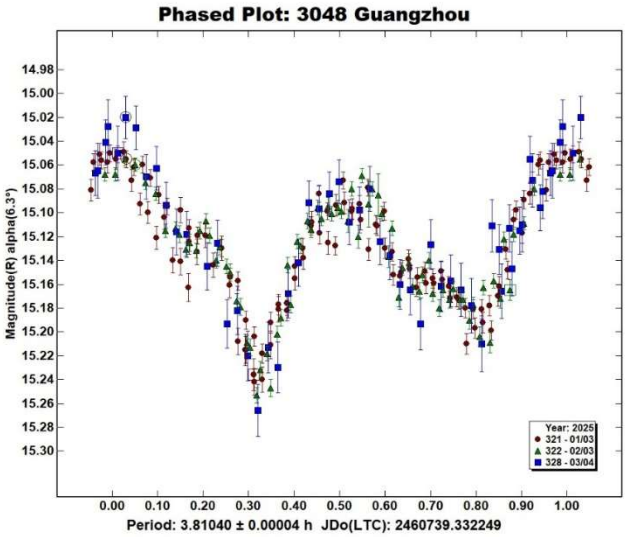

Figure 1: Phased lightcurve of 3048 Guangzhou.

Number	Name	yyyy mm/dd	Phase	L_{PAB}	B_{PAB}	Period(h)	P.E.	Amp	A.E.	Grp
3048	Guangzhou	2025 01/03-03/04	6.3,23.7	115.1	-2.7	3.81040	0.00004	0.18	0.01	MB

Table I. Observing circumstances and results. The phase angle is given for the first and last date. If preceded by an asterisk, the phase angle reached an extrema during the period. L_{PAB} and B_{PAB} are the approximate phase angle bisector longitude/latitude at mid-date range (see Harris et al., 1984). Grp is the asteroid family/group (Warner et al., 2009).

LIGHTCURVE AND ROTATION PERIOD OF 4163 SAAREMAA

Melissa N. Hayes-Gehrke, Kathryn De Leon, Nalani Deredita, Ebony Dobson, Nathan Frenkel, Gautham Hari, Sean Hughes, Reni Kaza, Vanessa Li, William Schmitz, Dereck Shirland Jr., Hannah Sitther, Marc Wagger
University of Maryland
Astronomy Department
1113 PSC bldg 415
College Park, MD 20742 USA
mhayesge@umd.edu

Stephen M. Brincat
Flarestar Observatory (MPC: 171)
F1.5 George Tayar Street
San Gwann SGN 3160, MALTA

Marek Buček
Luckystar Observatory (MPC: M55)
Dr. Lučanského 547, Važec, 032 61, SLOVAKIA

Charles Galdies
Znith Observatory
Armonie, E. Bradford Street
Naxxar NXR 2217, MALTA

(Received: 2025 June 3)

We report photometric observations for main-belt asteroid 4163 Saaremaa. The observations were performed during March and April 2025, from the T21 Telescope at Beryl Junction, Utah; Flarestar Observatory in Malta; Luckystar Observatory in Slovakia; and Znith Observatory in Malta. Lightcurve analysis indicates a rotation period of 26.315 ± 0.025 h and amplitude of 0.56 ± 0.07 mag. A rotation period of 26.3268 ± 0.0002 h was previously observed by Ďurech, et al. (2019) using Gaia spacecraft photometry, but no lightcurve was published.

4163 Saaremaa is a main-belt asteroid discovered on 1941 April 19 in Turku, Finland by L. Oterma. It has a diameter of 19.930 km, with an absolute magnitude of 11.49, and a geometric albedo of 0.086. It has an orbital eccentricity of 0.044 and an orbital semi-major axis of 3.02 AU (JPL, 2025).

The main-belt asteroid was observed between 2025 March 19 and 2025 April 23. Four independent teams observed in parallel during the timeframe. Table I provides observation details for 4163 Saaremaa. A clear filter was used for all images, and exposure times varied between 180 s (Luckystar), 240 s (Flarestar), and 300 s (T21 and Znith). Multiple acquisition softwares were used to capture images: *itelescope.net* (USA; 2002), *Sequence Generator Pro* (Malta; 2022), and *N.I.N.A.* (Slovakia; 2023). *MPO Canopus* software version 12 (Warner, 2021) was used to analyze the images, perform differential aperture photometry, and generate lightcurves.

The analysis of the data shows a period of 26.315 ± 0.025 h with an approximate amplitude of 0.56 ± 0.07 mag. The phased lightcurve shows two maxima and two minima, showcasing data across various nights and geographical locations that covered the majority of the asteroid's rotation period. These new observations confirm the previous result of 26.3268 ± 0.0002 h (Ďurech, et al., 2019). However, because Ďurech, et al., utilized mass survey data from the Gaia spacecraft, there is no previously published lightcurve. The publication of the first lightcurve provides novel data on the shape of 4163 Saaremaa. Specifically, the lightcurve has a substantial amplitude, meaning the asteroid is elongated.

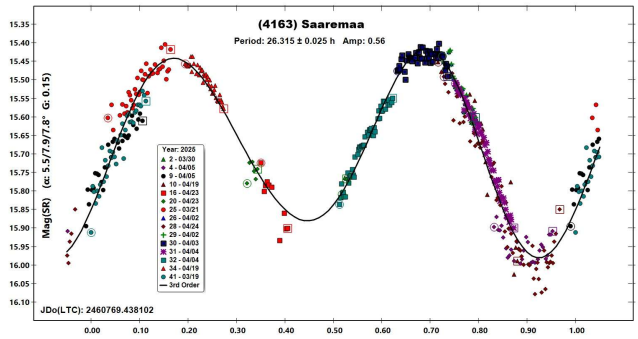

References

Automated night Sky Imaging. Sequence Generator Pro. (2022). *https://www.sequencegeneratorpro.com/*

Ďurech, J.; Hanuš, J.; Vančo, R. (2019). "Inversion of asteroid photometry from Gaia DR2 and the Lowell Observatory photometric database." *Astronomy & Astrophysics* **631**, 1-4.

Harris, A.W.; Young, J.W.; Scaltriti, F.; Zappala, V. (1984). "Lightcurves and phase relation of the asteroids 82 Alkeme and 444 Gyptis." *Icarus* **57**, 251-258.

Observatory	Telescope	Camera	Dates Observed 2025 (mm/dd)
Utah Desert Remote Obs. (T21) USA	0.43-m CDK	FLI PL6303E	03/29, 04/04, 04/18, 04/22
Flarestar Obs. Malta, Brincat	0.25-m SCT	Moravian G2-1600	03/21, 04/02, 04/22, 04/24
Luckystar Obs. Slovakia, Bucek	0.25-m SCT	Atik 460EX	04/02, 04/03, 04/04, 04/16, 04/19
Znith Astronomy Obs. Malta, Galdies	0.20-m SCT	Moravian G2-1600	03/19

Table I. Instrumentation and observation runs (2025). SCT: Schmidt-Cassegrain Telescope. CDK: Corrected Dall-Kirkham Telescope.

Number	Name	yyyy mm/dd	Phase	L_{PAB}	B_{PAB}	Period(h)	P.E.	Amp	A.E.	Grp
4163	Saaremaa	2025 03/19-04/23	7.5, 8.7	194.6	12.7	26.315	0.025	0.56	0.07	MB-M

Table II. Observing circumstances and results. The phase angle is given for the first and last date. If preceded by an asterisk, the phase angle reached an extrema during the period. L_{PAB} and B_{PAB} are the approximate phase angle bisector longitude/latitude at mid-date range (see Harris et al., 1984). Grp is the asteroid family/group (Warner et al., 2009).

iTelescope (2002). "Telescope 21." *https://www.itelescope.net/*

JPL (2025). Small-Body Database Browser. *https://ssd.jpl.nasa.gov/tools/sbdb_lookup.html#/*

N.I.N.A. - Berg, S. (2023). "Nightime Imaging 'N' Astronomy (NINA) website." *https://nighttime-imaginge.eu/*

Warner, B.D.; Harris, A.W.; Pravec, P. (2009). "The Asteroid Lightcurve Database." *Icarus* **202**, 134-146. Updated 2016 Sep. *http://www.minorplanet.info/lightcurvedatabase.html*

Warner, B.D. (2021). MPO Software, MPO Canopus v12.0.6.9. Bdw Publishing. *http://minorplanetobserver.com*

A LIGHTCURVE ANALYSIS OF MAIN BELT ASTEROID 5295 MASAYO

Melissa N. Hayes-Gehrke, Carmen Benitez, Jack Bibbo, Adith Chandrasekaran, Stina Drill, Brayson Fleegle, Ryan Kaplan, Hana Lerdboon, Jackson Nagy, Sriya Peddinti, Aadi Trivedi, Yiwen Zhang
University of Maryland
Astronomy Department
1113 PSC bldg 415
College Park, MD 20742 USA
mhayesge@umd.edu

Stephen M. Brincat
Flarestar Observatory (MPC: 171)
FL5 George Tayar Street
San Gwann SGN 3160, MALTA

Charles Galdies
Znith Observatory
Armonie, E. Bradford Street
Naxxar NXR 2217, MALTA

Marek Buček
Luckystar Observatory (MPC: M55)
Dr. Lučanského 547, Važec, 032 61, SLOVAKIA

(Received: 2025 June 3)

Using *MPO Canopus* to conduct lightcurve analysis of eight nights of observation from 2025 March 30 to 2025 April 23, we developed a periodic lightcurve and determined the preliminary rotation period of asteroid 5295 Masayo as 4.13 ± 0.01 h.

5295 Masayo is a main-belt asteroid that was discovered by Mizuno and Furata on 1991 February 5 in Kani, Japan. This asteroid has an absolute magnitude of 12.00, a diameter of 21.045 km, and a geometric albedo of 0.100. As well, it has a semi-major axis of 3.146 AU, an eccentricity of 0.0921, an inclination of 6.305°, and an orbital period of 5.580 yr (JPL, 2023).

Our team at the University of Maryland observed asteroid 5295 Masayo on five nights of observation between 2025 March 30 and 2025 April 23 using Telescope 21 from the Utah Desert Remote Observatory at Great Basin Desert, Beryl Junction, Utah, USA (MPC: U94). The telescope is equipped with a 0.43-m f/6.8 reflector, an FLI-PL6303E CCD camera with an array of 3072 × 2048 pixels, and an f/4.5 focal reducer. All images were taken using the luminance filter, an exposure time of 300 s, binned 1 × 1 pixels, and in sets of five (iTelescope Support Document).

Our team collaborated with Stephen Brincat and Charles Galdies from Malta, as well as Marek Buček from Slovakia. Brincat observed from Flarestar Observatory, San Gwann, Malta on 2025 April 4, using CCD G2-1600 with 0.20-m SCT, C filter, and an exposure of 240 s. Galdies observed from nith Observatory, Naxxar, Malta on 2025 March 21, using CCD G2-1600 with 0.20-m SCT, C filter, and exposure time of 360 s. Buček observed from Luckystar Observatory, Važec, Slovakia on 2025 April 2, using a CCD Atik-460exm with a Meade ACF 254, C filter, and an exposure time of 180 s.

After capturing the images, *SAOImage DS9* (SAO, 2023) was used to discard any images deemed unsuitable for our analysis. As a result, our final dataset consisted of 250 images, including the collaborators' data. The data were then processed through the software *MPO Canopus* (Warner, 2025), which identified comparison stars and provided the differential magnitude of the asteroid via aperture photometry. The rotation period was determined by conducting a Fourier analysis on all of our data an and adjusting zero points across all nights of observation. Towards the end of our analysis, we excluded 3 data points from our plot due to large deviations from the rest of the dataset.

Our analysis resulted in a typical double-peaked lightcurve. No previous data on this asteroid, regarding the rotation period, were found in the *Asteroid Lightcurve Database* (Warner et al., 2009). Based on our observations, we have determined a rotation period of 4.13 ± 0.01 h.

Number	Name	yyyy mm/dd	Phase	L_{PAB}	B_{PAB}	Period(h)	P.E.	Amp	A.E.	Grp
5295	Masayo	2025 03/21-04/22	17.9,17.0	270.6	0.3	4.13	0.01	0.38	0.04	HYG

Table I. Observing circumstances and results. The phase angle is given for the first and last date. If preceded by an asterisk, the phase angle reached an extrema during the period. L_{PAB} and B_{PAB} are the approximate phase angle bisector longitude/latitude at mid-date range (see Harris et al., 1984). Grp is the asteroid family/group (Warner et al., 2009).

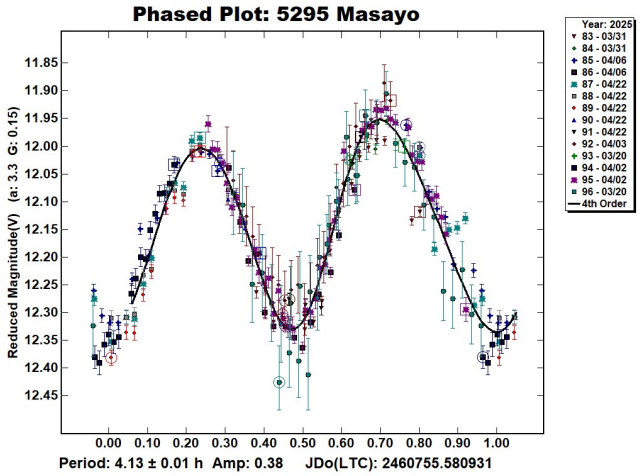

Acknowledgements

This research was conducted as part of an undergraduate astronomy course taught by Dr. Melissa Hayes-Gehrke at the University of Maryland. We thank Dr. Hayes-Gehrke for her instruction throughout the project. Her knowledge of observational astronomy was vital to our success. The chance to engage in hands-on research in this course enhanced our understanding of asteroid lightcurve analysis and the broader scientific process involved in minor planet studies.We are thankful to iTelescope.net for providing access to their network of remotely operated telescopes, which let us obtain high-quality data across multiple nights under optimal observing conditions. We are also thankful for the use of the *MPO Canopus* software, which was key in reducing our data and creating lightcurves for rotational analysis.

References

Harris, A.W.; Young, J.W.; Scaltriti, F.; Zappala, V. (1984). "Lightcurves and phase relations of the asteroids 82 Alkmene and 444 Gyptis." *Icarus* **57**, 251-258.

iTelescope - Leaders in Internet Astronomy since 2006. (n.d.). *https://itelescope.net/*

JPL (2023). Small-Body Database Lookup. *https://ssd.jpl.nasa.gov/tools/sbdb_lookup.html#/*

Smithsonian Astrophysics Observatory. (2023). "SAOImage DS9: A utility for displaying astronomical images in the X11 window environment." *Astrophysics Source Code Library*, ascl: 0003.002

Telescope 21 (n.d.). Support. *https://support.itelescope.net/support/solutions/articles/231906-telescope-21*

Warner, B.D.; Harris, A.W.; Pravec, P. (2009). "The Asteroid Lightcurve Database." *Icarus* **202**, 134-146. Updated 2016 Sep. *http://www.minorplanet.info/lightcurvedatabase.html*

Warner, B.D. (2025). MPO Software, *MPO Canopus* version 12.0.6.6. Bdw Publishing. *http://www.bdwpublishing.com/*

DISCOVERY OF THE BINARITY OF THE MAIN-BELT ASTEROID 8297 GERARDFAURE

Gerard Faure
Vaison la Romaine
FRANCE
gpmfaure@club-internet.fr

Yves Jongen
1348 Louvain la Neuve
BELGIUM

Petr Pravec
Academy of Sciences of Czech Republic
CZECH REPUBLIC

Anaël Wünsche
Observatoire des Baronnies Provençales
FRANCE

(Received: 2025 June 22 Revised: 2025 August 5)

We report the discovery of the binarity of the asteroid (8297) Gerardfaure during its near-perihelic opposition at the end of 2025 January. From 2025 January 27 to February 8, 21 imaging sessions were carried out, 10 of which made it possible to discover that 8297 has a synodic rotation period of 3.0459 ± 0.0003 h, with a lightcurve amplitude of 0.14 mag. In addition, it is accompanied by a satellite with an orbital period of 18.82 ± 0.01 h. Mutual eclipse/occultation events with a depth of 0.13 magnitudes indicate a lower limit on the secondary to primary mean diameter ratio of 0.36.

Minor planet 8297 Gerardfaure (*H* =14.8) was discovered by Belgian Professional Astronomer Eric W. Elst on 1993 August 18 at the Caussols Observatory in France. It belongs to the Flora asteroid family (rocky S-type and relatively high albedo) and is located in the inner zone of the asteroid main-belt. With orbital elements of a = 2.2373 au, e = 0.0613, and i = 3.590°, it revolves around the Sun every 3.35 years. On 2025 January 27, it reached opposition at 1.168 au from Earth. A few days later, February 6, it reached perihelion at r = 2.100 au.

Neither the Asteroid Lightcurve Data Exchange Format (ALCDEF. 2025) database nor R. Johnston's "Asteroids with Satellites" list (Johnson, 2025) mentioned a reliable lightcurve or known binarity for 8297 prior to our work. No listing was found in the Asteroid Lightcurve Database (Warner et al., 2009) for a period or evidence of being a binary (Warner et al., 2021).

After an unsuccessful attempt to obtain a good lightcurve for the asteroid at its 2022 opposition, the main author proposed to Yves Jongen (Jongen, 2021) to image it during the 2025 opposition with his two Planet Wave CDK 420 mm telescopes, on Planet Wave L500 Direct drive mounts and equipped with Moravian CCD G4-16000 CCD cameras. One was located in Chile on the Deep Sky Chile site and the other in France in Rasteau (Provence). Anaël Wünsche from the Observatoire des Baronnies de la Drôme Provençale (France) also joined the project to image the asteroid with the OBP's T 820 mm.

Number	Name	yyyy/mm/dd	Phase	L_{PAB}	B_{PAB}	Period(h)	P.E	Amp	A.E.
8297	Gerardfaure	2025/01/27-2025/02/06	*1.95,6.33	127.2	-3.1	3.0459	0.0003	0.14	0.04
						18.82	0.01	0.13	0.06

Table I. Observing circumstances and results. The first line gives the results for the primary of a binary system. The second line gives the orbital period of the satellite and the maximum attenuation. The phase angle is given for the first and last date. If preceded by an asterisk, the phase angle reached an extrema during the period. L_{PAB} and B_{PAB} are the approximate phase angle bisector longitude/latitude at mid-date range (see Harris et al., 1984).

Although the imaging was performed during a period of perihelic opposition, the *V* magnitude, still weak, decreased from *V* = 16.9 to 17.2 during the observations. Monitoring was done using unfiltered C images, all calibrated using standard procedures (bias, darks, and flats).

Yves Jongen imaged the asteroid every day of the period, which was decisive for the subsequent identification of the characteristics of the lightcurves of the target. A total of 21 imaging sessions were performed, but eight of them were not retained since they did not achieve sufficient SNR due to the low magnitude of 8297 or poor observing conditions. The average SNR was 46 (range 52 to 37). Only sessions with an average SNR greater than 35 were retained.

The analysis of the unfiltered images in *r*-band was then carried out by Gerard Faure with *MPO Canopus* (Warner, 2020) and its MPOSC3 catalog, including in particular the CMC 14. All images were "light-time corrected." All sessions were adjusted to a common zero-point using the CompAdjust feature in *MPO Canopus*, based on methods described in Warner (2016).

Despite multiple tests using periods from 2 to 1000 h and up to 15 Fourier orders, the simple lightcurves of 8297 showed a fairly chaotic and non-repetitive appearance, again as in 2022, with no possibility of obtaining a bimodal or plausible curve.

The most frequently recurring curve indicated a period of 9.460 hours, but with an RMS still too high by more than 5 and numerous peaks and minimums at intervals of about 1.5 hours.

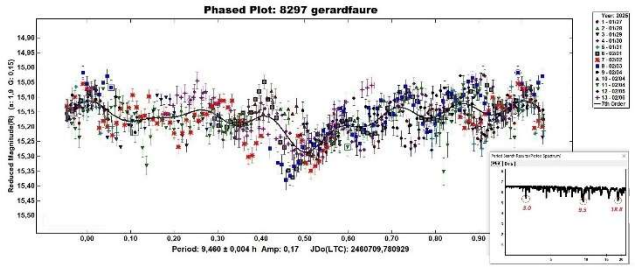

Sometimes, a period of 18.84 hours appeared, depending on the orders used, but always with a multiplicity of peaks and minimums, without a low RMS. This period was almost double the 9.46h period most often obtained from *MPO Canopus*.

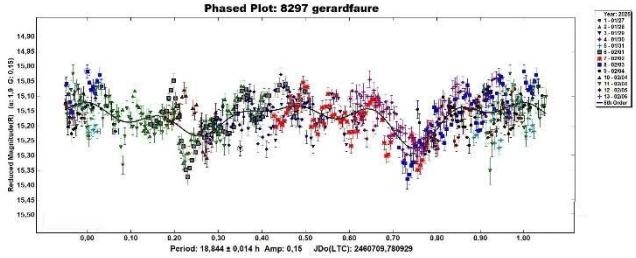

It was decided to look at the possibility that the asteroid was binary by following a tutorial for the *MPO Canopus* dual-period search.

After subtracting the lightcurve for the presumed primary body, which had period of 3.0464 ± 0.0003 h and amplitude of 0.15 mag (RMS fit of 0.036 mag), we found two probable secondary periods of 9.4 h and 18.9 h.

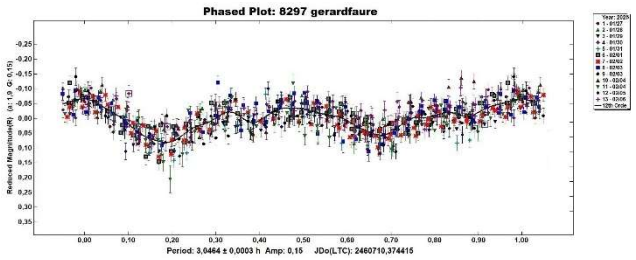

Although the 9.4 h period came up often in simple period calculations, it did not seem suitable for the orbital period of a satellite, having only a single apparent minimum that could represent an eclipse or partial occultation.

On the other hand, the period curve of 18.8348 ± 0.0095 h clearly showed two minima, one of which was weaker and an RMS of 3.687. This made the lightcurve a good candidate to represent the curve of a secondary body.

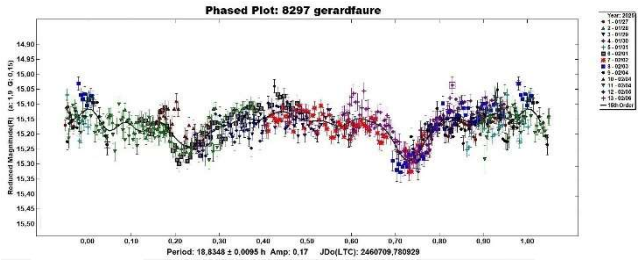

Following these results, we contacted Petr Pravec of the Czech Academy of Sciences, an expert in binary asteroids, to ask his opinion on the curves obtained for the main and secondary bodies and, if in agreement, to kindly provide additional results concerning the rotation period of the secondary and the minimum diameter ratio between the main and the secondary. We built our analysis on the fundamentals and methods of Pravec (2005), Pravec and Harris (2007), and Pravec et al. (2012a; 2012b).He agreed to verify our data and confirmed that 8297 Gerardfaure is indeed a binary asteroid. He obtained a satisfactory and unique solution, with an RMS of 0.026 mag, and further refined our lightcurves, removing some inappropriate measurements. This made it possible to obtain the following results for the final lightcurves only with 10 sessions.

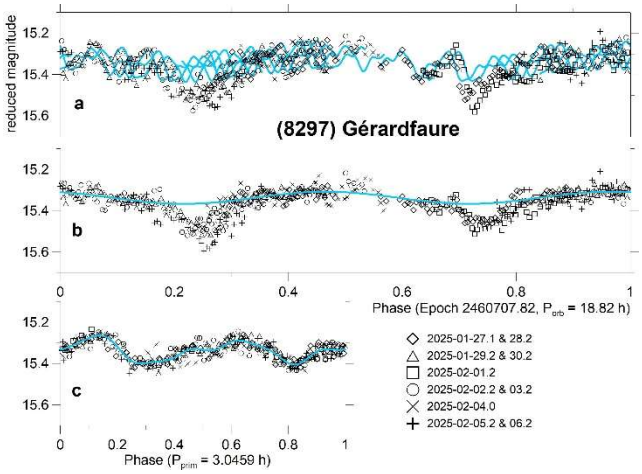

The International Astronomical Union announced the binary of (8297) Gerardfaure by CBET No. 5536 of 2025 April 4.

- Main body: rotation period of 3.0459 h ± 0.0003 h with a light amplitude of 0.14 magnitude.
- Secondary body: revolution period of 18.82 h +/-0.01h and synchronous rotation period with the secondary lightcurve amplitude (in the combined light from the primary and the secondary) of 0.06 magnitude.

Finally, following estimates of the binary parameters were obtained with the method of Pravec and Harris (2007):

- Mean diameter of the main body = 3.0 ± 0.6 km (estimated from the asteroid's *H* and assuming the geometric albedo p_V = 0.20 ± 0.05 that is the mean albedo for S-type asteroids (see Pravec et al., 2012).
- Lower limit on the secondary body's diameter = 1.1 ± 0.2 km.
- Orbital semi-major axis = 6 ± 2 km (assuming the primary's bulk density 2.0 g/cm^3 with uncertainty by a factor of 1.5).
- Separation Radius As/Rp = 4.2 ± 0.6°.

References

ALCDEF (2025). Asteroid Lightcurve Data Exchange Format website. Accessed on March 30, 2025. *https://alcdef.org/*

Baronnies Provençales Observatory, France. *https://www.obs-bp.net/*

Harris, A.W.; Young, J.W.; Scaltriti, F.; Zappala, V. (1984). "Lightcurves and phase relations of asteroids 82 Alkmene and 444 Gyptis." *Icarus* **57**, 251-258.

Johnston, R. (2025). Asteroids with satellites website. Accessed on March 30, 2025. *https://www.johnstonsarchive.net/astro/asteroidmoons.html*

Jongen, Y. (2021). "Les collaborations pro-am dans les mesures de transit d'exoplanètes - RCE 2021." *https://media.afastronomie.fr/RCE/PresentationsRCE2020/S2-19-JONGEN.pdf*

Minor Planet Center (2025). MPCORB.dat. Accessed on February 25, 2025. *https://www.minorplanetcenter.net/iau/MPCORB.html*

Pravec, P. (2005). "Photometric Survey for Asynchronous Binary Asteroids." Proceedings of the Symposium on Telescope Science The 24th Annual Conference of the Society for Astronomical Science, pp 61-67.

Pravec, P.; Harris, A.W. (2007). "Binary asteroid population: 1. Angular momentum content." *Icarus* **190**, 250-259.

Pravec, P. Scheirich, P.; Vokrouhlický, D.; Harris, A.W.; Kušnirák, P. and 37 collegues (2012a). "Binary Asteroid population - Anisotropic distribution of orbit poles of small, inner main-belt binaries." *Icarus* **218**, 125-143.

Pravec, P.; Harris, A.W.; Kušnirak P.; Galad, A.; Hornoch, K. (2012b). "Absolute magnitudes of asteroids and a revision of asteroid albedo estimates from WISE thermal observations." *Icarus* **221**, 365-387.

Warner, B.D. (2016). A Practical Guide to Lightcurve Photometry and Analysis. Second Edition.

Warner, B.D. (2020). MPO Canopus (version 10.8.6.12). *https://minplanobs.org/BdwPub/php/displayhome.php*

Warner, B.D.; Harris, A.W.; Pravec, P. (2009). "The Asteroid Lightcurve Database." *Icarus* **202**, 134-146. Updated 2023 June. *http://www.minorplanet.info/lightcurvedatabase.html*

Warner, B.D.; Stephens R.D.; Harris A.W. (2021). "On Confirmed and Suspected Binary Asteroids Observed at the Center for Solar System Studies." *Minor Planet Bulletin* **48**, 40-49.

LIGHTCURVE AND ROTATION PERIOD ANALYSIS FOR 19774 DIAMONDBACK

Melissa N. Hayes-Gehrke, Justin Kerns, Collin Sullivan,
Ethan Lau, Chayanika Sinha, Benjamin Weintraub,
Jonathan Hale, Chase Sunter, Rishi Anusuri, Brian Zajac,
Jimmy Yang, CC Lizas, Zahra Schenck
University of Maryland
Astronomy Department
1113 PSC bldg 415
College Park, MD 20742 USA
mhayesge@umd.edu

(Received: 2025 June 3)

An approximate rotation period and lightcurve are presented for 19774 Diamondback (preliminary designation 2000 OS51). We found a tentative period of 51.17± 0.53 h with an amplitude of 0.63 ± 0.11 mag.

We report photometric observations for 19774 Diamondback (preliminary designation 2000 OS51) from four nights on 2025 April 4, 18, 28, and 29. Observations were made remotely from the Siding Spring Observatory (Coonabarabran, Australia, MPC code Q62) courtesy of iTelescope (2025). The first half (2025 Apr 4 and 18) of observations were made using a 0.51-m f/4 Corrected Call-Kirkham telescope and FLI-PL6303E CCD camera with a binning of 1 × 1. The remaining half (2025 Apr 28 and 29) were made using a 0.43-m f/6.8 Corrected Dall-Kirkham telescope with a ZQO ASI 6200MM Pro CMOS using a binning of 2 × 2. Both telescopes used a luminance filter with 300-s exposure time to take images.

Ephemerides and finder charts were made using the Lowell Observatory Minor Planet Services (Lowell Observatory, 2025). *MPO Canopus* V12 was used for period analysis (Warner, 2025).

19774 Diamondback (2000 OS51) is a middle main-belt asteroid, discovered by Lincoln Near-Earth Asteroid Research (LINEAR) at Socorro on 2000 July 30 (Small-Body Database Lookup, 2025). The asteroid has an estimated diameter between 7.631 and 17.062 km (Mou and Webster, 2021). Its orbit has an inclination of 11.07°, semi-major axis of 2.653 AU, with an eccentricity of 0.2406 (Small-Body Database Lookup, 2025).

Through our photometric analysis for this asteroid, we discovered a probable rotation period of 51.17 ± 0.53 h with an amplitude of 0.63 ± 0.11 mag.

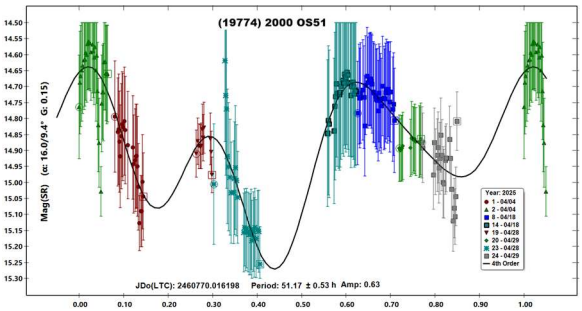

We note observation irregularities that might be sources of noise and data scatter. There was interference from cloud clover on April 4th, possibly explaining the variation in magnitude. April 18th experienced some light pollution from the Moon. April 28th was largely uneventful. April 29th experienced some cloudy weather.

Checking against the Asteroid Lightcurve Database shows one paper associated with (19774) 2000 OS51 but no previously published rotation period estimates (Warner et al., 2009). However, we were able to reference two other past observations of (19774) 2000 OS51 via an internet search, but only one of those contained a lightcurve analysis. The other observations were conducted by Pan-STARRS (Veres et al., 2015) and Gaia (Colazo et al., 2021), which imaged thousands of objects, including our asteroid, but did not find a rotation period. A study by Moravec et al. (2021) observed (19774) 2000 OS51 but did not report a period. This may suggest that the asteroid is a slow rotator. Through additional research, we discovered the PhD thesis of a Lehigh University astronomer, P.M. Christodoulou (2023), whose analysis based on KELT imaging created a lightcurve for which he determined a 25.41-h rotation period.

Our RMS plot does not show a singular clear fit for a period, suggesting that many of these periods are as likely as the period we found. We selected this period after surveying many of the good fits by considering the presence of data along the Fourier curve, along with the presence of two noticeable peaks. The slight downward trend in the RMS plot is due to the data becoming less concentrated in the graph, leading to many of the longer periods having less-supported fits. With more data, a longer period may be able to be supported.

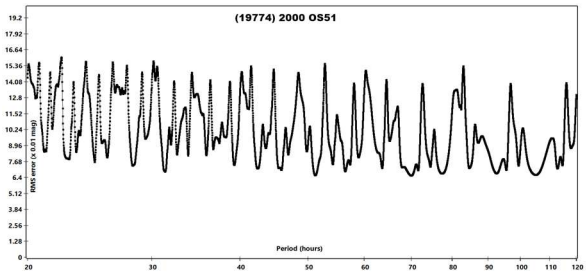

Number	Name	yyyy mm/dd	Phase	L_{PAB}	B_{PAB}	Period(h)	P.E.	Amp	A.E.	Grp
19774	Diamondback	2025 04/04-04/29	16.2, 9.5	217.6	-14.8	51.17	0.53	0.63	0.11	MB-M

Table I. Observing circumstances and results for (19774) 2000 OS51 permanently named as 19774 Diamondback. The phase angle is given for the first and last date. If preceded by an asterisk, the phase angle reached an extrema during the period. L_{PAB} and B_{PAB} are the approximate phase angle bisector longitude/latitude at mid-date range (see Harris et al., 1984). Grp is the asteroid family/group (Warner et al., 2009).

Our data disagree with the result of 25.41 h by Christodoulou. We include a plot of our data phased to a period of 25.41 h. There is a clear distinction between the two-phase plots for the nights of observation after the first peak in our data. Additionally, there is also only one distinct peak and trough in the lightcurve, which is evidence against the shorter period. The 25.41-h period is roughly half of the period we found in our observations, so we suggest that it is potentially a half-period for the asteroid.

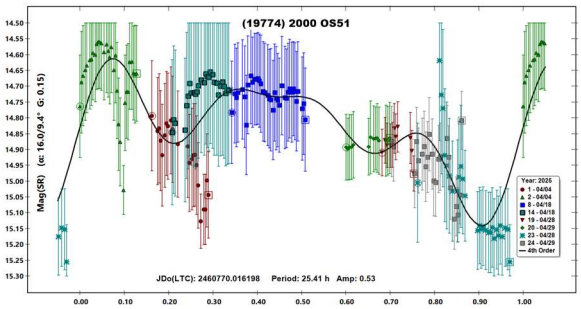

Acknowledgements

We would like to thank Brian Warner for taking time to debug an issue with *MPO Canopus* and providing a patch to the software. This allowed us to complete our data analysis in line with our deadlines.

References

Christodoulou, P.M. (2023). "Rotation Periods of Slowly Rotating Asteroids with KELT Photometry." [Doctoral thesis, Lehigh University]. Lehigh Preserve Institutional Repository. *https://preserve.lehigh.edu/_flysystem/fedora/2023-11/preserve30919.pdf*

Colazo, M.; Duffard, R.; Weidmann, W. (2021). "The determination of asteroid H and G phase function parameters using Gaia DR2." *Monthly Notices of the Royal Astronomy Society* **504**, 761-768.

Harris, A.W.; Young, J.W.; Scaltriti, F.; Zappala, V. (1984). "Lightcurves and phase relations of the asteroids 82 Alkmene and 444 Gyptis." *Icarus* **57**, 251-258.

iTelescope (2025). iTelescope website. *https://www.itelescope.net/*

Lowell Observatory (2025). Lowell Minor Planet Services. *https://asteroid.lowell.edu/*

Moravec, P.; Cochren, J.; Gerhartd, M.; Harris, A.; Karnemaat, R.; Melton, E.; Stolze, K.; West, J.; Ditteon, R. (2021). "Asteroid Lightcurve Analysis at the Oakley Southern Sky Observatory: 2012 January - April." *Minor Planet Bulletin* **39**, 213-216.

Mou, J.; Webster, I. (2021). Space Reference. *https://www.spacereference.org/asteroid/19774-2000-os51*

NASA, (2025). Small Body Database Lookup. *https://ssd.jpl.nasa.gov/tools/sbdb_lookup.html#/*

Veres, P.; Jedicke, R.; Fitzsimmons, A.; Denneau, L.; Granvik, M.; Bolin, B.; Chastel, S.; Waiscoat, R.J.; Burgett, W.S.; Chambers, K.C.; Flewelling, H.; Kaiser, N.; Magnier, E.A.; Morgan, J.S.; and 2 colleagues (2015). "Absolute magnitudes and slope parameters for 250,000 asteroids observed by Pan-STARRS PS1 - Preliminary results." *Icarus* **261**, 34-47.

Warner, B.D.; Harris, A.W.; Pravec, P. (2009). "The Asteroid Lightcurve Database." *Icarus* **202**, 134-146. Updated 2023 Oct. *http://www.minorplanet.info/lighcurvedatabase.html*

Warner, B.D. (2025). MPO Canopus V12. *https://minplanobs.org/BdsPub/php/displayhome.php*

LIGHTCURVE AND ROTATION PERIOD FOR 3507 VILAS AND 4185 PHYSTECH

Michael Fauerbach
Florida Gulf Coast University
and SARA Observatories
10501 FGCU Blvd.
Ft. Myers, FL 33965-6565 USA
mfauerba@fgcu.edu

(Received: 2025 July 6)

Photometric observations of two main-belt asteroids were obtained to verify their synodic rotation periods. We found: 3507 Vilas P = 4.755 ± 0.001 h with A = 0.29 ± 0.02 mag; 4185 Phystech P = 4.668 ± 0.001 h with A = 0.47 ± 0.04 mag.

Photometric observations of asteroids 3507 Vilas and 4185 Phystech were obtained with the 0.6m telescope of the Southeastern Association for Research in Astronomy (SARA) consortium at Cerro Tololo Inter-American Observatory. The telescope is coupled with an Andor iKon-L series CCD, and a SDSS R filter was used for all images. A detailed description of the instrumentation and setup can be found in the paper by Keel et al. (2017). Images were calibrated with dark and flat frames and converted to standard magnitudes using solar colored field stars from the ATLAS catalogue, distributed with *MPO Canopus* (Warner, 2021). All the new data for these asteroids can be found in the Asteroid Lightcurve Data Exchange Format (ALCDEF) database.

3507 Vilas is a member of the Themis family. The asteroid was observed on 4 nights over a period of four weeks with 196 total observations. The lightcurve database (LCDB; Warner et al., 2009) lists a period of 3.959 h based on (Wisniewski et al., 1997). However, two later papers by Erasmus et al. (2020, 4.755 h) and Ďurech et al. (2020, 4.75497 h), both using ATLAS data disagree with this value. This current work derived a rotational period of 4.755 ± 0.001 h with an amplitude of 0.29 mag in excellent agreement with the later two results. We expect that the result in the LCDB will be updated to reflect the new results.

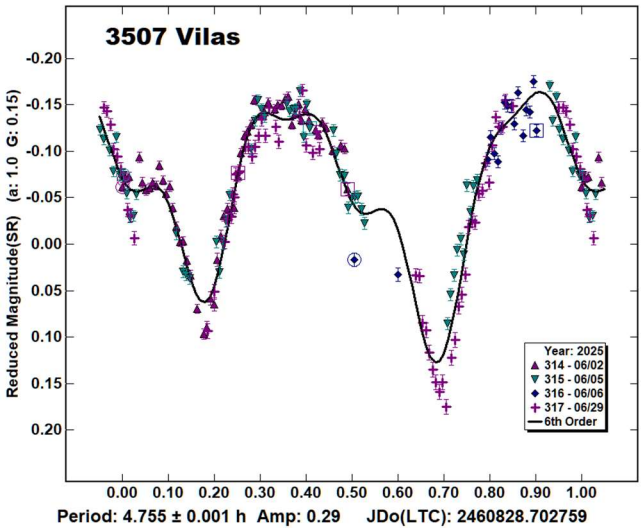

4185 Phystech. This inner main-belt asteroid was observed on three nights over a roughly three-week time span with 272 total observations. The derived rotational period of 4.668 ± 0.001 h with an amplitude of 0.47 mag in excellent agreement with the only prior measured rotation period by Dykhuis et al. (2016, 4.66904 h).

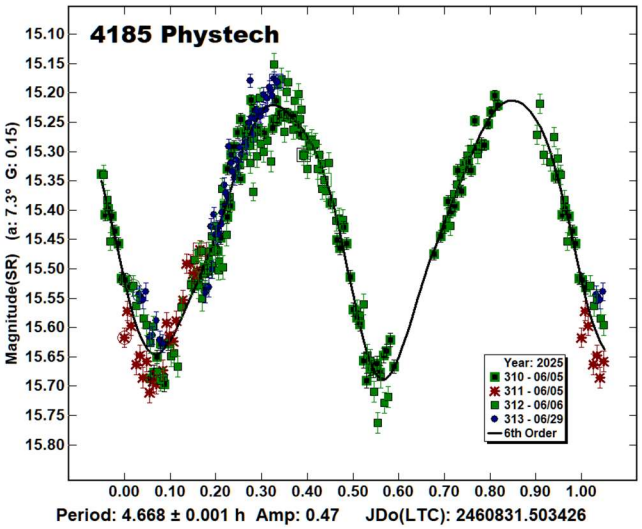

References

Dykhuis, M.J.; Molnar, L.A.; Gates, C.J.; Gonzales, J.A.; Huffman, J.J.; Maat, A.R.; Maat, S.L.; Marks, M.I.; Massey-Plantinga, A.R.; McReynolds, N.D.; Schut, J.A.; Stoep, J.P.; Stutzman, A.J.; Thomas, B.C.; Vander Tuig, G.W.; Vriesema, J.W.; Greenberg, R. (2016). "Efficient spin sense determination of Flora-region asteroids via the epoch method." *Icarus* **267**, 174-203.

Erasmus, N.; Navarro-Meza, S.; McNeill, A.; Trilling, D.E.; Sickafoose, A.A.; Denneau, L.; Flewelling, H.; Heinze, A.; Tonry, J.L. (2020). "Investigating Taxonomic Diversity within Asteroid Families through ATLAS Dual-band Photometry." *The Astrophysical Journal Supplement Series* **247**, 7 pp.

Ďurech, J.; Tonry, J.; Erasmus, N.; Denneau, L.; Heinze, A.N.; Flewelling, H.; Vančo, R. (2020). "Asteroid models reconstructed from ATLAS photometry." *Astronomy & Astrophysics* **643**, 5 pp.

Harris, A.W.; Young, J.W.; Scaltriti, F.; Zappala, V. (1984). "Lightcurves and phase relations of the asteroids 82 Alkmene and 444 Gyptis." *Icarus* **57**, 251-258.

Keel, W.C.; Oswalt, T.; Mack, P.; Henson, G.; Hillwig, T.; Batcheldor, D.; Berrington, R.; De Pree, C.; Hartmann, D.; Leake, M.; Licandro, J.; Murphy, B.; Webb, J.; Wood, M.A. (2017). "The Remote Observatories of the Southeastern Association for Research in Astronomy (SARA)." *Publications of the Astronomical Society of the Pacific* **129:015002** (12pp). *http://iopscience.iop.org/article/10.1088/1538-3873/129/971/015002/pdf*

Warner, B.D.; Harris, A.W.; Pravec, P. (2009). "The Asteroid Lightcurve Database." *Icarus* **202**, 134-146. Updated 2023 Oct 01. *http://www.minorplanet.info/lightcurvedatabase.html*

Number	Name	yyyy mm/dd	Phase	L_{PAB}	B_{PAB}	Period(h)	P.E.	Amp	A.E.	Grp
3507	Vilas	2025 06/02-06/29	1.0,11.8	250.2	1.1	4.755	0.001	0.29	0.02	THM
4185	Phystech	2025 06/05-06/29	7.2,19.1	244.7	-0.8	4.668	0.001	0.47	0.04	MB-I

Table I. Observing circumstances and results. The phase angle is given for the first and last date. If preceded by an asterisk, the phase angle reached an extrema during the period. L_{PAB} and B_{PAB} are the approximate phase angle bisector longitude/latitude at mid-date range (see Harris et al., 1984). Grp is the asteroid family/group (Warner et al., 2009): MB-I = main-belt inner, THM = Themis

Warner, B.D. (2021). MPO Software, MPO Canopus v10.8.5.0. Bdw Publishing. *http://minorplanetobserver.com*

Wisniewski, W.Z.; Michałowski, T.M.; Harris, A.W.; McMillan, R.S. (1997). "Photometric Observations of 125 Asteroids." *Icarus* **126**, 395-449.

LIGHTCURVES AND ROTATION PERIODS OF 57 MNEMOSYNE, 818 KAPTEYNIA, 896 SPHINX, AND 992 SWASEY

Frederick Pilcher
Organ Mesa Observatory (G50)
4438 Organ Mesa Loop
Las Cruces, NM 88011 USA
fpilcher35@gmail.com

(Received: 2025 July 5)

Synodic rotation periods and amplitudes at their year 2025 oppositions are found for 57 Mnemosyne 25.308 ± 0.001 h, 0.04 ± 0.01 mag; 818 Kapteynia 17.462 ± 0.001 h, 0.11 ± 0.01 mag with an irregular monomodal lightcurve; 896 Sphinx 21.072 ± 0.001 h, 0.24 ± 0.02 mag with an irregular lightcurve; 992 Swasey 13.295 ± 0.001 h, 0.15 ± 0.02 mag with an irregular lightcurve.

Observations to produce the results reported in this paper were made at the Organ Mesa Observatory with a Meade 35 cm LX200 GPS Schmidt-Cassegrain, SBIG STL-1001E CCD, 40 second exposures for 57 Mnemosyne, 60 second exposures for 818 Kapteynia, 896 Sphinx, and 992 Yerkes, unguided, clear filter. Image measurement and lightcurve construction were with *MPO Canopus* software with calibration star magnitudes for solar colored stars from the CMC15 catalog reduced to the Cousins R band. Zero-point adjustments of a few × 0.01 magnitude were made for best fit. To reduce the number of data points on the lightcurves and make them easier to read, data points have been binned in sets of 3 with maximum time difference 5 minutes.

57 Mnemosyne. Earlier published periods are by Harris et al. (1992), 12.463 hours; Ditteon and Hawkins (2007), 12.66 hours; Behrend (2016), 12.64 hours; Behrend (2020), 12.648 hours. All of these values can now be ruled out. The irregular lightcurve presented here for year 2025 observations consists of 14 sessions 2025 Apr. 7 - June 3 and shows a synodic period 25.308 ± 0.001 h, amplitude 0.04 ± 0.01 magnitudes. The real error in the period is considerably larger than the formal error. This lightcurve is the sixth dense lightcurve at consecutive oppositions published by this author. The results for the five previous lightcurves (Pilcher, 2019, 2020, 2022, 2023, 2024) and from the new observations are summarized in the table below.

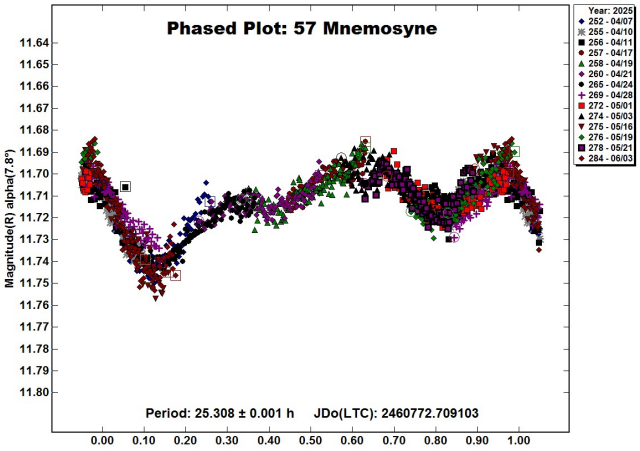

Figure 1: Lightcurve of 57 Mnemosyne phased to 25.308 hours.

Mid-date	L_{PAB}	B_{PAB}	P(h)	P.E.	Amp	A.E.
2019/05/09	197	1	25.324	0.002	0.09	0.01
2020/05/23	258	15	25.281	0.002	0.10	0.01
2021/08/23	331	14	25.308	0.001	0.08	0.01
2022/11/08	66	-13	25.316	0.002	0.08	0.01
2024/02/22	157	-13	25.303	0.002	0.06	0.01
2025/05/05	220	7	25.308	0.001	0.04	0.01

Column headings are, respectively; Mid-date half way between first and last observations; L_{PAB} and B_{PAB}, the respective celestial longitude and latitude of phase angle bisector on mid-date; P(h), synodic rotation period in hours; P.E., probable error in hours of the synodic rotation period; Amp, amplitude of the lightcurve; A.E., probable error of the lightcurve amplitude.

The errors of the observed synodic periods are much smaller than the variation of period from one opposition to the next. The differing amplitudes indicate that the observations were made at different asterocentric latitudes. None of the lightcurves are dominated by the usual bimodal shape. Both the small amplitudes and irregular shapes of the lightcurves from all six oppositions show that surface irregularities dominate over the usual ellipsoidal elongation. It will be a challenge to construct an LI model, but the model will have a unique and interesting shape. Will one of the readers of this manuscript accept the challenge?

818 Kapteynia. Previously published lightcurves with synodic rotation periods are by Behrend (2002), 15.98 h; Stephens (2002), 16.35 h; and Behrend (2005), 15.95 h. Durech et al. (2020) provide a sidereal period of 17.461 h, which is presented on the DAMIT website. New observations on eight nights 2025 Apr. 23 - June 4 provide an excellent fit to an irregular monomodal lightcurve with period 17.462 ± 0.001 h, amplitude 0.11 ± 0.01 magnitudes (Fig. 2). In the split halves plot of the double period (Fig. 3), nearly 90% of the lightcurve is covered by both halves and, in the doubly covered segments, the two halves are the same within the scatter of the data points. A period spectrum (Fig. 4) between 12 and 42 hours is also shown. Together, these plots show that the 15.9 hour and 16.35-hour periods can be rejected. Further evidence supporting the 17.462-hour synodic period comes from the DAMIT website (Durech et al. 2020), whose 17.461-hour sidereal period is almost identical with the synodic rotation period found in this study.

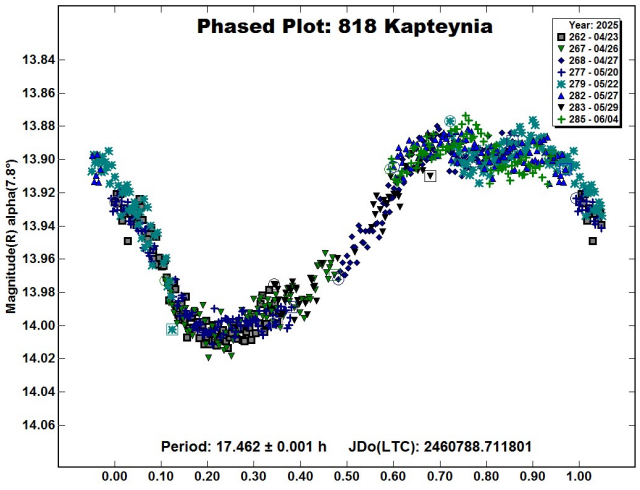

Figure 2: Lightcurve of 818 Kapteynia phased to 17.462 hours.

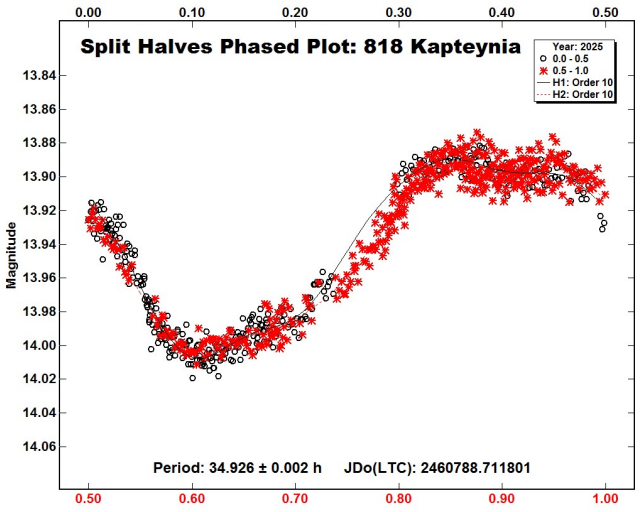

Figure 3: Split halves plot for 818 Kapteynia phased to the double period of 34.926 hours.

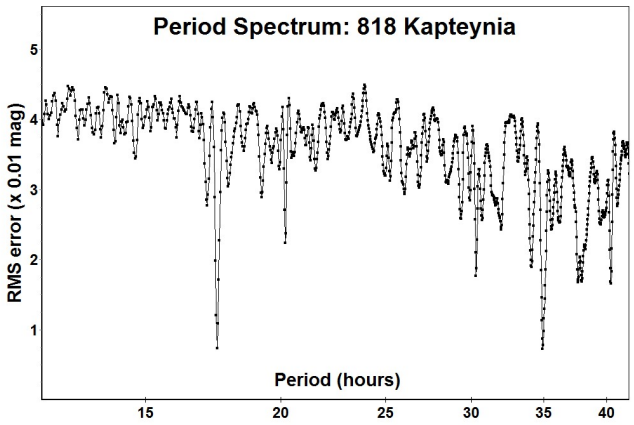

Figure 4: Period spectrum of 818 Kapteynia between 12 hours and 42 hours.

896 Sphinx. Previously published synodic rotation periods are by Behrend (2001), 26.27 hours; and Polakis (2018), 21.038 hours. Sidereal periods based on lightcurve inversion modeling of sparse data are by Durech et al. (2018), 12.95209 hours; and by Martikainen et al. (2021), 12.95198 hours. New observations on eleven nights 2025 June 5 - July 4 provide an excellent fit to a synodic rotation period 21.072 ± 0.001 hours, amplitude 0.24 ± 0.02 magnitudes with a somewhat irregular lightcurve (Fig. 5). This result is compatible with Polakis (2018) and rules out periods near 12.952 hours by Durech et al. (2018) and Martikainen et al. (2021), and 26.27 hours by Behrend (2001).

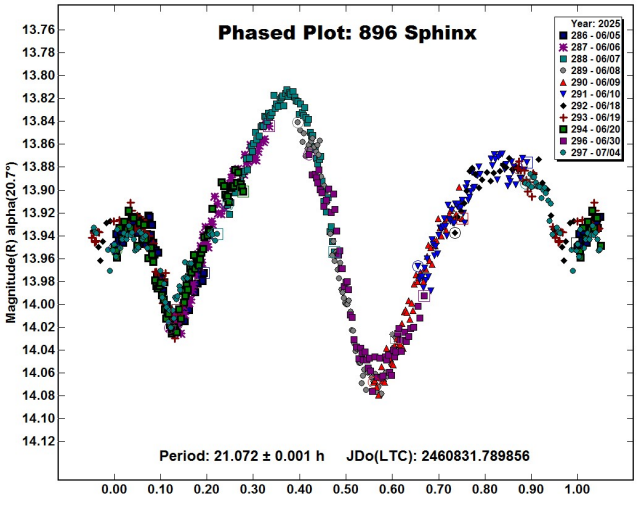

Figure 5: Lightcurve of 896 Sphinx phased to 21.072 hours.

992 Swasey. Previously published rotation periods are by Behrend (2004), 13.308 h; Behrend (2020), 13.31 h; Marchini et al. (2020), 13.305 h; Pál et al. (2020), 26.3193 h; Polakis (2020), 13.29 h; and Behrend (2021), 13.336 h. New observations on six nights 2025 Apr. 6-30 provide a good fit to a synodic period of 13.295 ± 0.001 h, amplitude 0.15 ± 0.02 magnitudes with an irregular lightcurve (Fig. 6). This value is consistent with all previously published periods except Pál et al. (2020).

Number	Name	2025/mm/dd	Phase	LPAB	BPAB	Period(h)	P.E	Amp	A.E.
57	Mnemosyne	04/07-06/03	* 7.8, 10.4	220	7	25.308	0.001	0.04	0.01
818	Kapteynia	04/23-06/04	* 7.8, 6.8	235	5	17.462	0.001	0.11	0.01
896	Sphinx	06/05-07/04	20.7, 7.1	288	6	21.072	0.001	0.24	0.02
992	Swasey	04/06-04/30	* 4.6, 5.7	207	1	13.295	0.001	0.15	0.02

Table I. Observing circumstances and results. The phase angle is given for the first and last date, except that a * denotes a minimum was reached between these dates. LPAB and BPAB are the approximate phase angle bisector longitude and latitude at mid-date range (see Harris et al., 1984).

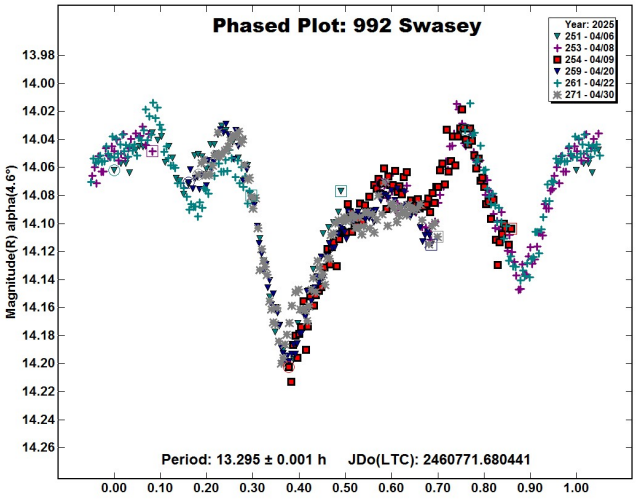

Figure 6: Lightcurve of 992 Swasey phased to 13.295 hours.

References

Behrend, R. (2001, 2002, 2004, 2005, 2016, 2020, 2021). Observatoire de Geneve web site. *http://*obswww.unige.ch/*~behrend/page_cou.html*

DAMIT website. *https://astro.troja.mff.cuni.cz/projects/damit/*

Ditteon, R.; Hawkins, S. (2007). "Asteroid lightcurve analysis at the Oakley Observatory - November 2006." *Minor Planet Bull.* **34**, 59-64.

Durech, J.; Hanus, J.; Ali-Lagoa, V. (2018). "Asteroid models reconstructed from the Lowell Photometric Database and WISE data." *Astron. Astrophys.* **617**, A57.

Durech, J.; Tonry, J.; Erasmus, N.; Denneau, L.; Heinze, A.N.; Flewelling, H.; Vanco, R. (2020). "Asteroid models reconstructed from ATLAS photometry." *Astron. Astrophys.* **643**, A59.

Harris, A.W.; Young, J.W.; Scaltriti, F.; Zappala, V. (1984). "Lightcurves and phase relations of the asteroids 82 Alkmene and 444 Gyptis." *Icarus* **57**, 251-258.

Harris, A.W.; Young, J.W.; Dockweiler, T.; Gibson, J.; Poutanen, M.; Bowell, E. (1992). "Asteroid lightcurve observations from 1981." *Icarus* **95**, 115-147.

Marchini, A.; Conti, M.; Vallerani, C.; Papini, R.; Salvaggio, F. (2020). "Rotation period determination for asteroids 992 Swasey and 3096 Bezruc." *Minor Planet Bull.* **47**, 265-267.

Martikainen, J.; Muinonen, K.; Penttila, A.; Cellino, A.; Wang, X.-B. (2018). "Asteroid absolute magnitudes and phase curve parameters from Gaia photometry." *Astron. Astrophys.* **649**, A98.

Pál, A.; Szakáts, R.; Kiss, C.; Bódi, A.; Bognár, Z.; Kalup, C.; Kiss, L.L.; Marton, G.; Molnár, L.; Plachy, E.; Sárneczky, K.; Szabó, G.M.; Szabó, R. (2020). "Solar System Objects Observed with TESS - First Data Release: Bright Main-belt and Trojan Asteroids from the Southern Survey." Astrophys. J. Suppl. Series **247**, 26.

Pilcher, F. (2019). "New lightcurves of 50 Virginia, 57 Mnemosyne, 59 Elpis, 444 Gyptis, and 997 Priska." *Minor Planet Bull.* **46**, 445-448.

Pilcher, F. (2020). "Lightcurves and rotation periods of 50 Virginia, 57 Mnemosyne, 58 Concordia, 59 Elpis, 78 Diana, and 529 Preziosa." *Minor Planet Bull.* **47**, 344-346.

Pilcher, F. (2022). "Lightcurves and rotation periods of 57 Mnemosyne and 58 Concordia." *Minor Planet Bull.* **49**, 9-10.

Pilcher, F. (2023). "Lightcurves and rotation periods of 57 Mnemosyne, 645 Agrippina, and 987 Wallia." *Minor Planet Bull.* **50**, 162-163.

Pilcher, F. (2024). "Lightcurves and rotations periods of 57 Mnemosyne, 58 Concordia, and 78 Diana." *Minor Planet Bull.* **51**, 235-236.

Polakis, T. (2018). "Lightcurve analysis for fourteen main-belt minor planets." *Minor Planet Bull.* **45**, 347-352.

Polakis, T. (2020). "Photometric observations of twenty-seven minor planets." *Minor Planet Bull.* **47**, 314-325.

Stephens, R.D. (2002). "Photometry of 769 Tatjana, 818 Kapteynia, 1922 Zulu, and 3687 Dzus." *Minor Planet Bull.* **29**, 72-73.

Warner, B.D.; Harris, A.W.; Pravec, P. (2009). "The Asteroid Lightcurve Database." *Icarus* **202**, 134-146. Updated 2023 Oct. *https://minplanobs.org/MPInfo/php/lcdb.php*

SYNODIC ROTATION PERIODS AND LIGHTCURVE AMPLITUDES FOR 12 MINOR PLANETS FROM GORA COLLABORATION

Milagros Colazo
Astronomical Observatory Institute, Faculty of Physics, Adam Mickiewicz University, ul. Słoneczna 36, 60-286 Poznań, POLAND
Grupo de Observadores de Rotaciones de Asteroides (GORA)
ARGENTINA - https://aoacm.com.ar/gora/index.php
milirita.colazovinovo@gmail.com

Víctor Amelotti
Observatorio Astronómico Naos (GORA NAO)
Observatorio Astronómico Naos 2 (GORA NA2)
- Alta Gracia (Córdoba, ARGENTINA)

Giuliat Navas
Observatorio Astronómico Nacional Llano del Hato (OAN)
Centro de Investigaciones de Astronomía Francisco J. Duarte (CIDA) - Apartaderos (Mérida, VENEZUELA)

Zlatko Orbanic
Osservatorio Explorer (MPC M19) - Pula (Istria, CROACIA)

Gerard Tàrtalo
Dark Energy Observatory (DEO) - Àger (Lleida, ESPAÑA)

Raúl Melia
Observatorio de Raúl Melia Carlos Paz (GORA RMC)
- Carlos Paz (Córdoba, ARGENTINA)

Francisco Santos
Observatorio Astronómico Giordano Bruno (MPC G05)
- Piconcillo (Córdoba, ESPAÑA)

Néstor Suárez
Observatorio Antares (MPC X39)
- Pilar (Buenos Aires, ARGENTINA)

Nicola Montecchiari
Elijah Observatory (MPC M27) - Lajatico (Pisa, ITALIA)

Alberto García
Observatorio Río Cofio (MPC Z03)
- Robledo de Chavela (Madrid, ESPAÑA)

Damián Scotta
Observatorio de Damián Scotta 1 (GORA ODS)
- San Carlos Centro (Santa Fe, ARGENTINA)

José Álvarez
Observatorio Astronómico Corgas (MPC Z65)
- Corgas-Taboadela-Ourense (Galicia, ESPAÑA)

Bruno Monteleone
OsservatorioAstronomico "La Macchina del Tempo" (MPC M24)
- Ardore Marina (Reggio Calabria, ITALIA)

Marcos Anzola
Observatorio Astronómico Vuelta por el Universo (GORA OMA)
- Córdoba (Córdoba, ARGENTINA)

Carlos Colazo
Observatorio Astronómico El Gato Gris (MPC I19)
- Tanti (Córdoba, ARGENTINA)

(Received: 2025 May 16)

Synodic rotation periods and amplitudes are reported for: 637 Chrysothemis, 1079 Mimosa, 1155 Aenna, 1287 Lorcia, 1409 Isko, 1841 Masaryk, 3731 Hancock, 3857 Cellino, 4350 Shibecha, 5438 Lorre, 5802 Casteldelpiano, 19793 2000 RX42.

The periods and amplitudes of asteroid lightcurves presented in this paper are the product of collaborative work by the GORA (Grupo de Observadores de Rotaciones de Asteroides) group. In all the studies, we have applied relative photometry assigning V magnitudes to the calibration stars.

The image acquisition was performed without filters and with exposure times of a few minutes. All images used were corrected using dark frames and, in some cases, bias and flat-field corrections were also used. Photometry measurements were performed using *FotoDif* software and for the analysis, we employed *Períodos* software (Mazzone, 2012).

Below, we present the results for each asteroid studied. The lightcurve figures contain the following information: the estimated period and period error and the estimated amplitude and amplitude error. In the reference boxes, the columns represent, respectively, the marker, observatory MPC code, or - failing that - the GORA internal code, session date, session offset, and several data points.

Targets were selected based on the following criteria: 1) those asteroids with magnitudes accessible to the equipment of all participants, 2) those with favorable observation conditions from Argentina, Venezuela, Spain, Italy, or Croatia, i.e. with negative or positive declinations δ, and 3) objects with few periods reported in the literature and/or with Lightcurve Database (LCDB) (Warner et al., 2009) quality codes (U) of less than 3.

637 Chrysothemis. This outer main-belt asteroid was discovered in 1971 by L. Kohoutek. It is classified as a CX-type asteroid according to the SDSS-based Asteroid Taxonomy (Carvano et al., 2010), with an estimated diameter of 40.24 km. The reported rotational period for this asteroid is P = 3.7 h (based on fragmentary lightcurve; Warner, 2017). In this work, we propose a considerably longer period of P = 23.088 ± 0.034 h with Δm = 0.16 ± 0.05.

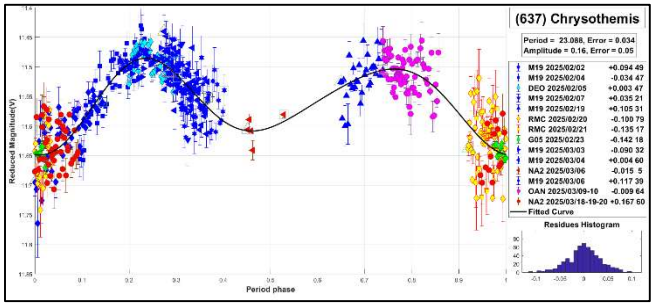

1079 Mimosa. Mimosa is a main-belt Asteroid discovered in 1927 by G. Van Biesbroeck. Classified as an S-type asteroid according to the Tholen taxonomy, it is a member of the Koronis family (Nesvorny et al., 2015). The reported rotational period for this asteroid is P = 64.6 h (Ďurech et al., 2020). In this work, we propose a shorter period of P = 20.243 ± 0.033 h with Δm = 0.15 ± 0.05.

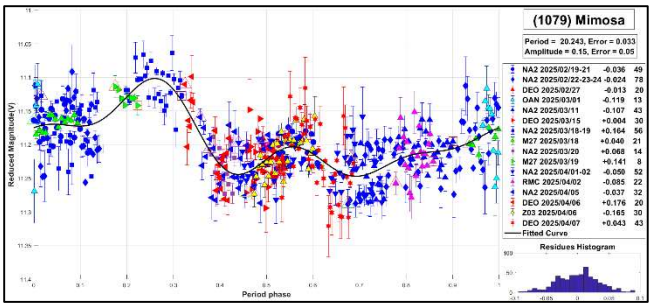

1155 Aenna. Aenna is a main-belt asteroid discovered in 1928 by K. Reinmuth. The estimated diameter is 9.284 km. The reported rotational period for this asteroid is 8.07 h (McNeill et al., 2019). Our measurement of the period, P = 7.908 ± 0.018 h, with Δm = 0.27 ± 0.03, agrees well with the value reported by the authors.

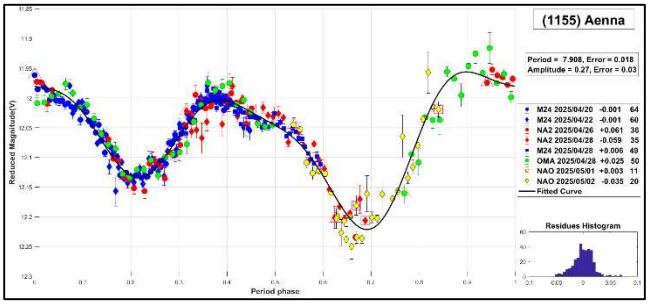

1287 Lorcia. Lorcia is main-belt asteroid with an estimated diameter of 35.54 km, discovered in 1933 by S. Arend. It is classified as an LS-type asteroid according to the SDSS-based Asteroid Taxonomy (Carvano et al., 2010). It is a member of the Eos family (Nesvorny et al., 2015). The reported rotational period for this asteroid is 8.8776 h (based on less than full coverage; Pál et al., 2020). Our measurement of the period, P = 8.876 ± 0.028 h, with Δm = 0.45 ± 0.04, agrees well with the value reported by the authors.

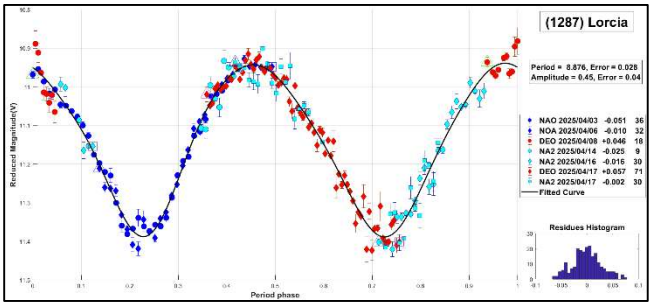

1409 Isko. Isko is a main-belt asteroid with an estimated diameter of 35.54 km, discovered in 1937 by K. Reinmuth. It is classified as a C-type asteroid according to the SDSS-based Asteroid Taxonomy (Carvano et al., 2010). The reported rotational period for this asteroid is 11.639 h (Ďurech et al., 2020). Our measurement of the period, P = 11.639 ± 0.029 h, with Δm = 0.21 ± 0.04, agrees well with the value reported by the authors.

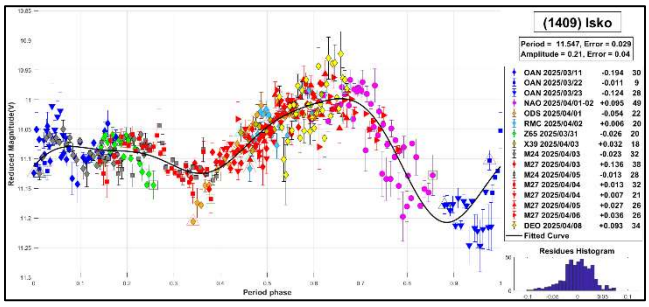

1841 Masaryk. This outer main-belt asteroid has an estimated diameter of 40.24 km, discovered in 1971 by L. Kohoutek. It is classified as a CX-type asteroid according to the SDSS-based Asteroid Taxonomy (Carvano et al., 2010). The reported rotational period for this asteroid is 7.53 h (based on less than full coverage; Ďurech et al., 2016). Our measurement of the period, P = 7.543 ± 0.030 h, with Δm = 0.56 ± 0.04, agrees well with the value reported by the author.

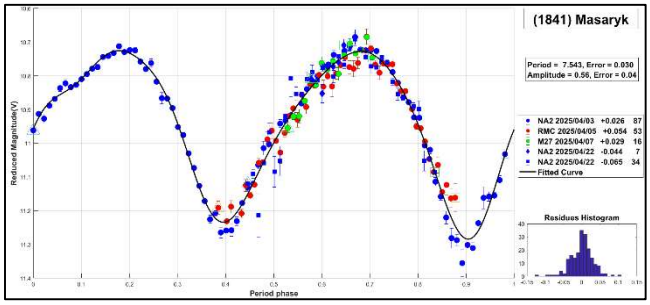

3731 Hancock. This outer main-belt asteroid has an estimated diameter of 53.112 km, discovered in 1984 at Perth. The reported rotational period for this asteroid is P = 6.712 h (based on fragmentary lightcurve; Clark, 2011). Our observations suggest a longer period, yielding a value of P = 29.744 ± 0.020 h with Δm = 0.05 ± 0.03.

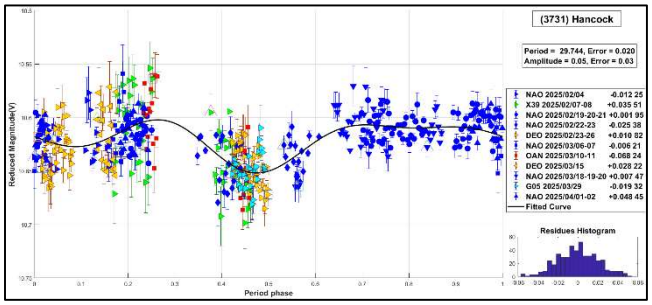

3857 Cellino. Cellino is a main-belt asteroid discovered in 1984 by E. Bowell. It is a member of the Nysa family (Nesvorny et al., 2015), with an estimated diameter of 5.839 km. The reported rotational period for this asteroid is 3.656529 h (Erasmus et al., 2020). We measured a period of P = 3.656 ± 0.044 h, with Δm = 0.46 ± 0.06.

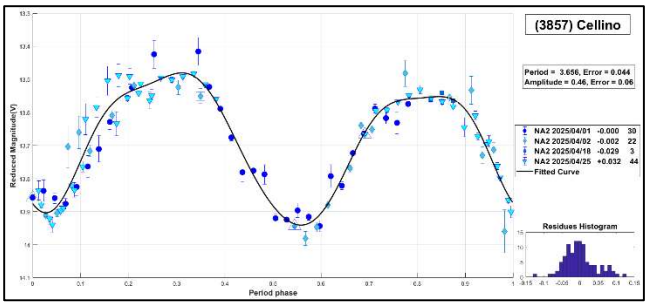

4350 Shibecha. This main-belt asteroid was discovered in 1989 by Ueda y Kaneda, with an estimated diameter of 11.489 km The reported rotational period for this asteroid is P = 2.89 h (Pál et al., 2020). Our observations also support the short-period hypothesis, yielding a value of P = 2.890 ± 0.038 h with Δm = 0.11 ± 0.05.

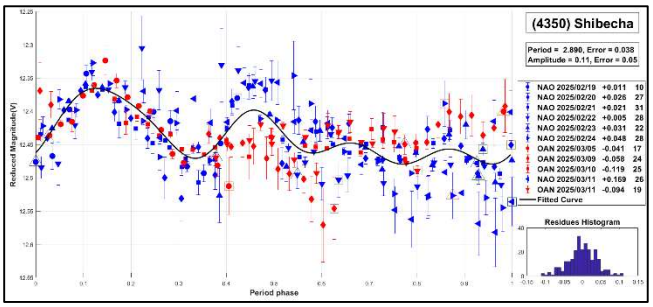

5438 Lorre. Lorre is a main-belt asteroid with an estimated diameter of 28.072 km, discovered in 1990 by E. Helin. The reported rotational period for this asteroid is P = 25.3 h (Polakis, 2020). In this work, we propose a period of P = 24.376 ± 0.015 h with Δm = 0.05 ± 0.02 mag.

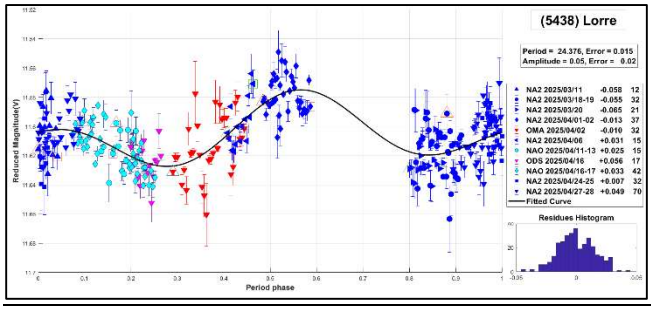

5802 Casteldelpiano. This main-belt asteroid was discovered in 1984 by V. Zappala, with an estimated diameter of 4.894 km The reported rotational period for this asteroid is P = 2.9705 h (Dose, 2021). Our observations also support the short-period hypothesis, yielding a value of P = 2.971 ± 0.022 h with Δm = 0.10 ± 0.03.

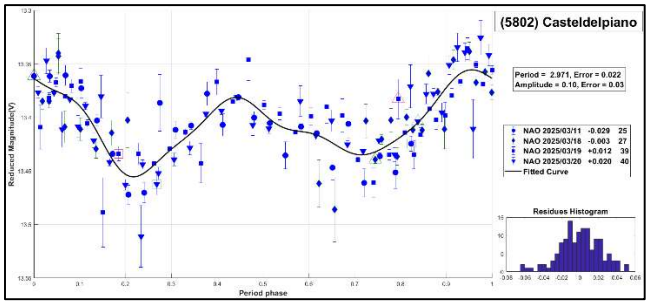

(19793) 2000 RX42. This main-belt asteroid was discovered in 2000 by LINEAR. It is a member of the Eunomia family (Nesvorny et al., 2015), with an estimated diameter of 8.534 km. The reported rotational period for this asteroid is 3.102 h (Waszczak et al., 2015). We measured a period of P = 2.973 ± 0.042 h, with Δm = 0.42 ± 0.06.

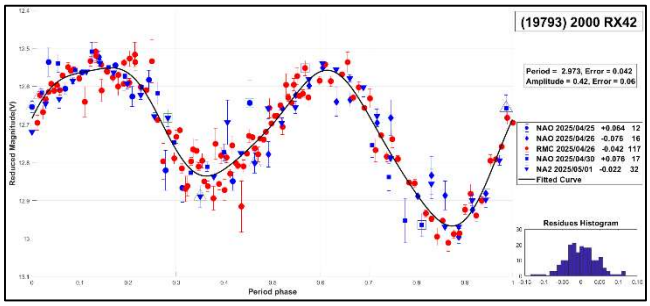

Acknowledgements

We want to thank Julio Castellano as we used his *FotoDif* program for preliminary analyses, Fernando Mazzone for his *Períodos* program, which was used in final analyses, and Matías Martini for his *CalculadorMDE_v0.2* used for generating ephemerides used in the planning stage of the observations. This research has made use of the Small Bodies Data Ferret (*https://sbnapps.psi.edu/ferret/*), supported by the NASA Planetary System. This research has made use of data and/or services provided by the International Astronomical Union's Minor Planet Center.

Number	Name	yy/ mm/dd- yy/ mm/dd	Phase	L_{PAB}	B_{PAB}	Period(h)	P.E.	Amp	A.E.	Grp
637	Chrysothemis	25/02/02-25/03/20	*5.3,12.8	146	0	23.088	0.034	0.16	0.05	Them
1079	Mimosa	25/02/19-25/04/07	*7.7,10.9	169	-1	20.243	0.033	0.15	0.05	Kor
1155	Aenna	25/04/20-25/05/02	2.7,09.3	206	2	7.908	0.018	0.27	0.03	MB-I
1287	Lorcia	25/04/03-25/04/18	0.9,06.1	193	-2	8.876	0.028	0.45	0.04	Eos
1409	Isko	25/03/11-25/04/08	*3.6,08.2	179	0	11.547	0.029	0.21	0.04	MB-M
1841	Masaryk	25/04/03-25/04/23	*1.2,06.5	196	1	7.543	0.030	0.56	0.04	MB-O
3731	Hancock	25/02/04-25/04/02	*9.8,17.4	145	-24	29.744	0.020	0.05	0.03	MB-O
3857	Cellino	25/04/01-25/04/25	15.7,02.9	218	1	3.656	0.044	0.46	0.06	Her
4350	Shibecha	25/02/19-25/03/11	19.5,11.6	188	10	2.890	0.038	0.11	0.05	MB-M
5438	Lorre	25/03/11-25/04/29	*20.2,25.1	182	-35	24.376	0.015	0.05	0.02	Lorr
5802	Casteldelpiano	25/03/11-25/03/20	6.8,01.4	181	1	2.971	0.022	0.10	0.03	MB-I
19793	2000 RX42	25/04/25-25/05/01	6.3,03.5	226	-4	2.973	0.042	0.42	0.06	Euno

Table I. Observing circumstances and results. The phase angle is given for the first and last date. If preceded by an asterisk, the phase angle reached an extremum during the period. L_{PAB} and B_{PAB} are the approximate phase angle bisector longitude/latitude at mid-date range (see Harris et al., 1984). Grp is the asteroid family/group (Warner et al., 2009). Them: 24 Themis; Kor: 158 Koronis; MB-I: main-belt inner; Eos: 221 Eos; MB-M: main-belt middle; MB-O: main-belt outer; Her: 135 Hertha; Lorr: 5438 Lorre; Euno: 15 Eunomia.

Observatory	Telescope	Camera
G05 Obs.Astr.Giordano Bruno	SCT (D=203mm; f=6.3)	CCD Atik 420 m
M19 Osservatorio Explorer	Newtonian (D=254mm; f=3.8)	CCD Moravian G2 4000
M24 Oss.Astr.LaMacchina del Tempo	RCT (D250mm; f=8.0)	CMOS ZWO ASI 1600MM
M27 Elijah Observatory	RCT (D250mm; f=8.0)	CCD QSI 683
X39 Obs.Astr.Antares	Newtonian (D=250mm; f=4.72)	CCD QHY9 Mono
Z03 Obs.Astr.RíoCofio	SCT (D=254mm; f=6.3)	CCD SBIG ST-8XME
Z65 Obs.Astr.Corgas	Newtonian (D=310mm; f=4.8)	CMOS ZWO ASI 294 MM
DEO Dark Energy Observatory	Refractor (D=115mm; f=7.0)	CMOS QHY 294M pro
NAO Obs.Astr.Naos	Newtonian (D=250mm; f=4.0)	CMOS QHY 163M
NA2 Obs.Astr.Naos 2	Newtonian (D=200mm; f=5.0)	CMOS ZWO ASI 174
OAN Obs.Astr.Nacional Llano del Hato	Cámara Schmidt (D=1000mm; f=3.0)	CMOS Fujifilm GFX 50R
ODS Obs.Astr.de Damián Scotta 1	Newtonian (D=300mm; f=4.0)	CMOS QHY 174M
OMA Obs.Astr.Vueltaporel Universo	Newtonian (D=150mm; f=5.0)	CMOS POA Neptune-M
RMC Obs.Astr.de Raúl Melia Carlos Paz	Newtonian (D=254mm; f=4.7)	CMOS QHY 174M

Table II. List of observatories and equipment.

References

Carvano, J.M.; Hasselmann, P.H.; Lazzaro, D.; Mothe-Diniz, T. (2010). "SDSS-based taxonomic classification and orbital distribution of main belt asteroids." *Astronomy and Astrophysics* **510**, id. A43.

Clark, M. (2011). "Asteroid Lightcurves from the Preston Gott and McDonald Observatories." *Minor Planet Bulletin* **38**, 187-189.

Dose, E.V. (2021). "Lightcurves of Eighteen Asteroids." *Minor Planet Bulletin* **48**, 125-132.

Ďurech, J.; Hanuš, J.; Oszkiewicz, D.; Vančo, R. (2016). "Asteroid models from the Lowell photometric database." *Astronomy & Astrophysics* **587**, A48.

Ďurech, J.; Tonry, J.; Erasmus, N.; Denneau, L.; Heinze, A.N.; Flewelling, H.; Vančo, R. (2020). "Asteroid models reconstructed from ATLAS photometry." *Astronomy & Astrophysics* **643**, A59.

Erasmus, N.; Navarro-Meza, S.; McNeill, A.; Trilling, D.E.; Sickafoose, A.A.; Denneau, L.; Flewelling, H.; Heinze, A.; Tonry, J.L. (2020). "Investigating taxonomic diversity within asteroid families through ATLAS dual-band photometry." *The Astrophysical Journal Supplement Series* **247**, 13.

Harris, A.W.; Young, J.W.; Scaltriti, F.; Zappala, V. (1984). "Lightcurves and phase relations of the asteroids 82 Alkmene and 444 Gyptis." *Icarus* **57**, 251-258.

Mazzone, F.D. (2012). Periodos sotware, version 1.0. *http://www.astrosurf.com/salvador/Programas.html*

McNeill, A.; Mommert, M.; Trilling, D.E.; Llama, J.; Skiff, B. (2019). "Asteroid Photometry from the Transiting Exoplanet Survey Satellite: A Pilot Study." *The Astrophysical Journal Supplement Series* **245**, 29.

Nesvorny, D.; Broz, M.; Carruba, V. (2015). "Identification and dynamical properties of asteroid families." arXiv preprint. arXiv:1502.01628.

Pál, A.; Sazkáta, R.; Kiss, C.; Bódi, A.; Bognár, Z.; Kalup, C.; Kiss, L.; Marton, G.; Molnár, L.; Plachy, E.; Sárneczky, K.; Szabó, G.; Szabó, R. "Solar System Objects Observed with TESS - First Data Release: Bright Main-belt and Trojan Asteroids from the Southern Survey." *The Astrophysical Journal Supplement Series* **247**(1), id. 26. 9pp. *axXiv:2001.05822.*

Polakis, T. (2020). "Photometric Observations of Thirty Minor Planets." *Minor Planet Bulletin* **47**, 177-186.

Warner, B.D.; Harris, A.W.; Pravec, P. (2009). "The Asteroid Lightcurve Database." *Icarus* **202**, 134-146. *https://minplanobs.org/mpinfo/ph*

Warner, B.D. (2017). "Asteroid Lightcurve Analysis at CS3-Palmer Divide Station: 2016 July-September." *The Minor Planet Bulletin* **44**, 22-36.

Waszczak, A.; Chang, C.K.; Ofek, E.O.; Laher, R.; Masci, F.; Levitan, D.; Surace, J.; Cheng, Y.-C.; Ip, W.-H; Kinoshita, D.; Helou, G.; Prince, T.A.; Kulkarni, S. (2015). "Asteroid light curves from the Palomar Transient Factory survey: rotation periods and phase functions from sparse photometry." *The Astronomical Journal* **150**, 75.

SYNODIC ROTATION PERIODS AND LIGHTCURVE AMPLITUDES FOR ELEVEN MAIN BELT ASTEROIDS

Milagros Colazo
Astronomical Observatory Institute, Faculty of Physics,
Adam Mickiewicz University, ul. Słoneczna 36, 60-286 Poznań, POLAND
Grupo de Observadores de Rotaciones de Asteroides (GORA)
ARGENTINA - https://aoacm.com.ar/gora/index.php
milirita.colazovinovo@gmail.com

Bruno Monteleone
OsservatorioAstronomico "La Macchina del Tempo" (MPC M24)
- Ardore Marina (Reggio Calabria, ITALIA)

Zlatko Orbanic
Osservatorio Explorer (MPC M19) - Pula (Istria, CROACIA)

Gerard Tàrtalo
Dark Energy Observatory (DEO) - Àger (Lleida, ESPAÑA)

Víctor Amelotti
Observatorio Astronómico Naos (GORA NAO)
- Alta Gracia (Córdoba, ARGENTINA)
Observatorio Astronómico Naos 2 (GORA NA2)
- Alta Gracia (Córdoba, ARGENTINA)

Raúl Melia
Observatorio de Raúl Melia Carlos Paz (GORA RMC)
- Carlos Paz (Córdoba, ARGENTINA)

Mario Morales
Observatorio de Sencelles (MPC K14)
- Sencelles (Mallorca-Islas Baleares, ESPAÑA)

Néstor Suárez
Observatorio Antares (MPC X39)
- Pilar (Buenos Aires, ARGENTINA)

Nicola Montecchiari
ElijahObservatory (MPC M27) - Lajatico (Pisa, ITALIA)

Francisco Santos
Observatorio Astronómico Giordano Bruno (MPC G05)
- Piconcillo (Córdoba, ESPAÑA)

Marcos Anzola
Observatorio Astronómico Vuelta por el Universo (GORA OMA)
- Córdoba (Córdoba, ARGENTINA)

Alberto García
Observatorio Río Cofio (MPC Z03)
- Robledo de Chavela (Madrid, ESPAÑA)

Giuliat Navas
Observatorio Astronómico Nacional Llano del Hato (OAN)
Centro de Investigaciones de Astronomía Francisco J. Duarte (CIDA) - Apartaderos (Mérida, VENEZUELA)

José Álvarez
Observatorio Astronómico Corgas (MPC Z65)
- Corgas-Taboadela-Ourense (Galicia, ESPAÑA)

Carlos Colazo
Observatorio Astronómico El Gato Gris (MPC I19)
- Tanti (Córdoba, ARGENTINA)

(Received: 2025 May 12)

Synodic rotation periods and amplitudes are reported for: 526 Jena, 1033 Simona, 1341 Edmee, 1408 Trusanda, 1926 Demiddelaer, 2350 von Lude, 2843 Yeti, 3041 Webb, 3134 Kostinsky, 3774 Megumi, 4725 Milone.

The periods and amplitudes of asteroid lightcurves presented in this paper are the product of collaborative work by the GORA (Grupo de Observadores de Rotaciones de Asteroides) group. In all the studies, we have applied relative photometry assigning V magnitudes to the calibration stars.

The image acquisition was performed without filters and with exposure times of a few minutes. All images used were corrected using dark frames and, in some cases, bias and flat-field corrections were also used. Photometry measurements were performed using *FotoDif* software and for the analysis, we employed *Períodos* software (Mazzone, 2012).

Below, we present the results for each asteroid studied. The lightcurve figures contain the following information: the estimated period and period error and the estimated amplitude and amplitude error. In the reference boxes, the columns represent, respectively, the marker, observatory MPC code, or - failing that - the GORA internal code, session date, session offset, and several data points.

Targets were selected based on the following criteria: 1) those asteroids with magnitudes accessible to the equipment of all participants, 2) those with favorable observation conditions from Argentina or Spain or Italy, i.e. with negative or positive declinations δ, respectively; and 3) objects with few periods reported in the literature and/or with Lightcurve Database (LCDB) (Warner et al., 2009) quality codes (U) of less than 3.

In this work, we present measurements of periods corresponding to asteroids previously analyzed by our team. These lightcurves display improved results and are part of a new long-term project that we are initiating.

526 Jenna. This main-belt asteroid was discovered in 1904 by M. Wolf. Classified as a B-type asteroid according to the Tholen taxonomy, it is a member of the Themis family (Nesvorny et al., 2015). The diameter is 44.84 km. The reported rotational period for this asteroid is 11.877 h (Martkainen et al., 2021). Our measurement of the period, P = 11.878 ± 0.015 h, with Δm = 0.25 ± 0.02, agrees well with the value reported by the authors.

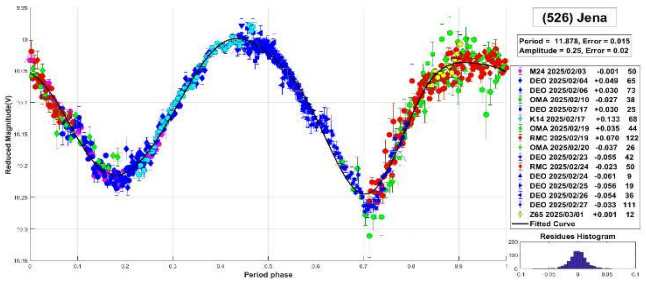

1033 Simona. Simona is a main-belt asteroid discovered in 1924 by G. Van Biesbroeck. It is a member of the Eos family (Nesvorny et al., 2015), with a diameter of 19.195 km. The reported rotational period for this asteroid is P = 10.07 h (Shipley et al., 2008). In this work, we propose a period of P = 11.69 ± 0.03 h with Δm = 0.09 ± 0.05 mag. The very low amplitude observed may be attributed to a near pole-on viewing geometry.

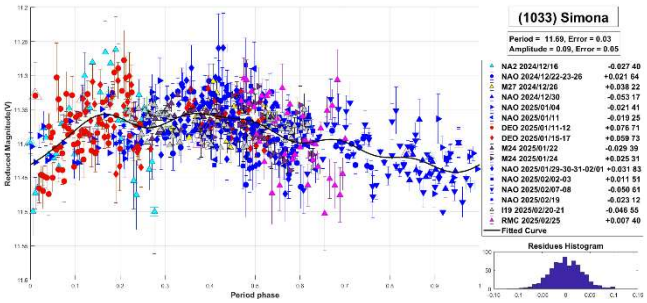

1341 Edmee. Edmee is a main-belt asteroid discovered in 1935 by E. Delporte. It is classified as a XB-type asteroid, with a diameter of 23.859 km. The reported rotational period for this asteroid is 23.745 h (Stephens, 2015). We measured a period of P = 23.779 ± 0.036 h, with Δm = 0.27 ± 0.05 mag.

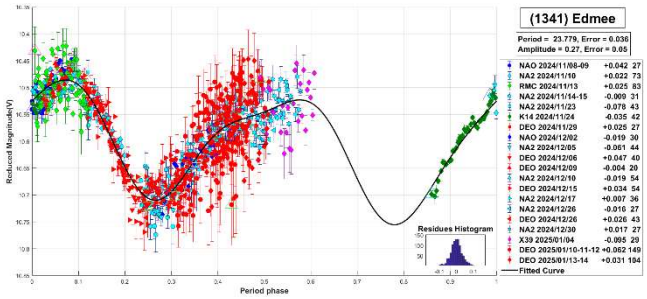

1408 Trusanda. This main-belt asteroid was discovered in 1936 by K. Reinmuth. It is classified as a X-type asteroid according to the Tholen taxonomy, with a diameter of 35.423 km. Interestingly, we could not find a reported rotational period for this object in the literature. Based on our observations and thorough analysis, we propose a period of P = 29.39 ± 0.02 h and Δm = 0.23 ± 0.08 mag.

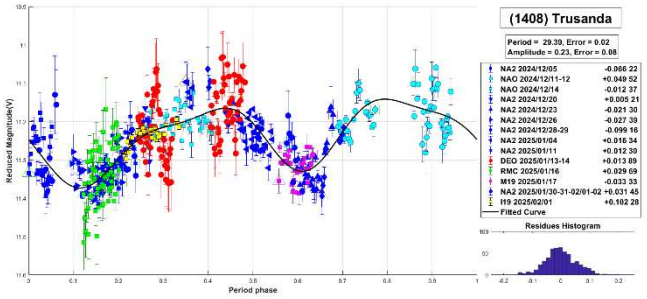

1926 Demiddelaer. This main-belt asteroid was discovered in 1935 by E. Delporte. It is a member of the Eunomia family (Nesvorny et al., 2015), with a diameter of 17.752 km. It is classified as an L-type asteroid. The reported rotational period for this asteroid is P = 32.095 h (Polakis and Skiff, 2017). Our observations suggest a longer period, yielding a value of P = 46.48 ± 0.03 h with Δm = 0.74 ± 0.05 mag.

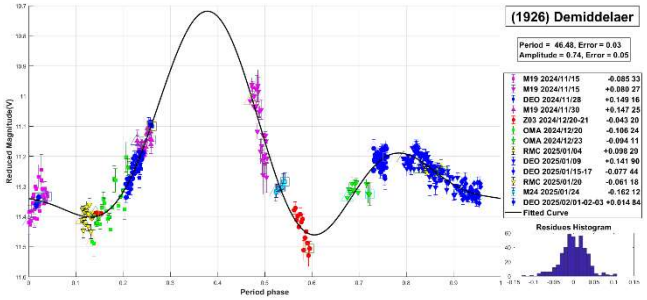

2350 von Lude. This main-belt asteroid is classified as an LS-type and a member of the Flora family, with a diameter of 5.786 km. It was discovered in 1938 by A. Bohrmann. No previously published rotational periods were found in the literature. In this work, we propose a period of P = 6.034 ± 0.038 h with an amplitude of Δm = 0.15 ± 0.05 mag.

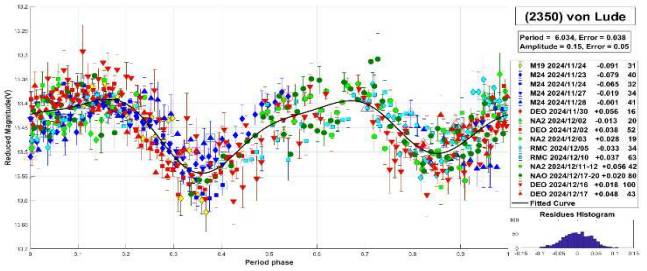

2843 Yeti. This main-belt asteroid has an estimated diameter of 7.587 km, discovered in 1975 by P. Wild. The reported rotational period for this asteroid is P = 156.718 h (Ďurech et al., 2020). Our observations also support the long-period hypothesis, yielding a value of P = 155.0 ± 1.7 h with Δm = 0.65 ± 0.05 mag.

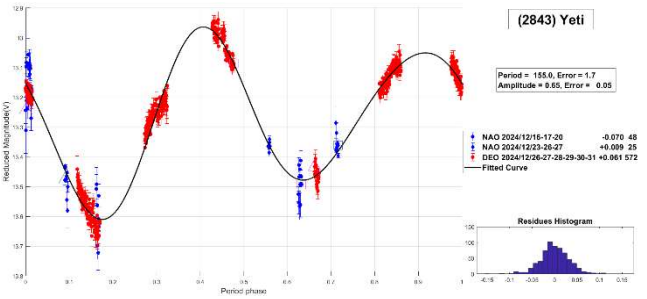

3041 Webb. This main-belt asteroid was discovered in 1980 by E. Bowell. It is a member of the Eunomia family (Nesvorny et al., 2015), with an estimated diameter of 8.221 km. A review of the literature revealed no published rotational periods for this asteroid. In this work, we propose a long period of P = 23.693 ± 0.037 h with Δm = 0.21 ± 0.05 mag.

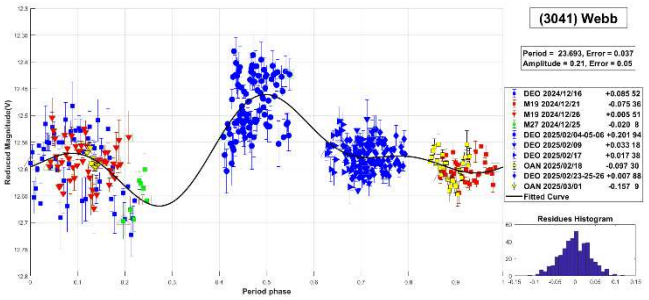

3134 Kostinsky. Kostinsky is an outer main-belt asteroid, discovered in 1921 by S. Belyavskij. It is a member of the Hilda family (Nesvorný et al., 2015), with an estimated diameter of 50.389 km. Pál et al. (2020) reported a rotational period of 14.7 h. Our measurement, P = 14.667 ± 0.025 h with an amplitude of Δm = 0.34 ± 0.03 mag, is in good agreement with their result.

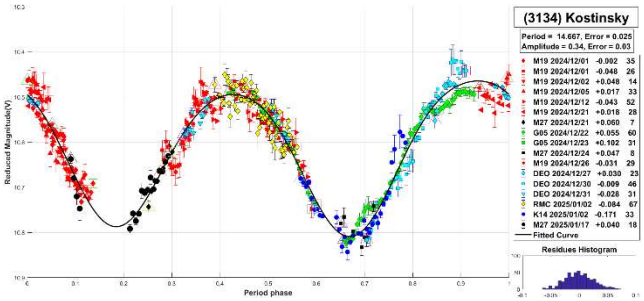

3774 Megumi. This main-belt asteroid was discovered in 1987 by T. Kojima. Classified as an L-type asteroid according to the Tholen taxonomy, it is a member of the Eos family (Nesvorny et al., 2015). The diameter is 18.251 km. For this asteroid, we couldn't find published periods in the literature either. In this work, we propose a short period of P = 3.573 ± 0.031 h with Δm = 0.22 ± 0.04 mag.

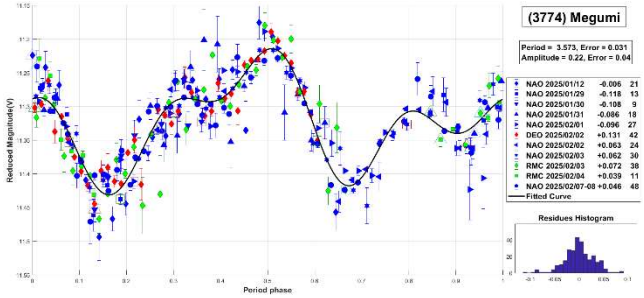

4725 Milone. Malone is a main-belt asteroid with an estimated diameter of 10.47 km, discovered in 1975 by the Felix Aguilar Observatory (El Leoncito). For this asteroid, we couldn't find published periods in the literature. In this work, we propose a long period of P = 136.7 ± 0.5 h with Δm = 0.62 ± 0.06 mag.

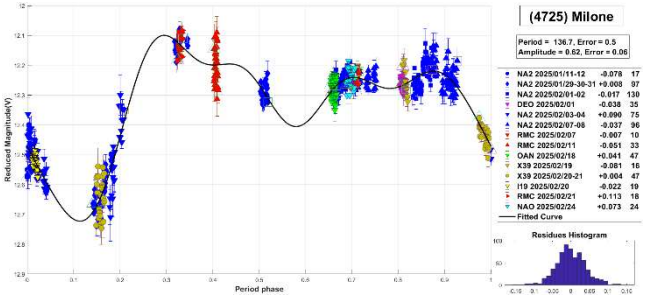

Acknowledgements

We want to thank Julio Castellano as we used his *FotoDif* program for preliminary analyses, Fernando Mazzone for his *Períodos* program, which was used in final analyses, and Matías Martini for his *CalculadorMDE_v0.2* used for generating ephemerides used in the planning stage of the observations. This research has made use of the Small Bodies Data Ferret (*https://sbnapps.psi.edu/ferret/*), supported by the NASA Planetary System. This research has made use of data and/or services provided by the International Astronomical Union's Minor Planet Center.

References

Ďurech, J.; Tonry, J.; Erasmus, N.; Denneau, L.; Heinze, A.N.; Flewelling, H.; Vančo, R. (2020). "Asteroid models reconstructed from ATLAS photometry." *Astronomy & Astrophysics* **643**, A59.

Harris, A.W.; Young, J.W.; Scaltriti, F.; Zappala, V. (1984). "Lightcurves and phase relations of the asteroids 82 Alkmene and 444 Gyptis." *Icarus* **57**, 251-258.

Martikainen, J.; Muinonen, K.; Penttilä, A.; Cellino, A.; Wang, X.B. (2021). "Asteroid absolute magnitudes and phase curve parameters from Gaia photometry." *Astronomy & Astrophysics* **649**, A98.

Mazzone, F.D. (2012). Periodos sotware, version 1.0. *http://www.astrosurf.com/salvador/Programas.html*

Observatory	Telescope	Camera
G05 Obs.Astr.Giordano Bruno	SCT (D=203mm; f=6.3)	CCD Atik 420 m
I19 Obs.Astr.El Gato Gris	SCT (D=355mm; f=10.6)	CCD SBIG STF-8300M
K14 Obs.Astr.de Sencelles	Newtonian (D=250mm; f=4.0)	CCD SBIG ST-7XME
M19 Osservatorio Explorer	Newtonian (D=254mm; f=3.8)	CCD Atik 414EX
M24 Oss.Astr.LaMacchina del Tempo	RCT (D250mm; f=8.0)	CMOS ZWO ASI 1600MM
M27 Elijah Observatory	RCT (D250mm; f=8.0)	CCD QSI 683
X39 Obs.Astr.Antares	Newtonian (D=250mm; f=4.72)	CCD QHY9 Mono
Z03 Obs.Astr.RioCofio	SCT (D=254mm; f=6.3)	CCD SBIG ST-8XME
Z65 Obs.Astr.Corgas	Newtonian (D=310mm; f=4.8)	CMOS ZWO ASI 294 MM
DEO Dark Energy Observatory	Refractor (D=115mm; f=7.0)	CMOS QHY 294M pro
NAO Obs.Astr.Naos	Newtonian (D=250mm; f=4.0)	CMOS QHY 163M
NA2 Obs.Astr.Naos 2	Newtonian (D=200mm; f=5.0)	CMOS ZWO ASI 174
OAN Obs.Astr.Nacional Llano del Hato	Cámara Schmidt (D=1000mm; f=3.0)	CMOS Fujifilm GFX 50R
OMA Obs.Astr.Vueltaporel Universo	Newtonian (D=150mm; f=5.0)	CMOS POA Neptune-M
RMC Obs.Astr.de Raúl Melia Carlos Paz	Newtonian (D=254mm; f=4.7)	CMOS QHY 174M

Table II. List of observatories and equipment.

Number	Name	yy/mm/dd-yy/mm/dd	Phase	L_{PAB}	B_{PAB}	Period(h)	P.E.	Amp	A.E.	Grp
526	Jena	25/02/03-25/03/03	*06.9,04.7	150	1	11.878	0.015	0.25	0.02	Themis
1033	Simona	24/12/16-25/02/26	*13.7,14.3	119	-12	11.69	0.03	0.09	0.05	Eos
1341	Edmee	24/11/08-25/01/14	06.4,19.1	40	-13	23.779	0.036	0.27	0.05	MB-O
1408	Trusanda	24/12/05-25/02/02	*11.2,11.5	102	-10	29.39	0.02	0.23	0.08	Eos
1926	Demiddelaer	24/11/15-25/02/03	*14.7,17.3	90	-1	46.48	0.03	0.74	0.05	Euno
2350	von Lude	24/11/23-24/12/20	*09.9,09.2	75	-7	6.034	0.038	0.15	0.05	Flora
2843	Yeti	24/12/16-25/01/01	20.7,14.2	122	-5	155.0	1.7	0.65	0.05	MB-I
3041	Webb	24/12/16-25/03/01	*19.0,17.2	125	13	23.693	0.037	0.21	0.05	Euno
3134	Kostinsky	24/12/01-25/01/17	*07.1,09.4	89	-2	14.667	0.025	0.34	0.03	Hilda
3774	Megumi	25/01/12-25/02/08	14.4,06.2	153	-7	3.573	0.031	0.22	0.04	Eos
4725	Milone	25/01/11-25/02/24	*16.2,07.8	144	-13	136.7	0.5	0.62	0.06	MB-O

Table I. Observing circumstances and results. The phase angle is given for the first and last date. If preceded by an asterisk, the phase angle reached an extremum during the period. L_{PAB} and B_{PAB} are the approximate phase angle bisector longitude/latitude at mid-date range (see Harris et al., 1984). Grp is the asteroid family/group (Warner et al., 2009). Themis: 24 Themis; Eos: 221 Eos; MB-O: main-belt outer; Euno: 15 Eunomia; Flora: 8 Flora; MB-I: main-belt inner; Hilda: 153 Hilda.

Nesvorny, D.; Broz, M.; Carruba, V. (2015). "Identification and dynamical properties of asteroid families." arXiv preprint. arXiv:1502.01628.

Pál, A.; Sazkáta, R.; Kiss, C.; Bódi, A.; Bognár, Z.; Kalup, C.; Kiss, L.; Marton, G.; Molnár, L.; Plachy, E.; Sárneczky, K.; Szabó, G.; Szabó, R. "Solar System Objects Observed with TESS - First Data Release: Bright Main-belt and Trojan Asteroids from the Southern Survey." *The Astrophysical Journal Supplement Series* **247**(1), id. 26. 9pp. *axXiv:2001.05822.*

Polakis, T.; Skiff, B.A. (2017). "Lightcurve Analysis for 341 California, 594 Mireille, 1115 Sabauda, 1504 Lappeenranta, and 1926 Demiddelaer." *Minor Planet Bull.* **44**, 299-302.

Shipley, H.; Dillard, A.; Kendall, J.; Reichert, M.; Sauppe, J.; Shaffer, N.; Kleeman, T.; Ditteon, R. (2008). "Asteroid Lightcurve Analysis at the Oakley Observatory – September 2007." *The Minor Planet Bulletin* **35**, 99-102.

Stephens, R.D. (2015). "Asteroids Observed from CS3: 2014 July-September." *Minor Planet Bull.* **42**, 70-74.

Warner, B.D.; Harris, A.W.; Pravec, P. (2009). "The Asteroid Lightcurve Database." *Icarus* **202**, 134-146.
https://minplanobs.org/mpinfo/ph

PHOTOMETRIC OBSERVATIONS AND LIGHTCURVE ANALYSYS OF FOUR MAIN-BELT ASTEROIDS

Marek Buček
Luckystar Observatory (MPC: M55)
Dr. Lučanského 547, Važec, 032 61, SLOVAKIA
marbucek1@gmail.com

Stephen M. Brincat
Flarestar Observatory (MPC: 171)
Fl.5 George Tayar Street,
San Gwann SGN 3160, MALTA
stephenbrincat@gmail.com

Normand Rivard
À la belle étoile Observatory
796, rang des Écossais
Sainte-Brigide-d'Iberville (Québec)
J0J 1X0 CANADA
normandrivard@icloud.com

(Received: 2025 June 9)

We report results of photometric observations and lightcurve analysis of four main-belt asteroids: 2383 Bradley, 6512 de Bergh, 7309 Shinkawakami and 31828 Martincordiner. The asteroids were observed by a network of observatories located in Slovakia, Malta and Canada.

We conducted photometric observations of following asteroids: 2383 Bradley, 6512 de Bergh, 7309 Shinkawakami, 31828 Martincordiner. Observations were made from network of observatories located in Europe (Malta and Slovakia) and North America (Canada) listed in Table 1. This table displays the details of the instrumentation and number of observation nights for each target. We employed an unfiltered observation - clear filter with Sloan R zero point for all images. Frames were calibrated by using dark and flat-field master subtractions images.

All observatory equipment was remotely controlled over the internet or from a nearby location. We used *Sequence Generator Pro* software (Binary Star Software) for image acquisition by Maltese Observatory. Slovak and Canadian stations used the *NINA* (Nighttime imaging ´N´ astronomy) image acquisition software (Berg, 2025).

We used *MPO Canopus* software version 10 and 12 (Warner, 2017) for image analysis, to acquire differential aperture photometry, to construct lightcurves and for Fourier analysis of gained light curves. We selected near-solar color comparison stars ($0.5 \leq$ B-V ≤ 0.9) using the Comparison Star Selector (CSS) feature of *MPO Canopus*. We based all brightness measurements on the Asteroid Terrestrial-impact Last Alert System (ATLAS) catalogue (Tonry et al., 2018).

Observatory/ Country	Scope and Type	Camera	Observed Asteroids (#Nights)
Flarestar Obs. (MPC: 171)/ MALTA	0.25-m SCT	Moravian G2-1600	# 2383 (4)
Luckystar Obs. (MPC: M55)/ SLOVAKIA	0.25-m SCT	Atik 460EX	# 7309 (5) # 31828 (4) # 6512 (9)
A la belle étoile Obs. /CANADA	0.2-m MK	Moravian G2-1600	# 6512 (1)

Table 1: Instrumentation and Observation Runs. SCT: Schmidt-Cassegrain Telescope, MK: Maksutov-Cassegrain.

2383 Bradley is a main-belt asteroid discovered on 1981 April 5 by E. Bowell at Anderson Mesa Station of Lowell Observatory. This asteroid's orbit is situated in the inner part of the main-belt with semi-major axis of 2.22 AU, eccentricity 0.11, inclination 3.57° and an orbital period of 3.3 years (JPL, 2025).

2383 Bradley was observed on 4 nights between 2024, April 6 and May 21 by Flarestar observatory. Fourier period analyses lead to the multiple solutions with similar RMS but for the asteroid with amplitude higher than 0.3 magnitude the bimodal solution is most probable. So, we have chosen estimated period of 5.8707 ± 0.0001 h with amplitude A = 0.52 ± 0.05 mag which is line with the previously reported period for this target: 5.871 ± 0.001 h, (Fornas et al, 2025), respectively 5.823 ± 0.003 h (Warell, 2017).

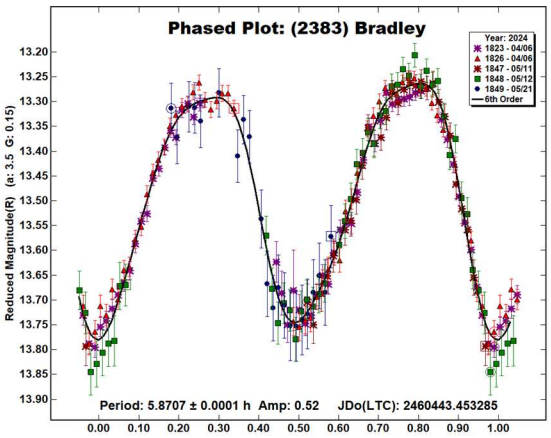

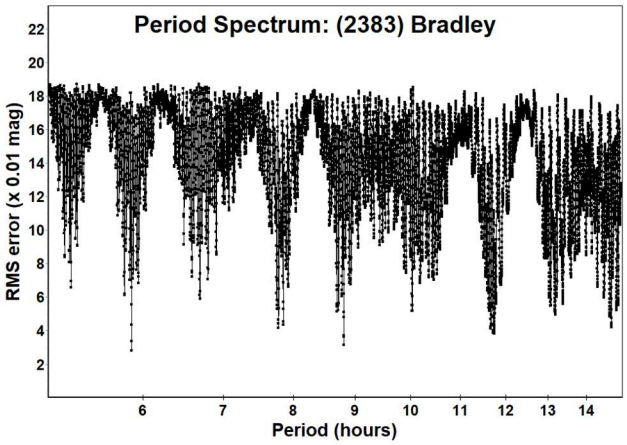

6512 de Bergh - is an inner main-belt asteroid discovered on 1987 September 21 by E. Bowell at Anderson Mesa Station of Lowell Observatory. Estimated diameter of this object is about 5.184 ± 0.457 km and recorded absolute magnitude is 13.49 mag (JPL, 2025).

6512 de Bergh was observed by Luckystar observatory on 9 nights between 2024 August 28 and September 29. Additional observational data from one session have been added from À la belle étoile Observatory. We have processed 490 individual observations of this target and period analyses showed estimated period of 12.6358 ± 0.0103 h. with corresponding amplitude of 0.22 ± 0.03 mag as a most probable solution. We found no prior rotation period reports for this asteroid.

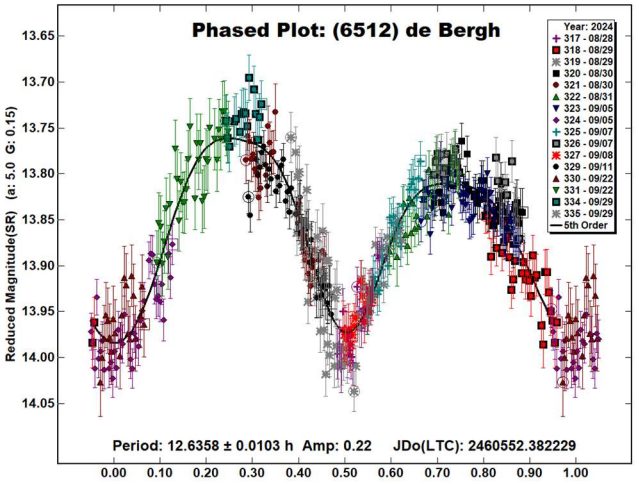

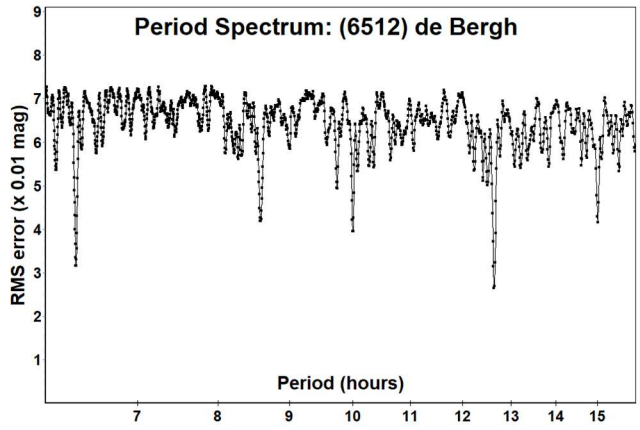

7309 Shinkawakami - is a main-belt asteroid discovered on 1995 March 28 by T. Kobayashi at Oizumi. This asteroid is named in honor of Shin-ichi Kawakami a professor of Earth and Planetary Sciences in the Faculty of Education at Gifu University.

7309 Shinkawakami was observed by Luckystar observatory on 5 nights between 2024, April 1 - 9. In total 245 observations were included in our period analysis which leads to two possible solutions. One with the monomodal and second with standard binodal behavior. No matter the lower RMS for monomodal solution, split halves diagram shows different behavior for each maximum, so we have preferred bimodal solution with period of 4.9801 ± 0.0063 h and amplitude of 0.64 ± 0.06 mag. We have found previous report of period results for this target, P= 4.982 ± 0.001 h by Dose (2024).

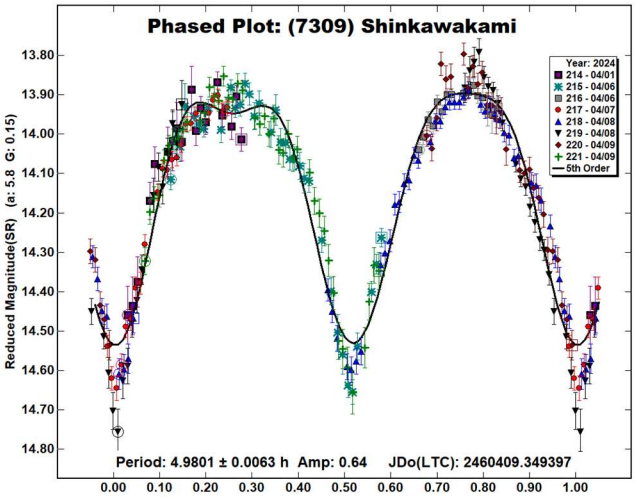

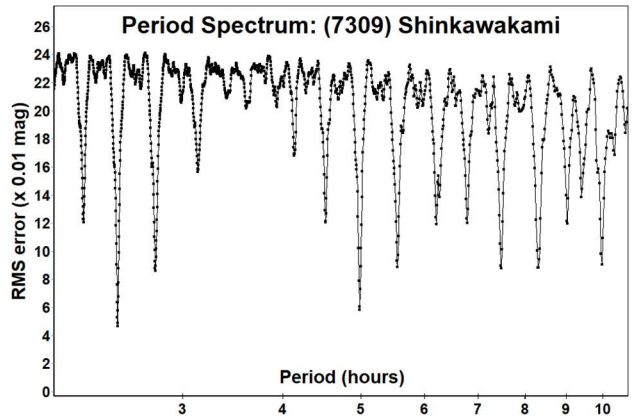

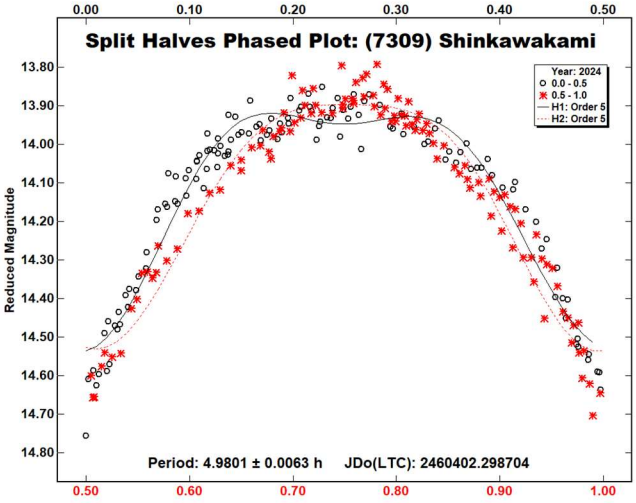

31828 Martincordiner - is a main-belt asteroid discovered on 1999 November 4 by LONEOS at Anderson Mesa. This asteroid is named after the British astronomer Martin Cordiner who is an expert in astrochemistry and planetary science.

Number	Name	yyyy mm/dd	Phase	L_{PAB}	B_{PAB}	Period(h)	P.E.	Amp	A.E.	Grp
2383	Bradley	2024 04/06-05/21	7.8,10.5	202.9	-0.8	5.8707	0.0001	0.52	0.05	MB-inner
6512	de Bergh	2024 08/28-09/29	5.1,13.5	341.2	6.0	12.6358	0.0103	0.22	0.03	MB-inner
7309	Shinkawakami	2024 04/01-04/09	5.8,10.2	183.8	3.8	4.9801	0.0063	0.64	0.05	MB-inner
31828	Martincordiner	2024 04/10-04/29	13.3,11.0	217.4	20.6	6.045	0.001	0.14	0.02	Unknown

Table I. Observing circumstances and results. The phase angle is given for the first and last date. L_{PAB} and B_{PAB} are the approximate phase angle bisector longitude and latitude at mid-date range (see Harris et al., 1984). Grp is the asteroid family/group (Warner et al., 2009).

Luckystar observatory observed 31828 Martincordiner on 4 nights between 2024, April 10 - 29. During this period 181 individual records of the target have been obtained and analyzed. Fourier period analysis showed several potential solutions with the very similar RMS. Best fitted solution for standard bimodal behavior of the asteroid is the one with P = 6.045 ± 0.001 h and A = 0.14 ± 0.02 mag. We haven´t found any previous reports for the period of this asteroid.

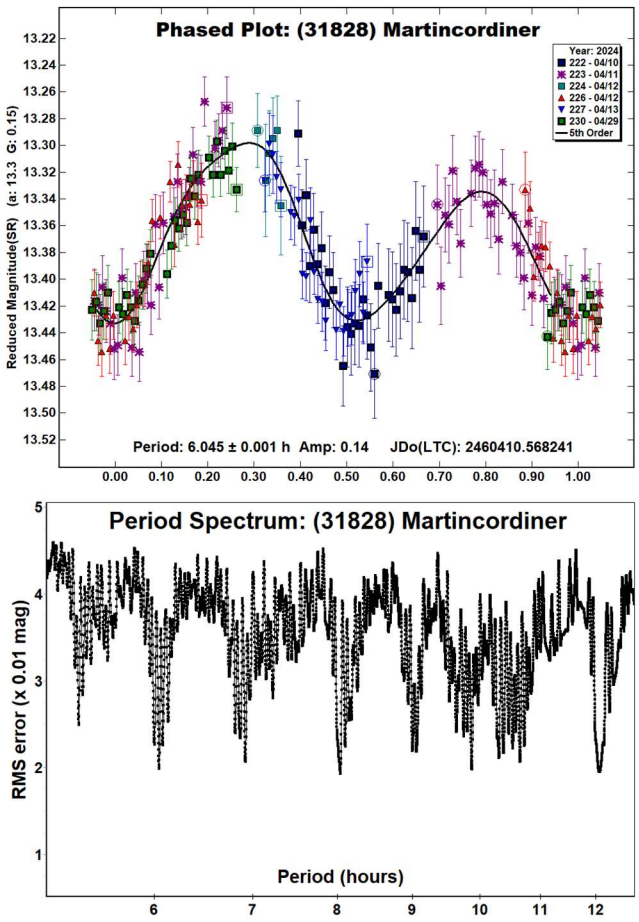

Acknowledgements

We would like to thank Brian Warner for his work in the development of *MPO Canopus* and for his efforts in maintaining the CALL website (Warner, 2016; 2021). This research has made use of the JPL's Small-Body Database (JPL, 2025).

References

Berg, S. (2025). Nightime Imaging 'N' Astronomy (NINA) website. *https://nighttime-imaging.eu/*. Last accessed 20 May 2025.

Dose, E. V. (2024). "Lightcurves of Eleven Asteroids." *Minor Planet Bull.* **51-4**, 324-330.

Fornas, G.; Fornas, A.; Huet, F.; Rathmann, E.; Arce, E.; Barberá, E.; Mas, V. (2025). "Lightcurve analysis for thirteen main-belt and three near Earth asteroids.", *Minor Planet Bull.* **52-1**, 38-44.

Harris, A.W.; Young, J.W.; Scaltriti, F.; Zappala, V. (1984). "Lightcurves and phase relations of the asteroids 82 Alkmene and 444 Gyptis." *Icarus* **57**, 251-258.

JPL, (2025). Small-Body Database Browser - JPL Solar System Dynamics web site. *http://ssd.jpl.nasa.gov/sbdb.cgi*. Last accessed: 18 December 2024.

Tonry, J.L.; Denneau, L.; Flewelling, H.; Heinze, A.N.; Onken, C.A.; Smartt, S.J.; Stalder, B.; Weiland, H.J.; Wolf, C. (2018). "The ATLAS All-Sky Stellar Reference Catalog." *Astrophys. J.* **867**, A105.

Warell, J. (2017). "Lightcurve observations of nine main-belt asteroids." *Minor Planet Bull.* **44-4**, 304-305.

Warner, B.D.; Harris, A.W.; Pravec, P. (2009). "The Asteroid Lightcurve Database." *Icarus* **202**, 134-146. Updated 2021 June. *https://www.minorplanet.info/php/lcdb.php*

Warner, B.D. (2016). Collaborative Asteroid Lightcurve Link website. *http://www.minorplanet.info/call.html* Last accessed: 20 May 2025.

Warner, B.D. (2017). MPO Software, MPO Canopus version 10.7.10.0. Bdw Publishing. *http://www.minorplanetobserver.com/*

Warner, B.D. (2021). Asteroid Lightcurve Photometry Database (ALCDEF) at *https://minplanobs.org/alcdef/index.php*

PHOTOMETRIC OBSERVATIONS AND LIGHTCURVE ANALYSIS OF FIVE ASTEROIDS FROM AN INTERNATIONAL NETWORK OF OBSERVATORIES

Marek Buček
Luckystar Observatory (MPC: M55)
Dr. Lučanského 547, Važec, 032 61, SLOVAKIA
marbucek1@gmail.com

Stephen M. Brincat
Flarestar Observatory (MPC: 171)
Fl.5 George Tayar Street,
San Gwann SGN 3160, MALTA

Charles Galdies
Znith Observatory
Armonie, E. Bradford Street
Naxxar NXR 2217, MALTA

Normand Rivard
À la belle étoile Observatory
796, rang des Écossais, Sainte-Brigide-d'Iberville
(Québec) J0J 1X0 CANADA

Vincent Zammit
Stellar Horizon Observatory
No.8, Maranatha, Triq Tal-Fieres
Kirkop KKP 1502, MALTA

Results of extensive observation campaigns of five asteroids from a network of observatories situated in Slovakia, Malta and Canada are presented in this paper. We have conducted more than 80 individual sessions during these campaigns targeting asteroids 3595 Gallagher, 5704 Schumacher, 7068 Minowa, 10143 Kamogawa and (12528) 1998 KL31.

We report results of photometric observation campaigns of five asteroids with long periods: 3595 Gallagher, 5704 Schumacher, 7068 Minowa, 10143 Kamogawa and (12528) 1998 KL31. Campaigns have been conducted by a network of observatories located in Malta (3), Slovakia (1) and Canada (1). Table 1 displays the details of the instrumentation and number of observation nights for each target.

All equipment was remotely controlled and networked to main observatories from nearby locations. Two types of acquisition software have been used by the network - *NINA* (Nighttime imaging ´N´ astronomy; Berg, 2023) in the case of Slovak and the Canadian observatories, as well as by Stellar Observatory located in Malta. The remaining two observatories used the *Sequence Generator Pro* software (Binary Star Software) for their image acquisition. We acquired all images (unfiltered) through a clear filter with Sloan R zero point. FITS frames were calibrated by using dark and flat-field master frames.

We used *MPO Canopus* software version 10 and 12 (Warner, 2017) for image analysis. The differential aperture photometry procedure was used to construct lightcurves for Fourier analysis. We selected near-solar color comparison stars ($0.5 \leq$ B-V ≤ 0.9) using the Comparison Star Selector (CSS) feature of *MPO Canopus*. We based all brightness measurements on the Asteroid Terrestrial-impact Last Alert System (ATLAS) catalogue (Tonry et al., 2018).

Observatory/ Country	Scope and Type	Camera	Observed Asteroids (#Nights)
A la belle étoile Obs. / CANADA	0.20-m MK	Moravian G2-1600	# 12528 (1)
Flarestar Obs. (MPC: 171) / MALTA	0.25-m SCT	Moravian G2-1600	# 5704 (2) # 7068 (8) # 12528 (3)
Luckystar Obs. (MPC: M55) / SLOVAKIA	0.25-m SCT	Atik 460EX	# 3595 (8) # 5704 (5) # 7068 (21) # 10143 (20) # 12528 (11)
Stellar Horizon Obs. / MALTA	0.30-m SCT	ASI 6200MM	# 3595 (1)
Znith Obs. / MALTA	0.20-m SCT	Moravian G2-1600	# 5704 (1) # 10143 (1)

Table 1: Instrumentation and Observation Runs. SCT: Schmidt-Cassegrain Telescope, MK: Maksutov-Cassegrain.

3595 Gallagher is a main-belt asteroid discovered on 1985 October 15 by E. Bowell at Flagstaff. The estimated diameter is 7.676 ± 0.226 km with an absolute magnitude H = 12. 96 mag based on the information provided JPL small-body database (JPL, 2025).

3595 Gallagher was observed during its favorable opposition between 2024 September 29 and October 28 from Luckystar and Stellar Horizon Observatories. In this month-long period, nine observation sessions have been completed and 499 individual frames obtained. Fourier data analysis derived its synodic rotation period as 87.2402 ± 0.6746 h with an amplitude of 0.43 ± 0.04 mag as the most probable solution, but limited amount of data lead to just partially covered lightcurve. Periodic spectral analysis shows another potential solution with the nearly the same RMS with half long period, but this solution has monomodal lightcurve behavior. Regarding the amplitude of the changes, which is more than 0.3 magnitude, we prefer to consider a bimodal solution as the most probable solution.

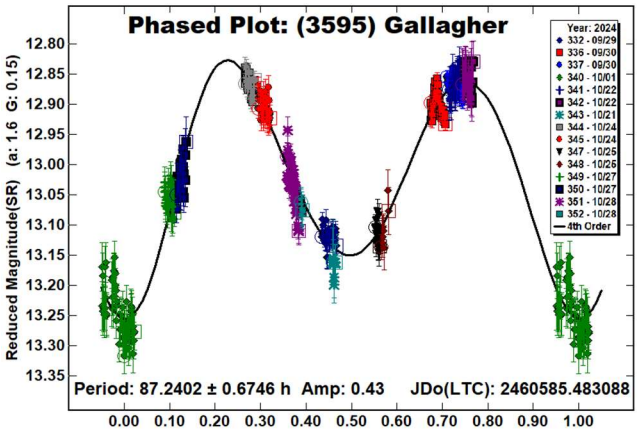

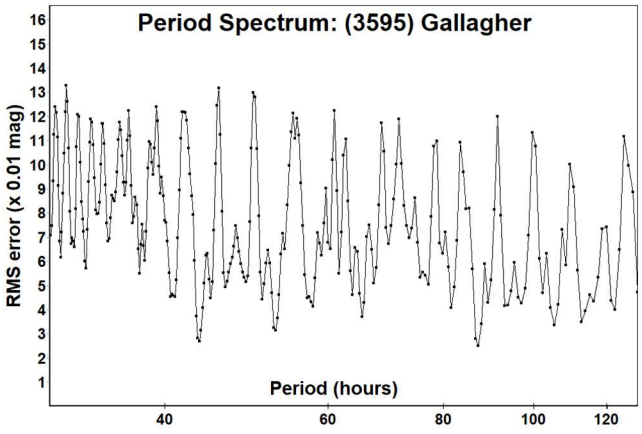

5704 Schumacher is an outer main-belt asteroid discovered on 1950 February 17 by K. Reinmuth at Heildelberg. The estimated diameter was derived to be 23.597 ± 0.304 km based on an absolute magnitude H = 12.18 (JPL, 2025).

5704 Schumacher was observed for eight nights between 2025 February 28 and April 3 from three different observatories of our network (Luckystar, Znith and Flarestar). A total of 427 individual frames have been processed and included to lightcurve analysis. From this data set we derived the synodic period to be 15.765 ± 0.003 h with an amplitude of 0.27 ± 0.06 mag. No published period could be found in the LCDB for this asteroid.

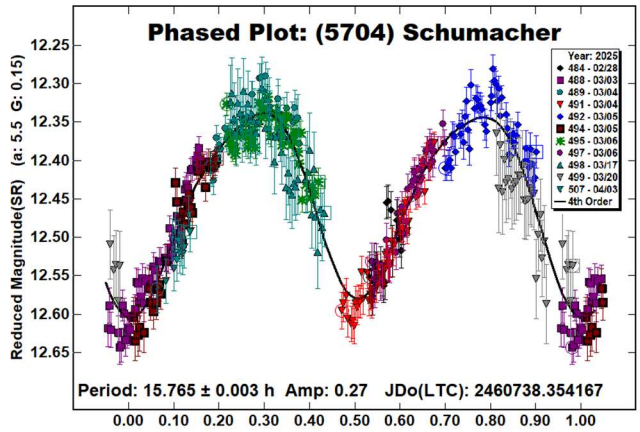

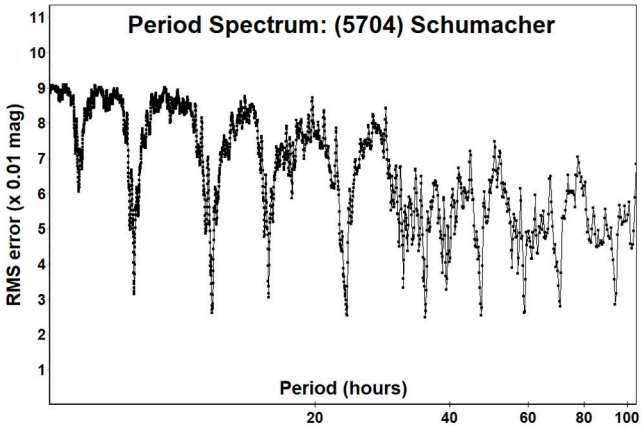

7068 Minowa is an inner main-belt asteroid which was discovered on 1994 November 26 by Y. Kushida and O. Muramatsu at Yatsugatake, Japan. The absolute magnitude is 13.63 mag and has corresponding diameter of about 5.84 ± 0.116 km.

7068 Minowa has been observed for an extensive period of 29 nights from Luckystar (21) and Flarestar (8) observatories, starting from late December 2024 until the second half of February 2025. While the 2024 sessions consisted of full night observations, the 2025 sessions consisted of batch observations that were one- to two-hours long. Data from three sessions have been excluded from analysis due to high RMS errors caused by high altitude clouds (46 points). In total 760 individual observations have been used for the lightcurve analysis which led to an estimated period of 157.6232 ± 0.8844 h and Amplitude of 0.93 ± 0.08 mag. In reality, the resulting amplitude should be bit lower because of a missing part in the lightcurve coverage around the secondary maxima. No published period could be found in the LCDB for this asteroid.

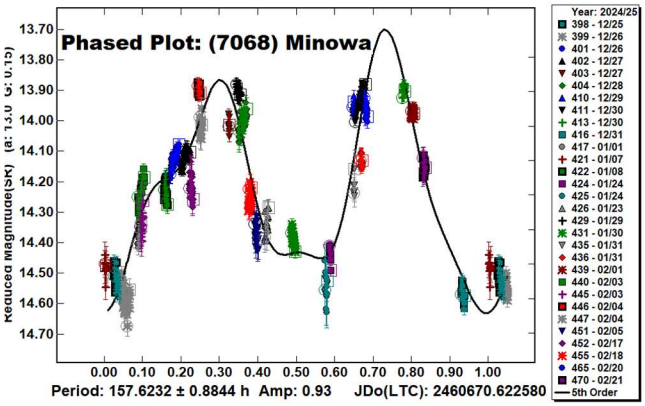

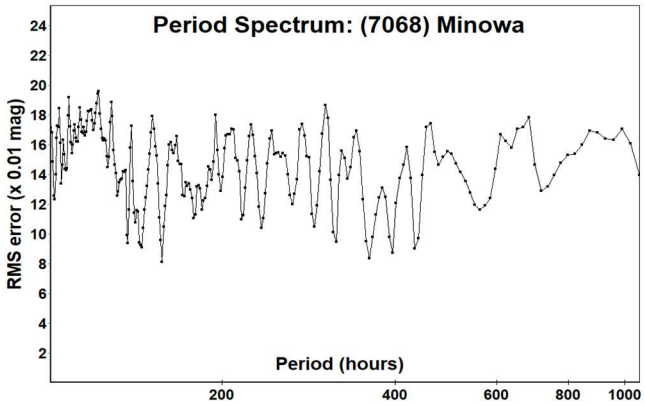

10143 Kamogawa is an outer main-belt asteroid discovered on 1994 January 8 by A. Sugie at Dynic Astronomical Observatory, Japan. This asteroid is named after the river that flows through the center of Kyoto city. The estimated diameter of this asteroid is 22.314 ± 0.078 km corresponding to H = 12.43 mag.

10143 Kamogawa was observed from late December 2024 till early March 2025, with a total of 21 sessions completed by Luckystar (20) and Znith (1) observatories. A total of 846 individual frames were obtained and analyzed. Fourier analysis leads to bimodal solution with an estimated period of P = 62.0305 ± 0.1211 h and an amplitude A = 0.16 ± 0.03 mag. A reported observation of 10143 Kamogawa is available, but no period has been published (Hess et al, 2017).

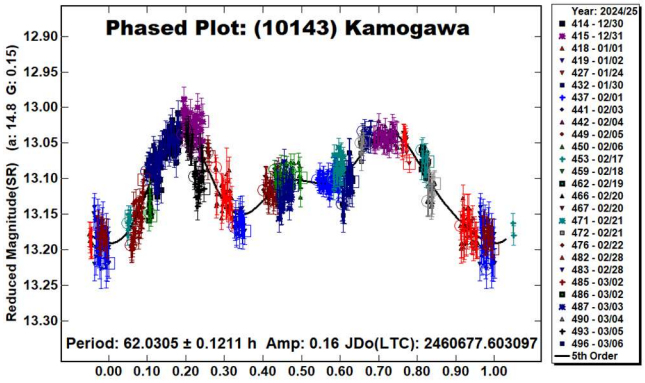

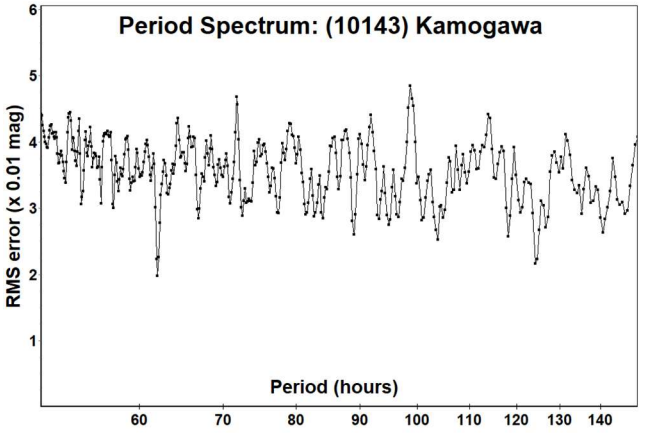

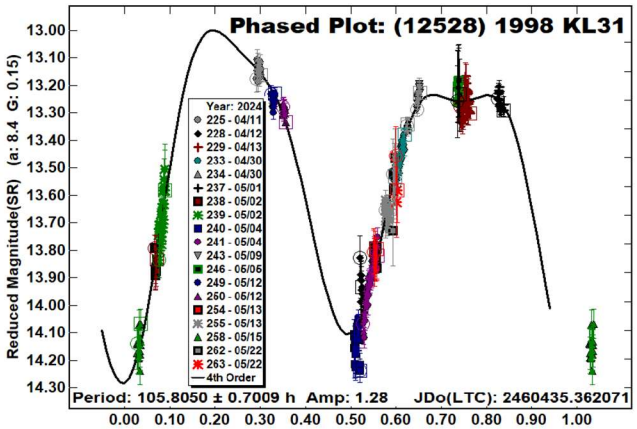

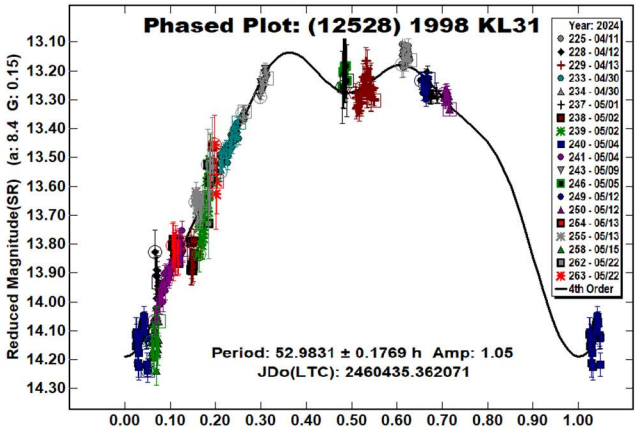

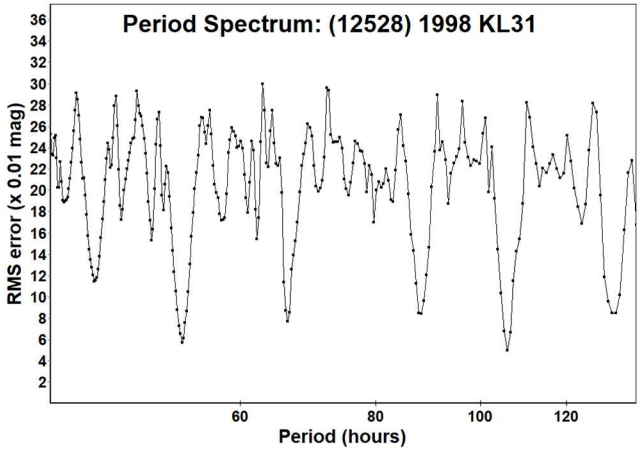

(12528) 1998 KL31 is a Eunomia asteroid family member discovered by the LINEAR system on 1998 May 22 at Socorro. This asteroid has an estimated diameter of 6.653 ± 0.146 km and a corresponding absolute magnitude of H = 12.94 mag.

(12528) 1998 KL31 was observed by our network of observatories between 2024 April 11 and 2024 May 22. Observations from three stations (Luckystar, Flarestar and À la belle étoile observatories) were used to determine the period and amplitude of this target. In total, 334 individual frames were obtained during 15 sessions. Fourier analysis of these observations leads to two potential solutions with basic period of P = 52.9831 ± 0.1769 h and double period P = 105.8050 ± 0.7009 h. The 105.8-hour period appears to be the correct solution, primarily due to physical constraints imposed by the high amplitude observed. Given an amplitude of 1.28 magnitudes, a true period solution would suggest a bimodal rotational state. The large photometric variation through a monomodal solution is far less likely to be the right one despite the lower RMS. Additional coverage to confirm the period of this asteroid is desirable. No previous report of the period for this asteroid has been published.

Number	Name	yyyy mm/dd	Phase	L_{PAB}	B_{PAB}	Period(h)	P.E.	Amp	A.E.	Grp
3595	Gallagher	2024 09/29-10/28	1.5,13.6	6.7	2.6	87.2402	0.6746	0.43	0.04	MB-middle
5704	Schumacher	2025 02/28-04/03	5.8,8.8	172.6	5.6	15.765	0.003	0.27	0.06	MB-outer
7068	Minowa	2024-2025 12/25-02/21	13.5,18.6	117.0	2.2	157.6232	0.8844	0.93	0.08	MB-inner
10143	Kamogawa	2024-2025 12/30-03/06	16.8,15.7	131.6	1.7	62.0305	0.1211	0.16	0.03	MB-outer
12528	1998 KL31	2024 04/11-05/22	8.5,17.8	204.4	15.4	105.8050	0.7009	1.28	0.06	Eunomia

Table II. Observing circumstances and results. The phase angle is given for the first and last date. L_{PAB} and B_{PAB} are the approximate phase angle bisector longitude and latitude at mid-date range (see Harris et al., 1984). Grp is the asteroid family/group (Warner et al., 2009).

Acknowledgements

We would like to thank Brian Warner for his work in the development of *MPO Canopus* and for his efforts in maintaining the CALL website (Warner, 2016; 2021). This research has made use of the JPL's Small-Body Database (JPL, 2025).

References

Berg, S. (2023). Nightime Imaging 'N' Astronomy (NINA) website. https://nighttime-imaging.eu/
Last accessed 6 January 2024.

Harris, A.W.; Young, J.W.; Scaltriti, F.; Zappala, V. (1984). "Lightcurves and phase relations of the asteroids 82 Alkmene and 444 Gyptis." *Icarus* **57**, 251-258.

Hess, K.; Bruner, M.; Ditteon, R. (2017). "Asteroid lightcurve analysis at the Oakley southern sky observatory: 2015 February - March." *Minor Planet Bull.* **44-1**, 3.

JPL (2025). Small-Body Database Browser - JPL Solar System Dynamics web site. *http://ssd.jpl.nasa.gov/sbdb.cgi*
Last accessed: 18 December 2024.

Tonry, J.L.; Denneau, L.; Flewelling, H.; Heinze, A.N.; Onken, C.A.; Smartt, S.J.; Stalder, B.; Weiland, H.J.; Wolf, C. (2018). "The ATLAS All-Sky Stellar Reference Catalog." *Astrophys. J.* **867**, A105.

Warner, B.D.; Harris, A.W.; Pravec, P. (2009). "The Asteroid Lightcurve Database." *Icarus* **202**, 134-146. Updated 2021 Jun. *https://minplanobs.org/MPInfo/php/lcdbsummaryquery.php*

Warner, B.D. (2016). Collaborative Asteroid Lightcurve Link website. *http://www.minorplanet.info/call.html*
Last accessed: 6 January 2024

Warner, B.D. (2017). MPO Software, MPO Canopus version 10.7.10.0. Bdw Publishing. *http://www.minorplanetobserver.com/*

Warner, B.D. (2021). Asteroid Lightcurve Photometry Database (ALCDEF) at https://minplanobs.org/alcdef/index.php

COLLABORATIVE ASTEROID PHOTOMETRY FROM UAI: 2025 APRIL-JUNE

Lorenzo Franco
Balzaretto Observatory (A81), Rome, ITALY
lor_franco@libero.it

Alessandro Marchini, Riccardo Papini
Astronomical Observatory, University of Siena (K54)
Via Roma 56, 53100 - Siena, ITALY

Nello Ruocco
Osservatorio Astronomico Nastro Verde (C82), Sorrento, ITALY

Giulio Scarfi
Iota Scorpii Observatory (K78), La Spezia, ITALY

Luca Buzzi
Schiaparelli Observatory (204), Varese, ITALY

Marco Iozzi
HOB Astronomical Observatory (L63)
Capraia Fiorentina, ITALY

Matteo Lombardo, Niccolò Lombardo
Zen Observatory (M26), Scandicci, ITALY

Gianni Galli
GiaGa Observatory (203), Pogliano Milanese, ITALY

(Received: 2025 July 10)

Photometric observations of five asteroids were made in order to acquire lightcurves for shape/spin axis modeling. Lightcurves were acquired for 992 Swasey, 1155 Aenna, 1326 Losaka, (9058) 1992 JB, and (424482) 2008 DG5.

Collaborative asteroid photometry was done inside the Italian Amateur Astronomers Union (UAI, 2025) group. The targets were selected mainly in order to acquire lightcurves for shape/spin axis modeling. Table I shows the observing circumstances and results.

The CCD observations were made in 2025 April-June using the instrumentation described in Table II. Lightcurve analysis was performed at the Balzaretto Observatory with *MPO Canopus* (Warner, 2023). All the images were calibrated with dark and flat frames and converted to standard magnitudes using solar colored field stars from CMC15 and ATLAS catalogues, distributed with *MPO Canopus*. For brevity, "LCDB" is a reference to the asteroid lightcurve database (Warner et al., 2009).

992 Swasey is a low albedo outer main-belt asteroid. The reflectance spectrum for 992 Swasey, extracted from Gaia ESA Archive (2025), is close to a D-type when compared with the Bus-DeMeo taxonomy (DeMeo et al., 2009). Multiband photometry was acquired by M. Iozzi (L63) on 2025 June 15, from which we found a color index V-R = 0.47 ± 0.05, consistent with a D-type asteroid (Pravec et al., 2012; 0.455 ± 0.033).

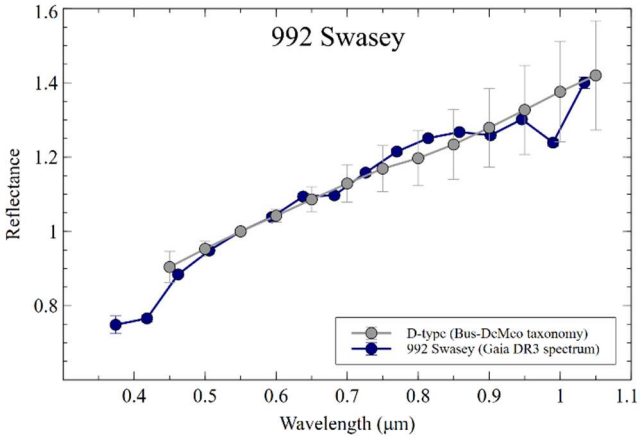

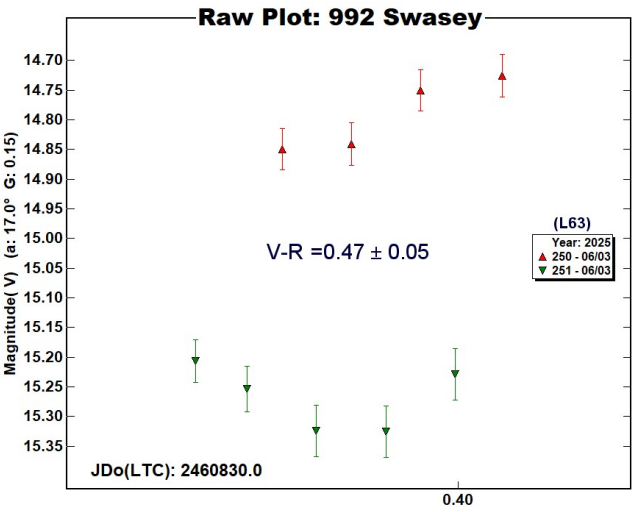

1155 Aenna is a Xe-type (Bus and Binzel, 2002) inner main-belt asteroid. Observations by N. Ruocco (C82) were made over seven nights. The period analysis shows a synodic period of P = 7.905 ± 0.001 h with an amplitude A = 0.26 ± 0.03 mag. The period is close to the previously published results in the LCDB.

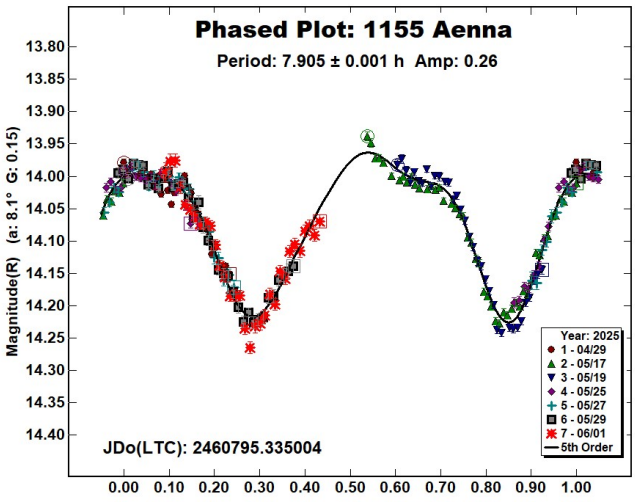

1326 Losaka is a CSU-type (Tholen, 1984) middle main-belt asteroid. Observations by A. Marchini and R. Papini (K54) were made over seven nights. The period analysis shows a quadrimodal solution with a synodic period of P = 5.279 ± 0.001 h and an amplitude A = 0.07 ± 0.03 mag. This period differs from the solution found by Warner (2006; 6.900 ± 0.001).

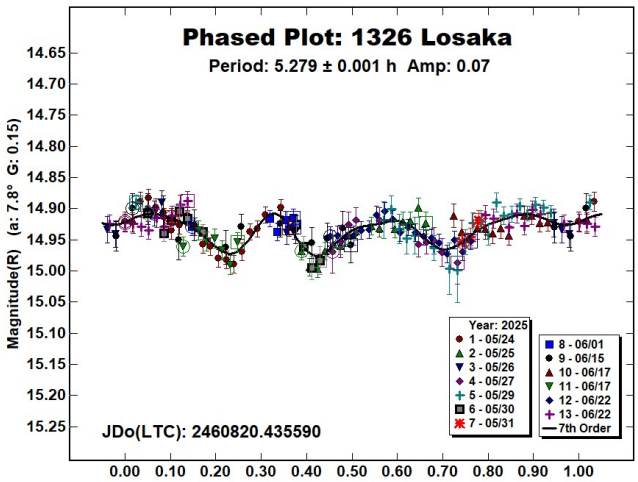

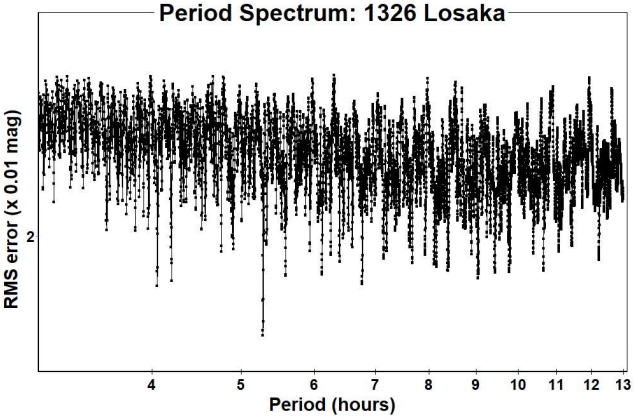

(9058) 1992 JB is an Apollo Near-Earth asteroid. Collaborative observations were made over six nights. We found a bimodal solution with a synodic period of P = 10.508 ± 0.002 h and an amplitude A = 0.39 ± 0.10 mag. No others periods were found in the LCDB.

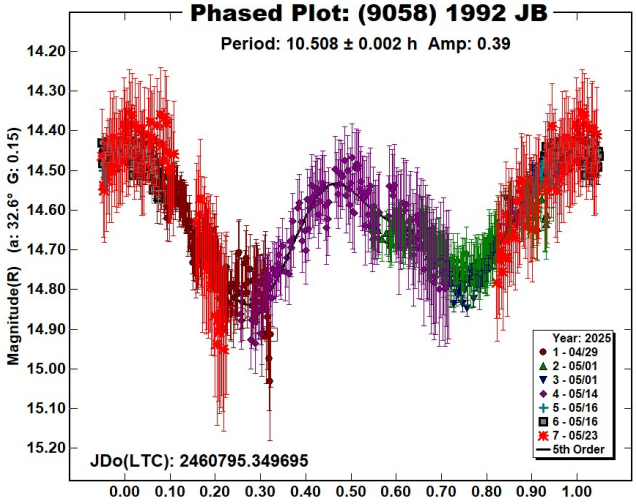

Number	Name	2025 mm/dd	Phase	L_{PAB}	B_{PAB}	Period(h)	P.E.	Amp	A.E.	Grp
992	Swasey	06/03	17.0	209	1					MB-O
1155	Aenna	04/29-06/01	8.1-22.7	208	1	7.905	0.001	0.26	0.03	MB-I
1326	Losaka	05/24-06/22	*7.7-5.7	260	8	5.279	0.001	0.07	0.03	MB-M
9058	1992 JB	04/29-05/23	*32.6-34.9	212	9	10.508	0.002	0.39	0.10	NEA
424482	2008 DG5	05/25-06/04	25.6-68.7	230	8	11.12	0.01	0.25	0.04	NEA

Table I. Observing circumstances and results. The first line gives the results for the primary of a binary system. The second line gives the orbital period of the satellite and the maximum attenuation. The phase angle is given for the first and last date. If preceded by an asterisk, the phase angle reached an extrema during the period. L_{PAB} and B_{PAB} are the approximate phase angle bisector longitude/latitude at mid-date range (see Harris et al., 1984). Grp is the asteroid family/group (Warner et al., 2009).

Observatory (MPC code)	Telescope	CCD	Filters	Observed Asteroids (#Sessions)
Astronomical Observatory, University of Siena (K54)	0.30-m MCT f/5.6	SBIG STL-6303e (bin 2×2)	C, V, Rc, Ic	1326(7) 424482(4)
Osservatorio Astronomico Nastro Verde (C82)	0.35-m SCT f/6.3	SBIG ST10XME (bin 2x2)	C	1155(7)
Iota Scorpii(K78)	0.40-m RCT f/6.1	CMOS QHY 268 (bin 4x4)	C	9058(5)
Schiaparelli Observatory (204)	0.84-m NRT f/3.5	Moravian C3-61000 PRO (bin 4×4)	C	9058(2)
HOB Astronomical Observatory (L63)	0.20-m SCT f/6.0	ATIK 383L+ (bin 2x2)	C, V, Rc	992(1) 424482(1)
Zen Observatory (M26)	0.30-m RCT f/7.4	ATIK 383L+ (bin 2x2)	C	424482(2)
GiaGa Observatory (203)	0.36-m SCT f/5.8	Moravian G2-3200	C	9058(1)

Table II. Observing Instrumentations. MCT: Maksutov-Cassegrain, NRT: Newtonian Reflector, RCT: Ritchey-Chretien, SCT: Schmidt-Cassegrain.

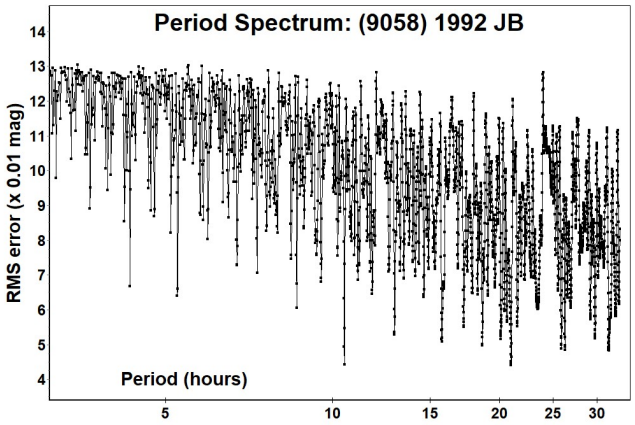

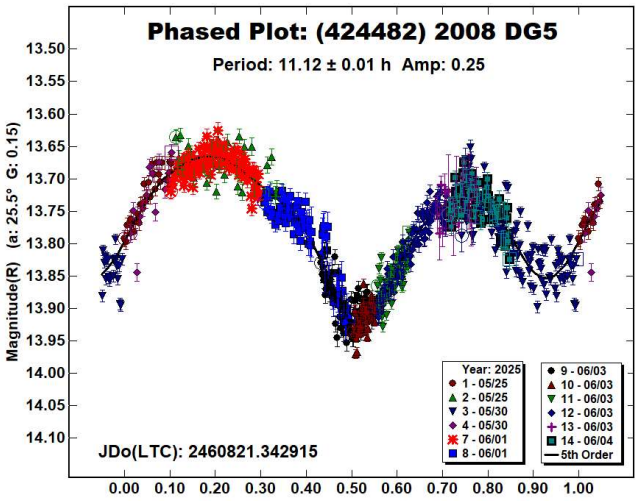

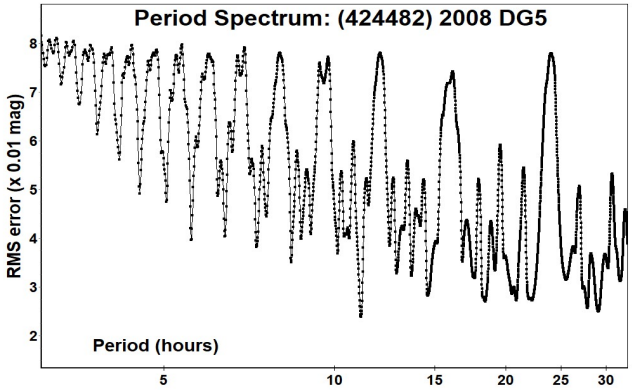

(424482) 2008 DG5 is an Apollo Near-Earth asteroid, classified as Potentially Hazardous Asteroid (PHA). Collaborative observations were made over four nights. We found a bimodal solution with a synodic period of P = 11.12 ± 0.01 h and an amplitude A = 0.25 ± 0.04 mag. No others periods were found in the LCDB. Multiband photometry was acquired by A. Marchini and R. Papini (K54) on 2025 May 30, from which we found the color indices V-R = 0.48 ± 0.03; R-I = 0.37 ± 0.04. both close to a S-type asteroid (Shevchenko and Lupishko, 1998; 0.49 ± 0.05; 0.41 ± 0.06).

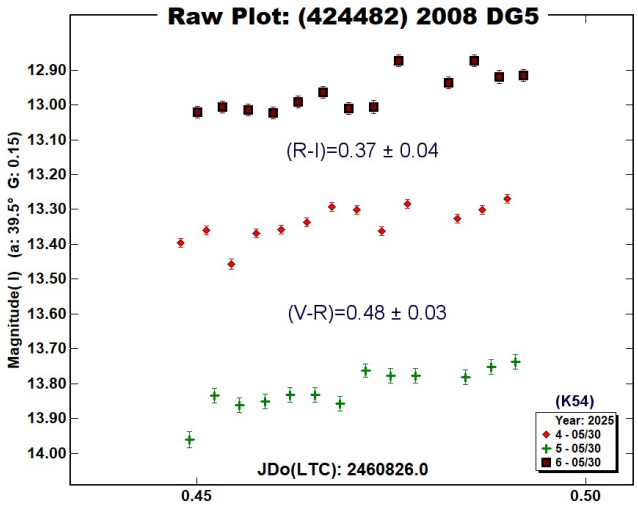

References

Bus, S.J.; Binzel, R.P. (2002). "Phase II of the Small Main-Belt Asteroid Spectroscopic Survey - A Feature-Based Taxonomy." *Icarus* **158**, 146-177.

DeMeo, F.E.; Binzel, R.P.; Slivan, S.M.; Bus, S.J. (2009). "An extension of the Bus asteroid taxonomy into the near infrared." *Icarus* **202**, 160-180.

Gaia ESA Archive (2025), version 3.7. *https://gea.esac.esa.int/archive/*

Harris, A.W.; Young, J.W.; Scaltriti, F.; Zappala, V. (1984). "Lightcurves and phase relations of the asteroids 82 Alkmene and 444 Gyptis." *Icarus* **57**, 251-258.

Pravec, P.; Harris, A.W.; Kušnirák, P.; Galád, A.; Hornoch, K. (2012). "Absolute magnitudes of asteroids and a revision of asteroid albedo estimates from WISE thermal observations." *Icarus* **221**, 365-387.

Shevchenko, V.G.; Lupishko, D.F. (1998). "Optical properties of Asteroids from Photometric Data." *Solar System Research* **32**, 220-232.

Tholen, D.J. (1984). "Asteroid taxonomy from cluster analysis of Photometry." Doctoral Thesis. University Arizona, Tucson.

UAI (2025), "Unione Astrofili Italiani" web site. *https://www.uai.it*

Warner, B.D. (2006). "Asteroid lightcurve analysis at the Palmer Divide Observatory - February - March 2006." *Minor Planet Bulletin* **33**, 82-84.

Warner, B.D.; Harris, A.W.; Pravec, P. (2009) "The asteroid lightcurve database." *Icarus* **202**, 134-146. Updated 2025 June 26. *https://minplanobs.org/alcdef/index.php*

Warner, B.D. (2023). MPO Software, MPO Canopus v10.8.6.20. Bdw Publishing. *http://minorplanetobserver.com*

V-R COLOR INDICES FOR NINE MAIN-BELT ASTEROIDS

Marco Iozzi
H.O.B Astronomical Observatory
Capraia Fiorentina, ITALY
mioxzy@gmail.com

(Received: 2025 July 14)

We present V-R color indices for a sample of nine main-belt asteroids. Observations were conducted from the H.O.B. Astronomical Observatory (MPC code L63) between June 28 and July 04, 2025.

All observations were conducted at the H.O.B. Astronomical Observatory (MPC code L63). The instrumentation consists of a 0.20-m f/6 Schmidt-Cassegrain telescope. Images were acquired with an ATIK 383L+ monochrome CCD camera, featuring a Kodak KAF-8300 sensor. The image scale is 1.9 arcsec/pixel. All observations were performed with the targets at an altitude greater than 30 degrees above the horizon. For each target, a time-series of exposures was acquired by alternating between the Johnson-Cousins V and Rc filters.

All science frames were calibrated in a standard manner using dark and flat-field frames and converted to standard magnitudes using solar-colored field stars from ATLAS catalogues distributed with *MPO Canopus* (Warner, 2019). Instrumental magnitudes were extracted by aperture photometry in *MPO Canopus* (Warner, 2019). Each calibrated frame was analysed by differential photometry against five solar-coloured ATLAS comparison stars, common to both V and Rc filters. The V-R color index is reported as the mean of these measurements, with its uncertainty given by the standard error of the mean.

329 Svea is a C-type (Bus and Binzel, 2002) inner main-belt asteroid. Observations were made on 2025 June 28. We found a color index of V-R = 0.41 ± 0.02. Our value lies near the upper end for C-Type asteroids (V-R = 0.38 ± 0.05; Shevchenko and Lupishko, 1998).

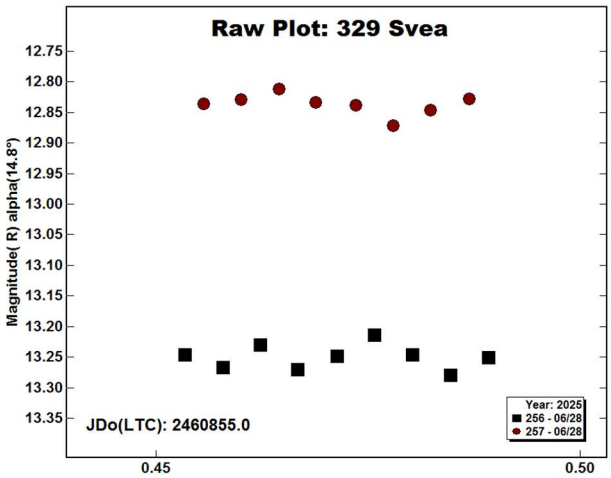

347 Pariana is an M-type (Tholen, 1984) middle main-belt asteroid. Observations were made on 2025 July 01. We found a color index of V-R = 0.43 ± 0.06. This value falls within the expected range for M-type asteroids (V-R = 0.42 ± 0.04; Shevchenko and Lupishko, 1998).

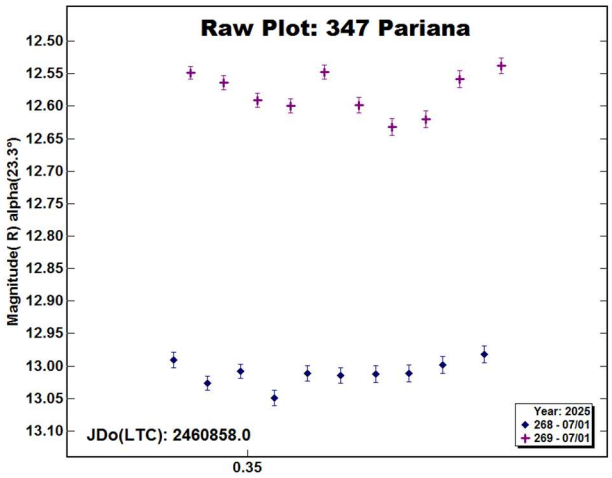

451 Patientia is a Cb-type (Bus and Binzel, 2002) outer main-belt asteroid. Observations were made on 2025 June 28. We found a color index of V-R = 0.36 ± 0.03. This value falls within the expected range for C-Type asteroids (V-R = 0.38 ± 0.05; Shevchenko and Lupishko, 1998).

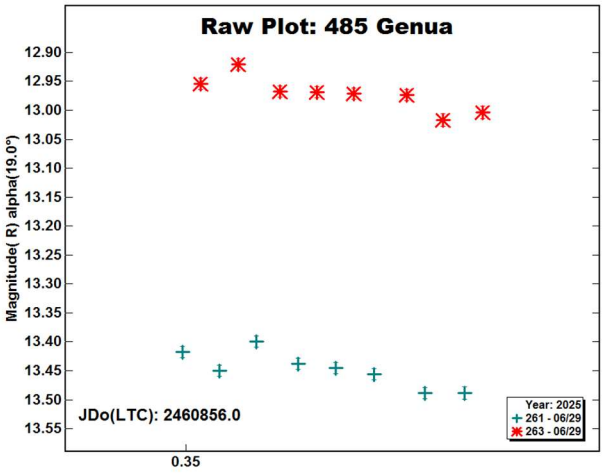

582 Olympia is an S-type (Bus and Binzel, 2002) middle main-belt asteroid. Observations were made on 2025 July 03. We found a color index of V-R = 0.50 ± 0.04. This value falls within the expected range for S-type asteroid (V-R = 0.49 ± 0.05; Shevchenko and Lupishko, 1998).

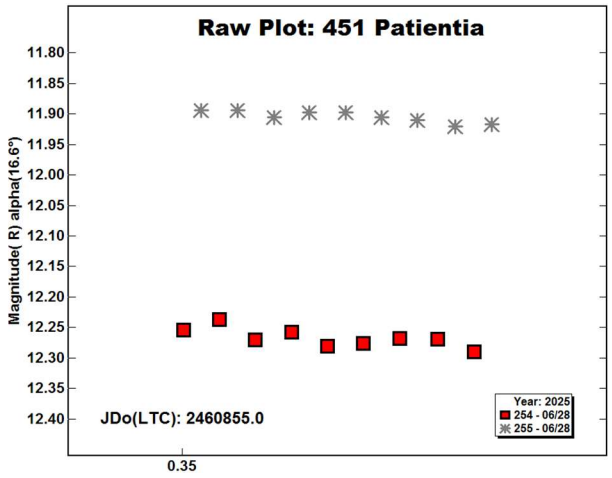

485 Genua is an S-type (Bus and Binzel, 2002) middle main-belt asteroid. Observations were made on 2025 June 29. We found a color index of V-R = 0.48 ± 0.03. This value falls within the expected range for S-type asteroids (V-R = 0.49 ± 0.05; Shevchenko and Lupishko, 1998).

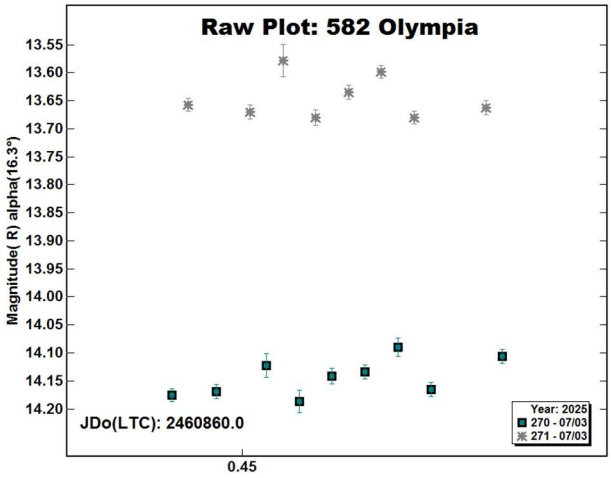

619 Triberga is an S-type (Bus and Binzel, 2002) middle main-belt asteroid. Observations were made on 2025 July 01. We found a color index of V-R = 0.51 ± 0.03. This value falls within the expected range for S-type asteroid (V-R = 0.49 ± 0.05; Shevchenko and Lupishko, 1998).

Number	Name	2025 mm/dd	Phase	L_{PAB}	B_{PAB}	Period(h)	P.E.	Amp	A.E.	Grp
329	Svea	06/28	14.8	255	21					MB-I
347	Pariana	07/01	23.3	225	7					MB-M
451	Patientia	06/28	16.6	219	11					MB-O
485	Genua	06/29	19.0	217	9					MB-M
582	Olympia	07/03	16.3	245	35					MB-M
619	Triberga	07/01	11.3	265	18					MB-M
670	Ottegebe	07/04	5.3	289	9					MB-M
788	Hohensteina	06/29	8.7	268	18					MB-O
805	Hormuthia	06/29	12.3	258	20					MB-O

Table I. Observing circumstances and results. The phase angle is given for the first and last date. If preceded by an asterisk, the phase angle reached an extrema during the period. L_{PAB} and B_{PAB} are the approximate phase angle bisector longitude/latitude at mid-date range (see Harris et al., 1984). Grp is the asteroid family/group (Warner et al., 2009).

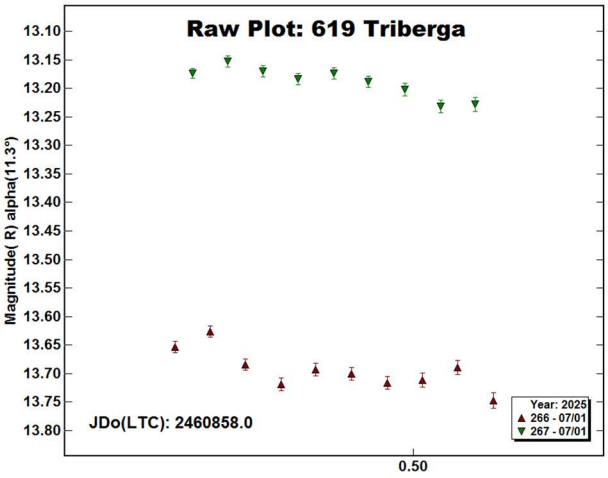

670 Ottegebe is an S-type (Bus and Binzel, 2002) middle main-belt asteroid. Observations were made on 2025 July 04. We found a color index of V-R = 0.47 ± 0.04. This value falls within the expected range for S-type asteroid (V-R = 0.49 ± 0.05; Shevchenko and Lupishko, 1998).

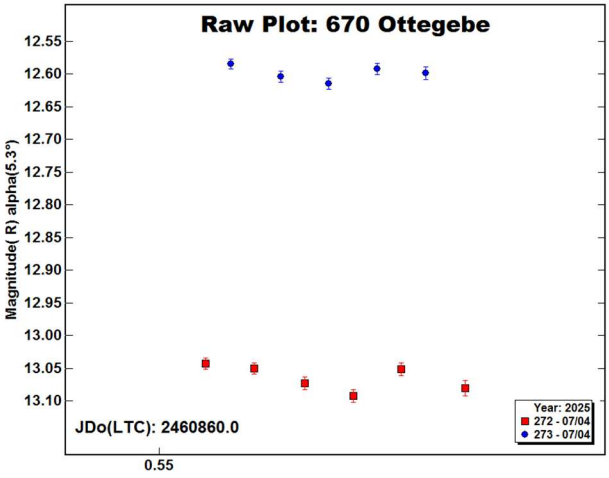

788 Hohensteina is a Ch-type (Bus and Binzel, 2002) outer main-belt asteroid. Observations were made on 2025 June 29. We found a color index of V-R = 0.38 ± 0.04. This value is in agreement with the reference for C-Type asteroid (V-R = 0.38 ± 0.05; Shevchenko and Lupishko, 1998).

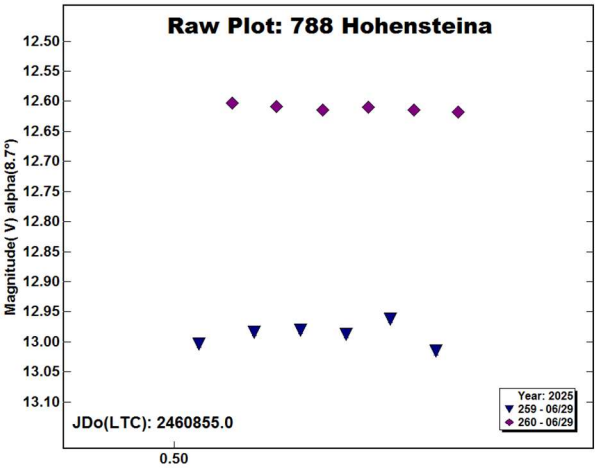

805 Hormuthia is a CX-type (Tholen, 1984) outer main-belt asteroid. Observations were made on 2025 June 29. We found a color index of V-R = 0.42 ± 0.02. This value agrees with a M-type asteroid (V-R = 0.42 ± 0.04; Shevchenko and Lupishko, 1998).

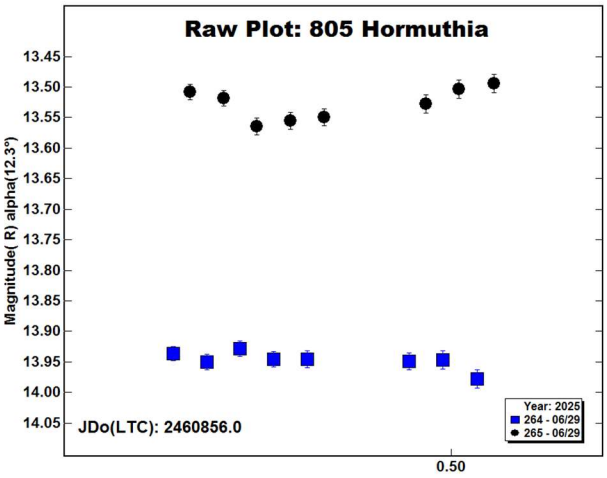

Acknowledgements

We would like to thank Lorenzo Franco for helpful discussions and for insightful comments that greatly improved this manuscript. We are deeply grateful to Maura Tombelli for introducing us to the field of asteroid studies and for her continued guidance and mentorship.

References

Bus, S.J., Binzel, R.P. (2002). "Phase II of the Small Main-Belt Asteroid Spectroscopic Survey: A Feature-Based Taxonomy." *Icarus* **158**, 146-177.

Harris, A.W.; Young, J.W.; Scaltriti, F.; Zappala, V. (1984). "Lightcurves and phase relations of the asteroids 82 Alkmene and 444 Gyptis." *Icarus* **57**, 251-258.

JPL (2016). Small Body Database Search Engine. *http://ssd.jpl.nasa.gov/sbdb_query.cgi*

Shevchenko, V.G.: Lupishko, D.F. (1998). "Optical properties of Asteroids from Photometric Data." *Solar System Research* **32**, 220-232.

Tholen, D.J. (1984). "Asteroid taxonomy from cluster analysis of Photometry." Doctoral Thesis. University Arizona, Tucson.

Warner, B.D.; Harris, A.W.; Pravec, P. (2009). "The Asteroid Lightcurve Database." *Icarus* **202**, 134-146. Updated 2016 Sep. *http://www.minorplanet.info/lightcurvedatabase.html*

Warner, B.D. (2019). MPO Software, MPO Canopus v10.8.1.1. Bdw Publishing. *http://minorplanetobserver.com*

A STUDY AND REVIEW OF THE LIGHTCURVES AND ROTATION PERIODS OF 10 ASTEROIDS

Rafael González Farfán (Z55)
Observatorio Uraniborg
Écija, Sevilla, SPAIN
uraniborg16@gmail.com

Faustino García de la Cuesta (J38)
La Vara, Valdés
Asturias, SPAIN

Esteban Reina Lorenz (232)
Masquefa, Can Parellada
Barcelona, SPAIN

Carlos Botana Albá (Y85)
Observatorio en Magalofes
Fene, A Coruña, SPAIN

Javier De Elías Cantalapiedra (L46)
Observatorio en Majadahonda
Madrid SPAIN

Javier Ruiz Fernández (J96)
Observatorio de Cantabria
Cantabria, SPAIN

Fernando Limón Martínez (Z50)
Observatorio Mazariegos
Mazariegos, Palencia, SPAIN

Juan Collada Bárcena (945)
Alfonso Coya Lozano
Observatorio Monte Deva
Gijón, SPAIN

Javier Polancos Ruiz
Observatorio La Portilla
Llanes, Asturias, SPAIN

(Received: 2025 June 30 Revised: 2025 August 15)

This paper presents the results of a photometric study of ten asteroids and their rotation periods. The 10 asteroids studied were: 498 Tokio (41.843 h), 502 Sigune (10.929 h), 790 Pretoria (10.385 h), 1055 Tynka (5.951 h), 1254 Erfordia (12.286 h), 1263 Varsavia (7.166 h), 1318 Nerina (2.527 h), 1342 Brabantia (4.172 h), 3774 Megumi (3.573 h), and 5632 Ingelehmann (3.780 h).

We report observations that were conducted during the first half of 2025. In some cases, we were able to confirm the published results for the rotation period. However, in other cases, we could not find any such results in the literature, so we present our own as a contribution in the hope that they may be confirmed (or not) by other authors.

As on other occasions, the images obtained were calibrated in the conventional mode, without photometric filter, and with the application of darks, bias and flats. Data analysis and processing were performed using *FotoDif* (2021), *Tycho Tracker* (2023) and *Períodos* (2020) software. In addition, all data were light-time corrected. The results are summarized below. Individual lightcurve plots along additional comments as required are also presented.

498 Tokio. This asteroid, discovered in December 1902 from the Nice Observatory, was observed again in 2018 and 2020 (Pal et al., 2020) and found to have a rotation period of 41.85 hours. Our observations were carried out from February to May 2025 and obtained a rotation period that was very similar to that previously published: P = 41.843 ± 0.009 hours, and an amplitude A = 0.170 ± 0.014. Our plotted curve had more than 2000 points.

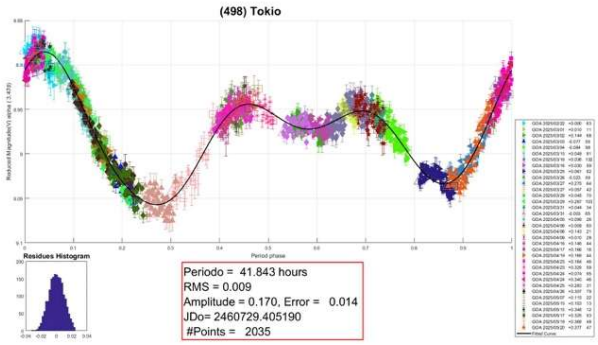

502 Sigune. One of the most recently published rotation periods for this asteroid, which was discovered in January 1903, is from 2014 (Stephens, 2014). This is very consistent with the value obtained by our team during observations in March and April 2025: P = 10.929 ± 0.018 hours and A = 0.450 ± 0.025 magnitude units, with a curve comprising approximately 840 data points.

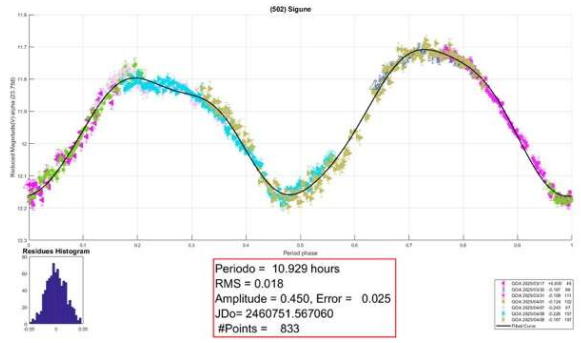

790 Pretoria. Most of the observations of this asteroid were carried out by our team in March and April 2025. Behrend (2021web) reports results which coincide with our findings for the rotation period: P = 10.385 ± 0.010 hours and A = 0.070 ± 0.014.

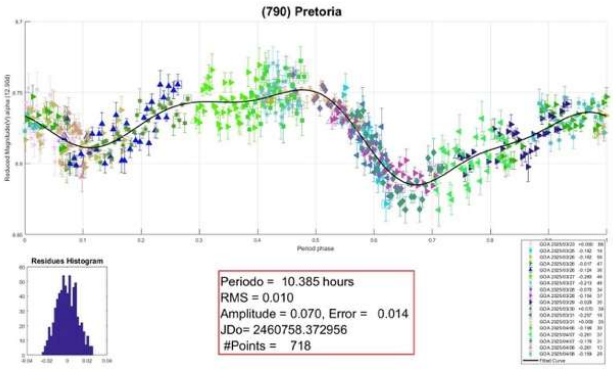

1055 Tynka. Discovered in November 1925, Tynka belongs to the main-belt. While multiple results are reported in the ALCDEF, the data obtained by our team in April and May 2025 are more in agreement with those reported by Behrend (2021web). We obtained P = 5.951 ± 0.026 hours and A = 0.240 ± 0.037.

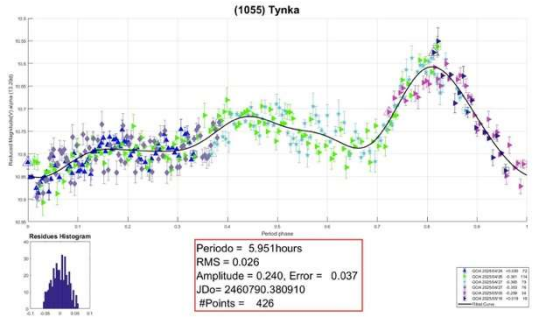

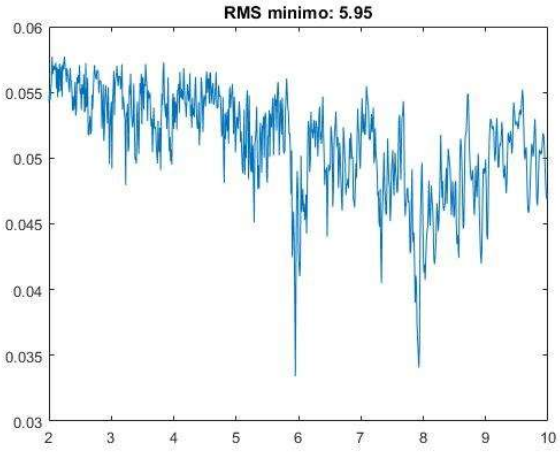

In addition, we have combined our lightcurves with dense lightcurves from ALCDEF and DAMIT, as well as AstDys sparse data (from ATLAS, CATALINA, LONEOS, PALOMAR and USNO), applying the lightcurve inversion method implemented in the MPO package *LCInvert* (BDW Publishing, 2016). We obtained a spin axis of Lambda = 248.301, Beta = 11.231 and P = 5.94678042.

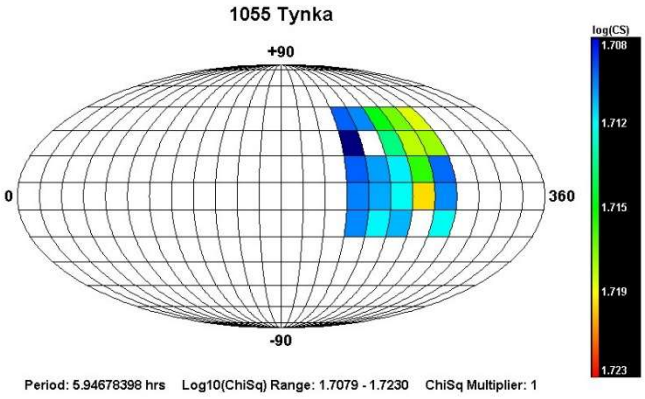

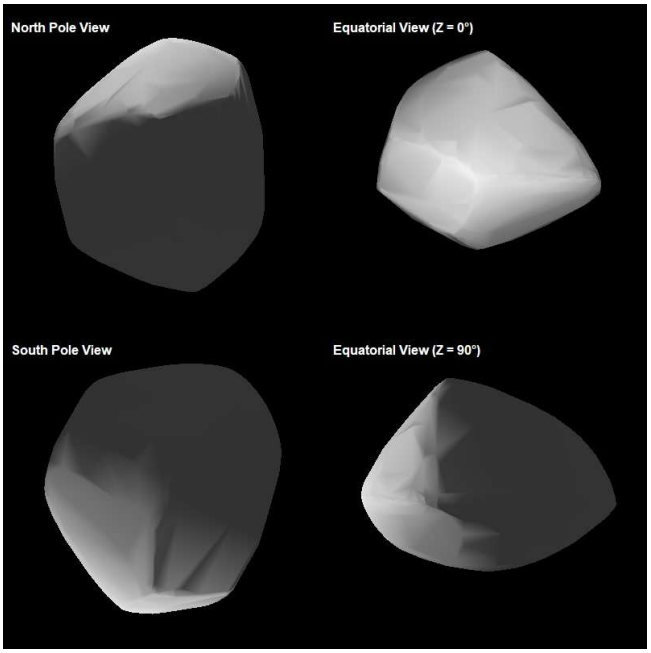

1254 Erfordia. The latest published data on the rotation period of this asteroid is from Durech et al. (2019). Similarly, ALCDEF provides a result that coincides with that obtained by our team in January 2025: P = 12.286 ± 0.025 hours and A = 0.550 ± 0.035.

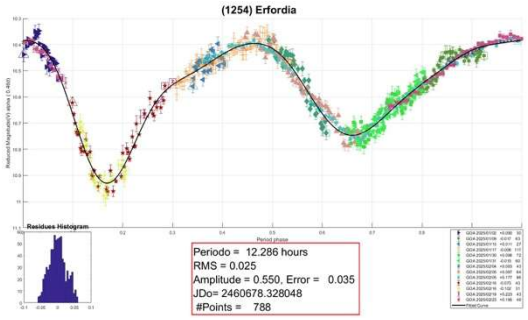

1263 Varsavia. This asteroid, belonging to the main asteroid belt and discovered in 1933, was studied by our team in May 2025. The latest observations recorded in the ALCDEF database correspond to 2018, although Pal et al. (2020) appear to have made observations more recently. Our current results confirm previous studies, as we obtained a coincident rotation period: P = 7.166 ± 0.011 hours and A = 0.260 ± 0.016.

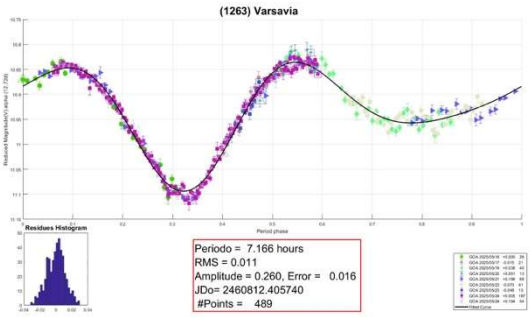

Number	Asteroid	20yy mm/dd	Phase	Period(h)	P.E.	Amp	A.E.
498	Tokio	25/02/22-25/05/20	3.5,18.2	41.843	0.009	0.170	0.014
502	Sigune	25/03/17-25/04/08	23.6,20.1	10.929	0.018	0.450	0.025
790	Pretoria	25/03/23-25/04/08	14.9,14.6	10.385	0.010	0.070	0.014
1055	Tynka	25/04/23-25/05/16	12.3,20.6	5.951	0.026	0.240	0.03
1254	Erfordia	25/01/02-25/02/25	10.5,16.2	12.286	0.025	0.550	0.035
1263	Varsavia	25/05/16-25/05/24	12.7,13.5	7.166	0.011	0.260	0.016
1318	Nerina	25/03/09-25/04/01	6.2,17.3	2.527	0.018	0.080	0.025
1342	Brabantia	25/02/19-25/02/23	7.2, 9.4	4.172	0.017	0.160	0.024
3774	Megumi	25/02/22-25/03/09	3.2, 7.2	3.573	0.026	0.200	0.036
5632	Ingelehmann	25/04/27-25/05/17	10.3, 5.3	3.780	0.015	0.080	0.021

Table I. Observing circumstances and results. Phase is the solar phase angle given at the start and end of the date range. If preceded by an asterisk, the phase angle reached an extrema during the period.

1318 Nerina. The most recent observations of this asteroid in the literature date from Franco et al. (2018). Our results, obtained in May 2025, confirm the same values for P = 2.527 ± 0.018 hours and A = 0.080 ± 0.025.

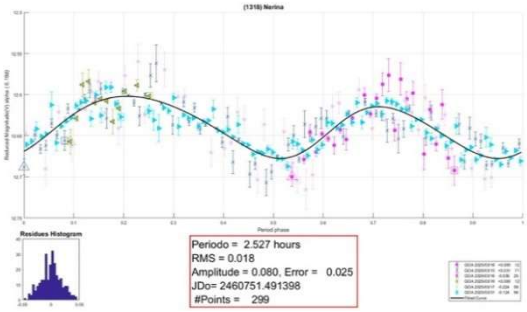

1342 Brabantia. This asteroid, which has been widely studied in recent years, was part of our February 2025 observing campaign. We obtained a result for the rotation period that is in very good agreement with previous results (Franco et al. 2018). P = 4.172 ± 0.017 hours and A = 0.160 ± 0.024.

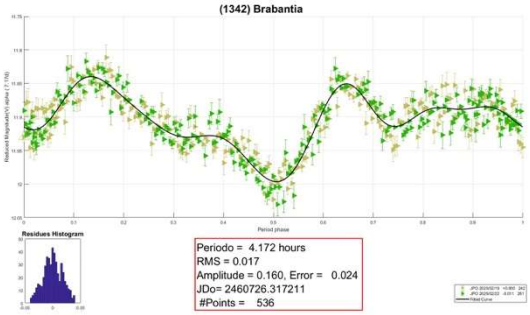

3774 Megumi. At the time of writing, we had not located any previous data on this asteroid's rotation period or any published lightcurve in the literature. During our studies in February and March 2025, we obtained a rotation period of P = 3.573 ± 0.026 hours and an amplitude of A = 0.200 ± 0.036.

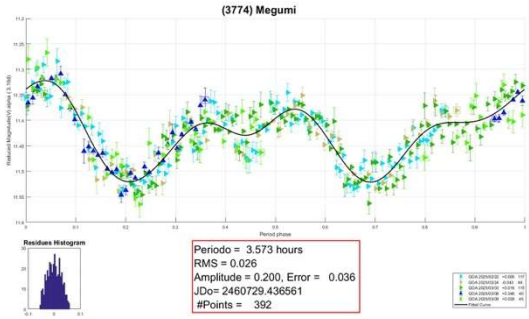

5632 Ingelehmann. As we could not find any results for this asteroid's rotation period or lightcurve in the literature, our team observed it in April and May 2025. We were able to determine a rotation period of P = 3.780 ± 0.015 and an amplitude of A = 0.080 ± 0.021.

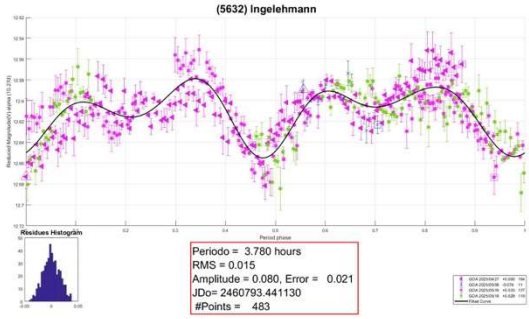

Its periodogram gives support to this result.

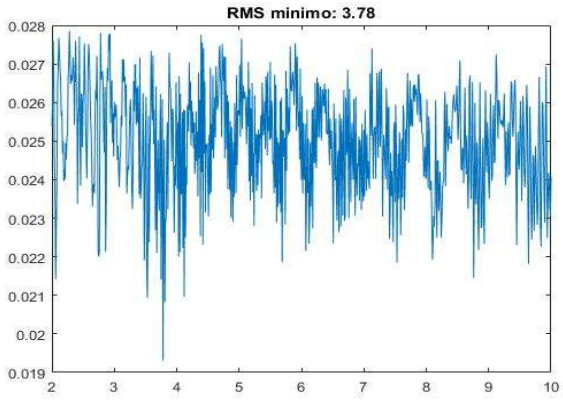

Observer	Telescope	Camera
Botana Albá, Carlos (Y85)	Newton 8”	ZWO ASI183M Pro
Collada Bárcena, Juan (945) Coya Lozano, Alfonso	SC 14”	ZWO 294MM Pro
De Elías Cantalapiedra, Javier (L46)	CDK 12.5”	QHY268m
García de la Cuesta, Faustino (J38)	RCX 10”	SBIG ST8XE
González Farfán, Rafael (Z55)	SC 11”	Atik414ex m
Limón Martínez, Fernando (Z50)	SC 8”	ZWO ASI533MM Pro
Polancos Ruiz, Javier	Vixen ED103S	QHY5III200M
Reina Lorentz, Esteban (232)	SC 10”	ZWO 294MM
Ruiz Fernández, Javier (J96)	RC 16”	ST8XME

Table II. Observers and equipment.

References

ALCDEF. Asteroid Lightcurve Data Exchange Format web site. *http://alcdef.org*

Behrend, R. (2021web) Observatoire de Geneve web site. *http://obswww.unige.ch/~behrend/page_cou.html*

DAMIT. *https://damit.cuni.cz/*

Durech, J.; Hanus, J.; Vanco, R. (2019). “Inversion of Asteroid Photometry from Gaia DR2 and the Lowell Observatory Photometric Database.” *Astron. Astrophys.* **631**, A2.

FotoDif (2021) software.
http://astrosurf.com/orodeno/fotodif/index.htm

Franco, L.; De Pieri, A.; Brosia, A.; Papini, R.; Salvaggio, F. and 17 colleagues (2021). “Collaborative Asteroid Photometry from UAI: 2020 October-December.” *Minor Planet Bull.* **48**, 120-122.

Franco, L.; Marchini, A.; Baj, G.; Scarfi, G.; Casalnuovo, G.B.; Luna, V.; Bachini, M.; Bacci, P.; Maestripieri, M.; Bacci, R; Galli, G. (2018). “Lightcurves for 1318 Nerina, 1342 Brabantia, 1981 Midas, and 3951 Zichichi.” *Minor Planet Bull.* **4**5, 273-275.

JPL. Small-Body Database Lookup.
https://ssd.jpl.nasa.gov/tools/sbdb_lookup.html#/?sstr=52768

MPO Canopus.
https://minplanobs.org/bdwpub/php/mpocanopus.php

Pal, A.; Sazkáta, R.; Kiss, C.; Bódi, A.; Bognár, Z.; Kalup, C.; Kiss, L.; Marton, G.; Molnár, L.; Plachy, E.; Sárneczky, K.; Szabó, G.; Szabó, R. “Solar System Objects Observed with TESS - First Data Release: Bright Main-belt and Trojan Asteroids from the Southern Survey.” *The Astrophysical Journal Supplement Series* **247**(1), id. 26. 9pp.

Períodos (2020) software.
http://www.astrosurf.com/salvador/Programas.html

Stephens, R.D. (2014). “Asteroids Observed from CS3: 2014 January - March.” *Minor Planet Bull.* **4**1, 171-175.

Tycho Tracker (2023) software.
https://www.tycho-tracker.com

LIGHTCURVES AND SYNODIC ROTATIONAL PERIODS FOR 16 ASTEROIDS: 2025 FEBRUARY - JUNE

Vladimir Benishek
Belgrade Astronomical Observatory
Volgina 7, 11060 Belgrade 38, SERBIA
vlaben@yahoo.com

(Received: 2025 July 15)

Lightcurves and synodic rotation periods for 16 asteroids determined from photometric observations conducted at the Sopot Astronomical Observatory in the time span 2025 February - June are presented.

Photometric observations of 16 asteroids were conducted at Sopot Astronomical Observatory (SAO) from 2025 February through June in order to determine the asteroids' synodic rotation periods. For this purpose, two 0.35-m *f*/6.3 Meade LX200GPS Schmidt-Cassegrain telescopes were employed. The telescopes are equipped with a SBIG ST-8 XME and a SBIG ST-10 XME CCD cameras. The exposures were unfiltered and unguided for all targets. Both cameras were operated in 2×2 binning mode, which produces image scales of 1.66 arcsec/pixel and 1.25 arcsec/pixel for ST-8 XME and ST-10 XME cameras, respectively. Prior to measurements, all images were corrected using dark and flat field frames.

Photometric reduction was conducted using *MPO Canopus* (Warner, 2018). Differential photometry with up to five comparison stars of near solar color ($0.5 \leq$ B-V ≤ 0.9) was performed using the Comparison Star Selector (CSS) utility. This helped ensure a satisfactory quality level of night-to-night zero-point calibrations and correlation of the measurements within the standard magnitude framework. Field comparison stars were calibrated using standard Cousins R magnitudes derived from the Carlsberg Meridian Catalog 15 (VizieR, 2025) Sloan r' magnitudes using the formula: R = r' - 0.22 in all cases presented in this paper. In some instances, small zero-point adjustments were necessary in order to achieve the best match between individual data sets in terms of achieving the most favorable statistical indicators of Fourier fit goodness.

Lightcurve construction and period analysis was performed using *Perfindia* custom-made software developed in the R statistical programming language (R Core Team, 2025) by the author of this paper. The essence of its algorithm is reflected in finding the most favorable solution for rotational period by minimizing the *residual standard error* of the lightcurve Fourier fit. A description of the method implemented in the Perfindia algorithm is given in the reference Benishek (2025).

The lightcurve plots presented in this paper show so-called 2% error for rotational periods, i.e. an error that would cause the last data point in a combined data set by date order to be shifted by 2% (Warner, 2012) and represented by the following formula:

$$\Delta P = \frac{0.02 \cdot \mathrm{T}}{P^2}$$

where P and T are the rotational period and the total time span of observations, respectively. Both of these quantities must be expressed in the same units.

Table I gives the observing circumstances and results.

Observations and results

2159 Kukkamaki. A bimodal period of P = 3.8234 ± 0.0007 h obtained from data collected over 4 nights in 2025 April-May is quite consistent with the previously found rotation period result by Behrend (2021web, 3.867 h).

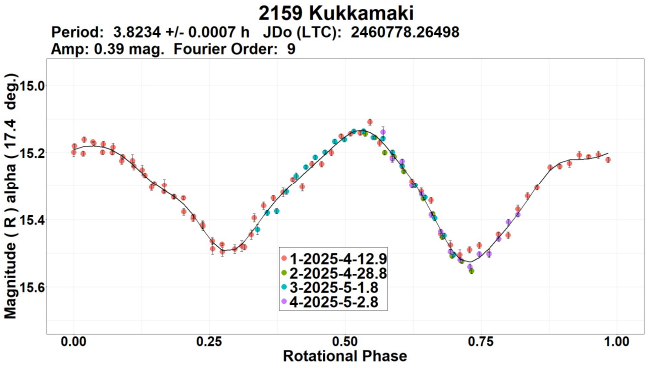

2820 Iisalmi. A bimodal solution for rotational period of P = 2.7581 ± 0.0004 h is almost identical to the two previously known period results present in the Asteroid Lightcurve Database records (LCDB; Warner et al., 2009): 2.7580 h (Behrend, 2020web) and 2.7579 h (Benishek, 2023).

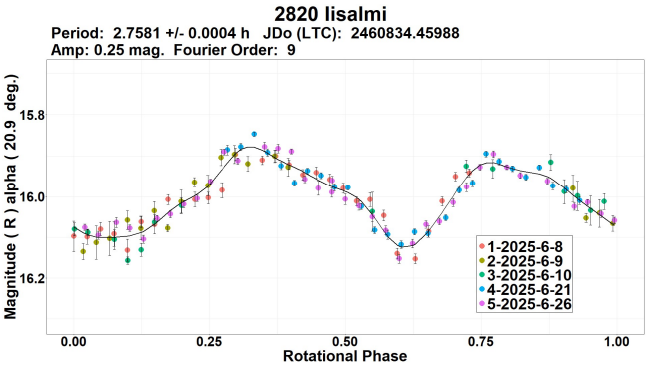

3636 Pajdusakova. No previous rotation period determinations are known for this asteroid. Observations carried out at SAO over 4 nights in 2025 April show a bimodal lightcurve of fairly high amplitude (A = 0.3 mag.), phased to a period of P = 5.141 ± 0.002 h, as the statistically most favorable solution.

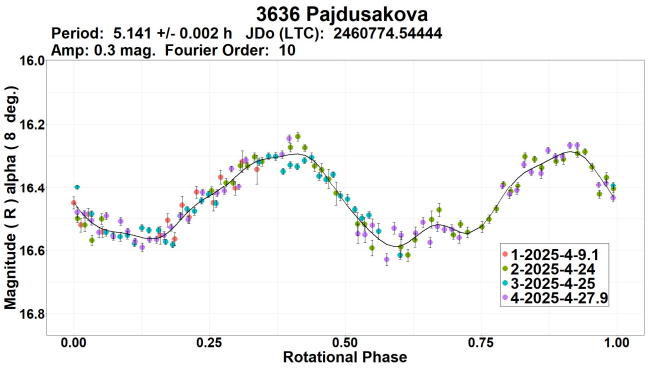

3760 Poutanen. An insight to several previous period determination results in the LCDB shows a high degree of agreement with the newly established rotation period value of P = 2.9557 ± 0.0005 h. Some of the previously determined periods are as follows: 2.956 h (Salvaggio et al., 2017), 2.95588 h (Pal et al., 2020), 2.9558 h (Benishek, 2022).

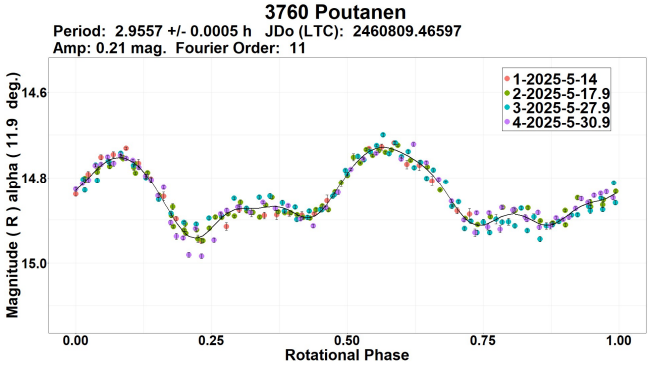

3857 Cellino. Although the data obtained at SAO on two consecutive nights in 2025 April do not provide double the full coverage of the rotational cycle found, the determined bimodal period value of P = 3.66 ± 0.02 h is quite consistent with the two values found previously by Durech et al. (2018, 3.656529 h; sidereal period) and Erasmus et al. (2020, 3.656 h).

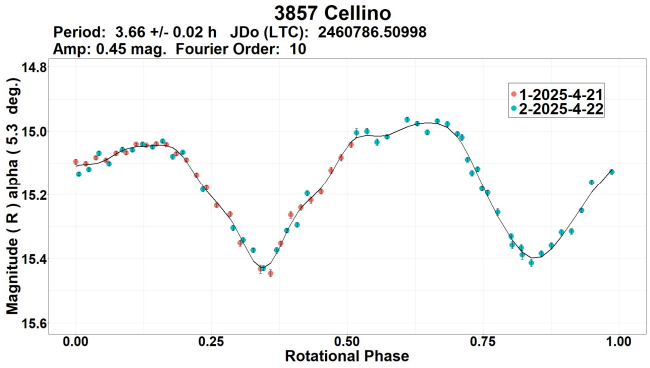

4875 Ingalls. A dense combined photometric dataset obtained over 5 nights in 2025 April points to a bimodal period solution of P = 3.7754 ± 0.0009 h, which is very close to the two previous results present in the LCDB: 3.78 h (Garceran et al., 2016) and 3.7783 h (Benishek, 2020).

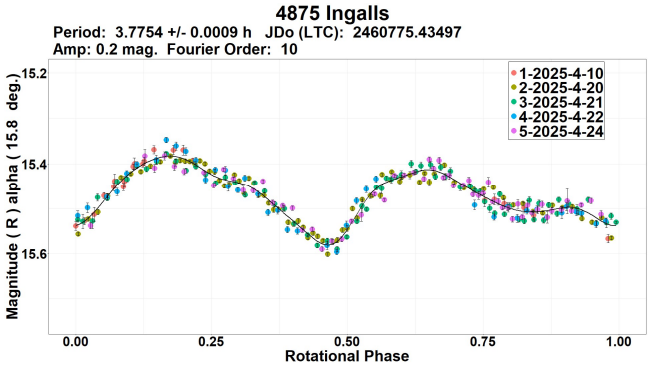

6521 Pina. Period result shown here (P = 2.9122 ± 0.0004 h) is in full agreement with the only previously reported result by Pravec (2014web, 2.911 h).

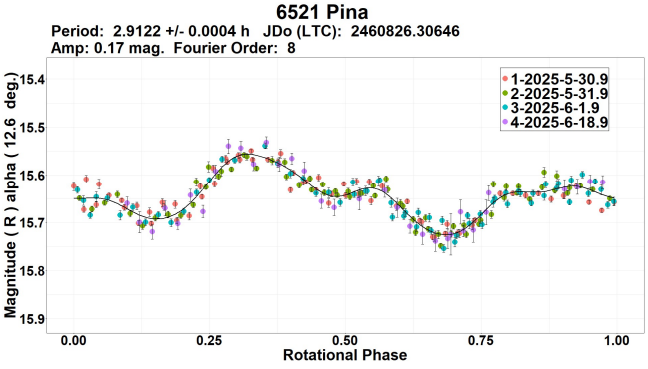

(6823) 1988 ED1. The period result of P = 2.5460 ± 0.0002 h, derived from a very dense photometric dataset obtained on 11 nights in 2025 February - March is in high agreement with numerous previous period determinations presented in the LCDB, some of which are as follows: 2.541 h (Stephens, 2008), 2.546 h (Durkee, 2012), 2.546 h (Waszczak et al., 2015).

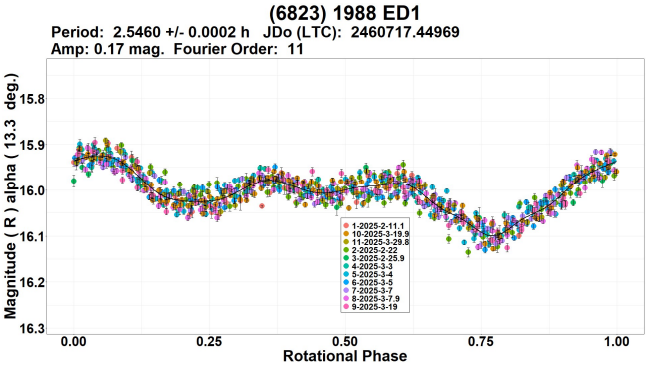

6976 Kanatsu. Period analysis of data obtained at SAO on 2 nights in late 2025 April and early 2025 May reveal a bimodal rotation period solution of P = 4.032 ± 0.003 h, which matches well with the value found by Carbo et al. (2009, 4.025 h).

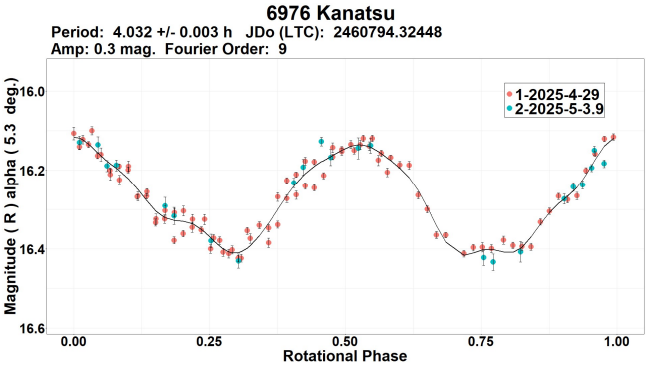

(10349) 1992 LN. Data collected over 4 consecutive nights in 2025 April - May yielded a dense combined dataset and show a rotation period of P = 2.861 ± 0.003 h, which is in good agreement with the only previously known result by Waszczak et al. (2015, 2.867 h).

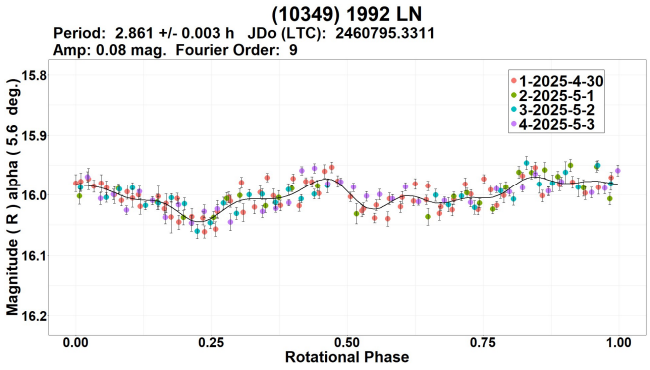

(13236) 1998 HF96. Three consecutive nights of observations in 2025 April - May show a bimodal lightcurve of particularly large amplitude (1.13 mag.) and a period of P = 7.21 ± 0.02 h. The obtained period result is in good accordance with previously reported ones: 7.20099 h (Durech et al., 2018; sidereal period) and 7.201 h (Erasmus et al., 2020).

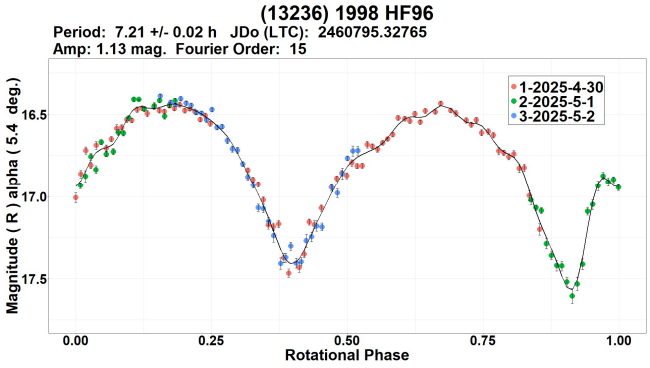

(13299) 1998 RU15. A Flora family asteroid without previously determined rotation period. A bimodal solution of P = 6.39 ± 0.02 h was derived as the statistically most favorable one, from data acquired over 4 nights in 2025 April - May.

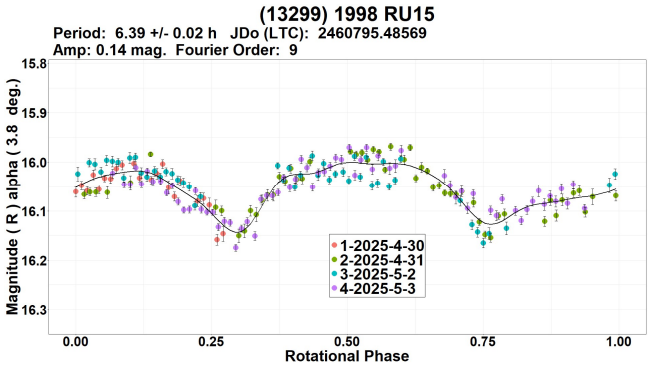

(14665) 1999 CC5. The newly determined period of P = 3.0084 ± 0.0007 h corroborates the only previously known value of 3.00857 h, found by Pal et al. (2020).

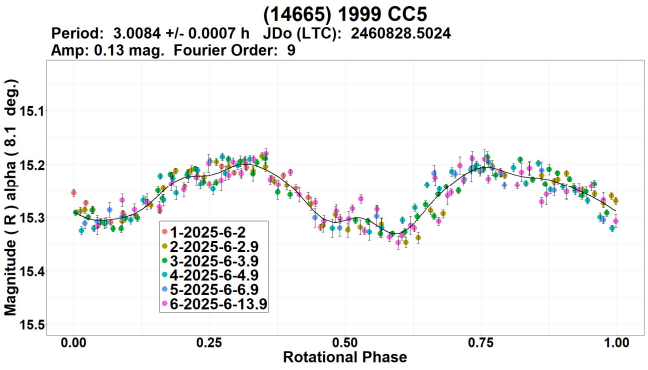

(17006) 1999 CH63. No previous rotation period determination reports were found. Dense photometric data for this object were obtained over 10 nights in 2025 June. Period analysis upon the combined dataset yields a period of P = 8.615 ± 0.005 h. This solution stands out as the statistically most favorable, but the lightcurve has a very small amplitude of only 0.05 mag. with weakly pronounced features. Their repetitiveness can still be recognized above noise level in different individual datasets. Further thorough photometric observations to unambiguously determine the rotation period are strongly encouraged.

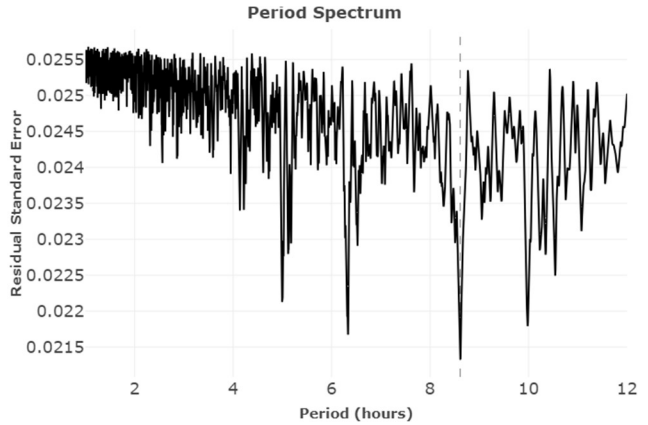

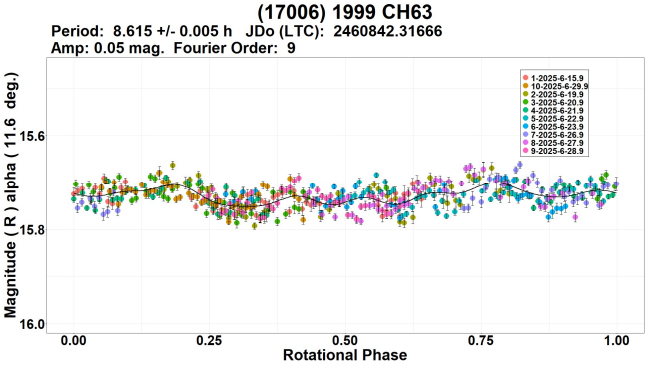

(29168) 1990 KJ. Several previously reported rotation period determination results found in the LCDB (e.g. 2.58247 h by Pravec, 2011web; 2.5827 h by Stephens, 2018; 2.588 h by Skiff et al., 2023) are in good agreement with the result (P = 2.5824 ± 0.0004 h) presented here.

Number	Name	20yy/mm/dd	Phase	L_{PAB}	B_{PAB}	Period (h)	P.E.	Amp	A.E.	Grp
2159	Kukkamaki	25/04/12-25/05/02	17.4,22.1	166	0	3.8234	0.0007	0.39	0.02	MB-I
2820	Iisalmi	25/06/07-25/06/26	20.9,14.6	298	4	2.7581	0.0004	0.25	0.03	FLOR
3636	Pajdusakova	25/04/09-25/04/27	*8.0, 2.6	213	0	5.141	0.002	0.30	0.04	MB-I
3760	Poutanen	25/05/13-25/05/30	11.9,17.8	221	14	2.9557	0.0005	0.21	0.03	MB-I
3857	Cellino	25/04/21-25/04/22	5.3, 4.7	219	1	3.66	0.02	0.45	0.03	HER
4875	Ingalls	25/04/09-25/04/24	15.8, 9.5	225	8	3.7754	0.0009	0.20	0.02	FLOR
6521	Pina	25/05/30-25/06/18	12.6,21.7	233	8	2.9122	0.0004	0.17	0.02	MB-I
6823	1988 ED1	25/02/10-25/03/29	*13.2,13.5	165	21	2.5460	0.0002	0.17	0.03	MB-I
6976	Kanatsu	25/04/28-25/05/04	5.3, 4.2	225	8	4.032	0.003	0.30	0.02	MB-I
10349	1992 LN	25/04/29-25/05/03	5.6, 4.6	226	7	2.861	0.003	0.08	0.02	V
13236	1998 HF96	25/04/29-25/05/02	5.4, 4.7	226	7	7.21	0.02	1.13	0.04	FLOR
13299	1998 RU15	25/04/29-25/05/03	*3.8, 3.5	222	5	6.39	0.02	0.14	0.04	FLOR
14665	1999 CC5	25/06/02-25/06/14	*8.1, 9.7	252	13	3.0084	0.0007	0.13	0.02	EUN
17006	1999 CH63	25/06/15-25/06/29	11.6,15.2	259	18	8.615	0.005	0.05	0.04	EUN
29168	1990 KJ	25/05/13-25/05/28	17.8,20.4	223	25	2.5824	0.0004	0.13	0.03	PHO
49981	1999 YJ13	25/06/14-25/06/20	9.7,11.8	254	10	3.636	0.003	0.13	0.03	MB-I

Table I. Observing circumstances and results. Phase is the solar phase angle given at the start and end of the date range. If preceded by an asterisk, the phase angle reached an extrema during the period. L_{PAB} and B_{PAB} are the average phase angle bisector longitude and latitude. Grp is the asteroid family/group (Warner et al., 2009): MB-I = main-belt inner, PHO = Phocaea, HER = Hertha, FLOR = Flora, EUN = Eunomia, V = Vesta.

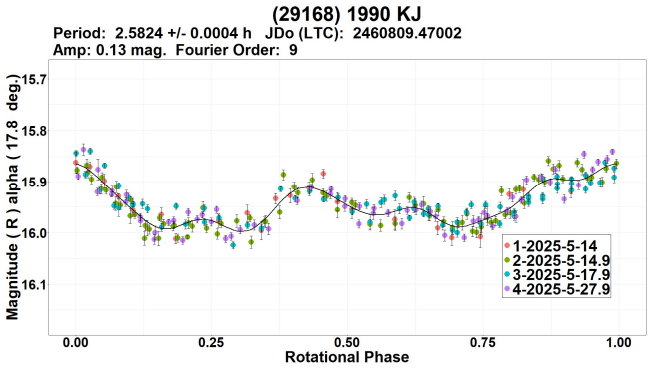

(49981) 1999 YJ13. There are no previous records of rotation period determinations for this asteroid in the LCDB. Observations on 5 nights in 2025 June indicate a period of P = 3.636 ± 0.003 h.

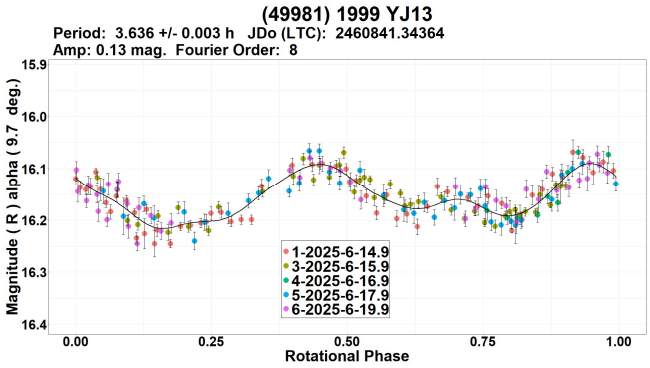

Acknowledgements

Observational work at Sopot Astronomical Observatory is generously supported by Gene Shoemaker NEO Grants awarded by the Planetary Society in 2018 and 2022.

References

Behrend, R. (2020web, 2021web). Observatoire de Geneve web site. *http://obswww.unige.ch/~behrend/page_cou.html*

Benishek, V. (2020). "Photometry of 39 Asteroids at Sopot Astronomical Observatory: 2019 September - 2020 March." *Minor Planet Bull.* **47**, 231-241.

Benishek, V. (2022). "CCD Photometry of 29 Asteroids at Sopot Astronomical Observatory: 2020 July - 2021 September." *Minor Planet Bull.* **49**, 38-44.

Benishek, V. (2023). "Lightcurves and Synodic Rotation Periods for 17 Asteroids from Sopot Astronomical Observatory: 2022 June - 2023 January." *Minor Planet Bull.* **50**, 142-147.

Benishek, V. (2025). "Synodic Rotation Periods and Lightcurves for 26 Asteroids from Sopot Astronomical Observatory: 2024 October - 2025 March." *Minor Planet Bull.* **52**, 239-245.

Carbo, L.; Green, D.; Kragh, K.; Krotz, J.; Meiers, A.; Patino, B.; Pligge, Z.; Shaffer, N.; Ditteon, R. (2009). "Asteroid Lightcurve Analysis at the Oakley Southern Sky Observatory: 2008 October thru 2009 March." *Minor Planet Bull.* **36,** 152-157.

Durech, J.; Hanus, J.; Ali-Lagoa, V. (2018). "Asteroid models reconstructed from the Lowell Photometric Database and WISE data." *Astron. Astrophys.* **617**, A57.

Durkee, R.I. (2012). "Lightcurves of 1940 Whipple and (6823) 1988 ED1." *Minor Planet Bull.* **39**, 92-93.

Erasmus, N.; Navarro-Meza, S.; McNeill, A.; Trilling, D.E.; Sickafoose, A.A.; Denneau, L.; Flewelling, H.; Heinze, A.; Tonry, J.L. (2020). "Investigating Taxonomic Diversity within Asteroid Families through ATLAS Dual-band Photometry." *Astrophys. J. Suppl. Ser.* **247**, A13.

Garceran, A.C.; Aznar, A.; Mansego, E.A.; Rodriguez, P.B.; de Haro, J.L.; Silva, A.F.; Silva, G.F.; Martinez, V.M.; Chiner, O.R. (2016). "Nineteen Asteroid Lightcurves at Asteroids Observers (OBAS) - MPPD: 2015 April - September." *Minor Planet Bull.* **43**, 92-97.

Pal, A.; Szakáts, R.; Kiss, C.; Bódi, A.; Bognár, Z.; Kalup, C.; Kiss, L.L.; Marton, G.; Molnár, L.; Plachy, E.; Sárneczky, K.; Szabó, G.M.; Szabó, R. (2020). "Solar System Objects Observed with TESS - First Data Release: Bright Main-belt and Trojan Asteroids from the Southern Survey." *Ap. J. Supl. Ser*. **247**, 26-34.

Pravec, P. (2011web, 2014web). Photometric Survey for Asynchronous Binary Asteroids web site. *http://www.asu.cas.cz/~ppravec/newres.txt*

R Core Team (2025). R: A language and environment for statistical computing. R Foundation for Statistical Computing. Vienna, Austria. *https://www.R-project.org/*

Salvaggio, F.; Marchini, A.; Papini, R. (2017). "Rotation Period Determination for 3760 Poutanen and 14309 Defoy." *Minor Planet Bull.* **44**, 354-355.

Skiff, B.A.; McLelland, K.P.; Sanborn, J.J.; Koehn, B.W. (2023). "Lowell Observatory Near-Earth Asteroid Photometric Survey (NEAPS): Paper 5." *Minor Planet Bull.* **50**, 74-101.

Stephens, R.D. (2008). "Asteroids Observed from GMARS and Santana Observatories - Late 2007 and Early 2008." *Minor Planet Bull.* **35**, 126-128.

Stephens, R D. (2018). "Asteroids Observed from CS3: 2018 April - June." *Minor Planet Bull.* **45**, 353-355.

VizieR (2025). *http://vizier.u-strasbg.fr/viz-bin/VizieR*

Warner, B.D.; Harris, A.W.; Pravec, P. (2009). "The Asteroid Lightcurve Database." *Icarus* **202**, 134-146. *https://www.minorplanet.info/php/lcdb.php*

Warner, B.D. (2012). The MPO Users Guide: A Companion Guide to the MPO Canopus/PhotoRed Reference Manuals. BDW Publishing, Eaton, CO.

Warner, B.D. (2018). MPO Canopus software, version 10.7.11.3. *http://www.bdwpublishing.com*

Waszczak, A.; Chang, C.-K.; Ofek, E.O.; Laher, R.; Masci, F.; Levitan, D.; Surace, J.; Cheng, Y.-C.; Ip, W.-H.; Kinoshita, D.; Helou, G.; Prince, T.A.; Kulkarni, S. (2015). "Asteroid Light Curves from the Palomar Transient Factory Survey: Rotation Periods and Phase Functions from Sparse Photometry." *Astron. J.* **150**, A75.

LIGHTCURVE AND ROTATION PERIOD ANALYSIS OF (9058) 1992 JB AND (424482) 2008 DG5

Wayne Hawley
Old Orchard Observatory (Z09)
Fiddington, UK
hawley.wayne@gmail.com

Patrick Wiggins (718)
University of Utah
Utah, USA

James D. Armstrong
University of Hawaii Institute for Astronomy|
(L09) (Q58) (Q59) (V38) (T04) (W89) (Z21)
34 Ohia Ku Street
Pukalani, HI 96768 USA

Rui Gonçalves
Linhaceira (938)
Tomar, PORTUGAL

Kent DeGroff
Whiskey Creek Observatory (V19)
New Mexico, USA

Brian Scott
Calne (247)
Wiltshire, UK

Mohammad Shawkat Odeh
Al Khatim Observatory (M44)
Abu Dhabi, UAE

Tim Haymes
Southside Observatory (Y98)
Steeple Aston, UK

Jean-Francois Gout
Tree Gate Farm Observatory (W05)
Starkville, Mississippi, USA

Grant Privett
LPMR Observatory (Y82)
Broad Chalke, UK

Joan Genebriera
Astropriorat Observatory (M02)
Catalonia, SPAIN

(Received: 2025 July 4)

Photometric observations of asteroid (9058) 1992 JB were obtained during 2025 April and May while observations of (424482) 2008 DG5 were obtained during 2025 May and June. For (9058) 1992 JB, we found P = 10.52 ± 0.01 h, A = 0.32 ± 0.03 mag. For (424482) 2008 DG5, the results were P = 11.256 ± 0.006 h, A = 0.25 ± 0.03 magnitudes.

CCD photometric observations of minor planets (9058) 1992 JB and (4244482) 2008 DG were made by a collaboration of observers from 2025 April to June. Images were obtained from observatories around the globe. Several of the co-authors used their own equipment and some used the Las Cumbres Observatory facilities.

Photometry and period determination were carried out with *TychoTracker Pro* Version 12.5.5. (TT).

The photometric analysis was performed using standard differential techniques on images with the comparison stars employed selected by TT to be within the color range of +0.50 < (B-V) < +0.90. The Asteroid Terrestrial-impact Last Alert System (ATLAS) catalog (Tonry et al, 2015; Kostov and Bonev, 2017) was used as the source of reference stars. TT's period determination operates by finding model light curves based on a user-defined number of Fourier components which best fit the asteroid photometric data. The program lists the candidate periods found within a user-defined period range and sampling frequency, based on minimizing Root Mean Square Errors (RMSE), between the modelled and photometric magnitudes. The candidate periods are listed in increasing RMSE value and the entire suite of RMSE values is plotted as a "periodogram" for quality control. In these periodograms each object yielded a clear 'best-fit' period solution having well defined minima as shown in the following figures.

Periodograms often exhibit several possible candidate periods, in which case an examination of the rotational phase plot for each of these is then conducted looking for a credible lightcurve. Where the object shape is the dominant factor in producing the observed magnitude changes, (typically having lightcurve amplitudes of >0.2 mag), the rotational phase plot often has two peaks and two troughs (bimodal) and this is usually chosen as the most likely for such asteroids.

In this paper no attempt is made to find an absolute magnitude and a value of G = 0.15 has been used throughout the calculations. Time-series magnitude estimates from different nights and observing locations using a variety of imaging equipment were offset in magnitude to bring them into alignment when producing the raw and rotational-phase plots. The same offset was used for each instance of an individual imaging setup. When this paper is accepted for publication all the observations will be loaded into the Asteroid Lightcurve Data Exchange Format (ALCDEF) database. Some individual datapoints have been combined by stacking during period analysis to improve the signal-to-noise ratio.

The results are summarized in the table below. Column 3 gives the span of dates over which the observations were made. Column 4 is the range of phase angles for each date range, if this is preceded by an asterisk this means the asteroid passed through minimum phase angle during the observing period. Columns 5 and 6 give the range of values for the Phase Angle Bisector (PAB) longitude and latitude respectively, for the mid date of the observation set. Column 7 gives the period and Column 8 the minimum possible formal error in hours given by TT. Columns 9 and 10 give the amplitude and its associated uncertainty in magnitude. Dips in the results from the period analysis have been checked to see if they are monomodal or bimodal and a bimodal period has been chosen for the best-fit result. Information given for the object is taken from the NASA Jet Propulsion Laboratory (JPL) Small-Body Database Lookup webpage.

(9058) 1992 JB is an Apollo asteroid that that was discovered on 1992 May 1 by J. Alu and K.J. Lawrence at Palomar. The lightcurve period and amplitude results reported here are based on 20 observing sessions (a total of 1297 exposures) obtained from 2025 April-May. Our analysis found a synodic rotation period of 10.52 ± 0.01 h and peak-to-peak amplitude of 0.32 ± 0.03 mag.

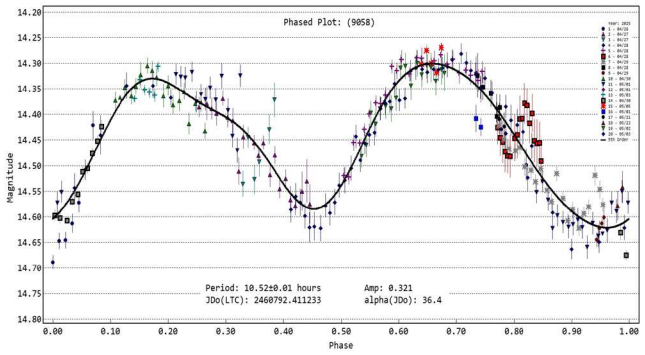

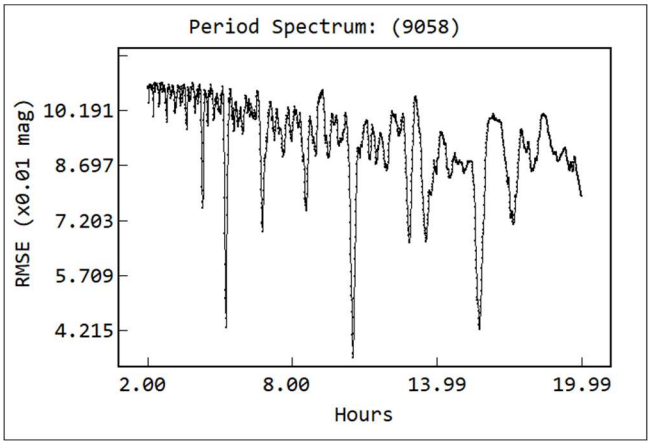

(424482) 2008 DG5 is an Apollo asteroid that was discovered on 2008 Feb 28 by the Catalina Sky Survey at Catalina. We used data from 43 observing sessions (a total of 566 exposures) made from 2025 May-June. The analysis found P = 11.256 ± 0.006 h and A = 0.25 ± 0.03 mag.

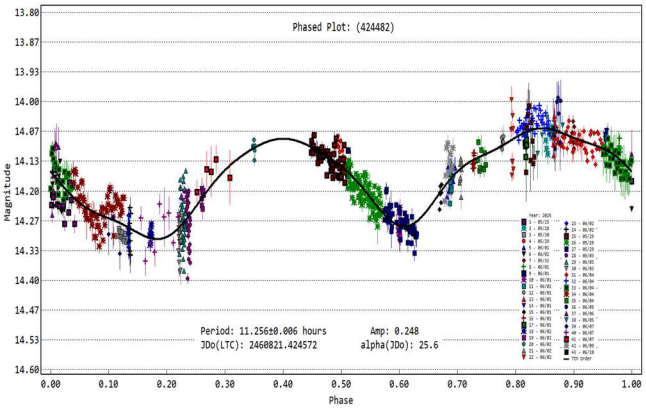

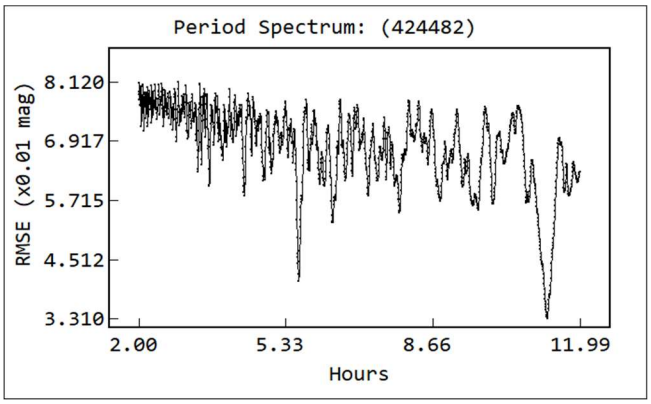

Number	Name	yyyy mm/dd	Phase	L_{PAB}	B_{PAB}	Period (h)	P.E.	Amp	A.E.	Grp
9058	1992 JB	2025 04/26-05/22	*30.5,36.4	201	-1	10.52	0.01	0.32	0.03	9101
424482	2008 DG5	2025 05/25-06/07	25.6,99.7	230	16	11.26	0.006	0.25	0.03	9101

Table I. Observing circumstances and results. The phase angle is given for the first and last date. If preceded by an asterisk, the phase angle reached a minimum during the period. L_{PAB} and B_{PAB} are the approximate phase angle bisector longitude/latitude at mid-date range (see Harris et al., 1984). Grp is the asteroid family/group (Warner et al., 2009).

Observatory	Telescope (m)	Camera	Filter	Object (sessions)
Old Orchard (Z09) Hawley	0.35 *f*/6.7 SCT	SX694 Trius Pro (2x2)	SR	9058 (5), 424482 (3)
Univ. of Utah, (718), Wiggins	0.35 *f*/5.5 SCT	ST-10XME (3x3)	C	9058 (4), 424482 (5)
Sutherland LC-Aqawan A (L09) Armstrong	0.40 *f*/8	SBIG STL-6303 (1x1)	SR	424482 (3)
Siding Spring LCO Clamshell #2 (Q59), Armstrong	0.40 *f*/8	SBIG STL-6303 (1x1)	SR	424482 (1)
Haleakala LCO Clamshell #1 (T04), Armstrong	0.40 *f*/8	SBIG STL-6303 (1x1)	SR	424482 (5)
Cerro Tololo LCO Clamshell #1 (W89), Armstrong	0.40 *f*/8	SBIG STL-6303 (1x1)	SR	424482 (4)
Tenerife LCO Aqawan A #1 (Z21), Armstrong	0.40 *f*/8	SBIG STL-6303 (1x1)	SR	424482 (1)
McDonald LCO Aqawan A (V38), Armstrong	0.40 *f*/8	SBIG STL-6303 (1x1)	SR	424482 (1)
Al Katim (M44), Odeh	0.36 *f*/7.7	ASI 2600MM Pro	V	9058 (3), 424482 (4)
Whiskey Creek (V19), DeGroff	0.46 *f*/4.2 Newtonian	QHY 268M	V	9058 (1), 424482 (4)
Linhaceira (938), Gonclaves	0.35 *f*/5.6	SBIG ST-7XME (1x1)	C	9058 (1), 424482 (3)
Southside (Y98), Haymes	0.28 *f*/5.8	QHY 174J-GPS	C	9058 (1)
LPMR (Y82), Privett	0.30 *f*/4	SX694 Trius Pro	C	9058 (2)
Astropriorat (M02), Genbriera	0.41 *f*/8	Moravian G4-16000	V	9058 (3), 424482 (2)
Calne UK (247), Scott	0.28 *f*/7	SX694 Trius Pro	Lum	9058 (2)
Tree Gate (W05), Gout	0.28 *f*/2.2 C11 Hyperstar	ASI 2600MM	C	9058 (1)

Table II. List of observers and equipment. The number in parentheses in the last column is the number of sessions for the given object.

Acknowledgements

Our thanks are extended to Daniel Parrott, author of *TychoTracker Pro*. This work has made use of data from the Asteroid Terrestrial-impact Last Alert System (ATLAS) project. ATLAS is primarily funded to search for near earth asteroids through NASA grants NN12AR55G, 80NSSC18K0284, and 80NSSC18K1575; byproducts of the NEO search include images and catalogs from the survey area. The ATLAS science products have been made possible through the contributions of the University of Hawaii Institute for Astronomy, the Queen's University Belfast, the Space Telescope Science Institute, and the South African Astronomical Observatory. The ATLAS Catalog makes use of the formulae to convert Pan-STARRS gri to BVRI (Kostov and Bonev, 2017). This work makes use of observations from the Las Cumbres Observatory global telescope network.

References

Harris, A.W.; Young, J.W.; Scaltriti, F.; Zappala, V. (1984). "Lightcurves and phase relations of the asteroids 82 Alkmene and 444 Gyptis." *Icarus* **57**, 251-258.

JPL (2023). Small-Body Database Lookup. *https://ssd.jpl.nasa.gov/tools/sbdb_lookup.html*

Kostov, A.; Bonev, T. (2017). "Transformation of Pan-STARRS1 gri to Stetson BVRI magnitudes. Photometry of small bodies observations." *Bulgarian Astron. J.* **28**, 3 (ArXiv:1706.06147v2).

Tonry, J.L.; Denneau, L.; Flewelling, H.; Heinze, A.N.; Onken, C.A.; Smartt, S.J.; Stadler, B.; Weiland, H.J.; Wolf, C. (2018). "The ATLAS All-Sky Stellar Reference Catalog." *Ap. J.* **867**, A105.

Warner, B.D.; Harris, A.W.; Pravec, P. (2009). "The Asteroid Lightcurve Database." *Icarus* **202**, 134-146. Updated 2023 Oct 1. *http://www.minorplanet.info/lightcurvedatabase.html*

LIGHTCURVE ANALYSIS FOR THREE MAIN-BELT, TWO MARS-CROSSING AND TWO NEAR-EARTH ASTEROIDS

Gonzalo Fornas (J57)
Asocación Valenciana de Astronomía
(Centro Astronómico Alto Turia)
C/ Profesor Blanco 16. 46014 Valencia, SPAIN
gon@iicv.es

Alvaro Fornas (J57)
Asociación Valenciana de Astronomía (CAAT)

Alfonso Carreño (Y76)
Nova Canet Observatory

Fernando Huet (Z93)
Asociación Valenciana de Astronomía.
Polop Observatory

Enrique Rathmann (Y78)
Asociación Valenciana de Astronomía
Tros Alt Observatory

Vicente Mas, AVA (J57)
Asociación Valenciana de Astronomía (CAAT)

(Received: 2025 July 9)

Photometric observations are reported for three main-belt, two Mars-crossing, and two near-Earth asteroids. We derived the following rotational synodic periods: 5066 Garradd, 3.7791 ± 0.0024 h; 5972 Harryatkinson, 3.3859 ± 0.0018; 18404 Kenichi, 3.44084 ± 0.00008 h; (21183) 1994 EO2, 8.73188 ± 0.00024 h; (27174) 1999 BB2, 4.88420 ± 0.00029 h; (137126) 1999 CF9, 6.7056 ± 0.0008 h; (137170) 1999 HF1, binary, P1 = 2.31921 ± 0.00002 h, P2 = 14.2087 ± 0.0022 h.

We report on the photometric analysis for seven asteroids by Asociación Valenciana de Astronomía (AVA). The data were obtained during the last quarter of 2024 and the first months of 2025. We present graphic results of data analysis, mainly lightcurves, with the plot phased to a given period. We managed to obtain several accurate and complete lightcurves and calculating their rotation periods as accurately as possible.

Observatory	Telescope	CCD
C.A.A.T. J57	17" DK	QHY- 600
C.A.A.T. J57	10" NW	ZWO ASI 1600
Z93	SC 8"	SBIG ST8300
Y78	SC 8"	ZWO ASI 294 MM PRO
Y76	SC 9.25"	ATIK 314L+

Table I. List of instruments used for the observations.

We focused on asteroids with no reported period and those where the reported period was poorly established and needed confirmation. The targets were selected from the Collaborative Asteroid Lightcurve (CALL) website (*http://www.minorplanet.info/call.html),* the Minor Planet Center (*http://www.minorplanet.net*) and Brian D. Warner et al. (2025). The Asteroid Lightcurve Database (LCDB; Warner et al., 2009) was consulted to locate previously published results.

Images were measured using *MPO Canopus* (Bdw. Publishing) with a differential photometry technique. The comparison stars were restricted to near solar-color to minimize color dependencies, especially at larger air masses. The lightcurves show the synodic rotation period. The amplitude (peak-to-peak) that is shown is that for the Fourier model curve and not necessarily the true amplitude.

Results

5066 Garradd. This Mars-crossing asteroid was discovered on 1990 Jun 22 at Sidind Spring by R.H. McNaught. We made observations on 2025 May 24 to 25. From our data we derive a synodic rotation period of 3.7791 ± 0.0024 h and an amplitude of 0.07 mag. We have no previous information about its rotation period.

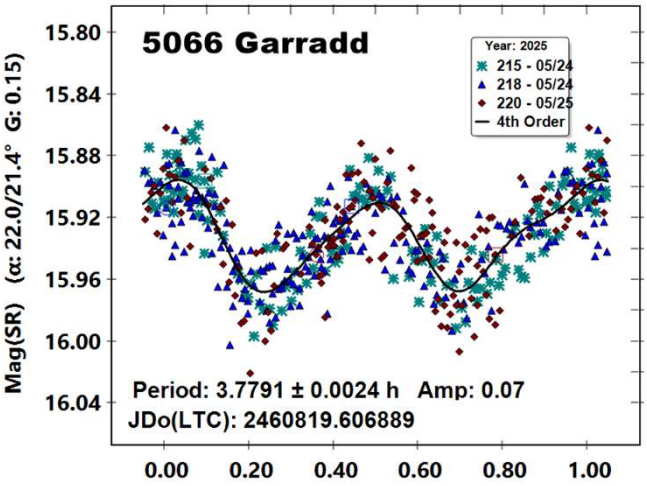

5972 Harryatkinson. This middle main-belt asteroid was discovered on 1991 Aug 5 at Palomar by H.E. Holt. We made observations on 2025 May 19 to 22. From our data we derive a synodic rotation period of 3.3859 ± 0.0018 h and an amplitude of 0.11 mag. Pál et al. (2020) got a period of 3.38813 h; Bonamico (2020) found 3.376 h and Benishek (2022) got 3.3889 h. All of them are consistent with our results.

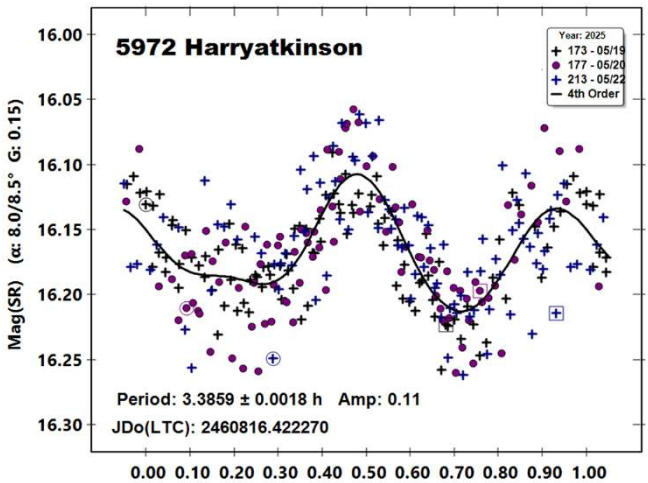

18404 Kenichi. This middle main-belt asteroid was discovered on 1993 March 20 at Kitami by K. Endate and K. Watanabe. We made observations on 2025 Feb 5 to March 28. From our data we derive a synodic rotation period of 3.44084 ± 0.00008 h and an amplitude of 0.23 mag. We have no previous information about its rotation period.

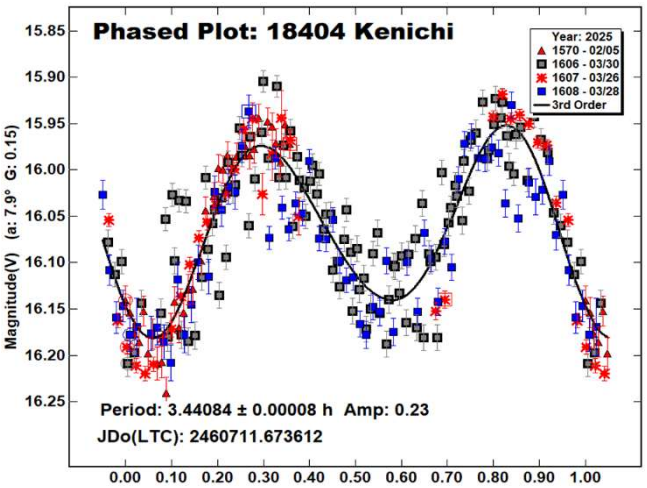

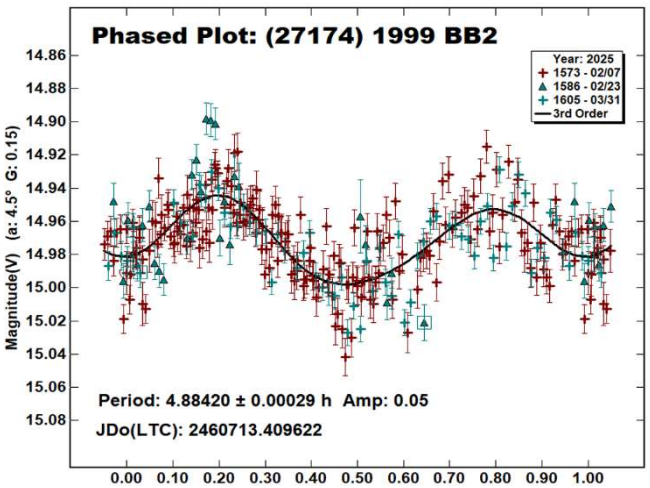

(21183) 1994 EO2. This Mars-crossing asteroid was discovered on 1994 March 9 at Palomar by E.F. Helin. We made observations on 2025 Feb 6 to March 31. From our data we derive a synodic rotation period of 8.73188 ± 0.00024 h and an amplitude of 0.76 mag. We have no previous information about its rotation period.

(137126) 1999 CF9. This near-Earth asteroid was discovered on 1999 Feb 2 at Socorro by LNEAR. We made observations on 2025 Feb 20 to 24. From our data we derive a synodic rotation period of 6.7056 ± 0.0008 h and an amplitude of 0.69 mag. We have no previous information about its rotation period.

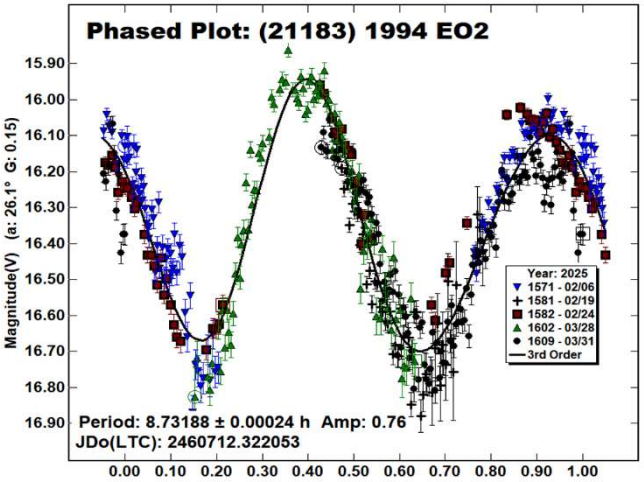

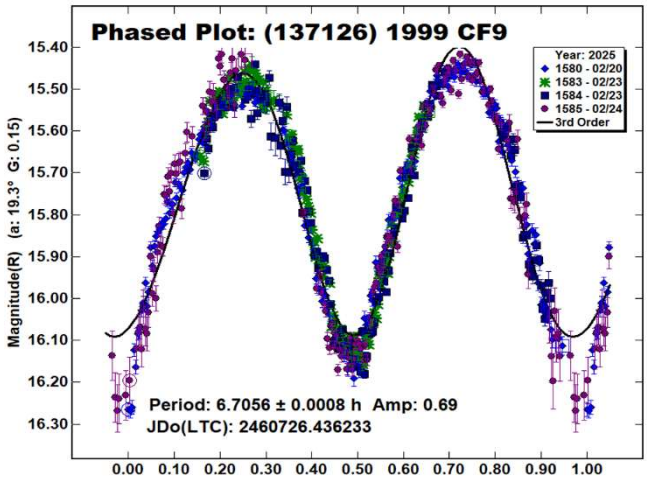

(27174) 1999 BB2. This middle main-belt asteroid was discovered on 1999 Jan 19 at Črni Vrh Observatory. We made observations on 2025 Feb7 to March 31. From our data we derive a synodic rotation period of 4.88420 ± 0.00029 h and an amplitude of 0.05 mag. We have no previous information about its rotation period.

(137170) 1999 HF1. This near-Earth asteroid of the Phocaea family was discovered on 1999 Apr 12 at Anderson Mesa by LONEOS. We made observations on 2025 March 31 to April 25. From our data we think it is a binary asteroid. We show our full data set assuming a single period, followed by a binary asteroid model with separate primary and secondary periods.

Number	Name	yyyy mm/dd	Phase	L_{PAB}	B_{PAB}	Period(h)	P.E.	Amp	A.E.	Grp
5066	Garradd	2025 05/24-25	5.7,10.6	290.9	8.9	3.7791	0.0024	0.07	0.03	MC
5972	Harryatkinson	2025 05/19-22	7.9,8.3	232.7	17.5	3.3859	0.0018	0.11	0.03	MB-M
18404	Kenichi	2025 02/05-3/28	12.3,14.3	159.2	9.25	3.44084	0.00008	0.23	0.03	MB-M
21183	1994 EO2	2025 02/06-03/31	26.1,31.2	122.8	24.3	8.73188	0.00024	0.76	0.05	MC
27174	1999 BB2	2025 02/07-03/31	18.9,26.9	277.7	-1.4	4.88420	0.00029	0.05	0.02	MB-M
137126	1999 CF9	2025 02/20-24	23.8,25.5	169.5	0.2	6.7056	0.0008	0.69	0.03	NEA
137170	1999 HF1	2025 03/31-04/25	70.6,59	203.7	50.2	2.31921	0.00002	0.15	0.05	NEA
					P2=	14.2087	0.0022	0.07	0.02	

Table I. Observing circumstances and results. The phase angle is given for the first and last date. If preceded by an asterisk, the phase angle reached an extrema during the period. L_{PAB} and B_{PAB} are the approximate phase angle bisector longitude/latitude at mid-date range (see Harris et al., 1984). Grp is the asteroid family/group (Warner et al., 2009).

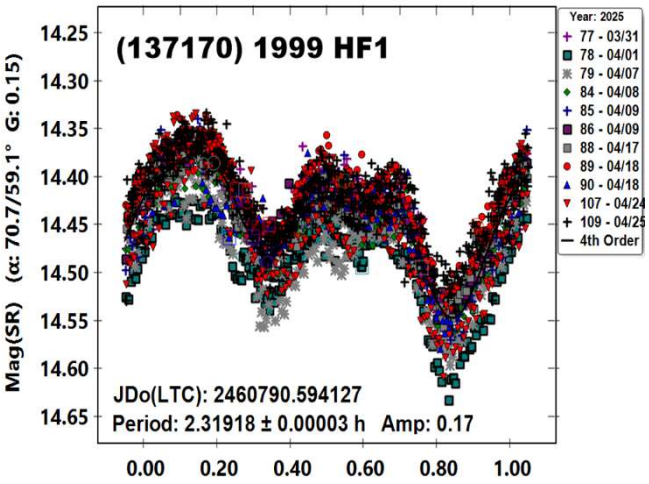

(137170) 1999 HF1 full data, for a single body.

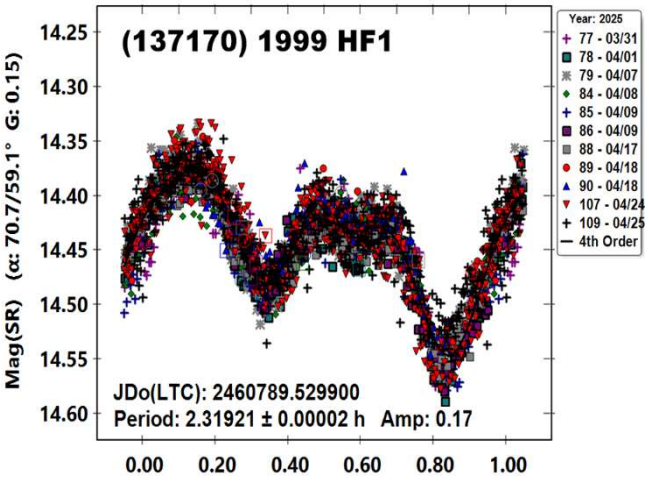

(137170) 1999 HF1, solving for a primary period P1.

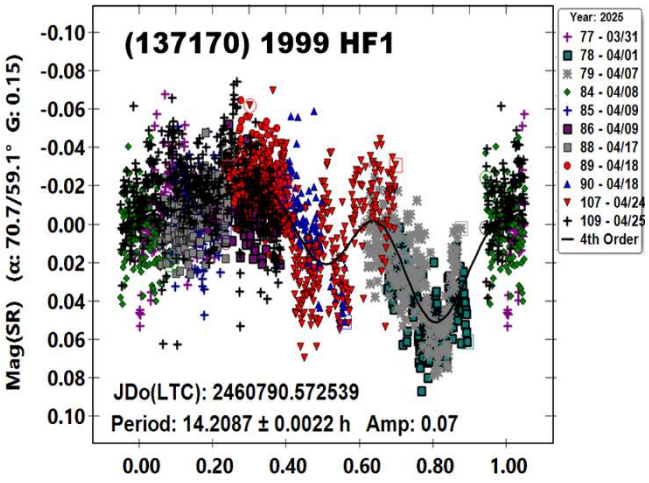

(137170) 1999 HF1, solving for a secondary period P2.

If we process it as a binary asteroid, we get a main synodic period of 2.31921 ± 0.00002 h and an amplitude of 0.17 mag and a secondary period of 14.2087 ± 0.0022 h with an amplitude of 0.07 mag. Pravec et al. (2002) found both periods P1 = 2.319 h and P2 = 14.017 h; Pravec et al. (2006) found again P1 = 2.3192 h and P2 = 14.03 h; Marchis et al. (2012) got P1 = 2.319 h and P2 = 14.04 h. All of them are consistent with our results.

References

Benishek, V. (2022). "CCD Photometry of 29 Asteroids at Sopot Astronomical Observatory: 2020 July-2021 September." *Minor Planet Bull.* **49**, 38-44.

Bonamico, R. (2020). "Rotational Periods of Five Asteroids." *Minor Planet Bull.* **47**, 222-223.

Marchis, F.; Enriquez, J.E.; Emery, J.P.; Mueller, M.; Baek, M.; Pollock, J.; Assafin, M.; Vieira Martins, R.; Berthier, J.; Vachier, F.; Cruikshank, D.P.; Lim, L.F.; Reichart, R.E.; Ivarsen, K.M.; Haislip, J.B.; LaCluyze, A.P. (2012). "Multiple asteroid systems: Dimensions and thermal properties from Spitzer Space Telescope and ground-based observations." *Icarus* **221**, 1130-1161.

Pál, A.; Sazkáta, R.; Kiss, C.; Bódi, A.; Bognár, Z.; Kalup, C.; Kiss, L.; Marton, G.; Molnár, L.; Plachy, E.; Sárneczky, K.; Szabó, G.; Szabó, R. "Solar System Objects Observed with TESS - First Data Release: Bright Main-belt and Trojan Asteroids from the Southern Survey." *The Astrophysical Journal Supplement Series* **247**(1), id. 26. 9pp.

Pravec, P.; Sarounova, L.; Hicks, M.D.; Rabinowitz, D.L.; Wolf, M.; Scheirich, P.; Krugly, Y.N. (2002). "Doubly-periodic Lightcurve of 1999 HF1 - A Binary NEA Candidate," *Minor Planet Bull.* **29**, 23-25.

Pravec, P.; Scheirich, P.; Kušnirák, P. and 54 colleagues (2006). "Photometric survey of binary near-Earth asteroids." *Icarus* **181**, 63-93.

Warner, B.D.; Harris, A.W.; Pravec, P. (2009). "The Asteroid Lightcurve Database." *Icarus* **202**, 134-146. Updated 2016 Sep. *http://www.minorplanet.info/lightcurvedatabase.html*

Warner, B.D.; Harris, A.W.; Durech J.; Lance, A.M. (2025). "Lightcurve Photometry Opportunities: 2025 January - Aprl". *Minor Planet Bull.* **52**, 90-93.

LIGHTCURVES, ROTATIONAL PERIODS AND SPECTRAL CLASSIFICATION OF TWO NEAR-EARTH ASTEROIDS OBSERVED WITH TRAPPIST: 2020 WG AND (458122) 2010 EW45

Brankica Apostolova
MAUCA - Master track in Astrophysics
Université Côte d'Azur & Observatoire de la Côte d'Azur
Parc Valrose, 06100 Nice, FRANCE
brankica.apostolova@oca.eu

Mohamed Amine Miftah
Space Sciences, Technologies & Astrophysics Research (STAR) Institute, Université de Liège, Liège, BELGIUM
Cadi Ayyad University (UCA), Oukaïmeden Observatory (OUCA), Faculté des Sciences Semlalia (FSSM), High Energy Physics, Astrophysics and Geoscience Laboratory (LPHEAG), Marrakech, MOROCCO

Emmanuël Jehin, Elisabeta Petrescu
Space Sciences, Technologies & Astrophysics Research (STAR) Institute, Université de Liège, Liège, BELGIUM

Marin Ferrais
Florida Space Institute, University of Central Florida
Orlando, Florida, USA

Abdelhadi Jabiri, Zouhair Benkhaldoun
Cadi Ayyad University (UCA), Oukaïmeden Observatory (OUCA), Faculté des Sciences Semlalia (FSSM), High Energy Physics, Astrophysics and Geoscience Laboratory (LPHEAG), Marrakech, MOROCCO

(Received: 2025 June 7)

We observed two near-Earth asteroids (NEAs) with TRAPPIST-North and TRAPPIST-South from October 2024 to January 2025. We obtained their lightcurves and estimated their synodic rotational periods and amplitudes, which have not been previously reported – 2020 WG: (0.5927 ± 0.0003 h) and (0.36 ± 0.02 mag); (458122) 2010 EW45: (2.4880 ± 0.0008 h) and (0.11 ± 0.01 mag). We also performed calculations of their color indices B-V, V-R and V-I, and according to them, classified the asteroids into spectral types – 2020 WG: S-type, 2010 EW45: Q-type. The acquired data have been submitted to the ALCDEF database.

We conducted CCD photometric observations of NEAs 2020 WG and (458122) 2010 EW45 with the TRAPPIST-North (TN; IAU code Z53) and TRAPPIST-South (TS; IAU code I40) robotic telescopes (Jehin et al., 2011), which are installed at the Oukaïmeden Observatory in Morocco and the ESO La Silla observatory in Chile, respectively. Both are 0.6-m Ritchey-Chrétien telescopes operating at f/8 on German Equatorial mounts. The TN camera is an Andor IKONL BEX2 DD (0.60 arcsec/pixel), and the TS camera is an FLI ProLine 3041-BB (0.64 arcsec/pixel).

All observations used for the lightcurves were made using a R filter. Additional observations in B, V and I filters were conducted in order to calculate the color indices, to infer spectral types. The raw images obtained with the two telescopes were calibrated with a Python script using standard flat fields, dark and bias frames. The aperture photometry was carried out with Photometry Pipeline developed by Mommert (2017), which integrates zero-point calibration by matching field stars with reference catalogs. The rotational periods were determined using the software *Peranso* (Paunzen and Vanmunster, 2016), utilizing the FALC method described by Harris et al. (1989).

The phased lightcurves are shown in Figure 1 and Figure 2. We display the variation of the magnitudes subtracted by the average magnitude. The associated errors are from the quality of the photometry. We fitted the data with a Fourier series of the form $F_n(\phi) = a_0 + \Sigma(a_n\cos(2\pi n\phi) + b_n\sin(2\pi n\phi))$, where ϕ is the rotational phase normalized between 0 and 1, and n refers to the different harmonic orders of the Fourier series. The residuals between the data and the fit are shown on the bottom of the figure. The amplitudes reported are from the Fourier series model. The color indices were calculated by taking the mean of the magnitudes in each filter for each night, then taking the mean of each index from all nights. Table 1 and Table 2 summarize the observation details and results.

2020 WG is an NEA that is categorized as a Potentially Hazardous Asteroid (PHA) belonging to the Apollo class (NASA/JPL, 2025). It was observed for five nights with TN and TS in October 2024 and November 2024 with a total time on target of 19.8 hours. The best-fitting period found is 0.5927 ± 0.0003 h, revealing a fast rotator (35.6 min), with a quite large amplitude of 0.36 ± 0.02 mag. The shape of the lightcurve shows shifting to a lower phase from the first to the second night, then consecutive shifting to a higher phase each night, with a magnitude drop during the last two nights. This can be attributed to the large phase angle change in the observing period – from 64.1° to 25.4° from October 25 to October 31, which is then followed by an increase of up to 34.0° on November 4. The colors of 2020 WG were calculated using observations with TN over two nights. The estimated color indices are B-V = 0.85 ± 0.01, V-R = 0.52 ± 0.01 and V-I = 0.87 ± 0.01. These values point to an asteroid of the S-type according to the Tholen classification (Dandy et al., 2003).

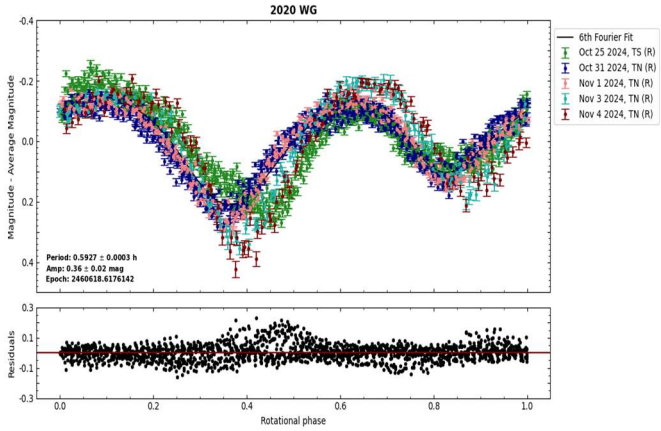

Fig. 1. Asteroid 2020 WG. Top: lightcurve, bottom: residuals.

Number	Name	yyyy	mm/dd	Pts	Phase angle (°)	L_{PAB}	B_{PAB}	Period (h)	P.E.	Amp (mag)	A.E.
	2020 WG	2024	10/25-11/04	1708	64.1, 34.0	32	12	0.5927	0.0003	0.36	0.02
458122	2010 EW45	2024-2025	12/23-01/06	2600	53.3, 24.3	92	-4	2.4880	0.0008	0.11	0.01

Table I. Observation details and results of the lightcurve photometry. Pts is the number of data points, i.e., number of images from which we acquired photometric magnitudes and phase angle corresponds to the first and last date (NASA/JPL, 2025). L_{PAB} and B_{PAB} represent the approximate phase angle bisector longitude/latitude at the midpoint of the observation period (Harris et al., 1984). We report the results for the rotational period and amplitude along with the uncertainties.

Number	Name	yyyy	mm/dd	Pts_B	Pts_V	Pts_R	Pts_I	(B-V)	σ_{B-V}	(V-R)	σ_{V-R}	(V-I)	σ_{V-I}	Spect. Type
	2020 WG	2024	11/03-11/04	8	7	18	8	0.85	0.01	0.52	0.01	0.87	0.01	S
458122	2010 EW45	2024-2025	12/23-01/15	33	32	61	30	0.84	0.02	0.45	0.02	0.71	0.02	Q

Table II. Observation details and results for the color indices and spectral type classification. We give the number of data points in each of the BVRI filters. We report the values of the color indices along with the uncertainties, as well as the asteroid spectral type.

(458122) 2010 EW45 is also an Apollo PHA (NASA/JPL, 2025; Bressi et al., 2010). Radar observations from Goldstone have shown that 2010 EW45 is a binary asteroid (*https://echo.jpl.nasa.gov/asteroids/Alinda.goldstone.planning.2024.html*). We observed it for 11 nights with both TN and TS from December 2024 to January 2025, with a total time on target of 35.5 hours. We found a best-fitting period of 2.4880 ± 0.0008 h and amplitude 0.11 ± 0.01 mag. Using BVRI observations from eight nights, the color indices were estimated to be B-V = 0.84 ± 0.02, V-R = 0.45 ± 0.02 and V-I = 0.71 ± 0.02, indicating a Q-type asteroid.

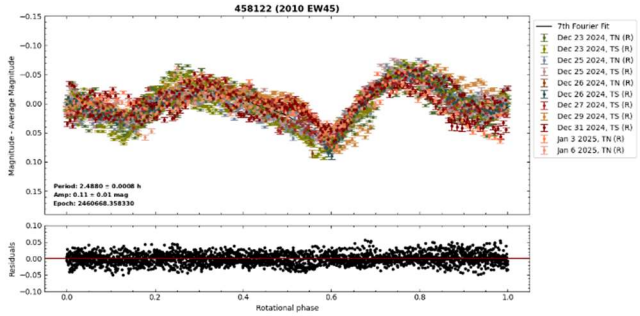

Fig. 2. Asteroid 2010 EW45. Top: lightcurve, bottom: residuals.

Acknowledgements

TRAPPIST is a project funded by the Belgian Fonds (National) de la Recherche Scientifique (F.R.S.-FNRS) under grant PDR T.0.120.21. TRAPPIST-North is a project funded by the University of Liège (Belgium), in collaboration with Cadi Ayyad University in Marrakech (Morocco). E. Jehin is FNRS senior Research Associate. The TRAPPIST project can be visited at the website *https://www.trappist.uliege.be*. Author Brankica Apostolova thanks Observatoire de la Côte d'Azur, the COMETA team at Université de Liège and the Erasmus+ program for making this joint research work possible.

References

Bressi, T.H.; Holvorcem, P.R.; Schwartz, M.; Kowalski, R.A.; Ahern, J.D.; Beshore, E.C.; Beshore, E.C.; Boattini, A.; Garradd, G.J.; Gibbs, A.R; Grauer, A.D.; Hill, R.E.; Larson, S.M.; McNaught, R.H.; Birtwhistle, P. (2010). "2010 EW45." *Minor Planet Electronic Circulars*, MPEC 2010-F05.

Dandy, C.L.; Fitzsimmons, A.; Collander-Brown, S.J. (2003). "Optical colors of 56 near-Earth objects: trends with size and orbit." *Icarus* **163(2)**, 363-373.

Harris, A.W.; Young, J.W.; Scaltriti, F.; Zappala, V. (1984). "Lightcurves and phase relations of the asteroids 82 Alkmene and 444 Gyptis." *Icarus* **57(2)**, 251-258.

Harris, A.W.; Young, J.W.; Bowell, E.; Martin, L.J.; Millis, R.L.; Poutanen, M.; Scaltriti, F.; Zappalà, V.; Schober, H.J.; Debehogne, H.; Zeigler, K.W. (1989). "Photoelectric observations of asteroids 3, 24, 60, 261, and 863." *Icarus* **77(1)**, 171-186.

Jehin, E.; Gillon, M.; Queloz, D.; Magain, P.; Manfroid, J.; Chantry, V.; Lendl, M.; Hutsemékers, D.; Udry, S. (2011). "TRAPPIST: TRAnsiting planets and PlanetesImals small telescope." *The Messenger* **145(2)**, 2-6.

Mommert, M. (2017). "PHOTOMETRYPIPELINE: An automated pipeline for calibrated photometry." *Astronomy and Computing* **18**, 47-53.

NASA/JPL (2025). HORIZONS System. Jet Propulsion Laboratory, California Institute of Technology. Accessed: April 26, 2025. *https://ssd.jpl.nasa.gov/horizons/*

Paunzen, E.; Vanmunster, T. (2016). "Peranso–light curve and period analysis software." *Astronomische Nachrichten* **337(3)**, 239-245.

LIGHTCURVE ANALYSIS FOR NINE NEAR-EARTH ASTEROIDS OBSERVED BETWEEN MARCH - JUNE 2025

Peter Birtwhistle
Great Shefford Observatory
Phlox Cottage, Wantage Road
Great Shefford, Berkshire, RG17 7DA
UNITED KINGDOM
peter@birtwhistle.org.uk

(Received: 2025 July 11)

Lightcurves and amplitudes for nine near-Earth asteroids observed from Great Shefford Observatory during close approaches between March and June 2025 are reported. All are small objects and all but one have rotation periods shorter than the spin barrier at ~2.2 h, with 2025 HP4 having the unusually short period of 10.6 s. Two are identified as having tumbling rotation with two others being possible tumblers.

Photometric observations of near-Earth asteroids during close approaches to Earth between March and June 2025 were made at Great Shefford Observatory using a 0.40-m Schmidt-Cassegrain and Apogee Alta U47+ CCD camera. All observations were made unfiltered and with the telescope operating with a focal reducer at f/6. The 1K×1K, 13-micron CCD was binned 2×2 resulting in an image scale of 2.16 arcsec/pix. All the images were calibrated with dark and flat frames and *Astrometrica* (Raab, 2025) was used to measure photometry using G band data from the Gaia DR3 catalogue. *MPO Canopus* (Warner, 2023), incorporating the Fourier algorithm developed by Harris (Harris et al., 1989) was used for lightcurve analysis.

No previously reported results have been found in the Asteroid Lightcurve Database (LCDB) (Warner et al., 2009), from searches via the Astrophysics Data System (ADS, 2025) or from wider searches unless otherwise noted. All size estimates are calculated using *H* values from the Small-Body Database Lookup (JPL, 2025a), using an assumed albedo for NEAs of 0.2 (LCDB readme.pdf file) and are therefore uncertain and offered for relative comparison only.

2025 FR13. This Aten (*H = 24.2, D ~590 m*) was discovered from the ATLAS South Africa, Sutherland station on 2025 Mar 26.0 UTC and passed Earth at 3.5 Lunar Distances (LD) on 2025 Mar 30.49 UTC (Denneau et al., 2025). It was observed for 6.75 h starting on 2025 Mar 30.82 UTC and a raw plot of the 3120 data points obtained shows large magnitude variations, but no obvious repeating lightcurve pattern, suggesting non-principal axis rotation (NPAR) or tumbling may be present. A period spectrum shows a potential solution at ~3.3 h and the Dual Period Search function in *MPO Canopus* was then used to locate potential periods for rotation and precession for a body in non-principal axis rotation. The best-fit pair of NPAR periods located produce lightcurves with periods of 3.265 h and 2.396 h with amplitudes of 1.0 mag and 0.5 mag respectively and plots for these are labelled P1 and P2. However, because each period is a significant fraction of the 6.75 h it was under observation the solution cannot be regarded as safe and is provided here as one possible, but necessarily uncertain solution.

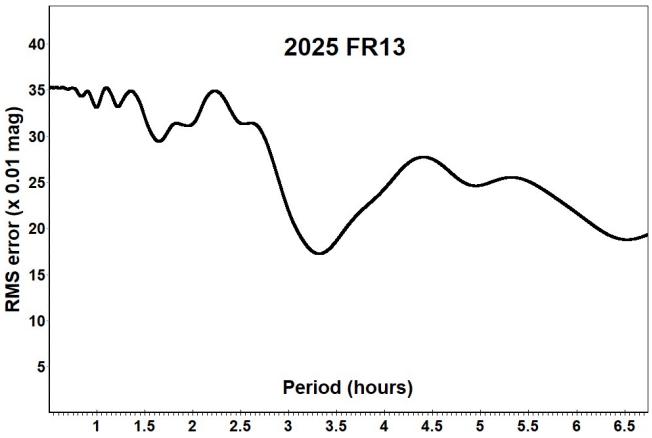

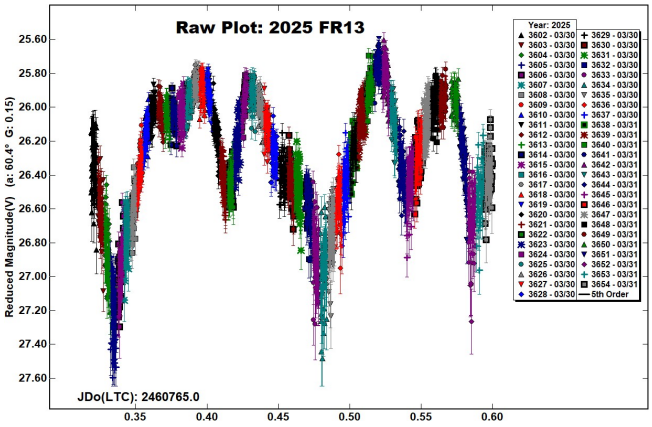

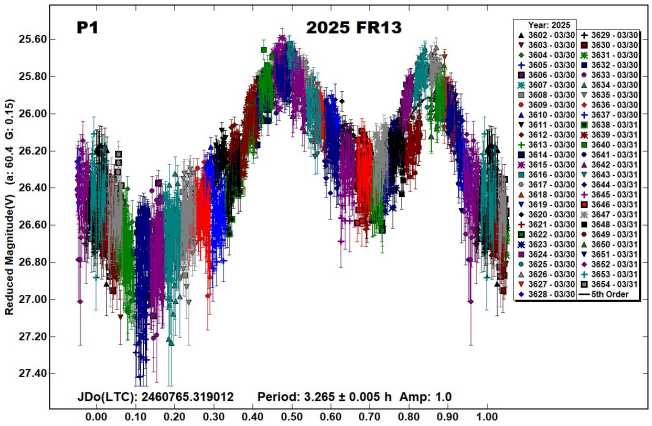

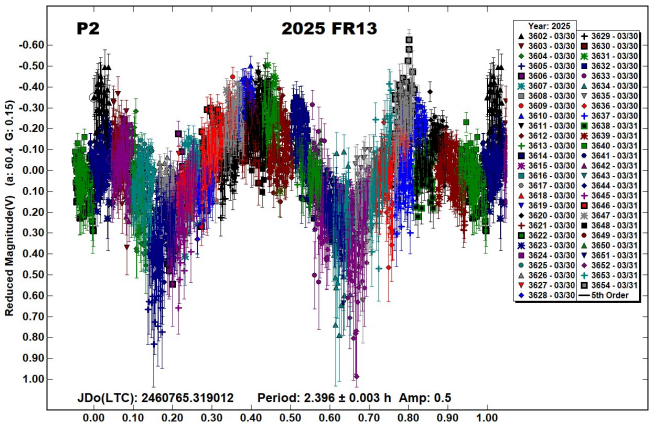

2025 GA. The discovery of this Apollo (*H = 28.7, D ~5 m*) was made on 2025 Apr 1.06 UTC from the MAP, San Pedro de Atacama observatory (Dupouy et al., 2025) and it made a very close approach, to 0.2 LD of Earth 25 hours later. It was observed for 69 minutes starting at 2025 Apr 1.83 UTC when it was 0.7 LD from Earth and with apparent speed accelerating above 160 arcsec/min exposures were limited to 3.5 s or shorter to keep the trailing of the target within the measurement annulus used in *Astrometrica*. The linearly plotted period spectrum reveals three well defined sets of equally spaced minima at multiples of 0.0059 h (21.2 s), 0.0079 h (28.4 s) and 0.0115 h (41.4 s) indicating that fast tumbling rotation is present. Again, the Dual Period Search function in *MPO Canopus* was used to determine tumbling solutions, with plots for the best-fit pair of lightcurves being labelled P1 and P2, where:

P1 = 0.015778 ± 0.000004 h (~57 s), amplitude 0.8
P2 = 0.02304 ± 0.00001 h (~83 s), amplitude 0.7

A weaker solution, consisting of the same dominant P1 period but with a secondary period of:

P3 = 0.011760 ± 0.000004 h (~42 s), amplitude 0.5

was also located, but it is noted that the frequency of the P3 period is just a linear combination of the frequencies of P1 and P2, where:

2/P1 + 1/P2 = 2/P3

and is therefore likely to just be an alias of the stronger solution. The NPAR solution indicates the full amplitude of the tumbling rotation is 1.5 mag and during the time 2025 GA was under observation it completed 72 rotations of the P1 period and 49 of the P2 period.

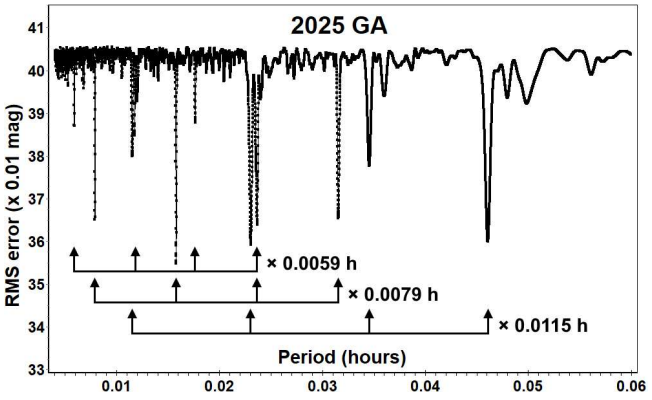

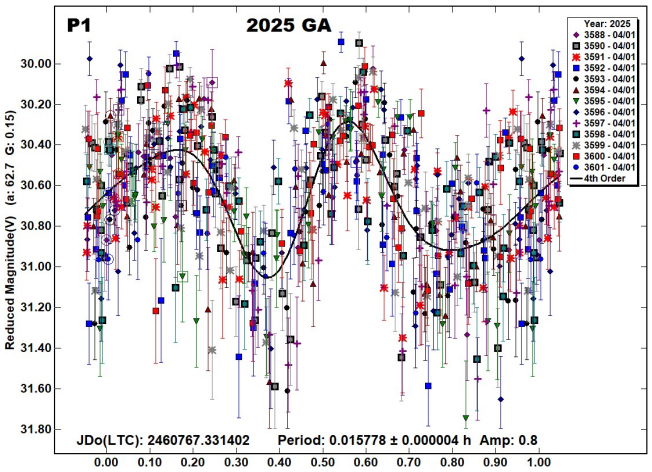

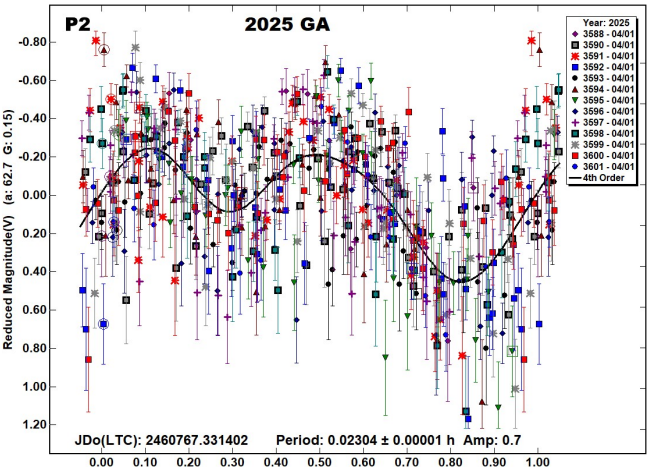

2025 GQ1. The Catalina Sky Survey discovered this Apollo (*H = 25.8, D ~20 m*) on 2025 Apr 15.15 UTC, 7 hours before it passed Earth at 2.7 LD (Leonard et al., 2025). It was observed for 18 min starting at 2025 Apr 16.91 UTC, then 1.4 h later was observed for a further 2.7 h, with 645 measurements being obtained in total. A period spectrum shows a well-defined set of solutions with the best-fit being represented by a slightly asymmetric bimodal lightcurve of period 0.06551 ± 0.00001 h (~3.9 min). 2025 GQ1 completed 45 rotations in the 3.0 h it was actively under observation.

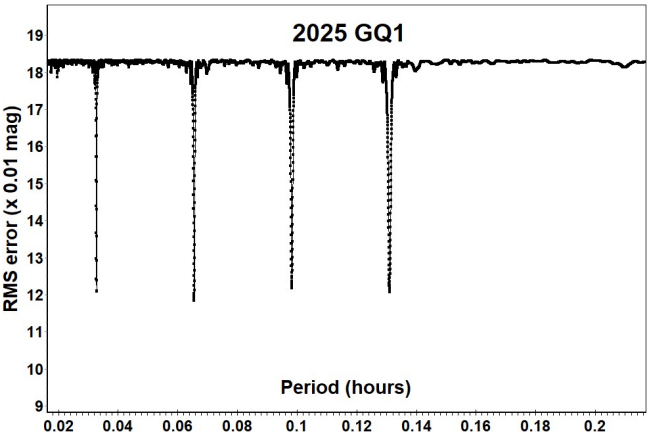

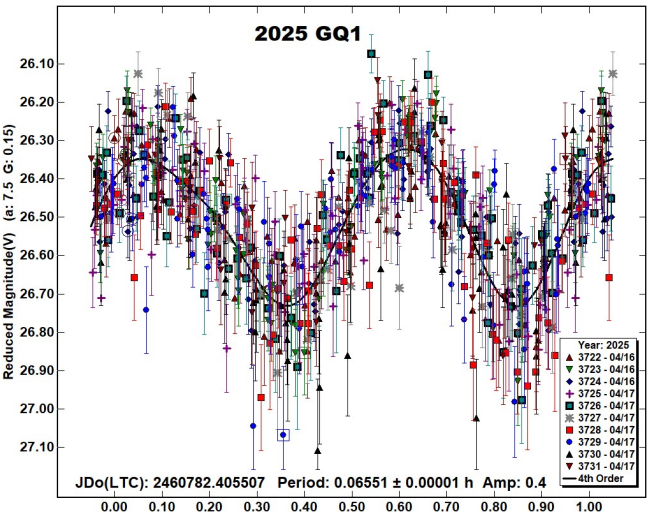

2025 HP4. Another discovery by the MAP, San Pedro de Atacama observatory, this Apollo (*H = 27.6, D ~9 m*) was first detected on 2025 Apr 26.1 UTC and made an approach to within 0.9 LD on 2025 Apr 28.2 (Ikari et al., 2025). It was observed for 2.75 h starting at 2025 Apr 27.96 UTC when it was at its peak apparent brightness of 15th mag but was poorly placed from Great Shefford with its altitude reaching 18° at best, apparent speed increasing from 275 to 335 arcsec/min and with it running into increasingly dense areas of the Milky Way in SCO and OPH. Exposures were trialled at 1.9 and 1.0 seconds due to the fast motion and, with the shorter exposures taken at a cadence of ~3 seconds, noticeable variations in magnitude were obvious between consecutive exposures. A total of 1917 photometry measurements were obtained with 92% using the shorter exposure length. Analysis of the period spectrum reveals some very tightly constrained solutions and the lightcurve plot shows the best-fit has an extremely short rotation period P of 0.0029532 ± 0.0000001 h (10.6 s). The guideline exposure length for a bimodal lightcurve, to maximise SNr before lightcurve smoothing becomes excessive (Pravec et al., 2000) is 0.185 × P, so in this instance the optimal exposure length would be 1.97s, indicating that due to the short exposures used, lightcurve smoothing is unlikely to have significantly affected the resultant lightcurve shape or amplitude. 2025 HP4 completed 932 rotations during the period it was under observation.

2025 HL5. This is another Catalina Sky Survey discovery of an Apollo (*H = 25.7, D ~22 m*) made on 2025 Apr 27.25 UTC (Naves et al., 2025). It was observed for 4.4 h starting on 2025 Apr 28.91 UTC and for a further 5.1 h starting on 2025 Apr 29.88 UTC. During that second session 2025 HL5 reached its closest point to Earth, at 1.6 LD on 2025 Apr 29.96 UTC. It was at high phase angles on both nights, reaching a minimum of 76.5° between the two sessions. Linearly scaled period spectra using data from both nights combined (see plot) and for each night independently show the same signs of tumbling rotation, with two sets of equally spaced minima at multiples of 0.421 h (~25.3 min) and 0.157 h (~9.4 min). With the effects of the high phase angle and changing geometry, independent determinations of possible tumbling rotation for each of the two nights were made using the *MPO Canopus* Dual Period Search function, with the best-fit solutions being similar for the two nights:

2025 Apr 28:
P1 = 0.4211 ± 0.0006 h (~25.3 min), amplitude 0.8
P2 = 0.3129 ± 0.0003 h (~18.8 min), amplitude 0.6

2025 Apr 29:
P1 = 0.4204 ± 0.0003 h (~25.2 min), amplitude 1.0
P2 = 0.3134 ± 0.0002 h (~18.8 min), amplitude 0.5

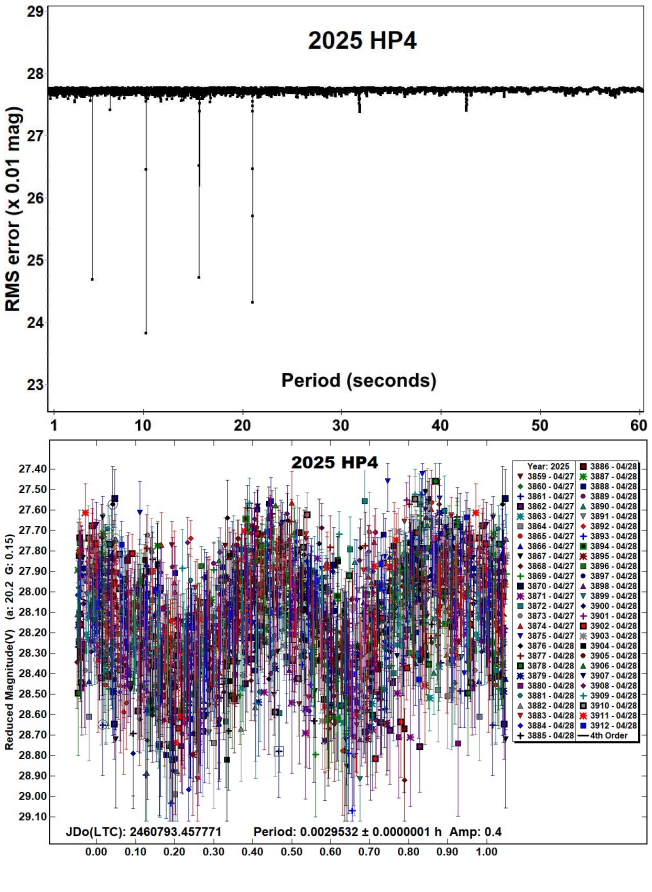

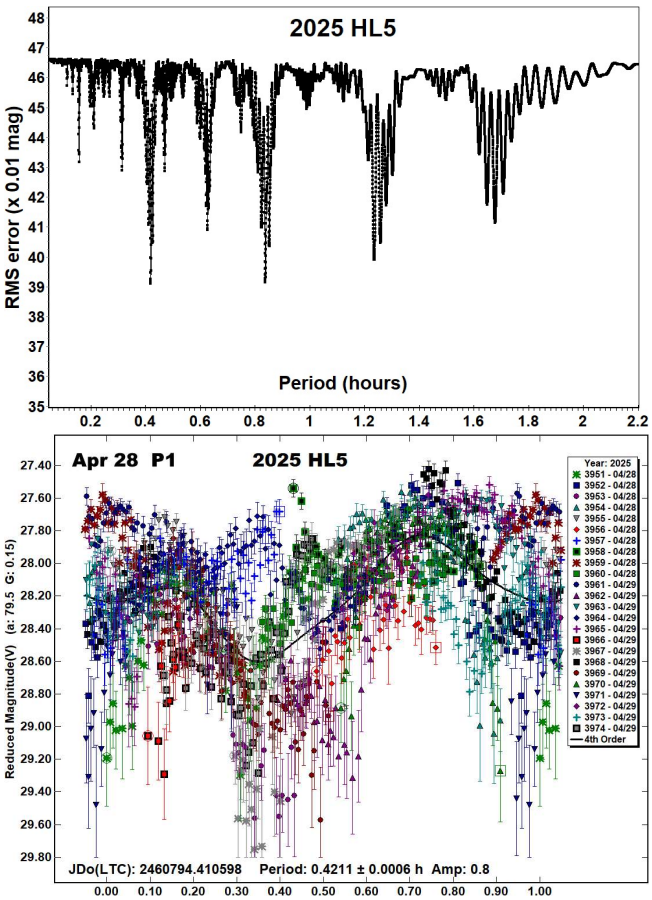

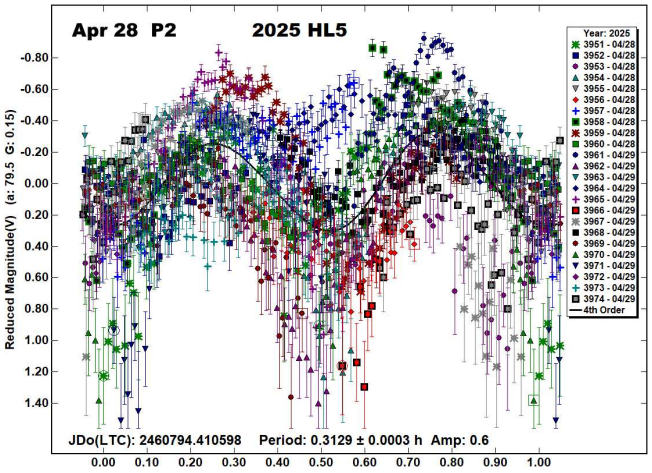

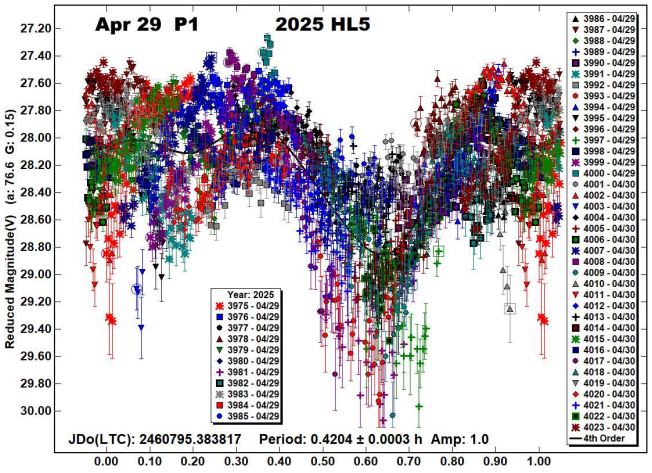

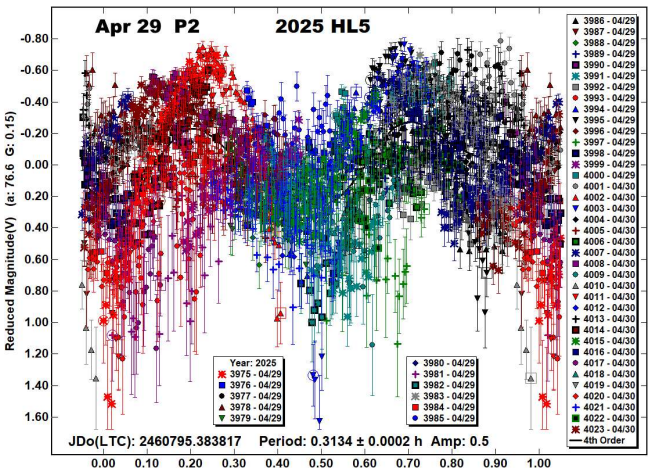

It is noted that on both nights, although the combined P1 and P2 Fourier series do model the times of maxima and minima well, the amplitude of those points are poorly represented, even with higher order solutions. As an example, this 36-minute segment of raw plot starting at 2025 Apr 30 00:40 UTC shows observed magnitude deltas together with the modelled NPAR lightcurve as a solid line.

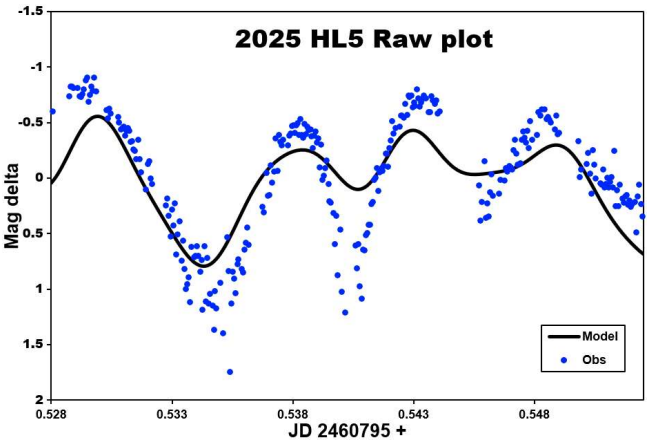

This poor fit is very likely due to shadowing effects as a result of viewing at phase angles > 76° and has resulted in the A.E. (Amplitude error) column in Table II, calculated from √2 × (lightcurve RMS residual) to be ~0.5 on both nights, much larger than the SNr of the individual measurements would suggest. The full amplitude of the tumbling lightcurve estimated from the raw lightcurves from both nights is given below and the value from the second night has been used in the calculation of Min a/b (minimum elongation of the asteroid) in Table I.

Estimated amplitude of the tumbling lightcurve:

2025 Apr 29.0 UTC, amp. 2.4 ± 0.2 mag (phase 79.2°)
2025 Apr 30.0 UTC, amp. 2.1 ± 0.2 mag (phase 76.9°)

2025 KA. The Catalina Sky Survey discovered this Apollo (*H = 25.9, D ~19 m*) on 2025 May 16.4 UTC and it made a relatively distant approach to Earth, to 4.2 LD on 2025 May 17.6 UTC (Galli et al., 2025). Photometry was collected for 1.5 h starting on 2025 May 16.95 UTC and analysis indicates the best-fit solution produces an asymmetric bimodal lightcurve with period 0.1225 ± 0.0001 h (~7.4 min).

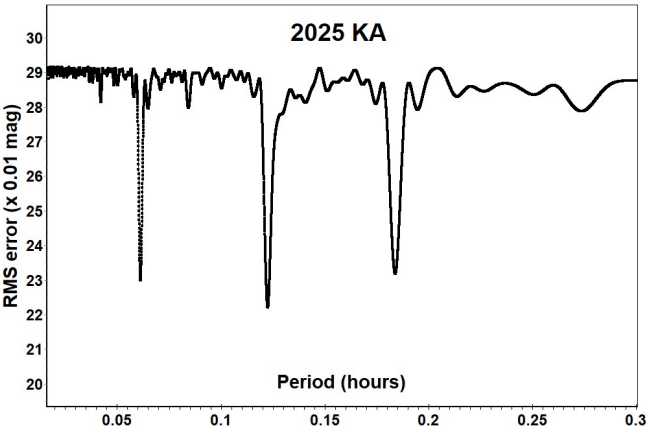

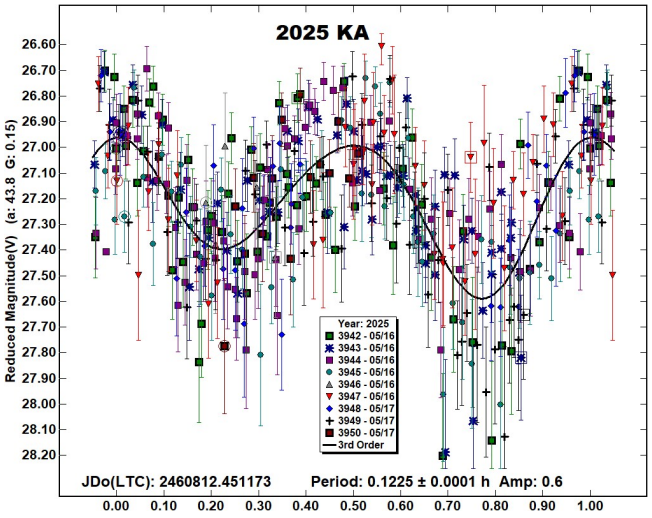

2025 KD. Another Apollo (*H = 25.8, D ~20 m*) discovered by the Catalina Sky Survey, this one from 2025 May 18.3 UTC, 2 h after it had passed Earth at 3.6 LD (Luongo et al., 2025). It was observed for 1.1 h starting on 2025 May 18.94 UTC and analysis reveals the best-fit solution gives an asymmetric bimodal lightcurve with period 0.2378 ± 0.0007 h (~14.3 min) and amplitude of 0.8.

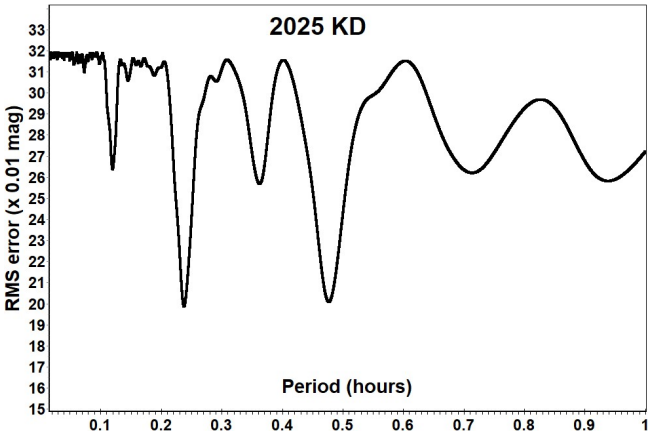

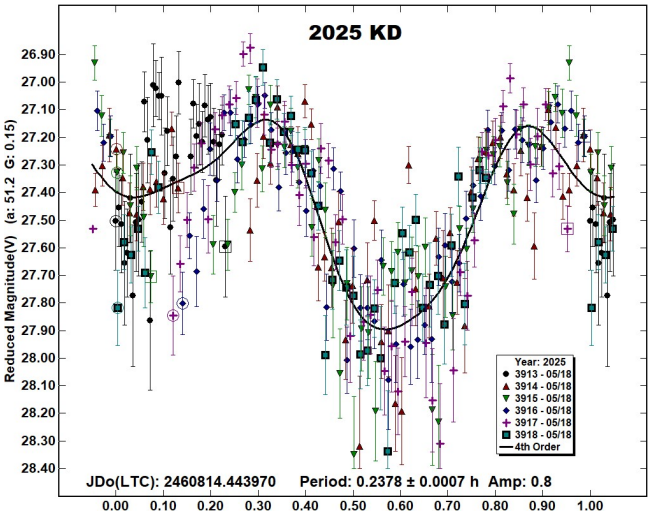

2025 KE1. Another Catalina Sky Survey discovery of an Apollo (*H = 26.5, D ~15 m*), made on 2025 May 21.4 UTC, on its way to an approach to within 0.5 LD of Earth on 2025 May 23.06 h (Gilmore et al., 2025). It was observed for 68 minutes starting on 2025 May 22.92 UTC when it had reached 13th mag but was very poorly placed, moving swiftly south, initially at an altitude of 14° reducing to 8° by the end of the session. The best-fit solution gives a period of 0.04177 ± 0.00003 h (~2.5 min) and a bimodal lightcurve.

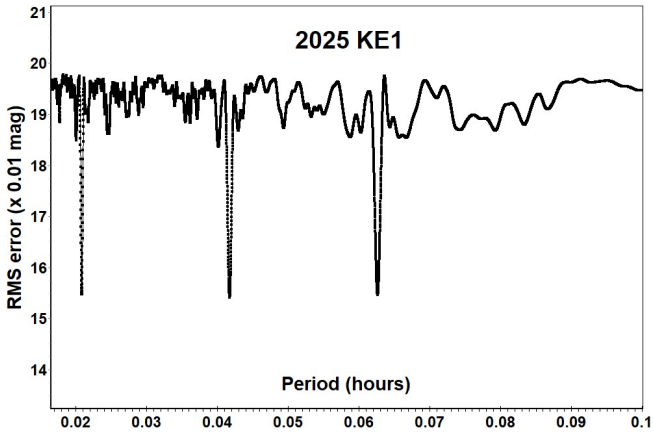

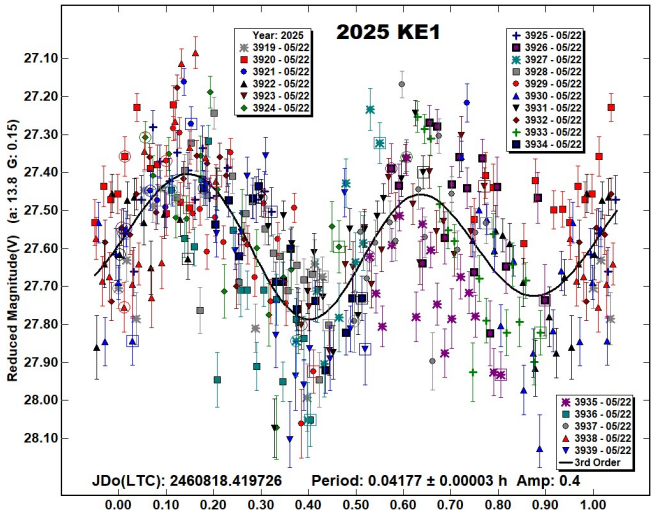

2025 ML2. The discovery of this Apollo (*H = 25.4, D ~24 m*) by the Catalina Sky Survey on 2025 June 23.3 UTC was made 10 hours before its closest approach to Earth at 4 LD (Kowalski et al., 2025). It is listed by the impact monitoring services Sentry (JPL, 2025b), Clomon-2 (NEODyS, 2025) and Aegis (ESA, 2025) with several very low probability potential impacts, the earliest in 2097. 2025 ML2 was observed for 2.7 h starting on 2025 June 23.94 UTC and again for 1.4 h starting 2025 June 24.91 UTC. A period spectrum using data from both dates suggests possible solutions near 0.6 h, 0.95 h and 1.2 h, each with multiple similar minima due to the ~24 h gap between the two short sets of observations.

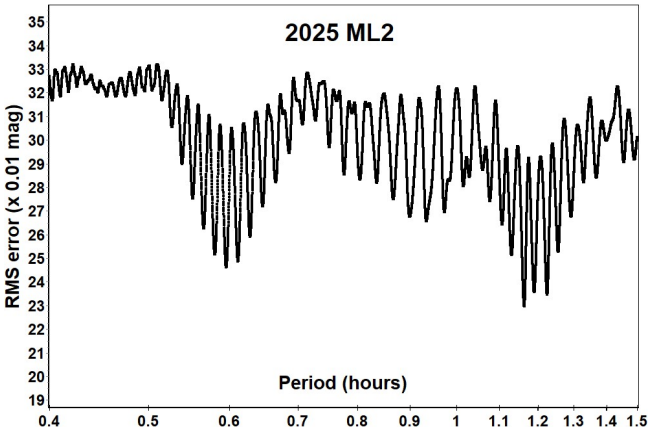

Initial lightcurve analysis using *MPO Canopus* resolves the best-fit principal axis rotation (PAR) period as 1.1638 ± 0.0004 h with amplitude 0.8, but this shows some indications that tumbling may be present. Further analysis with the Dual Period Search function of *MPO Canopus* does reveal potential NPAR (tumbling) solutions, with the best-fit pair of periods being:

P1 = 1.2241 ± 0.0003 h, amplitude 0.7
P2 = 0.9829 ± 0.0004 h, amplitude 0.5

However, due to the 24 h gap between the short sets of observations on the two nights, there are other similar NPAR solutions giving only slightly inferior RMS fits. The three best NPAR solutions are listed here as a), b) and c) together with the PAR solution d) in order of worsening RMS fit to their respective lightcurves:

```
a)  P1  = 1.2241 h,  P2 = 0.9829 h,  RMS = 0.179
b)  P1  = 1.1627 h,  P2 = 0.9415 h,  RMS = 0.183
c)  P1  = 1.1889 h,  P2 = 0.9041 h,  RMS = 0.185
d)  PAR = 1.1638 h,                  RMS = 0.230
```

All the NPAR solutions a), b) and c) are superior to the PAR solution d) and phased lightcurves labelled as P1 and P2 are given for the best-fit solution a). However, attempting to assign a rating on the PAR scale defined in Pravec et al., (2005) is somewhat problematic as the codes attributable to NPA rotation were developed for situations where a main period has been determined uniquely. In the case of 2025 ML2 there are a number of possible NPAR solutions for both the main and the secondary periods, however tumbling rotation is reasonably well detected in each and therefore it may be appropriate to rate as PAR = -2, where NPA rotation is detected based on deviations from a single period but the second period is not resolved. (Petr Pravec, personal communication). The full amplitude of the tumbling rotation for solution a) is 1.2 mag and this value has been used in the calculation of Min a/b (minimum elongation of the asteroid) in Table I.

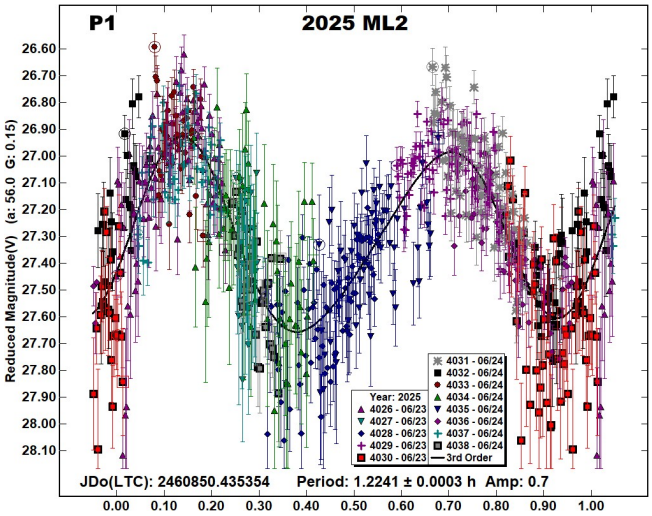

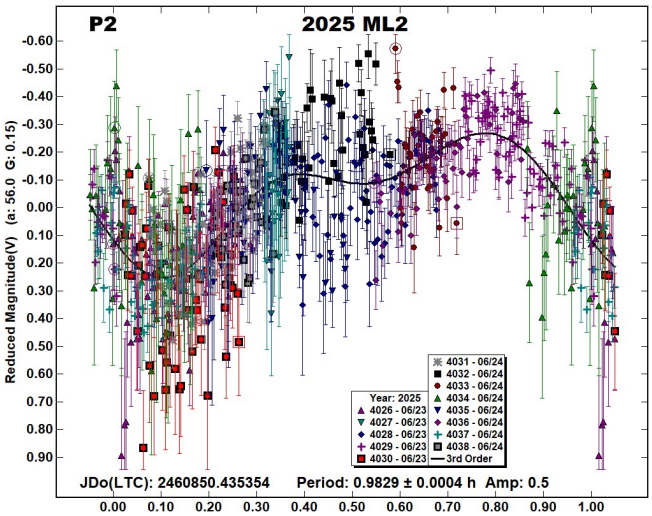

Number	Name	Integration times	Max intg/Pd	Min a/b	Pts	Flds
	2025 FR13	4.2-5.5	0.001[1]	1.5*	3120	53
	2025 GA	2.7-3.5	0.062[1]	1.2*	516	13
	2025 GQ1	12-14	0.060	1.4	645	10
	2025 HP4	1-1.9	0.177	1.2	1917	54
	2025 HL5	3.6-9	0.008[1]	1.8*	3813	73
	2025 KA	7.5	0.017	1.3*	391	9
	2025 KD	4-11.1	0.013	1.3*	310	6
	2025 KE1	0.8-1.3	0.009	1.3	334	21
	2025 ML2	3.5-12	0.003[1]	1.6*	720	13

Table I. Ancillary information, listing the integration times used (seconds), the fraction of the period represented by the longest integration time (Pravec et al., 2000), the calculated minimum elongation of the asteroid (Zappala et al., 1990), the number of data points used in the analysis and the number of times the telescope was repositioned to different fields. Note: * = Value uncertain, based on phase angle > 40°, 1 = Calculated using the shorter of the NPAR periods.

Number	Name	yyyy mm/dd	Phase	L_{PAB}	B_{PAB}	Period(h)	P.E.	Amp	A.E	PAR	H
2025	FR13	2025 03/30-03/31	60.3,74.1	168	27	3.265	0.005	1.0	0.2	-2	24.2
						2.396	0.003	0.5	0.2		
2025	GA	2025 04/01-04/01	62.8,65.8	162	-12	0.015778	0.000004	0.8	0.4	-3	28.7
						0.02304	0.00001	0.7	0.4		
2025	GQ1	2025 04/16-04/17	7.4,5.8	208	3	0.06551	0.00001	0.4	0.2		25.8
2025	HP4	2025 04/27-04/28	20.8,34.4	231	0	0.0029532	0.0000001	0.4	0.3		27.6
2025	HL5	2025 04/28-04/29	79.6,78.9	196	34	0.4211	0.0006	0.8	0.5	-3	25.7
						0.3129	0.0003	0.6	0.5		
2025	HL5	2025 04/29-04/30	76.7,77.1	235	36	0.4204	0.0003	1.0	0.5	-3	
						0.3134	0.0002	0.5	0.5		
2025	KA	2025 05/16-05/17	43.7,45.4	228	21	0.1225	0.0001	0.6	0.3		25.9
2025	KD	2025 05/18-05/18	51.1,50.6	215	13	0.2378	0.0007	0.8	0.3		25.8
2025	KE1	2025 05/22-05/22	13.4,13.5	248	1	0.04177	0.00003	0.4	0.2		26.5
2025	ML2	2025 06/23-06/24	56.0,41.7	263	22	1.2241	0.0003	0.7	0.3	-2	25.4
						0.9829	0.0004	0.5	0.3		

Table II. Observing circumstances and results. The phase angle is given for the first and last date. If preceded by an asterisk, the phase angle reached an extrema during the period. L_{PAB} and B_{PAB} are the approximate phase angle bisector longitude/latitude at mid-date range (see Harris et al., 1984). Amplitude error (A.E.) is calculated as $\sqrt{2}$ × (lightcurve RMS residual). PAR is the expected Principal Axis Rotation quality detection code (Pravec et al., 2005) and H is the absolute magnitude at 1 au from Sun and Earth taken from the Small-Body Database Lookup (JPL, 2025a).

Acknowledgements

The author is very grateful to Dr. Petr Pravec, Astronomical Institute, Czech Republic for his continuing help with the interpretation of tumbling asteroid lightcurves. The author also gratefully acknowledges a Gene Shoemaker NEO Grant from the Planetary Society (2005) and a Ridley Grant from the British Astronomical Association (2005), both of which facilitated upgrades to observatory equipment used in this study.

This work has made use of data from the European Space Agency (ESA) mission Gaia (*https://www.cosmos.esa.int/gaia*), processed by the Gaia Data Processing and Analysis Consortium (DPAC, *https://www.cosmos.esa.int/web/gaia/dpac/consortium*). Funding for the DPAC has been provided by national institutions, in particular the institutions participating in the Gaia Multilateral Agreement.

References

ADS (2025). Astrophysics Data System. *https://ui.adsabs.harvard.edu/*

Denneau, L.; Siverd, R.; Tonry, J.; Weiland, H.; Erasmus, N.; Fitzsimmons, A.; Robinson, J.; Thaluang, T. (2025). "2025 FR13." MPEC 2025-F218. *https://minorplanetcenter.net/mpec/K25/K25FL8.html*

Dupouy, P.; Laborde, J.; Felber, T.; Losse, F.; Birtwhistle, P.; Remmel, P.; Gerhard, C.; Duin, H.; Mari, J.-M.; Jasicki, C.; Maury, A.; Attard, G.; Parrott, D.; Signoret, F. (2025). "2025 G." MPEC 2025-G29. *https://minorplanetcenter.net/mpec/K25/K25G29.html*

ESA (2025) Risk List. *https://neo.ssa.esa.int/risk-list*

Galli, G.; Buzzi, L.; Carvajal, V.F.; Beuden, T.; Fay, D.; Fazekas, J.B.; Fuls, D.C.; Gibbs, A.R.; Grauer, A.D.; Groeller, H.; Hogan, J.K.; Kowalski, R.A.; Larson, S.M.; Leonard, G.J.; Rankin, D. and 28 colleagues (2025). "2025 KA." MPEC 2025-K03. *https://www.minorplanetcenter.net/mpec/K25/K25K03.html*

Gilmore, A.C.; Kilmartin, P.M.; Rankin, D.; Beuden, T.; Carvajal, V.F.; Fay, D.; Fazekas, J.B.; Fuls, D.C.; Gibbs, A.R.; Grauer, A.D.; Groeller, H.; Hogan, J.K.; Kowalski, R.A.; Larson, S.M.; Leonard, G.J. and 31 colleagues (2025). "2025 KE1" MPEC 2025-K49. *https://www.minorplanetcenter.net/mpec/K25/K25K49.html*

Harris, A.W.; Young, J.W.; Scaltriti, F.; Zappala, V. (1984). "Lightcurves and phase relations of the asteroids 82 Alkmene and 444 Gyptis." *Icarus* **57**, 251-258.

Harris, A.W.; Young, J.W.; Bowell, E.; Martin, L.J.; Millis, R.L.; Poutanen, M.; Scaltriti, F.; Zappala, V.; Schober, H.J.; Debehogne, H.; Zeigler, K. (1989). "Photoelectric Observations of Asteroids 3, 24, 60, 261, and 863." *Icarus* **77**, 171-186.

Ikari, Y.; Thinius, B.; Koch, B.; Lindner, P.; Urbanik, M.; Felber, T.; Hogan, J.K.; Beuden, T.; Carvajal, V.F.; Fay, D.; Fazekas, J.B.; Fuls, D.C.; Gibbs, A.R.; Grauer, A.D.; Groeller, H. and 26 colleagues (2025). "2025 HP4." MPEC 2025-H161. *https://minorplanetcenter.net/mpec/K25/K25HG1.html*

JPL (2025a). Small-Body Database Lookup. *https://ssd.jpl.nasa.gov/tools/sbdb_lookup.html*

JPL (2025b). Sentry: Earth Impact Monitoring *https://cneos.jpl.nasa.gov/sentry/*

Kowalski, R.A.; Gray, B.; Rankin, D.; Shelly, F.C.; Beuden, T.; Carvajal, V.F.; Fay, D.; Fazekas, J.B.; Fuls, D.C.; Gibbs, A.R.; Grauer, A.D.; Groeller, H.; Hogan, J.K.; Larson, S.M.; Leonard, G.J. and 12 colleagues (2025). "2025 ML2." MPEC 2025-M82. *https://www.minorplanetcenter.net/mpec/K25/K25M82.html*

Leonard, G.J.; Beuden, T.; Carvajal, V.F.; Fay, D.; Fazekas, J.B.; Fuls, D.C.; Gibbs, A.R.; Grauer, A.D.; Groeller, H.; Hogan, J.K.; Kowalski, R.A.; Larson, S.M.; Rankin, D.; Seaman, R.L.; Shelly, F.C. and 37 colleagues (2025). "2025 GQ1." MPEC 2025-H04. *https://minorplanetcenter.net/mpec/K25/K25H04.html*

Luongo, D.; Lachat, D.; Buzzi, L.; Naves, R.; Campas, M.; Fumagalli, A.; Testa, A.; Hogan, J.K.; Beuden, T.; Carvajal, V.F.; Fay, D.; Fazekas, J.B.; Fuls, D.C.; Gibbs, A.R.; Grauer, A.D. and 32 colleagues (2025). "2025 KD." MPEC 2025-K10. *https://minorplanetcenter.net/mpec/K25/K25K10.html*

Naves, R.; Campas, M.; Tichy, M.; Ticha, J.; Honkova, M.; D'Agostino, G.; Pettarin, E.; Beuden, T.; Carvajal, V.F.; Fay, D.; Fazekas, J.B.; Fuls, D.C.; Gibbs, A.R.; Grauer, A.D.; Groeller, H. and 46 colleagues (2025). "2025 HL5." MPEC 2025-H178. *https://minorplanetcenter.net/mpec/K25/K25HH8.html*

NEODyS (2025) Risk List. *https://newton.spacedys.com/neodys/index.php?pc=4.1*

Pravec, P.; Hergenrother, C.; Whiteley, R.; Sarounova, L.; Kusnirak, P.; Wolf, M. (2000). "Fast Rotating Asteroids 1999 TY2, 1999 SF10, and 1998 WB2." *Icarus* **147**, 477-486.

Pravec, P.; Harris, A.W.; Scheirich, P.; Kušnirák, P.; Šarounová, L.; Hergenrother, C.W.; Mottola, S.; Hicks, M.D.; Masi, G.; Krugly, Y.N.; Shevchenko, V.G.; Nolan, M.C.; Howell, E.S.; Kaasalainen, M.; Galád, A. and 5 colleagues. (2005). "Tumbling Asteroids." *Icarus* **173**, 108-131.

Raab, H. (2025). Astrometrica software, version 4.16.0.460. *http://www.astrometrica.at/*

Warner, B.D.; Harris, A.W.; Pravec, P. (2009). "The Asteroid Lightcurve Database." *Icarus* **202**, 134-146. Updated 2023 Oct. *https://www.minorplanet.info/php/lcdb.php*

Warner, B.D. (2023). MPO Software, Canopus version 10.8.6.20. Bdw Publishing, Colorado Springs, CO. *https://minplanobs.org/BdwPub/*

Zappala, V.; Cellini, A.; Barucci, A.M.; Fulchignoni, M.; Lupishko, D.E. (1990). "An analysis of the amplitude-phase relationship among asteroids." *Astron. Astrophys*. **231**, 548-560.

LIGHTCURVE OF COMET C/2024 M1 (ATLAS)

Sonka Adrian Bruno
Astronomical Institute of the Romanian Academy
5 Cuţitul de Argint, 040557 Bucharest, ROMANIA
Astronomical Observatory "Amiral Vasile Urseanu"
21, Bd. Lascar Catargiu, 010662, Bucharest, ROMANIA
sonka@astro.ro

Alin Nedelcu
Astronomical Institute of the Romanian Academy
Bucharest, ROMANIA

Mirel Birlan
Astronomical Institute of the Romanian Academy
Bucharest, ROMANIA
IMCCE, Observatoire de Paris
77 av Denfert Rochereau, 75014 Paris cedex, FRANCE

Mădălina Trelia
Astronomical Institute of the Romanian Academy
Bucharest, ROMANIA
Faculty of Physics, University of Bucharest
405, Atomistilor Street, 077125 Magurele, Ilfov, ROMANIA

(Received: 2025 June 12)

We present the lightcurve of comet C/2024 M1 (ATLAS) from two observatories, determined after noticing that it presents no cometary activity.

C/2024 M1 (ATLAS) was discovered on 2024 June 29, by the Asteroid Terrestrial-Impact Last Alert System (ATLAS) search program. On 2024 November 20, the comet crossed its perihelion at 1.703 AU, and the last orbit determined by the Minor Planet Center shows that C/2024 M1 is a periodic comet with P=163.752 years.

We first observed the comet on 2024 December 22, while it was at 0.828 AU from Earth and 1.752 AU from the Sun, from L54 Berthelot Observatory (Birlan et al., 2021), and failed to detect any visible coma or tail, even on a stack of images with a total exposure of 2.9 hours. Following this observation, we started to monitor the comet in order to determine the rotational period, also checking for any cometary activity. Very often, the coma of a comet hides the true properties of the nucleus, and while these objects can be observed at large heliocentric distances so that some physical properties can be determined, their small brightness makes them accessible to only very large telescopes. Comet C/2024 M1 (ATLAS) with its apparent lack of coma represented a good target to be monitored by small telescopes.

We observed the comet nucleus between 2024 December 22 and 2025 January 22, for 8 nights, using two identical telescopes, a 0.5-m, f/7, Riccardi Dall-Kirkham, with a SBIG STXL-6303 and FLI 16803 CCD cameras, located at Berthelot Observatory (IAU Code L54) and IAU code 073 Bucharest Observatory (Birlan et al, 2019). The images were taken without a filter and the exposure time varied from 90 to 120 seconds. For data reduction (bias, dark, and flat subtraction) and photometry we used *Tycho-Tracker* (Parrot, 2024) with reference stars from the ATLAS star catalog, V magnitude band (Tonry et al., 2018).

Number	Name	yyyy mm/dd	Phase	L_{PAB}	B_{PAB}	Period(h)	P.E.	Amp	A.E.	Grp
	C/2024 M1 (ATLAS)	2024 12/22-01/22	17.0,29.6	68	18	9.45	0.02	0.435	0.05	

Table I. Observing circumstances and results. The phase angle is given for the first and last date. If preceded by an asterisk, the phase angle reached an extrema during the period. L_{PAB} and B_{PAB} are the approximate phase angle bisector longitude/latitude at mid-date range (see Harris et al., 1984). Grp is the asteroid family/group (Warner et al., 2009).

We analyzed the comet activity by comparing the brightness profile of the comet and that of a star in the field (Galiazzo et al., 2016). If the comet exhibited a coma, the profile should be different, as the coma brightness should contribute to the overall brightness of the comet. However, in all our data we found that in every observing session the profile of stars was identical to that of the comet (Figure 1).

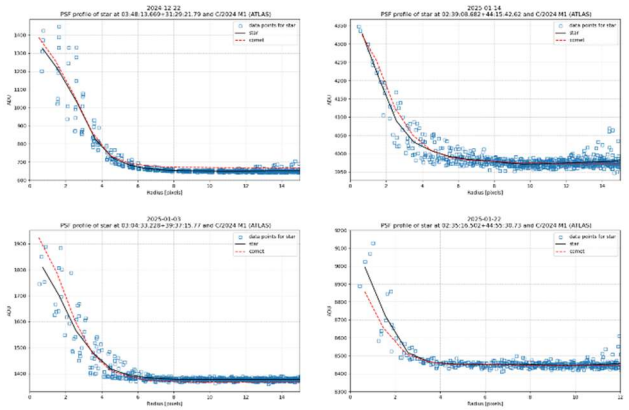

Figure 1: Brightness profiles of stars and comet during our observing period. We included the profile for 2025-01-22 even if we did not use this data in our light curve.

After finding that the comet shows little activity we proceeded to determine its rotational period, as we would do for an asteroid. Our analysis form observation made at the observatories shows that C/2024 M1 (ATLAS) has a rotation period of 9.45 ± 0.02 h, and an amplitude of 0.44 magnitudes. The composite lightcurve has equal amplitude minima (Figure 2).

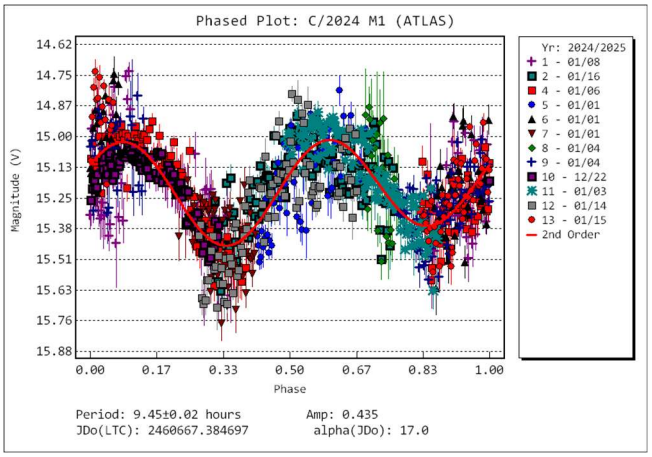

Figure 2: Phased lightcurve of C/2024 M1 (ATLAS).

C/2024 M1 (ATLAS) represents a rare type of comet which shows no activity even at small heliocentric distances, which allows the determination of the rotational period of the nucleus.

References

Birlan, M.; Sonka, A.; Nedelcu, D.A.; Balan, M.; Anghel, S.; Pandele, C.; Trusculescu, M.; Dragasanu, C.; Plesca, V.; Gandescu, C.H.; Banica, C.; Georgescu, T. (2019). "Telescope calibration for mobile platforms: first results." *Romanian Astronomical Journal* **29(1)**, 23-32.

Birlan, M.; Sonka, A.; Badescu, O.; Nedelcu, A.; Paraschiv, P.; Turcu, V.; Anghel, S.; Besliu-Ionescu, D.; Boaca, I.; Trelia, M.; Moldovan, D.; Petrescu, E.; Huzoni, A. (2021). "Berthelot, the new astronomical station in Romania." *Romanian Astronomical Journal* **31(1)**, 41-56.

Galiazzo, M.; de la Fuente Marcos, C.; de la Fuente Marcos, R.; Carraro, G.; Maris, M.; Montalto, M. (2016). "Photometry of Centaurs and trans-Neptunian objects: 2060 Chiron (1977 UB), 10199 Chariklo (1997 CU 26), 38628 Huya (2000 EB 173), 28978 Ixion (2001 KX 76), and 90482 Orcus (2004 DW)." *Astrophysics and Space Science* **361**, 1-15.

Harris, A.W.; Young, J.W.; Scaltriti, F.; Zappala, V. (1984). "Lightcurves and phase relations of the asteroids 82 Alkmene and 444 Gyptis." *Icarus* **57**, 251-258.

Parrott, D. (2024). Tycho Tracker Software. *https://www.tycho-tracker.com*

Tonry, J.L.; Denneau, L.; Flewelling, H.; Heinze, A.N.; Onken, C.A.; Smartt, S.J.; Stalder, B.; Weiland, H.J.; Wolf, C. (2018). "The ATLAS All-Sky Stellar Reference Catalog." *Astrophys. J.* **867**, A105.

Warner, B.D.; Harris, A.W.; Pravec, P. (2009). "The Asteroid Lightcurve Database." *Icarus* **202**, 134-146. *https://www.minorplanet.info/php/lcdb.php*

ON THE GAIA DR3 REFLECTANCE SPECTRA

Lorenzo Franco
Balzaretto Observatory (A81), Rome, ITALY
lor_franco@libero.it

(Received: 2025 July 10 Revised: 2025 July 13)

For the community of observers in the Minor Planets Section and beyond, we present a study on the reflectance spectra contained in the ESA Gaia DR3 database. This data set has great potential for the amateur astronomer community, especially for the classification of asteroids that do not have any previous classifications. A taxonomic classification has been carried out for 14954 asteroids. Of these, there are 1214 asteroids in common with the SMASSII catalogue, of which for 914 the taxonomic classification agrees (78%). The quality of the Gaia spectra sometimes is not very high, so it is advisable to proceed with caution, using a visual inspection in the most ambiguous cases.

The ESA Gaia database Data Release 3 (June 13, 2022) includes 60518 asteroid reflectance spectra, primarily from the main belt. The spectra cover the visible spectrum band and a part of the near infrared band, between the wavelengths of 374 and 1034 nm. The procedures and methods used for the reduction are reported by Galluccio et al. (2023), to which one can refer for further information and references.

The ESA Gaia DR3 reflectance spectra represent, due to their extensiveness, one of the main sources of information for the taxonomic classification of asteroids.

This study is inspired by that of Galluccio et al. (2023), with some simplifications. The main goal is to encourage the use of ESA Gaia DR3 spectro-photometric data by the amateur astronomer community, whose contribution is often limited to photometric lightcurves only. For this work we used *Scilab 6.11* (2021) for scripting language environment and *Orange 3.34* (Demsar et al., 2013) for data analysis.

The reflectance spectra were downloaded from the Gaia ESA Archive (2025) with an ADQL query (Astronomical Data Query Language; See Appendix). A total of 60518 reflectance spectra were extracted, relating to as many asteroids. Each reflectance spectrum is sampled in 16 wavelength band (between 374 and 1034 nm) and is normalized to the 550 nm wavelength. For each record a 'reflectance_spectrum_flag' is provided for indicates the quality of the single reflectance value (0=good, 1=poor, 2=compromised).

Most of the Gaia spectra have reflectance values with reflectance_spectrum_flag=2. It was therefore decided to limit this study only to the spectra with the quality flag set to 0 and 1. A total of 14966 spectra were selected (25% of the total), discarding 45552 (75% of the total).

For comparison and reference, the mean spectra of the Bus-DeMeo taxonomy (DeMeo et al., 2009) were used, downloadable from the Planetary Data System, Small Bodies Node (2020), cut at 1050 nm (13 wavelength samples for each reflectance spectrum), for homogeneity with the spectral extension, in wavelength, of the ESA Gaia sample.

Following the approach of DeMeo and Carry (2013) and Galluccio et al. (2023), for all the spectra (Gaia DR3 and the mean reflectance values from Bus-DeMeo taxonomy), we evaluated the spectral slope and *z-i* color, because these explain many of the distinctive taxonomic features of the asteroids. In the reflectance spectrum, the slope characterizes the UV wavelength region, while the *z-i* color takes into account the presence and the depth of the 1-μm absorption band.

First of all, the Gaia reflectance spectrum is sampled on slightly different wavelengths than the Bus-DeMeo taxonomy reference spectra. For homogeneity, we chose to resample the Gaia spectrum on the same wavelength intervals as the Bus-DeMeo reference spectra through a cubic spline interpolation. Specifically, we used the *Scilab* functions *splin*() and *interp*(), setting the wavelength range from 0.45 to 1.05 μm with 0.05 μm steps.

In detail, the slope parameter was determined from the regression line between the points of the reflectance spectrum between 0.45 and 0.75 μm. While the *z-i* color parameter was obtained calculating the follow expression from Galluccio et al. (2023): *z-i* = -2.5*log10(Rz/Ri), where Rz and Ri are respectively the reflectance value at wavelength of 0.75 and 0.90 μm. These last are a very close approximation to those used by Galluccio et al. (2023) at 748 and 893 nm.

The plot of the slope vs *z-i* parameters for the Gaia DR3 reflectance spectra sample shows a discrepancy on the overlap areas with respect to the reference parameters of the Bus-DeMeo taxonomy, differently from what one might have expected (Figure 1). In detail the *z-i* values appear all systematically higher respect to the values of the Bus-DeMeo reference taxonomy. Note, for example, that the S sub-classes, despite being one of the most populous classes, all appear off-center and fall within a low-density area occupied by the Gaia data.

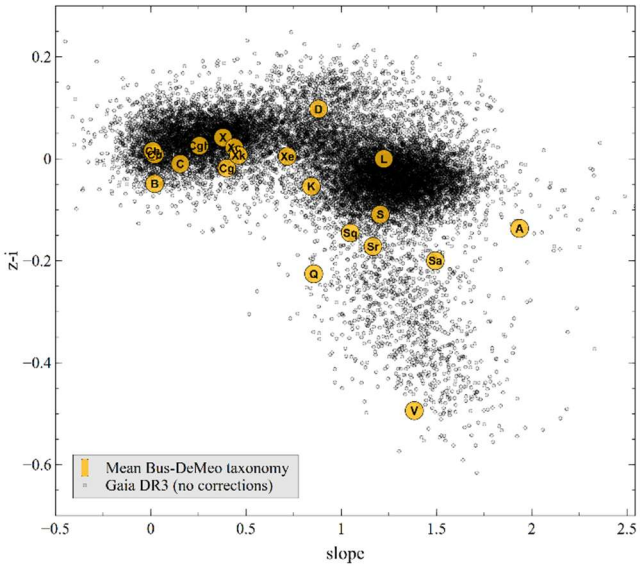

Figure 1: The Gaia DR3 sample distribution for the slope and *z-i* parameters. A discrepancy is noted on the overlap areas compared to the reference parameters represented by the Bus-DeMeo taxonomy. Note that the S sub-classes fall within a low-density area occupied by the Gaia data.

To investigate this discrepancy, we plotted the relation Gaia vs Bus-DeMeo for slope and *z-i* color, using as reference the sample of asteroids in common from the Gaia DR3 and the SMASSII (Bus and Binzel, 2002), grouped for each spectral class and averaging the

slope and the *z-i* color parameters (Figure 2). We confirm the *z-i* color difference for Gaia, compared to that of SMASSII (Bus and Binzel, 2002), with an average value of -0.06, close to that found by Galluccio et al. (2023; -0.08).

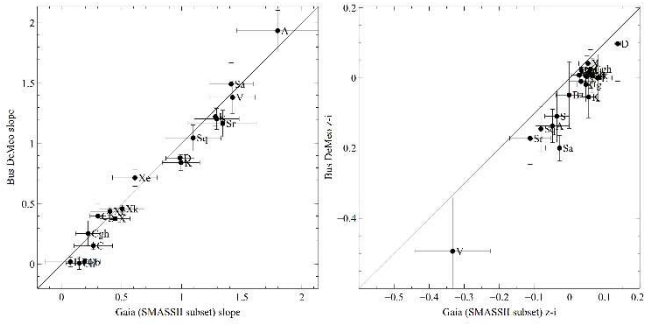

Figure 2: The relation for slope and *z-i* color for Gaia DR3 sample and Bus-DeMeo reference taxonomy, on the basis of the of the SMASSII sub-set. The *z-i* color color for Gaia DR3 is systematically below to Bus-DeMeo reference.

In order to correct this discrepancy we calculated the differences for slope and *z-i* from the Bus-DeMeo and the Gaia DR3 (SMASSII common sub-set). Plotting that differences respect to the Gaia slope and *z-i* color (Figure 3), we obtained the following regression line expressions:

(BusDeMeo_slope - Gaia_slope) = 0.02712 * Gaia_slope - 0.06128

(BusDemeo_zi - Gaia_zi) = -0.05559 * Gaia_slope - 0.02046

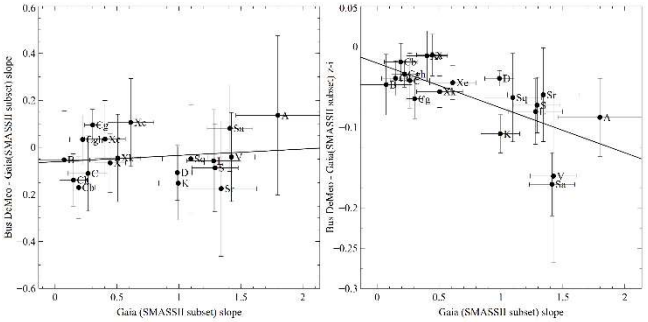

Figure 3: Differences for slope and *z-i* from the Bus-DeMeo and the Gaia DR3 (SMASSII common sub-set).

By applying these corrections to the slope and *z-i* color parameters we obtained a better distribution of the overlap areas with the Bus-DeMeo taxonomy and with the common SMASSII sub-set (Figure 4).

Once the distribution of the slope and *z-i* color parameters on the Gaia DR3 data had been corrected, it was possible to proceed with their taxonomic classification, following the approach proposed by DeMeo and Carry (2013) for the SDSS data.

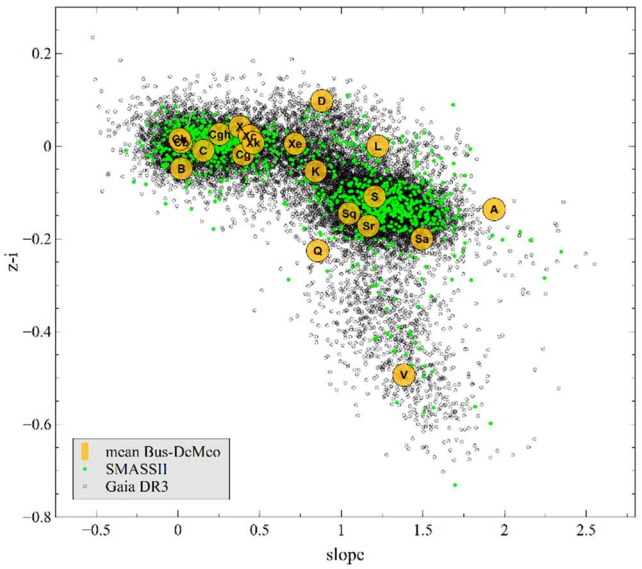

Figure 4: Slope vs *z-i* color parameters, once the linear correction has been applied. Gaia DR3 (gray), SMASSII (green), and the mean Bus-DeMeo taxonomy (orange) for each spectral class.

In detail, the sub-classes S, C, X have been merged into their broader complex, reducing the distinct taxonomic classes to the following A, B, C, D, K, L, Q, S, V, X. For each taxonomic class a specific area of the cartesian plane (slope vs *z-i*) was assigned, on the basis of the Table 3 of DeMeo and Carry (2013) and following a decision tree approach. The resulting taxonomic distribution of the Gaia DR3 sample is reported on Figure 5 with a total of 14954 assigned spectral classes and 12 undefined assignments. The catalogue of the assigned spectral classes is available in a .csv file format, with the following data fields: Num, Denomination, slope, *z-i*, and SpType (Balzaretto Observatory, 2025).

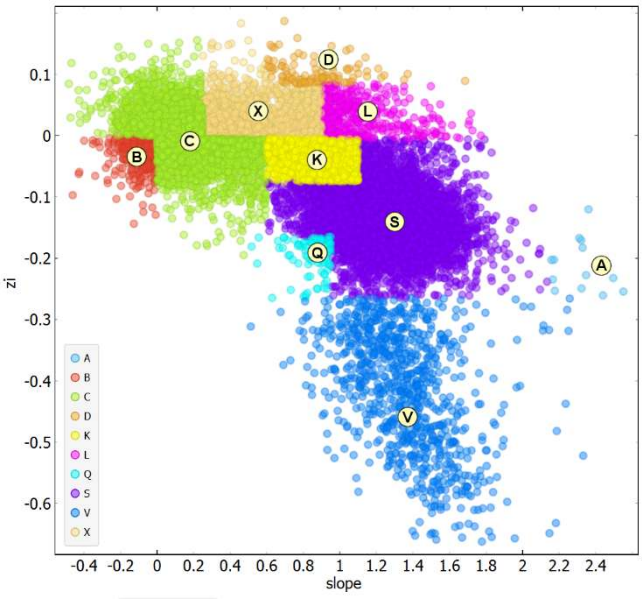

Figure 5: Taxonomic distribution for the Gaia DR3 sample, on the basis of the criteria defined by DeMeo and Carry (2013) for the areas of the plane (slope, *z-i* color).

The sample in common between Gaia DR3 and SMASSII (Bus and Binzel, 2002) is composed by 1214 asteroids, and for 914 of that sample (78%) was assigned the same taxonomic class, while for the

remain 270 asteroids (22%) the taxonomic class assigned was result different.

The Figure 6 compare the distribution of the taxonomic classes for the common SMASSII sub-set (1214) and for whole sample of the Gaia DR3 (14954). The distribution of spectral classes between SMASSII and Gaia DR3 is quite similar in percentage terms, although with some differences for the spectral classes V and K, where the percentage is clearly higher for Gaia DR3 data.

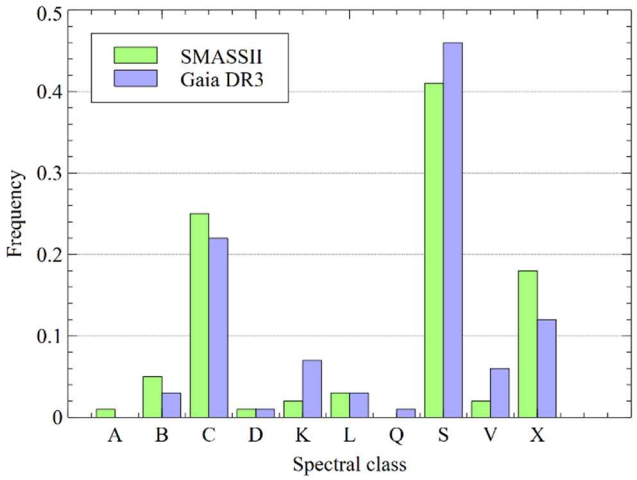

Figure 6: Histogram of the frequency for the spectral classes of the Gaia DR3 sample (sky blue) compared with the common SMASSII sub-set (light green).

In Figure 7 we plot a sample of the Gaia DR3 reflectance spectra. The first row reports the spectra for which the classification of this work, based on slope and *z-i*, coincides with that of SMASSII (Bus and Binzel, 2002). The second row instead reports the spectra for which the classification of this work differs from the SMASSII one. The third row report the classification of three asteroids for which there is no reference classification. Of these, for Nerina the classification based on slope and *z-i* assign a C-type, while the best fit suggests a X-type.

To conclude, this work confirms the potential of the Gaia DR3 reflectance spectra for the spectral classification of asteroids, in the absence of more detailed, and better quality, spectra. The automatic classification, based on slope and *z-i* color parameters, although very effective in most cases, still shows the need to resolve the most ambiguous cases with a direct inspection of the data. For the amateur astronomer community, ESA Gaia reflectance spectra can represent a useful resource for the taxonomic classification of asteroids, better if supported also by multi-band photometric observations.

References

Bus, S.J.; Binzel, R.P. (2002). "Phase II of the Small Main-Belt Asteroid Spectroscopic Survey - A Feature-Based Taxonomy." *Icarus* **158**, 146-177.

Balzaretto Observatory (2025). *https://digidownload.libero.it/A81_Observatory/data/gaia_asteroid_sptype.csv*

DeMeo, F.E.; Binzel, R.P.; Slivan, SM.; Bus, S. J. (2009). "An extension of the Bus asteroid taxonomy into the near-infrared." *Icarus* **202**, 160-180.

DeMeo, F.E.; Carry, B. (2013). "The taxonomic distribution of asteroids from multi-filter all-sky photometric surveys." *Icarus* **226**, 723-741.

Demsar, J.; Curk, T.; Erjavec, A.; Gorup, C.; Hocevar, T.; Milutinovic, M.; Mozina, M.; Polajnar, M.; Toplak, M.; Staric, A.; Stajdohar, M.; Umek, L.; Zagar, L.; Zbontar, J.; Zitnik, M.; Zupan, B. (2013), "Orange: Data Mining Toolbox in Python." *Journal of Machine Learning Research* **14 (Aug)**, 2349-2353.

Galluccio, L.; Delbo, M.; De Angeli, F.; Pauwels, T.; Tanga, P.; Mignard, F.; Cellino, A.; Brown, A.G.A.; Muinonen, K.; Penttilä, A.; Jordan, S.; Vallenari, A.; Prusti, T.; de Bruijne, J.H.J.; Arenou, F.; Babusiaux, C.; Biermann, M.; Creevey, O.L.; Ducourant, C. and 5 colleagues (2023). "Gaia Data Release 3. Reflectance spectra of Solar System small bodies." *A&A* **674**, A35, 29 pp.

Gaia ESA Archive (2025). version 3.7. *https://gea.esac.esa.int/archive/*

Planetary Data System. Small Bodies Node (2020). *https://sbn.psi.edu/pds/resource/busdemeotax.html*

Scilab (2021). *https://www.scilab.org/*

Appendix

Keywords for Astronomical Data Query Language

SELECT number_mp, denomination, wavelength, reflectance_spectrum, reflectance_spectrum_err, reflectance_spectrum_flag

FROM gaiadr3.sso_reflectance_spectrum

ORDER by number_mp, wavelength

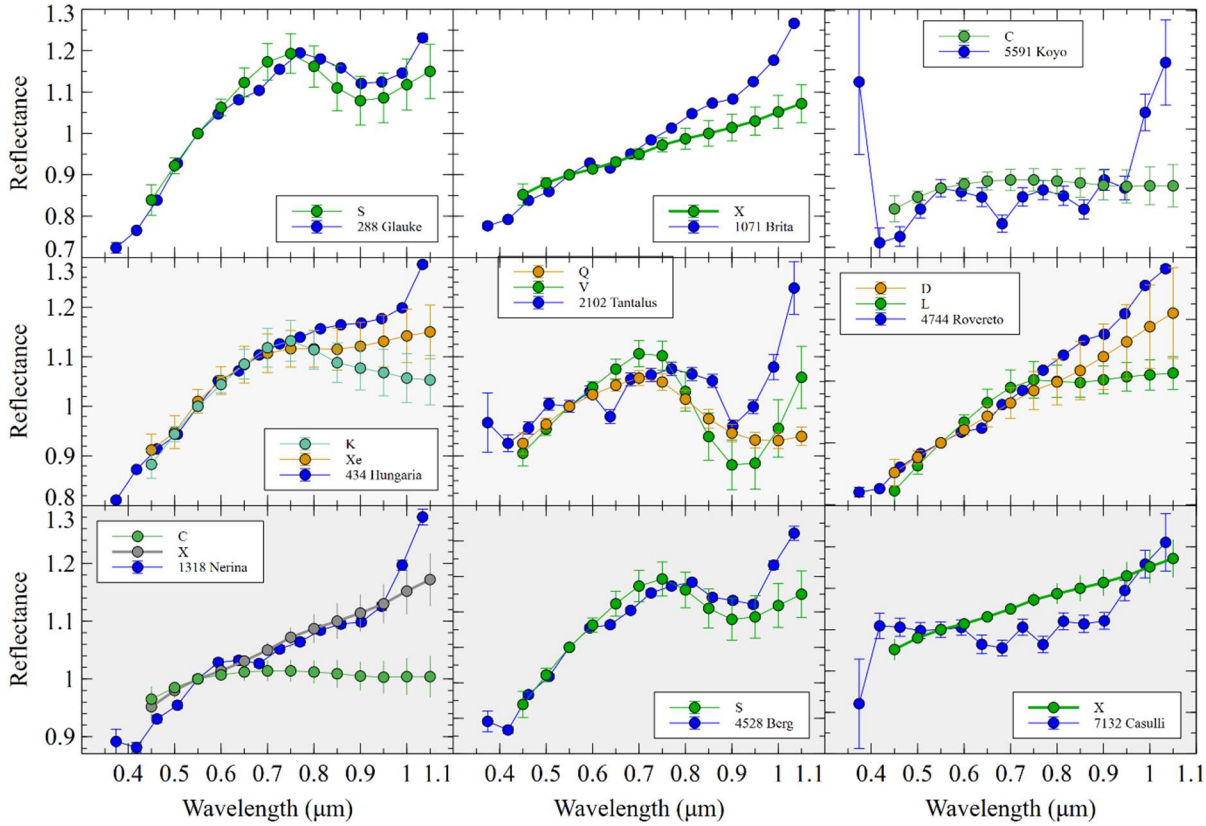

Figure 7: Sample of the Gaia DR3 reflectance spectra (blue color) compared with those from the mean Bus-DeMeo reference spectra. The first row reports the spectra of the asteroids 288 Glauke, 1071 Brita, and 5591 Koyo, for which the taxonomic classification of this work coincides with that of SMASSII (green color). The second row report the spectra of 434 Hungaria, 2102 Tantalus, and 4744 Rovereto, for which the classification of this work (green color) differs from the SMASSII one (orange color). The third row report the spectra of the asteroids 1318 Nerina, 4528 Berg, and 7132 Casulli, for which the classification of this work (green color) assign respectively the classes C, S and X. To note that for 1318 Nerina the most appropriate classification is X-type, on the best fit basis.

LIGHTCURVE PHOTOMETRY OPPORTUNITIES: 2025 OCTOBER – 2026 JANUARY

Brian D. Warner
Center for Solar System Studies (CS3)
446 Sycamore Ave.
Eaton, CO 80615 USA
brian@MinPlanObs.org

Alan W. Harris
Center for Solar System Studies (CS3)
La Cañada, CA 91011-3364 USA

Josef Ďurech
Astronomical Institute
Charles University
18000 Prague, CZECH REPUBLIC
durech@sirrah.troja.mff.cuni.cz

Lance A.M. Benner
Jet Propulsion Laboratory
Pasadena, CA 91109-8099 USA
lance.benner@jpl.nasa.gov

(Received: 2025 July 14)

We present lists of asteroid photometry opportunities for 2025 October - 2026 January. The extended four-month listing allows better observation planning, especially for those working in wide-spread collaborations. With the massive input of survey photometry, even if mostly sparse data, the small telescope researcher's role is moving away generic studies to those concentrating on specific needs and targets and so, we hope, leading to even more fulfilling and fruitful efforts.

We refer the reader to the lightcurve photometry opportunities article in *Minor Planet Bulletin* 51-4 (Warner et al., 2024) for a detailed discussion on the evolution of the lists presented here and the purpose behind each one. In addition, we refer the reader to other prior releases of this paper (e.g., Warner et al., 2023) for more detailed discussions about the requirements and considerations for the targets in the lists and to Warner et al. (2021a; 2021b).

On-Line Planning Tool

The ephemeris generator on the *https://MinorPlanet.info* web site allows creating custom lists for numbered objects reaching V ≤ 18.0 during a given month from 2020 through 2035 by setting search parameters based on a number of parameters.

https://www.minorplanet.info/php/callopplcdbquery.php

The updated page added data for the minimum phase angle of any object included in the search: the date (0.001 d), the minimum phase angle (0.1°), and the declination. Searches can limit results to a phase angle range between 0-120°. Also new is limiting the results to a range of rotation periods and so, for example, one can look for only long, or especially short, period objects.

Important and Useful Web Sites

The dates and values given on the MinorPlanet.info site are very good estimates in most cases. NEAs are sometimes an important exception. Use the site for preliminary planning for objects and then confirm those plans using the Minor Planet Center or JPL Horizons web sites.

MPC: *http://www.minorplanetcenter.net/iau/MPEph/MPEph.html*
JPL: *https://ssd.jpl.nasa.gov/sb/orbits.html*

Those doing work for modeling should contact Josef Ďurech at the email address above. If looking to add lightcurves for objects with existing models, visit the Database of Asteroid Models from Inversion Techniques (DAMIT) web site.

https://astro.troja.mff.cuni.cz/projects/damit/

to see what, if any, information it has on a chosen target.

For near-Earth asteroids in particular, check the list found on the Goldstone planned targets schedule at

http://echo.jpl.nasa.gov/asteroids/goldstone_asteroid_schedule.html

and keep in touch with Lance Benner at the email above. The radar team often needs updated astrometry and photometry (rotation period) prior to observing. Keep in mind as well that the *MinorPlanet.info* site opposition database includes only numbered objects. Keep a close eye on the MPC NEA pages.

Once you've obtained and analyzed your data, it's important to publish your results. Papers appearing in the *Minor Planet Bulletin* are indexed in the Astrophysical Data System (ADS) and so can be referenced by others in subsequent papers. It's also important to make the data available at least on a personal website or upon request. We urge you to consider submitting your raw data to the ALCDEF database. This can be accessed for uploading and downloading data at

http://www.alcdef.org

The database contains about 10.94 million observations for 24,639 objects (as of 2024 May 27), making it one of the more useful sources for raw data of *dense* time-series asteroid photometry.

The Planning Lists

The lists, excluding the one for NEAs, are usually restricted to objects reaching V ≤ 15.5 during the covered months. To include every object within a list that met this criterium alone resulted in far too many targets than the known community of asteroid photometrists could possibly handle, so only the "better" candidates are included. This is entirely subjective and the reader is encouraged to visit the *https://MinorPlanet.info* web site and use all the planning tools available there should our preferences not match yours.

Don't presume that something rated U ≥ 3– doesn't need more work nor, at the other end, that something not rated at all or 1– < U < 2+ or has a long period should be skipped in lieu of an "easier" project. The often-heard saying, "Past performance is not a guarantee of future results" should be part of your work ethic. Someone's "certain" result may not be so certain after all, especially if it's based on data that are minimal in quantity and/or quality.

Favorable Apparitions includes objects reaching one of the five brighter (favorable) apparitions from 1995 and 2050 and rated U < 3- in the LCDB.

No Pole Solutions includes objects rated U > 2+ but do not have a pole indicated on the LCDB summary line. This is list is the most likely needing further confirmation by checking the DAMIT web site, which grows in spurts large and small quite frequently and so the LCDB can lag considerably.

Poor Pole Solutions includes objects rated U < 3– that have a pole solution on the summary line. In this case, the period is often based on using sparse survey data, with or without support of dense lightcurve data. An additional set of dense data may help elevate both the U rating and the quality of the pole solution.

Low Phase Angles includes objects, regardless of U rating or even having a period, that reach a solar phase angle < 1°. You should refer to Warner et al. (2023) to review important information about low solar phase angle work.

Long Periods includes objects with $P \geq$ ~24 hours. These are often overlooked because they are very difficult for a single-station campaign. However, they are ideal for collaborations, especially those with stations well-separated in longitude.

NEAs (aka Radar Target) is limited to *known* near-Earth asteroids that might be on the radar team's radar (pun intended). It is common for newly discovered objects to move into or out of the list. We recommend that you keep up with the latest discoveries by using the Minor Planet Center observing tools.

The List Data

If the list includes the "Fam" column, this is the orbital group (> 9000) using criteria from the LCDB or the collisional family (< 9000) based on Nesvorny et al. (2015) and Nesvorny (2015). To convert the number to a name, see the LCDB documentation on the LCDB web site or use the One Asteroid Lookup page on the site:

https://www.minorplanet.info/php/lcdb.php
https://minorplanet.info/php/oneasteroidinfo.php

Table Columns

Num	Asteroid number, if any.
Name	Name (or designation) assigned by the MPC.
Fam	Orbital group or collisional family.
BMD	Date of maximum brightness (to 0.1 d precision).
BMg	Approximate V magnitude at brightest.
BDC	Approximate declination at brightest.
PD	Date of minimum phase angle (to 0.001 d precision).
PMn	Phase angle at minimum (solar elongation > 90°).
PDC	Approximate declination at minimum phase angle.
P (h)	Synodic rotation period from summary line in the LCDB summary table. An * indicates a sidereal period.
U	LCDB solution quality (U) from 1 (probably wrong) to 3 (secure).
Notes	Comments about the object.

Some asteroids may appear in more than one list. The reader is referred to the latest LCDB release and, where and when necessary, the original reference source should be used. The Notes column is rarely used, except for the NEAs list.

Calculations of brightest and minimum phase are by Brian D. Warner. For minimum phase, the observer should use the JPL Small Bodies Node Ephemeris site for more precise information. All periods are taken from the summary line of the LCDB. If needed, the LCDB should be checked to find the source of the summary line period.

Favorable Apparitions (U < 3-)

Num	Name	Fam	BMD	BMg	BDC	PD	PMn	PDC	P (h)	U	Notes
1767	Lampland	606	10 01.4	15.3	+5	10 02.993	0.2	+4	35.399	2	
1475	Yalta	9104	10 02.5	14.3	+5	10 02.285	0.9	+5	70.77	2	
3111	Misuzu	9104	10 04.8	15.1	+1	10 04.797	2.3	+1	40	2-	
1615	Bardwell	602	10 07.5	14.6	+4	10 06.828	0.7	+4	17	2	
3024	Hainan	9106	10 08.7	15.1	+2	10 08.849	1.6	+2	11.746	2+	
3641	Williams Bay	9106	10 14.1	15.3	+4	10 14.422	1.6	+4	9.035	2	
6024	Ochanomizu	9104	10 18.2	15.3	+5	10 18.219	2.2	+5	6	1	
2856	Roser	606	10 19.4	15.4	+13	10 19.809	0.8	+12	13.73	2+	
2263	Shaanxi	606	10 28.8	15.0	+8	10 29.036	2.2	+8	272.2	2	
3572	Leogoldberg	9106	10 31.5	15.3	+16	11 01.232	0.6	+16	10.101	2	
3597	Kakkuri	602	11 02.0	15.2	+12	11 02.127	1.2	+12	27	2	
2475	Semenov	606	11 08.3	15.4	+13	11 08.430	1.4	+13	12	2	
13165	1995 WS1	9104	11 08.4	15.4	+17	11 09.160	0.3	+17	64.19	2	
2490	Bussolini	502	11 09.2	14.8	+11	11 09.210	2.6	+11	24	1	
5062	Glennmiller	9104	11 11.1	15.3	+21	11 11.253	1.8	+21	9.243	2	
1122	Neith	9105	11 14.9	13.3	+17	11 14.868	0.9	+17	25.11	2	
11544	1992 UD3	9104	11 17.4	15.2	+18	11 17.591	0.7	+18	14.464	2	
2533	Fechtig	602	11 17.5	15.0	+17	11 16.680	0.5	+17	15.41	2-	
6514	Torahiko	9105	11 18.9	14.9	+17	11 18.716	1.0	+17	8.721	2	
1300	Marcelle	9106	11 22.8	15.3	+15	11 22.891	2.1	+15	565	2	
47592	2000 AO203	9104	11 23.4	15.3	+22	11 23.818	0.8	+22	17.507	2	
4215	Kamo	401	12 08.5	15.5	+21	12 08.406	0.7	+21	12.6	2	
5394	Jurgens	2004	01 04.5	15.3	+23	01 04.342	0.4	+23	6.073	2	
4689	Donn	9104	01 08.5	15.3	+23	01 07.719	0.2	+23	122.5	2+	
4214	Veralynn	9104	01 08.7	15.3	+29	01 08.831	3.1	+29	7.6	2-	
1586	Thiele	9104	01 12.5	14.5	+20	01 12.756	0.8	+20	3.086	2+	

Table I. A partial list of numbered asteroids reaching a favorable apparition and with an LCDB rating U < 3-.

Spin Axis and Modeling (Favorable Apparition, U > 2+, No LCDB pole, not in DAMIT)

Num	Name	Fam	BMD	BMg	BDC	PD	PMn	PDC	P (h)	U	Notes
4217	Engelhardt	9104	10 01.5	14.2	18	10 03.211	8.0	+19	3.066	3	
3677	Magnusson	402	10 01.6	15.0	6	10 01.889	1.5	+6	9.466	3	
1453	Fennia	9102	10 03.7	13.9	8	10 03.884	1.9	+8	4.412	3	
1346	Gotha	502	10 09.2	14.1	-5	10 08.283	5.6	-5	2.64	3	
4155	Watanabe	9104	11 08.7	15.0	23	11 09.492	3.2	+23	4.497	3	
5682	Beresford	9103	11 14.8	15.1	13	11 16.283	3.4	+13	3.769	3-	
4807	Noboru	9104	11 21.5	14.8	21	11 21.400	0.6	+21	4.042	3	
3577	Putilin	9107	11 30.5	14.8	24	11 30.328	0.9	+24	18.239	3-	
7369	Gavrilin	701	12 01.5	14.7	47	12 07.368	14.5	+45	49.12	3	
5080	Oja	2009	12 10.1	14.6	34	12 10.254	5.4	+34	7.222	3	
5035	Swift	502	12 10.4	15.2	34	12 09.965	4.8	+34	9.475	3	
3669	Vertinskij	402	12 21.5	15.1	23	12 21.269	0.2	+23	2.735	3	
3880	Kaiserman	3	12 28.4	15.5	23	12 29.016	0.2	+23	5.27	3	
1480	Aunus	9104	01 06.9	15.0	29	01 06.717	3.3	+29	5.16	3	
1262	Sniadeckia	9106	01 17.9	14.2	18	01 17.849	0.8	+18	17.57	3	
1587	Kahrstedt	9104	01 23.1	14.1	31	01 23.778	5.2	+31	7.971	3	
7225	Huntress	9104	01 29.1	14.7	10	01 29.374	4.3	+10	2.44	3	

Table II. A partial list of numbered asteroids reaching a favorable apparition that have high-quality periods solutions but do not have a pole solution in the LCDB or DAMIT databases.

Spin Axis and Modeling (Any Apparition, U < 3–, Pole in LCDB)

Num	Name	Fam	BMD	BMg	BDC	PD	PMn	PDC	P (h)	U	Notes
1475	Yalta	9104	10 02.5	14.3	+5	10 02.285	0.9	+5	70.77	2	
892	Seeligeria	9106	10 19.6	14.4	-5	10 18.793	5.2	-5	16.693	2+	
1118	Hanskya	2013	10 26.8	14.8	+31	10 27.616	5.9	+31	25.31	2	
1555	Dejan	9105	10 28.0	13.8	+25	10 29.650	5.7	+24	16.96	2+	
1551	Argelander	9104	11 14.2	15.0	+13	11 14.454	2.3	+13	4.063	2+	
923	Herluga	9105	11 19.2	14.1	+3	11 20.538	8.2	+2	30.61	2	
838	Seraphina	9106	11 28.4	13.6	+20	11 28.835	0.7	+20	11.69	2+	
1159	Granada	9104	12 01.3	15.1	+43	12 02.252	8.4	+43	77.28	2	
3679	Condruses	9104	12 12.6	15.3	+29	12 13.542	3.0	+29	172	2+	
1366	Piccolo	9106	12 26.0	15.1	+36	12 26.618	3.9	+36	16.57	2	
4533	Orth	701	01 08.2	15.3	-21	01 05.068	22.7	-22	>24	2	

Table III. A partial list of numbered asteroids reaching brightest magnitude that have a reported pole position but the LCDB rating is U < 3-. Bold indicates a favorable apparition.

Low Phase Angle (V ≤ 15.0, phase angle α ≤ 1.0°)

Num	Name	Fam	BMD	BMg	BDC	PD	PMn	PDC	P (h)	U	Notes
1686	De Sitter	602	10 04.4	14.9	+5	10 06.114	0.1	+5	11.292	3-	
76	Freia	9106	10 04.5	12.4	+4	10 02.592	0.3	+4	9.973	3	
1084	Tamariwa	9105	10 06.4	14.0	+5	10 07.945	0.3	+5	6.196	3	
697	Galilea	9106	10 06.4	12.4	+5	10 07.802	0.2	+5	16.538	3	
1207	Ostenia	606	10 12.5	14.6	+7	10 11.503	0.2	+7	9.073	3	
1358	Gaika	9104	10 13.4	15.0	+8	10 14.672	0.2	+8	10.1	3	
305	Gordonia	9106	10 14.5	12.7	+8	10 12.912	0.3	+8	12.893	3	
85	Io	502	10 16.4	10.3	+9	10 16.939	0.1	+9	6.875	3	
848	Inna	602	11 03.4	14.9	+15	11 05.009	0.1	+15	45.479	2	
617	Patroclus	9202	11 05.4	14.4	+17	11 08.561	0.2	+17	102.8	3	
104	Klymene	602	11 09.5	11.8	+17	11 08.196	0.2	+17	8.984	3	
235	Carolina	9106	11 24.4	12.9	+20	11 25.472	0.3	+20	17.61	3	
1888	Zu Chong-Zhi	2001	11 24.5	14.2	+21	11 24.034	0.3	+21	11.053	3	
564	Dudu	9106	12 02.4	14.8	+23	12 04.612	0.3	+23	8.882	3	
352	Gisela	402	12 02.4	11.4	+22	12 02.871	0.2	+22	7.49	3	
1645	Waterfield	9106	12 03.4	14.8	+23	12 04.892	0.1	+23	4.861	3	
441	Bathilde	9106	12 10.2	11.7	+22	12 09.099	0.3	+22	10.446	3	
4448	Phildavis	9104	12 16.5	14.6	+23	12 15.239	0.2	+23	14.914	3	
1061	Paeonia	9106	12 20.4	15.0	+23	12 21.995	0.0	+23	7.997	3-	
1319	Disa	9106	12 24.5	14.9	+22	12 22.719	0.3	+22	7.08	3	
431	Nephele	602	01 09.4	13.8	+22	01 10.971	0.1	+22	13.53	3	
465	Alekto	9106	01 17.5	14.1	+22	01 15.595	0.2	+22	10.936	3	
381	Myrrha	9106	01 24.5	13.0	+19	01 22.810	0.2	+19	6.572	3	
1142	Aetolia	9106	01 31.5	14.6	+18	01 29.490	0.2	+17	10.73	3-	

Table IV. A partial list of numbered asteroids reaching a minimum phase angle α ≤ 1.0°. Bold indicates a favorable apparition.

Long Period (Favorable Apparition, $P \geq 24$ h, U < 3)

Num	Name	Fam	BMD	BMg	BDC	PD	PMn	PDC	P (h)	U	Notes
1767	Lampland	606	10 01.4	15.3	+5	10 02.993	0.2	+4	35.399	2	
1475	Yalta	9104	10 02.5	14.3	+5	10 02.285	0.9	+5	70.77	2	
3111	Misuzu	9104	10 04.8	15.1	+1	10 04.797	2.3	+1	40	2-	
1024	Hale	9106	10 27.1	13.7	+1	10 28.162	5.4	+1	106.047	2+	
2263	Shaanxi	606	10 28.8	15.0	+8	10 29.036	2.2	+8	272.2	2	
3597	Kakkuri	602	11 02.0	15.2	+12	11 02.127	1.2	+12	27	2	
13165	1995 WS1	9104	11 08.4	15.4	+17	11 09.160	0.3	+17	64.19	2	
6562	Takoyaki	9104	11 09.2	15.3	+7	11 09.427	6.0	+7	31.202	2	
2490	Bussolini	502	11 09.2	14.8	+11	11 09.210	2.6	+11	24	1	
1570	Brunonia	605	11 11.8	15.4	+16	11 12.154	0.6	+16	157	2	
1952	Hesburgh	9106	11 12.8	14.1	+7	11 12.767	4.1	+7	47.52	2	
1122	Neith	9105	11 14.9	13.3	+17	11 14.868	0.9	+17	25.11	2	
923	Herluga	9105	11 19.2	14.1	+3	11 20.538	8.2	+2	30.61	2	
13249	Marcallen	9105	11 20.6	15.1	+37	11 20.648	8.1	+37	90.07	2	
1300	Marcelle	9106	11 22.8	15.3	+15	11 22.891	2.1	+15	565	2	
3171	Wangshouguan	9106	12 06.6	15.0	+35	12 07.055	4.4	+35	43.548	2+	
4293	Masumi	9106	12 16.8	14.7	+31	12 16.358	3.6	+31	36	2-	
4689	Donn	9104	01 08.5	15.3	+23	01 07.719	0.2	+23	122.5	2+	
1854	Skvortsov	9104	01 10.4	15.2	+13	01 10.513	3.9	+13	78.5	2	

Table V. A partial list of numbered asteroids reaching a favorable apparition and with a reported period $P \geq 24$ hours.

NEAs (aka Radar) Reaching Brightest for Year (Any Apparition, V ≤ 17.0, α ≤ 90°)

Num	Name	Fam	BMD	BMg	BDC	PD	PMn	PDC	P (h)	U	Notes
461397	2001 SD170	9101	10 10.8	14.9	+5	10 09.982	5.4	+07			
112985	2002 RS28	9101	10 20.8	15.7	+31	10 26.971	18.7	+20	4.787	2	
144900	2004 VG64	9101	10 26.1	15.9	-5	12 31.	41.3	-16			
164206	2004 FN18	9101	10 30.0	14	+8	10 27.947	6.0	+13			
433	Eros	9101	11 13.0	10.4	+45	10 22.931	24.8	+47	5.27	3	
3361	Orpheus	9101	11 14.3	14.8	-22	10 28.995	22.1	+08	3.533	3	PHA
4183	Cuno	9101	11 20.6	15.5	+28	11 10.005	7.2	+30	3.560	3	
516155	2016 DP	9101	11 26.8	15.8	+69	01 01.	27.0	+53			PHA
220839	2004 VA	9101	12 17.8	15.2	-5	11 18.292	8.8	+08	6.791	3	PHA
533722	2014 NE52	9101	12 20.0	16.5	+25	06 29.437	3.2	-29			
488789	2004 XK50	9101	12 22.5	15.9	-56	01 01.	22.3	-39			
3753	Cruithne	9101	12 31.	16.5	-16	01 01.	24.8	-16	27.310	3-	
36284	2000 DM8	9101	12 31.	16.4	-25	01 15.415	18.7	+70	3.844	3	
164400	2005 GN59	9101	12 31.	16.4	-82	08 01.040	11.8	+00	38.69	3	
6455	1992 HE	9101	12 31.	16.3	-41	02 12.864	14.5	+55	2.736	3	
1620	Geographos	9101	12 31.	16.3	+43	12 31.	23.0	+43	5.222	3	
141484	2002 DB4	9101	12 31.	16.1	-55	01 01.	53.2	-12	2.22	2	
2212	Hephaistos	9101	12 31.	16.1	+42	12 20.606	8.1	+42	48	2	
87684	2000 SY2	9101	12 31.	15.3	-18	12 31.	26.6	-18	2.571	2	
242708	2005 UK1	9101	01 03.4	15.5	+8	07 09.990	0.8	-21	63.8	2-	PHA
141484	2002 DB4	9101	01 08.4	16	-56	02 13.909	53.1	-39	2.22	2	
35107	1991 VH	9101	01 12.0	15.6	-11	01 18.809	26.7	-04	2.624	3	
164400	2005 GN59	9101	01 18.2	15.5	-45	02 26.391	20.0	-08	38.69	3	

Table VI. A list of near-Earth asteroids known as of 2025 July 15. Where the BMD (Brightest Date) is "12 31.", the asteroid was still brightening at the end of 2025. Green bar lines are on the Goldstone list of planned targets. PHA: Potentially Hazardous Asteroid. This is not necessarily a complete list of Goldstone targets. Check their web site.

References

Nesvorny, D. (2015). "Nesvorny HCM Asteroids Families V3.0." NASA Planetary Data Systems, id. EAR-A-VARGBET-5-NESVORNYFAM-V3.0.

Nesvorny, D.; Broz, M.; Carruba, V. (2015). "Identification and Dynamical Properties of Asteroid Families." In Asteroids IV (P. Michel, F. DeMeo, W.F. Bottke, R. Binzel, Eds.). Univ. of Arizona Press, Tucson, also available on astro-ph.

Warner, B.D., Harris, A.W., Pravec, P. (2009). "The Asteroid Lightcurve Database." *Icarus* **202**, 134-146. Updated 2023 Oct. *http://www.minorplanet.info/lightcurvedatabase.html*

Warner, B.D.; Harris, A.W.; Durech, J.; Benner, L.A.M. (2021a). "Lightcurve Photometry Opportunities: 2021 January-March." *Minor Planet Bull.* **48**, 89-97.

Warner, B.D.; Harris, A.W.; Durech, J.; Benner, L.A.M. (2021b). "Lightcurve Photometry Opportunities: 2021 October-December." *Minor Planet Bull.* **48**, 406-410.

Warner, B.D.; Harris, A.W.; Durech, J.; Benner, L.A.M. (2023). "Lightcurve Photometry Opportunities: 2023 July - September." *Minor Planet Bull.* **50***,* 240-244.

Warner, B.D.; Harris, A.W.; Durech, J.; Benner, L.A.M. (2024). "Lightcurve Photometry Opportunities: 2024 October - 2025 January." *Minor Planet Bull.* **51**, 379-384.

INDEX TO VOLUME 52

Colazo, M.; Amelotti, V.; Melia, R.; Santos, F.; Suárez, N.; Primucci, E.; Orbanic, Z.; Scotta, D.; Martini, M.; Anzola, M.; Monteleone, B.; Morales, M.; Tàrtalo, G.; Ciancia, G.; Colazo, C. "Photometric Analysis of Patroclus-Menoetius Mutual Events and 15 Other Asteroids" 168-173.

Colazo, M.; Colazo, C.; Amelotti, V.; Melia, R.; Suárez, N.; Santos, F.; Monteleone, B.; Ciancia, G.; Wilberger, A.; Morales, M.; Anzola, M.; Stechina, A.; Scotta, D.; García, A.; Primucci, E. "761 Brendelia: A Newly Identified Binary Asteroid from Pro-Am Collaboration" 284-287.

Colazo, M.; Amelotti, V.; Navas, G.; Orbanic, Z.; Tàrtalo, G.; Melia, R.; Santos, F.; Suárez, N.; Montecchiari, N.; García, A.; Scotta, D.; Álvarez, J.; Monteleone, B.; Anzola, M.; Colazo, C. "Synodic Rotation Periods and Lightcurve Amplitudes for 12 Minor Planets from GORA Collaboration" 306-309.

Colazo, M.; Monteleone, B.; Orbanic, Z.; Tàrtalo, G.; Amelotti, V.; Melia, R.; Morales, M.; Suárez, N.; Montecchiari, N.; Santos, F.; Anzola, M., García, A.; Navas, G.; Álvarez, J.; Colazo, C. "Synodic Rotation Periods and Lightcurve Amplitudes for Eleven Main Belt Asteroids" 310-313.

Dose, E.V. "Lightcurves of Eight Asteroids" 27-31.

Dose, E.V. "Lightcurves of Eighteen Asteroids" 125-133.

Dose, E.V. "Lightcurves of Fourteen Asteroids" 191-199.

Duin, H. "Lightcurves and Rotation Periods of Near-Earth Asteroids (137170) 1999 HF1 and 2025 GB" 279-280.

Fauerbach, M. "Lightcurve and Rotation Period for 3507 Vilas and 4185 Phystech" 302-303.

Faure, G.; Jongen, Y.; Pravec, P.; Wünsche, A. "Discovery of the Binarity of the Main-Belt Asteroid 8297 Gerardfaure" 297-299.

Fornas, G.; Pilcher, F. "Lightcurve Analysis for (36197) 1999 TZ91" 289.

Fornas, G.; Fornas, Á.; Huet, F.; Rathmann, E.; Arce, E.; Barberá, R.; Mas, V. "Lightcurve Analysis for Thirteen Main-Belt and Three Near Earth Asteroids" 38-44.

Fornas, G.; Fornas, A.; Carreño, A.; Huet, F.; Rathmann, E.; Arce, E.; Mas, V. "Lightcurve and Results for Eight Main-Belt Asteroids" 226-228.

Fornas, G.; Fornas, A.; Carreño. A.; Huet, F.; Rathmann, E. "Lightcurve Analysis for Three Main-Belt, Two Mars-Crossing and Two Near-Earth Asteroids" 337-339.

Franco, L. "On the Gaia DR3 Reflectance Spectra" 351-354.

Franco, L.; Scarfi, G.; Ruocco, N.; Lombardo, M.; Tombelli, M.; Lombardo, M.; Iozzi, M.; Galli, G.; Iozzi, M. "Collaborative Asteroid Photometry from UAI: 2024 July-September" 15-16.

Franco, L.; Scarfi, G.; Casalnuovo, G.B.; Marchini, A.; Papini, R.; Iozzi, M.; Bacci, P.; Maestripieri, M.; Galli, G.; Montigiani, N.; Mannucci, M.; Ruocco, N.; Lombardo, M.; Coffano, A.; Marinello, W.; Pizzetti, G.; Baj, G.; Tinelli, L. "Collaborative Asteroid Photometry from UAI: 2024 October-December" 146-148.

Franco, L.; Galli, G.; Buzzi, L. "Two Mutual Events Observed for Patroclus-Menoetius Binary System" 174.

Franco, L.; Pilcher, F.; Mortari, F.; Gabellini, D., Baj, G.; Iozzi, M. "Preliminary Spin-Shape Model for 49 Pales" 202-204.

Franco, L.; Marchini, A.; Papini, R.; Galli, G.; Scarfi, G.; Montigiani, N.; Mannucci, M.; Buzzi, L.; Bacci, P.; Maestripieri, M.; Iozzi, M.; Ruocco, N.; Lombardo, M.; Baj, G.; Tinelli, L. "Collaborative Asteroid Photometry for UAI: 2025 January - March" 235-238.

Franco, L.; Marchini, A.; Papini, R.; Ruocco, N.; Scarfi, G.; Buzzi, L.; Iozzi, M.; Lombardo, M.; Lombardo, N.; Galli, G. "Collaborative Asteroid Photometry from UAI: 2025 April-June" 320-323.

Galdies, C.; Brincat, S.M.; Bucek, M. "Photometric Observations and Analysis of Seven Asteroids" 24-26.

Gault, D.; Nosworthy, P, Herald, D. "A New Satellite of (172376) 2002 YE25 Detected by Stellar Occultation" 58-59.

González Farfán, R.; García de la Cuesta, F.; Reina Lorenz, E.; Botana Albá, C.; De Elías Cantalapiedra, J.; Ruiz Fernández, J.; Gómez Pinilla, F.; Martín Saura, A.; Fernández Andújar, J.M. "Analysis and Lightcurves of Eleven Asteroids" 31-34.

González Farfán, R.; García de la Cuesta, F.; Reina Lorenz, E.; Botana Albá, C.; De Elías Cantalapiedra, J.; Ruiz Fernández, J.; Limón Martínez, F.; Gómez Pinilla, F.; Fernández Andújar, J.M. "Analysis and Review of Rotation Curves and Periods of 12 Asteroids" 35-37.

González Farfán, R.; García de la Cuesta, F.; Delgado Casal, J.; Reina Lorenz, E.; Botana Albá, C.; De Elías Cantalapiedra, J.; Ruiz Fernández, J.; Limón Martínez, F.; Fernández Andújar, J.M.; Fernández Mañanes, E.; Graciá Ribes, N.; Collada Bárcena, J.; Coya Lozano, A.; Polacos Ruiz, J.; Cores, J.M. "Review of Rotation Curves and Periods of 32 Asteroids" 246-253.

González Farfán, R.; García de la Cuesta, F.; Reina Lorenz, E.; Botana Albá, C.; De Elías Cantalapiedra, J.; Ruiz Fernández, J.; Limón Martínez, F.; Collada Bárcena, J.; Coya Lozano, A.; Polancos Ruiz, J. "A Study and Review of the Lightcurves and Roataion Periods of 10 Asteroids" 326-329.

Hayes-Gehrke, M.N.; O'Brien, O.; Haugen, N.; Sanford, I.; Argueta, J.; Mekonnen, N.; Blaufuss, S.; Lu, Q.; Kleinman, J.; Breza, B. "Lightcurves from Three Mutual Events of Trojan Binary 617 Patroclus in October 2024" 175-177.

Hayes-Gehrke, M.N.; Delavan-Hoover, C.; Johnston, C.; Krishnamurthy, P.; Longkeng, C.; McNeal, E.; Mengistu, S.; Mooney, J.; Samblanet, A.; Scholz, T.; Ward, K.; White, H.; Whitken, G. "Lightcurve and Rotation Period of Main-Belt Asteroid 3961 Arthurcox" 293.

Hayes-Gehrke, M.N.; De Leon, K.; Deredita, N.; Dobson, E.; Frenkel, N.; Hari, G.; Hughes, S.; Kaza, R.; Li, V.; Schmitz, W.; Shirland Jr., D.; Sitther, H.; Wagger, M.; Brincat, S.M.; Buček, M.; Galdies, C. "Lightcurve and Rotation Period of 4163 Saaremaa" 295-296.

Hayes-Gehrke, M.N.; Benitez, C.; Bibbo, J.; Chandrasekaran, A.; Drill, S.; Fleegle, B.; Kaplan, R.; Lerdboon, H.; Nagy, J.; Peddinti, S.; Trivedi, A.; Zhang, Y.; Brincat, S.M.; Galdies, C.; Buček, M. "A Lightcurve Analysis of Main Belt Asteroid 5295 Masayo" 296-297.

Hayes-Gehrke, M.N.; Kerns, J.; Sullivan, C.; Lau, E.; Sinha, C.; Weintraub, B.; Hale, J.; Sunter, C.; Anusuri, R.; Zajac, B.; Yang, J.; Lizas, C.C.; Schenck, Z. "Lightcurve and Rotation Period Analysis for 19774 Diamondback" 300-301.

Hawley, W.; Wiggins, P.; Armstrong, J.D.; Leyland, P.C.; DeGroff, K.; Arnold, S.; Odeh, M.S.; Haymes, T.; Kardasis, E.; Takoudi, A.; Privett, G.; Genebriera, J. "Lightcurve and Rotation Period Analysis of 1908 Pobeda, 2168 Swope, and 5203 Pavarotti" 12-14.

Hawley, W.; Armstrong, J.D.; Marshall, J.; DeGroff, K.; Leyland, P.C.; Odeh, M.S.; Oey, J.; Fornas, A.; Gonçalves, R.; Kardasis, E.; Takoudi, A.; Usatov, M.; Drummond, J. "617 Patroclus-Menoetius Mutual Event Lightcurves" 70-73.

Hawley, W.; Wiggins, P.; Armstrong, J.D.; Gonçalves, R.; DeGroff, K.; Scott, B.; Odeh, M.S.; Haymes, T.; Gout, J.-F.; Privett, G., Genebriera, J. "Lightcurve and Rotation Period Analysis of (9058) 1992 JB and (424482) 2008 DG5" 344-346.

Huet, F.; Fornas, G.; Fornas, A. "A Lightcurve Analysis for Nine Main-Belt and One Mars-Crossing Asteroids" 141-145.

Hutton, L.J.; Fieber-Beyer, S.; Linder, T.R.; Reichart, D.E.; Haislip, J.B.; Kouprianov, V.V.; Moore, J.P. "Photometry of NEAs (187026) 2005 EK70 and (152787) 1999 TB10" 148-150.

Iozzi, M. "V-R Color Indices for Nine Main-Belt Asteroids" 323-325.

Kikwaya Eluo, J.-B.; Hergenrother, C.W. "Observations of Patroclus and Menoetius Mutual Events with Vatican Advanced Technology Telescope (VATT)" 74-76.

Kikwaya Eluo, J.-B.; Hergenrother, C.W. "Lightcurves and Colors of Five Small Near-Earth Asteroids: 2024 SY6, 2024 TU, 2024 TK1, 2024 TX13, 2024 UF9" 158-163.

Mannucci, M.; Montigiani, N. "Rotation Period Determination for 3048 Guangzhou" 294.

Marchini, A.; Papini, R. "Photometric Observations of Asteroids 1626 Sadeya, 5552 Studnicka and 5565 Ukyounodaibu" 113-114.

Marchini, A.; Papini, R.; Pilcher, F. "13441 Janmerlin, an Asteroid with an Earth Commensurate Rotation Period" 7-8.

Marchini, A.; Papini, R.; Pierguidi, L.; Savino, J.P.; Schintu, S. "Photometric Observations of Asteroids 229 Adelinda, 5802 Casteldelpiano and (27174) 1999 BB2" 217-219.

Marchini, A.; Papini, R.; Salvaggio, F. "Photometric Observations of Asteroid 3760 Poutanen" 291-292.

Miyashita, K.; Watanabe, H.; Yamamura, H.; Manago, N. "A New Satellite of Asteroid (6326) Idamiyoshi Discovered from Occultation Observation" 267-270.

Nobre, G. "Lightcurve Analysis and Rotation Period for NEA 2006 WB" 100.

Nobre, G. "Lightcurve Analysis and Rotation Period for PHA 2020 XR" 101.

Nobre, G. "Lightcurve Analysis and Rotation Period for (887) Alinda" 210-211.

Noschese, A. "Lightcurve and Rotation Period of Slow Rotator 6176 Horrigan" 103.

Petrescu, E.; Ferrais, M.; Jehin, E.; Vander Donckt, M.; Karateking, Ö.; Benkhaldoun, Z. "Lightcurves of Near-Earth Asteroids 2024 ON, 2024 MK and 1998 ST27 as Observed from TRAPPIST" 150- 152.

Pilcher, F. "Minor Planets at Unusually Favorable Elongations in 2025" 1-3.

Pilcher, F. "Lightcurves and Rotation Periods of 209 Dido, 268 Adorea, 2732 Witt, and 2836 Sobolev, with a Note on 1402 Eri" 19-20.

Pilcher, F. "Lightcurves and Rotation Periods of 691 Lehigh, 795 Fini, and 1302 Werra" 106-107.

Pilcher, F. "Lightcurves and Rotation Periods of 229 Adelinda, 413 Edburga, 1101 Clematis, 1342 Brabantia, and 1343 Nicole" 219-221.

Pilcher, F. "General Report of Position Observations by the ALPO Minor Planets Section for the Year 2024" 271.

Pilcher, F. "Lightcurves and Rotation Periods of 57 Mnemosyne, 818 Kapteynia, 896 Sphinx, and 992 Swasey" 303-305.

Pilcher, F.; Dose, E.V. "The Lightcurve and Rotation Period of 637 Chrysothemis" 206.

Pilcher, F.; Franco, L.; Oey, J. "The Ambiguous Rotation Period of 1269 Rollandia is Solved by a Global Collaboration of Observers" 104.

Pilcher, F.; Marchini, A.; Papini, R. "Lightcurve and Rotation Period of 1237 Genevieve" 105-106.

Pilcher, F.; Delgado Casal, J.; Stone, G. "Lightcurves and the Rotation Period of the Amor-Type Asteroid 887 Alinda" 208-209.

Polakis, T. "Photometry of Suspected and Confirmed Binary Asteroids" 222-225.

Pritchard, S.M. "Lightcurve and Rotation of 55 Pandora" 205.

Ramsey, A.G.; Wilkin, F.P.; Castro, E.; Hizmo, G.; Zora, D.-V. "Lightcurves of Asteroid (1363) Herberta in 2023 and 2024" 290-291.

Romanishin, W. "Period of the Flat-Topped Lightcurve of 1510 Charlois" 6.

Romanishin, W. "Two New Lightcurves for 1209 Pumma and its Obliquity and Lightcurve Amplitude" 288-289.

Rondón-Briceño, E.; Michimani, J.; Monteiro, F.; Pereira, W.; Arcoverde, P.; Evangelista-Santana, M.; Souza, R.; Rodrigues, T.; Lazzaro, D. "(167) Patroclus-Menoetius Mutual Events Observations from OASI Observatory" 77-78.

Siakas, A.; Gkolias, I.; Tsiaras, A.; Tsavdaridis, S.; Gaitanas, M.; Tsiganis, K.; Tsirvoulis, G. "Observations of (617) Patroclus-Menoetius Mutual Events by the Aristotle University of Thessaloniki" 199-201.

Sioulas, N. "Rotation Period Determination for Asteroid 2024 MK" 11.

Sioulas, N. "Patroclus and Menoetius Mutual Events: Support for the NASA Lucy Mission to the Trojan Asteroids" 86.

Stone, G. "Lightcurves of Twenty-Two Asteroids" 51-58.

Stone, G. "Lightcurves of 40 Asteroids" 115-125.

Stone, G. "Lightcurves of Twenty Asteroids" 229-234.

Wang, L. "Lightcurve and Rotation Period of 2266 Tchaikovsky" 102.

Warner, B.D.; Durkee, R.; Fauerbach, M.; Gebauer, J.; Cloutier, W.; Nastasi, A.; Oey, J.; Stephens, R.D.; Guimaraes Tedesco, D.; de Oliveira Barreto, C.H. "CCD Photometric Observations of 617 Patroclus-Menoetius Mutual Events" 64-69.

Warner, B.D.; Durkee, R.; Fauerbach, M.; Gebauer, J.; Cloutier, W.; Nastasi, A.; Oey, J.; Sioulas, N.; Stephens, R.D.; Guimaraes Tedesco, D.; de Olivera Barreto, C.H. "Follow-Up Observations of 617 Patroclus-Menoetius Mutual Events: 2024 November to 2025 January" 178-183.

Warner, B.D.; Harris, A.W.; Ďurech, J.; Benner, L.A.M. "Lightcurve Photometry Opportunities:"

2025 January - April 90 - 93.
2025 April - July 184 - 187.
2025 July - October 272 - 276.
2025 October - 2026 January 355 - 359.

Wiles, M. "Lightcurve and Rotation Period Analysis for Four Minor Planets" 17-18.

Wiles, M. "Lightcurve and Rotation Period Analysis for Twenty-Five Minor Planets" 134-140.

Wilkin, F.P. "Lightcurve and Period of Koronis Family Member (2837) Griboedov" 215.

Wilkin, F.P.; Castro, E. "Additional Observations of (617) Patroclus-Menoetius Mutual Events" 173-174.

Wilkin, F.P.; Castro, E.; Ramsey, A.; Hizmo, G. "Observations of (617) Patroclus Mutual Events in Support of the Lucy Mission to the Trojan Asteroids" 87-89.

Xiong, J. "Lightcurve and Rotation Period of 1318 Nerina" 214.

Xiong, J.; Lu, Y.; Guo, C. "Lightcurve and Rotation Period Analysis of (1685) Toro" 8-9.

IN THIS ISSUE

This list gives those asteroids in this issue for which physical observations (excluding astrometric only) were made. This includes lightcurves, color index, and H-G determinations, etc. In some cases, no specific results are reported due to a lack of or poor-quality data. The page number is for the first page of the paper mentioning the asteroid. EP is the "go to page" value in the electronic version.

Number	Name	EP	Page
57	Mnemosyne	25	303
329	Svea	45	323
347	Pariana	45	323
451	Patientia	45	323
485	Genua	45	323
498	Tokio	48	326
502	Sigune	48	326
526	Jena	32	310
582	Olympia	45	323
619	Triberga	45	323
637	Chrysothemis	28	306
670	Ottegebe	45	323
761	Brendelia	6	284
788	Hohensteina	45	323
790	Pretoria	48	326
805	Hormuthia	45	323
818	Kapteynia	25	303
896	Sphinx	25	303
992	Swasey	25	303
992	Swasey	42	320
1033	Simona	32	310
1055	Tynka	48	326
1079	Mimosa	28	306
1155	Aenna	28	306
1155	Aenna	42	320
1209	Pumma	10	288
1254	Erfordia	48	326
1263	Varsavia	48	326
1287	Lorcia	28	306
1318	Nerina	48	326
1326	Losaka	42	320
1341	Edmee	32	310
1342	Brabantia	48	326
1363	Herberta	12	290
1408	Trusanda	32	310
1409	Isko	28	306
1841	Masaryk	28	306
1926	Demiddelaer	32	310
2159	Kukkamaki	52	330
2350	von Lude	32	310
2383	Bradley	36	314
2820	Iisalmi	52	330
2843	Yeti	32	310
3041	Webb	32	310
3048	Guangzhou	16	294
3134	Kostinsky	32	310
3507	Vilas	24	302
3595	Gallagher	39	317
3636	Pajdusakova	52	330
3731	Hancock	28	306
3760	Poutanen	13	291
3760	Poutanen	52	330
3774	Megumi	32	310
3774	Megumi	48	326
3857	Cellino	28	306
3857	Cellino	52	330
3961	Arthurcox	15	293
4163	Saaremaa	17	295
4185	Phystech	24	302
4350	Shibecha	28	306
4725	Milone	32	310
4875	Ingalls	52	330
5066	Garradd	59	337
5295	Masayo	18	296
5438	Lorre	28	306
5632	Ingelehmann	48	326
5704	Schumacher	39	317
5802	Casteldelpiano	28	306
5972	Harryatkinson	59	337
6512	de Bergh	36	314
6521	Pina	52	330
6823	1988 ED1	52	330
6976	Kanatsu	52	330
7068	Minowa	39	317
7309	Shinkawakami	36	314
8297	Gerardfaure	19	297
9058	1992 JB	42	320
9058	1992 JB	56	334
10143	Kamogawa	39	317
10349	1992 LN	52	330
12528	1998 KL31	39	317
13236	1998 HF96	52	330
13299	1998 RU15	52	330
14665	1999 CC5	52	330
17006	1999 CH63	52	330
18404	Kenichi	59	337
19774	Diamondback	22	300
19793	2000 RX42	28	306
21183	1994 EO2	59	337
27174	1999 BB2	59	337
29168	1990 KJ	52	330
31828	Martincordiner	36	314
36197	1999 TZ91	11	289
49981	1999 YJ13	52	330
137126	1999 CF9	59	337
137170	1999 HF1	1	279
137170	1999 HF1	59	337
424482	2008 DG5	42	320
424482	2008 DG5	56	334
458122	2010 EW45	62	340
	2020 WG	62	340
	2025 EE4	3	281
	2025 FR13	64	342
	2025 GA	64	342
	2025 GB	1	279
	2025 GQ1	64	342
	2025 HL5	64	342
	2025 HP4	64	342
	2025 KA	64	342
	2025 KD	64	342
	2025 KE1	64	342
	2025 ML2	64	342
	C/2024 M1 (ATLAS)	71	349

THE MINOR PLANET BULLETIN (ISSN 1052-8091) is the quarterly journal of the Minor Planets Section of the Association of Lunar and Planetary Observers (ALPO, http://www.alpo-astronomy.org). Current and most recent issues of the *MPB* are available on line, free of charge from:

https://mpbulletin.org/

The Minor Planets Section is directed by its Coordinator, Prof. Frederick Pilcher, 4438 Organ Mesa Loop, Las Cruces, NM 88011 USA (fpilcher35@gmail.com). Robert Stephens (rstephens@foxandstephens.com) serves as Associate Coordinator. Dr. Alan W. Harris (MoreData! Inc.; harrisaw@colorado.edu), and Dr. Petr Pravec (Ondrejov Observatory; ppravec@asu.cas.cz) serve as Scientific Advisors. The Asteroid Photometry Coordinator is Brian D. Warner (Center for Solar System Studies), Palmer Divide Observatory, 446 Sycamore Ave., Eaton, CO 80615 USA (brian@MinorPlanetObserver.com).

The Minor Planet Bulletin is edited by Professor Richard P. Binzel, MIT 54-410, 77 Massachusetts Ave, Cambridge, MA 02139 USA (rpb@mit.edu). Brian D. Warner (address above) is Associate Editor. Assistant Editors are Dr. David Polishook, Department of Earth and Planetary Sciences, Weizmann Institute of Science (david.polishook@weizmann.ac.il) and Dr. Melissa Hayes-Gehrke, Department of Astronomy, University of Maryland (mhayesge@umd.edu). The *MPB* is produced by Dr. Pedro A. Valdés Sada (psada2@ix.netcom.com).

Effective with Volume 50, the *Minor Planet Bulletin* is an electronic-only journal; print subscriptions are no longer available. In addition to the free electronic download of the *MPB* as noted above, electronic retrieval of all *Minor Planet Bulletin* articles (back to Volume 1, Issue Number 1) is available through the Astrophysical Data System:

http://www.adsabs.harvard.edu/

Authors should submit their manuscripts by electronic mail (rpb@mit.edu). Author instructions and a Microsoft Word template document are available at the web page given above. All materials must arrive by the deadline for each issue. Visual photometry observations, positional observations, any type of observation not covered above, and general information requests should be sent to the Coordinator.

* * * * *

The deadline for the next issue (53-1) is October 15, 2025. The deadline for issue 53-2 is January 15, 2026.

THIS PAGE IS INTENTIONALLY LEFT BLANK